CANADIAN THESES ON MICROFICHE

THÈSES CANADIENNES SUR MICROFICHE

National Library of Canada
Collections Development Branch

Canadian Theses on
Microfiche Service

Ottawa, Canada
K1A 0N4

Bibliothèque nationale du Canada
Direction du développement des collections

Service des thèses canadiennes
sur microfiche

NOTICE

The quality of this microfiche is heavily dependent upon the quality of the original thesis submitted for microfilming. Every effort has been made to ensure the highest quality of reproduction possible.

If pages are missing, contact the university which granted the degree.

Some pages may have indistinct print especially if the original pages were typed with a poor typewriter ribbon or if the university sent us an inferior photocopy.

Previously copyrighted materials (journal articles, published tests, etc.) are not filmed.

Reproduction in full or in part of this film is governed by the Canadian Copyright Act, R.S.C. 1970, c. C-30. Please read the authorization forms which accompany this thesis.

THIS DISSERTATION
HAS BEEN MICROFILMED
EXACTLY AS RECEIVED

AVIS

La qualité de cette microfiche dépend grandement de la qualité de la thèse soumise au microfilmage. Nous avons tout fait pour assurer une qualité supérieure de reproduction.

S'il manque des pages, veuillez communiquer avec l'université qui a conféré le grade.

La qualité d'impression de certaines pages peut laisser à désirer, surtout si les pages originales ont été dactylographiées à l'aide d'un ruban usé ou si l'université nous a fait parvenir une photocopie de qualité inférieure.

Les documents qui font déjà l'objet d'un droit d'auteur (articles de revue, examens publiés, etc.) ne sont pas microfilmés.

La reproduction, même partielle, de ce microfilm est soumise à la Loi canadienne sur le droit d'auteur, SRC 1970, c. C-30. Veuillez prendre connaissance des formules d'autorisation qui accompagnent cette thèse.

LA THÈSE A ÉTÉ
MICROFILMÉE TELLE QUE
NOUS L'AVONS REÇUE

NL 339 (r. 86/06)

Canada

0-315-19605-X

National Library of Canada
Bibliothèque nationale du Canada

265

Canadian Theses Division
Division des thèses canadiennes

Ottawa, Canada
K1A 0N4

67513

PERMISSION TO MICROFILM — AUTORISATION DE MICROFILMER

- Please print or type — Écrire en lettres moulées ou dactylographier

Full Name of Author — Nom complet de l'auteur

CHUKWUMAEZE JULIAN IWUAGWU

Date of Birth — Date de naissance 24 Nov. 1947	Country of Birth — Lieu de naissance NIGERIA

Permanent Address — Résidence fixe

P.O.Box 56, EHIME, IMO STATE, NIGERIA — WEST AFRICA.

Title of Thesis — Titre de la thèse

LITHOFACIES ANALYSIS, DEPOSITIONAL ENVIRONMENT AND DIAGENESIS OF THE BASAL BELLY RIVER FORMATION, SOUTHERN AND CENTRAL FOOTHILLS, ALBERTA, CANADA.

University — Université

UNIVERSITY OF ALBERTA, EDMONTON.

Degree for which thesis was presented — Grade pour lequel cette thèse fut présentée

Ph.D

Year this degree conferred — Année d'obtention de ce grade 1983 (FALL)	Name of Supervisor — Nom du directeur de thèse PROF. J.F. LERBEKMO.

Permission is hereby granted to the NATIONAL LIBRARY OF CANADA to microfilm this thesis and to lend or sell copies of the film.

The author reserves other publication rights, and neither the thesis nor extensive extracts from it may be printed or otherwise reproduced without the author's written permission.

L'autorisation est, par la présente, accordée à la BIBLIOTHÈQUE NATIONALE DU CANADA de microfilmer cette thèse et de prêter ou de vendre des exemplaires du film.

L'auteur se réserve les autres droits de publication; ni la thèse ni de longs extraits de celle-ci ne doivent être imprimés ou autrement reproduits sans l'autorisation écrite de l'auteur.

Date 14/10/83	Signature

NL-91 (4/77)

THE UNIVERSITY OF ALBERTA

'Lithofacies Analysis, Depositional Environment and Diagenesis of the basal Belly River Formation, Southern and Central Foothills, Alberta, Canada'

by

Chukwumaeze Julian Iwuagwu

A THESIS
SUBMITTED TO THE FACULTY OF GRADUATE STUDIES AND RESEARCH
IN PARTIAL FULFILMENT OF THE REQUIREMENTS FOR THE DEGREE
OF Doctor of Philosophy

Department of Geology

EDMONTON, ALBERTA
Fall, 1983

THE UNIVERSITY OF ALBERTA

RELEASE FORM

NAME OF AUTHOR Chukwumaeze Julian Iwuagwu

TITLE OF THESIS 'Lithofacies Analysis, Depositional Environment and Diagenesis of the basal Belly River Formation, Southern and Central Foothills, Alberta, Canada'

DEGREE FOR WHICH THESIS WAS PRESENTED Doctor of Philosophy

YEAR THIS DEGREE GRANTED Fall, 1983

Permission is hereby granted to THE UNIVERSITY OF ALBERTA LIBRARY to reproduce single copies of this thesis and to lend or sell such copies for private, scholarly or scientific research purposes only.

The author reserves other publication rights, and neither the thesis nor extensive extracts from it may be printed or otherwise reproduced without the author's written permission.

(SIGNED) ....

PERMANENT ADDRESS:

P.O. Box 56
EHIME , IMO STATE
NIGERIA - WEST AFRICA.

DATED June 22 1983

THE UNIVERSITY OF ALBERTA

FACULTY OF GRADUATE STUDIES AND RESEARCH

The undersigned certify that they have read, and recommend to the Faculty of Graduate Studies and Research, for acceptance, a thesis entitled 'Lithofacies Analysis, Depositional Environment and Diagenesis of the basal Belly River Formation, Southern and Central Foothills, Alberta, Canada' submitted by Chukwumaeze Julian Iwuagwu in partial fulfilment of the requirements for the degree of Doctor of Philosophy.

J F Lerbekmo

Supervisor

F.J. Longstaffe

C R Stelck

External Examiner

Date June 22, 1983

DEDICATION

To my parents (Chief James I. Iwuagwu (late) and Roselynn Iwuagwu) for their love, help and encouragement, and my children yet unborn and their mother for their patience.

ABSTRACT

Lithofacies analysis, petrography and diagenetic study of Upper Cretaceous (Campanian) basal Belly River sediments was undertaken along the Southern and Central Foothills of Alberta. The aims of the study were to deduce the depositional environment, determine the diagenetic patterns of the sandstone lithofacies, relate the diagenesis to depositional environment, and predict the most likely subsurface petroleum reservoirs.

The Belly River Formation in the study area forms an upward coarsening sequence which grades from shale at its base through interstratified shale/sandstone interval to coaly mudstones, coal beds and scour-based sandstones. This facies sequence is interpreted as of a shoreline depositional setting consisting of prodelta marine environment, delta front (occasionally affected by storm-waves), delta marsh and fluvial environments. The sandstones are fine- to very fine-grained, well to very well sorted mature lithic sandstones. Their diagenesis is environment specific resulting in four basic facies-related diagenetic patterns, namely: early calcite cementation of the distal bar sandstones, compaction and authigenic clay cementation of stream mouth bar sands, mechanical compaction and occasional cementation of the crevasse splay sandstones, and extensive authigenic clay cementation of the channel sandstones. In all cases, diagenesis detrimentally affected the reservoir quality of these sands, resulting in observable thin section porosity of less than 5 percent and a maximum total porosity of approximately 10 percent. Petrographic data show the sands to be poor petroleum reservoirs in general, but the most promising facies are the stream mouth bar and channel sands. The Belly River sandstones are characterized by variations in detrital composition, texture, sedimentary structures and diagenesis, and can be differentiated at various levels from outcrop to subsurface core and drill-cuttings, thereby improving exploration predictions.

ACKNOWLEDGEMENTS

The author gratefully acknowledges the friendly supervision of Dr. J.F. Lerbekmo at all stages of the research and his constructive comments during the writing of this thesis. I thank Dr. R.A. Rahmani (Ray) for all his encouragement throughout the duration of this project. Dr. C.R. Stelck identified the fossils. Terry Belke assisted in the field measurement of the stratigraphic sections and my thanks are due to him. I thank Mary Willock and Lynda Davis for freely typing the manuscript and processing the microfossils, respectively.

The Natural Sciences and Engineering Research Council and Esso Resources Canada, Calgary contributed financial support in the form of research grants to Dr. Lerbekmo, and the Alberta Research Council provided field assistance to the author. Financial assistance in the form of a Graduate Teaching Assistantship from the Geology Department, University of Alberta is also gratefully acknowledged.

I thank my parents, brothers, sisters and beloved cousin (Ugo) for their help and encouragement throughout the duration of this project. Finally, I thank my close friends, Barbara and Rod Moore, for their hospitality and tolerance of my late nights during the preparation and writing of this thesis.

Table of Contents

Chapter Page

I. INTRODUCTION 1

A. Purpose and Scope of the Study 1

B. Methods of Study 4

II. STRATIGRAPHY 6

A. The Belly River Formation of the Southern and Central Foothills of Alberta 6

B. Nomenclature 8

III. LITHOFACIES ANALYSIS 10

A. Lithofacies Definitions and Descriptions 10

Evenly Laminated Fissile Shale Facies (A). 10

Interstratified Sandstone/Shale Facies (B). (Heterolithic Facies I). 13

Bioturbated/Distorted Sandstone Facies (C). 19

Horizontal to low-angle Cross-stratified Sandstone Facies (D). 26

Coaly Mudstone Facies (E). 31

Interstratified Mudstone/Sandstone Facies (F). 33

Scour-based High-angle Cross-stratified Sandstone Facies (G). 36

Load-structure-based Cross-stratified Sandstone Facies (H). 40

Scoured Surface Facies (SS). 43

B. Facies Sequence: Markov Chain Analysis 43

IV. FACIES AND FACIES SEQUENCE : DEPOSITIONAL ENVIRONMENTAL INTERPRETATION 57

V. DEPOSITIONAL HISTORY AND PALEOGEOGRAPHY OF THE WESTERN ALBERTA SHORELINE DURING BELLY RIVER TIME. 68

A. Sedimentation History 68

Delta Type 69

Channel Pattern 72

B. Paleogeography 76

Provenance of Belly River Sediments 81

Paleocurrent Analysis and the Dispersal Pattern of Basal Belly River Sediments. 87

VI. MINERALOGICAL COMPOSITION AND CLASSIFICATION 92

Classification 92

Quartz 92

Feldspars 101

Rock Fragments 101

Varietal/Accessory Minerals 106

VII. TEXTURE: GRANULOMETRIC ANALYSIS 110

A. Size Frequency Distribution 110

Parameters 110

Textural Maturity 117

B. Other Textural Attributes 117

C. Paleohydraulics : Interpretation of the Grain Size Curves 118

D. Textural Characterization of Basal Belly River Sandstone Lithofacies 120

E. Textural Summary 121

VIII. DIAGENESIS 124

A. Diagenesis of Facies B Sandstones 125

B. Diagenesis of Facies D Sandstones 125

C. Diagenesis of Facies F and H Sandstones 131

D. Diagenesis of Facies G Sandstones 131

E. Discussion 138

F. Reservoir Quality 148

IX. SUBSURFACE DATA FROM THE BASAL BELLY RIVER FORMATION IN THE STUDY AREA 153

A. Core description (lithofacies) 153

Interstratified sandstone/shale (Facies B) 160

Horizontal to low-angle cross-stratified sandstone (Facies D) 160

Coaly mudstone (Facies E) 160

Scour-based high-angle cross-stratified sandstone (Facies G) 160

Load-structure-based cross-stratified sandstone (Facies H) 161

Scoured surface (Facies SS) 161

B. Mechanical log characteristics 161

X. COMPARATIVE EVALUATION OF OUTCROP AND SUBSURFACE DATA : POSSIBLE APPLICATION OF OUTCROP INFORMATION TO SUBSURFACE EXPLORATION OF THE BASAL BELLY RIVER SANDSTONE RESERVOIR 164

XI. SUMMARY AND CONCLUSIONS 172

REFERENCES CITED 174

APPENDIX A: STRATIGRAPHIC SECTIONS 182

APPENDIX B: FACIES RELATIONSHIP DIAGRAMS (FRDS) FOR THE INDIVIDUAL STRATIGRAPHIC SECTIONS. 192

APPENDIX C: DATA SHEET FOR THE GRAIN SIZE ANALYSES (USING HUMPHRIES MICROMETER EYEPIECE AND THE COUNTER UNIT). 199

APPENDIX D: CUMULATIVE CURVES OF THE ANALYSED SAMPLES. 228

APPENDIX E: HISTOGRAMS OF THE ANALYSED SAMPLES. 244

TABLES

Table 1: List of wells in the study area with Belly River core 3

Table 2: Table of Formations of the Southern and Central Alberta Foothills and adjoining areas 7

Table 3: Composite transition count matrix (observed number of transitions between facies) derived from all the fourteen stratigraphic sections combined 48

Table 4: Summary statistics of the number of occurrences of the different lithofacies in all the fourteen stratigraphic sections combined 49

Table 5: Observed transition probability matrix (Observed transition probabilities) 50

Table 6: Random probability matrix (transition probabilities for random sequence) 51

Table 7a: Difference probability matrix (observed minus random transition probabilities) .. 52

Table 7b: Chi-square statistics to test the significance of facies transitions 53

Table 8: Total thickness of facies A,B,C, and D (the subaqueous deltic lithofacies) in the various sections 73

Table 9: Summary of paleocurrent data 77

Table 10: Essential components (recalculated to 100%) 93

Table 11: Quartz types as percentage of total essential components 96

Table 12: Feldspar types as percentage of total essential components 102

Table 13: Rock fragments as percentage of total essential components 104

Table 14: Summary statistics of granulometric analyses (phi units) of basal Belly River sandstones 113

Table 15: Cement types and percentages 129

Table 16: Total cement, thin section porosity, cement+porosity, framework, matrix, accessory minerals, opaques, and framework+matrix+accessory minerals+opaques as percentage of total components 150

Table 17: Check list of sediment properties for the differentiation of the basal Belly River sandstone lithofacies 168

FIGURES

Figure 1: Locations of measured outcrop sections 2

Figure 2: Legend for the stratigraphic sections 11

Figure 3: Facies types and representation for the Belly River Formation 12

Figure 4: Interstratified sandstone/shale facies (B) 14

Figure 5a: Schematic generalized sequence of sedimentary structures typical of sandstone beds of facies B 16

Figure 5b: Example of the sequence of sedimentary structures in the sandstones of facies B 16

Figure 5c: Example of sequence of sedimentary structures in the sandstones of facies B 17

Figure 6: Rhizocorallium in sandstones of facies B 18

Figure 7a: Bioturbated sandstone of facies C 20

Figure 7b: Distorted sandstone of facies C 20

Figure 7c: Deformed bedding common in facies C sandstones 21

Figure 8a: Interstratification of bioturbated homogenized and non-bioturbated sandstone layers of facies C 22

Figure 8b: Interstratification of bioturbated homogenized and non-bioturbated horizontal laminated sandstone layers of facies C 23

Figure 8c: Interstratification of bioturbated homogenized shaly sandstone layer and non-bioturbated low-angle planar tabular cross-stratified sandstone layer of facies C 24

Figure 9a: Horizontal to low-angle cross-stratified sandstone facies 27

Figure 9b: Closeup of fig. 9a above 28

Figure 9c: Horizontal bedding followed by low-angle cross-bedding of facies D 29

Figure 9d: Interstratification of clean horizontal laminated and ripple cross-laminated sandstone and bioturbated shaly sandstone layers of facies D 29

Figure 9e: Symmetrical straight crested ripples on the upper surface of a sandstone bed of facies D 30

Figure 9f: Interference ripples on a bedding plane of facies D sandstone 30

Figure 10a: Schematic idealized sequence of sedimentary structure typical of sandstone beds of facies D 32

Figure 10b: Sequence of sedimentary structures common within sandstone beds of facies D 32

Figure 11a: Interstratified mudstone/sandstone facies 34

Figure 11b: Interstratified mudstone/sandstone facies 34

Figure 11c: Ripple cross-lamination common in facies F sandstones 35

Figure 11d: Asymmetrical ripple marks on top of the top sandstone layer of Unit 22 of Trap Creek section (Fig. 11c) 35

Figure 12: Scour-based high-angle cross-stratified sandstone facies 37

Figure 13: Multistorey channel sandstone with shallow minor channels (scours) within facies G sandstone 38

Figure 14a: Load-structure-based cross-strataified sandstone facies 41

Figure 14b: Typical base of facies H sandstone 41

Figure 15: Plan view of scoured surface with mudclasts (facies SS) 44

Figure 16a: Composite simplified facies relationship diagram for the basal Belly River Formation 54

Figure 16b: A local facies model for basal Belly River sequence based on Markov diagram (Figure 16a) 55

Figure 17: Delta front subenvironments 58

Figure 18: Suspected position of Belly River delta on a schematic diagram illustrating the threefold division of deltas into fluvial-dominated, wave-dominated, and tide-dominated types 70

Figure 19: The seven partially overlapping lobes of the Mississippi delta which have developed during the last 5000 years 74

Figure 20: Dominant paleocurrent directions at measured outcrop sections 80

Figure 21: Comparison of Drywood River, Bow River and Cripple Creek section FRDs 82

Figure 22: Paleogeographic map of Western Canada for Belly River time 84

Figure 23: Flute casts on the sole of Unit 5 high-angle cross-stratified sandstone facies (G) at Morley 88

Figure 24: Detrital composition of basal Belly River sandstone in the study area 95

Figure 25: Size frequency of representative basal Belly River sandstones in the study area, determined by thin section analysis 111

Figure 26: Histograms of samples representative of basal Belly River sandstones in the study area 112

Figure 27: Sieve median diameter vs. percent finer than 4 phi of basal Belly River sandstones 122

Figure 28: Framework vs. cement-free porosity (a measure of degree of compaction before cementation) 128

Figure 29: Framework, cement and porosity characteristics of the different sandstone lithofacies 149

Figure 30: Lithologic and electric logs of well 3-36-40-9W5 156

Figure 31: Gamma ray-neutron and lithologic logs of well 3-36-40-9W5 157

Figure 32: Lithologic and electric logs of well 4-27-40-8W5 158

Figure 33: Lithologic and electric logs of well 12-31-40-8W5 159

Figure 34: Log-probability curves representative of outcrop sandstone samples of the basal Belly River sandstone 165

Figure 35: Log-probability curves representative of subsurface sandstone samples of the basal Belly River sandstone 166

PLATES

Plate 1: Photomicrographs of thin sections of basal Belly River sandstones 99

Plate 2: Photomicrographs of thin sections of basal Belly River sandstone 107

Plate 3: Photomicrographs of thin sections and SEM photomicrographs of basal Belly River sandstone 126

Plate 4: SEM photomicrographs of authigenic clays of the basal Belly River sandstone 132

Plate 5: SEM photomicrograph and spectral profiles of authigenic clays of the basal Belly River sandstone 134

Plate 6: Composition of authigenic clay cements of basal Belly River sandstone as displayed by the energy-dispersive X-ray spectrometer 136

Plate 7: Photomicrographs of thin sections of basal Belly River sandstone 143

Plate 8: Photomicrographs of thin sections of basal Belly River sandstones 145

Plate 9: Photographs of core slab typical of the basal Belly River Formation (Well: 3-36-40-9W5) 154

I. INTRODUCTION

A. Purpose and Scope of the Study

The purpose of this study was fourfold:

1. To characterize the sediments of the Belly River Formation in its outcrop belt of the Rocky Mountain Foothills, southwestern and west-central Alberta,
2. To decipher their depositional environments,
3. To investigate the relationship between depositional environment and diagenesis of the sandstone lithofacies, and
4. To reconstruct the characteristics of the western shoreline during the retreat of the Cretaceous seaway.

The discovery of shallow oil and natural gas accumulations in the Upper Cretaceous basal Belly River Sandstone at Pembina Field in the late 1950s attracted the interest of only a few companies until the mid-1960 when exploration for similar accumulations increased in surrounding areas of the central Alberta Plains and Foothills. Exploration and drilling programs indicated that the discovery of such accumulations was largely fortuitous (Oilweek, Oct. 26/64), and that the control for these accumulations is stratigraphic. There was need for a better understanding of the depositional environments of these sands. Following studies resulted in diverse interpretations spanning the gamut of major clastic depositional environments: floodplain (Shawa and Lee, 1975), coastal plain (Lerbekmo, 1963), delta (Lerand and Oliver, 1975; Nelson and Glaister, 1975; McLean, 1971), marginal-marine (Ogunyomi and Hills, 1977) and turbidite (Rosenthal, 1982). These workers, with the exception of Ogunyomi and Hills (1977) and Rosenthal (1982), concentrated their studies on single sections, and suffered from lack of knowledge of the variability of this lithostratigraphic unit in different geographic areas.

The present study involved the accessible good outcrops in the Foothills along with some very limited available subsurface core. It is believed that the knowledge gained from this study can be used as an exploration tool in the Plains where this lithostratigraphic unit contains hydrocarbons.

Figure 1 shows the locations of the studied outcrop sections and Table 1 is the list of examined well cores. The selection of the outcrop sections was based mainly on

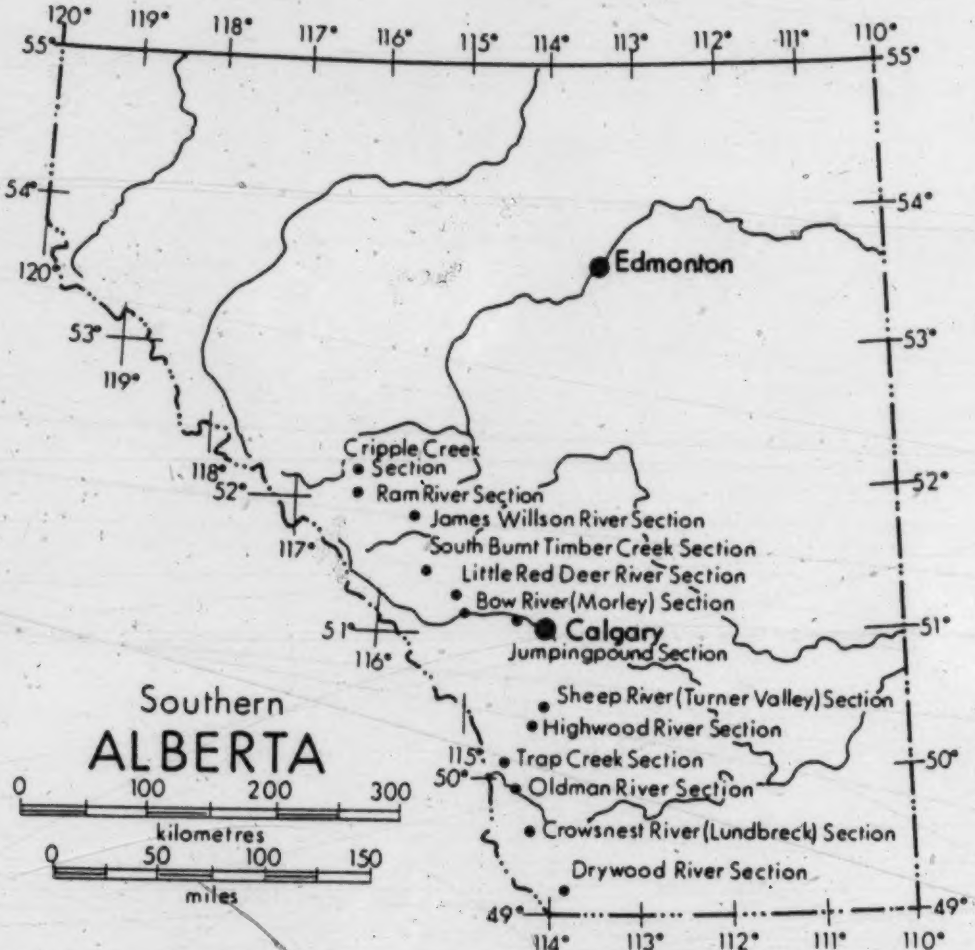
Southern
ALBERTA
0
100
200
300
kilometres
0
50
100
150
miles
Edmonton
Calgary
Cripple Creek Section
Ram River Section
James Willson River Section
South Burnt Timber Creek Section
Little Red Deer River Section
Bow River (Morley) Section
Jumpingpound Section
Sheep River (Turner Valley) Section
Highwood River Section
Trap Creek Section
Oldman River Section
Crowsnest River (Lundbreck) Section
Drywood River Section
120°
119°
118°
117°
116°
115°
114°
113°
112°
111°
110°
55°
54°
53°
52°
51°
50°
49°

Figure 1. Locations of measured outcrop sections.

Table 1. List of wells in the study area with Belly River core.

Well Name	Location	Cored Interval (Ft)	Rec. Core Footage	Top of Wapiabi Shale
Ricinus No.1	15-27-35-9W5	7380-7388	7.5	7430.0 Ft
Phillips Ancona No.1	8-27-39-11W5	7020-7023;	5.0	7450.0 Ft
		7158-7166		
		7228-7236	7.5	
Amerada CDN-SUP Ferrier	4-27-40-8W5	5515-5588	73.0	5641.0 Ft
Ammin W. Ferrier	12-31-40-8W5	5645-5578	60.0	5692.0 Ft
Ammin Ferrier	3-36-40-9W5	5659-5735	76.0	5730.0 Ft

accessibility and structural simplicity (unfaulted nature), whereas wells were chosen for availability of the necessary core. More than one thousand wells in the immediate vicinity of the outcrop belt were examined for availability of cores of the Wapiabi/Belly River (Brazeau) transition, but unfortunately only five wells (Table 1) were found to have such core. This particular interval was sought because it is the most controversial part of the Belly River (Brazeau) Formation with regard to the depositional environment. The limited available subsurface information was utilized along with the outcrop data to arrive at a comprehensive depositional environment for the Belly River (Brazeau) sediments in the study area.

B. Methods of Study

Fourteen outcrop sections (two sections located at Jumpingpound) and cores from five wells form the data base for this thesis. The sections were measured, described and sampled, and are the best exposed of the essentially unfaulted sections available. Each section was subdivided into lithofacies on the bases of sedimentary structures, textures, mineralogical composition and paleontology. The cores were described and sampled, and like the outcrop sections, subdivided into lithofacies. Laboratory investigations included grain size measurements, compositional and microfaunal analyses and diagenetic studies. One hundred and ninety six representative sandstone and ten shale/mudstone samples were selected for detailed analyses and study. Compositional analysis in thin section was achieved by recording 600 points within a 6 sq. cm grid, utilizing an automatic point-count mechanical stage. A check made after counting 300 points revealed that counting more than 600 points was unnecessary. The necessary data for granulometric analyses were also obtained from thin sections utilizing a Humphries' micrometer eyepiece because all the samples are lithified. A comparison with the data obtained from the first 400 grains, showed that measuring more than 600 grains was not justified. The shale and mudstone samples were soaked in water for several days to cause them to partially break down, and they were then washed through a nest of standard sieves. The less than 100 mesh fractions were boiled with "Sparkleen" detergent and water to further induce shale failure and free any foraminifers.

Local lithofacies sequences (local summaries) were arrived at by Markov chain analysis. The lithofacies and their local lithofacies sequences (lithofacies assemblages) are given depositional environmental interpretation by:

1. considering the possible depositional processes that might have given rise to them, as indicated by the primary sedimentary structures and textures (paleohydraulic information),
2. considering the likely environments in which these processes might have operated,
3. comparing and contrasting the local lithofacies sequences of the basal Belly River Formation with established facies models, and by
4. considering available paleontological information.

Sandstone samples from the inferred different subenvironments were then examined in greater detail to see if their diagenesis is environment specific, i.e., if there is any relationship between their diagenesis and depositional environment, and if so, to further characterize the different sandstones. Scanning electron microscopy was carried out using a Cambridge Stereoscan 150 equipped with energy dispersive unit (Kevex 7000), as well as thin section petrography, to achieve this objective.

II. STRATIGRAPHY

A. The Belly River Formation of the Southern and Central Foothills of Alberta

The Belly River Formation in the study area is part of an eastward thinning clastic wedge that records the progradation of continental conditions associated with the eastward withdrawal of the Lea Park sea during Cretaceous Campanian time (Williams and Burk, 1964; Jeletzky, 1971; Stott, 1963; Eisbacher et al., 1974). It represents part of the easterly prograding Belly River–Paskapoo molasse (Eisbacher et al, 1974), attaining a thickness of about 400 meters in the Plains of southern Alberta and increasing westwards to about 700 meters in the southern Foothills (Lerbekmo, 1961; 1963).

In the area of study in the Southern and Central Foothills, the Belly River Formation consists of horizontal and cross-stratified, light gray to greenish, lithic, fine- to medium-grained, moderately sorted sandstones, dark gray mudstone, minor amounts of siltstones, carbonaceous and bentonitic shales and minor conglomerates. It is conformable with both the underlying Wapiabi marine shale (Jeletzky, 1971;Stott, 1963) and with the overlying Bearpaw marine shale, but is diachronous, becoming younger to the east. In the Southern Foothills and Plains, the Bearpaw Shale separates the Belly River Formation from similar younger continental sediments (St. Mary's River and Edmonton Formations), but the Bearpaw Shale thins northward in the Foothills until at the Bow River it does not reach as far west as the outcrop belt. Therefore, the inability to separate the Belly River and Edmonton Formations where the sediments thicken farther north has necessitated the lumping of this continental sequence in the Central Foothills into the Brazeau Formation (Lerbekmo, 1963). Eastward from the Foothills, Belly River strata thin gradually under the Plains where the appearance of the thin Pakowki marine shale tongue and the distinctive Milk River Sandstone along with other lithologic variations permit the differentiation of four units of formational status within the Plains Belly River Group (Russell and Landes, 1940; Lerbekmo, 1963; Table 2).

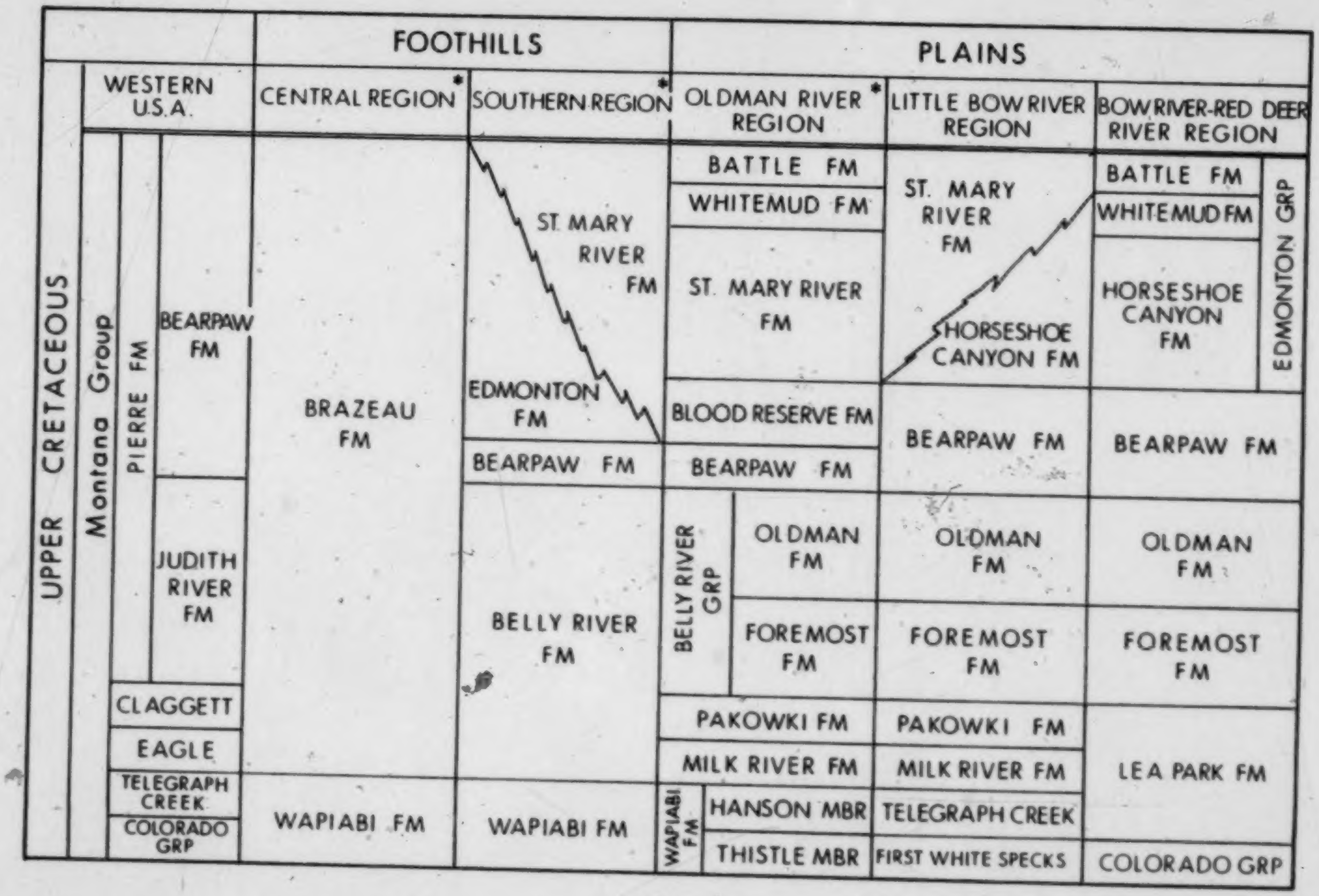

				FOOTHILLS		PLAINS				
UPPER CRETACEOUS	WESTERN U.S.A.			CENTRAL REGION*	SOUTHERN REGION*	OLDMAN RIVER REGION*		LITTLE BOW RIVER REGION	BOW RIVER-RED DEER RIVER REGION	
	Montana Group	PIERRE FM	BEARPAW FM	BRAZEAU FM	ST. MARY RIVER FM EDMONTON FM	BATTLE FM		ST. MARY RIVER FM	BATTLE FM	EDMONTON GRP
						WHITEMUD FM			WHITEMUD FM	
						ST. MARY RIVER FM		HORSESHOE CANYON FM	HORSESHOE CANYON FM	
						BLOOD RESERVE FM		BEARPAW FM	BEARPAW FM	
					BEARPAW FM	BEARPAW FM				
			JUDITH RIVER FM		BELLY RIVER FM	BELLY RIVER GRP	OLDMAN FM	OLDMAN FM	OLDMAN FM	
							FOREMOST FM	FOREMOST FM	FOREMOST FM	
		CLAGGETT				PAKOWKI FM		PAKOWKI FM	LEA PARK FM	
		EAGLE				MILK RIVER FM		MILK RIVER FM		
		TELEGRAPH CREEK		WAPIABI FM	WAPIABI FM	WAPIABI FM	HANSON MBR	TELEGRAPH CREEK		
		COLORADO GRP					THISTLE MBR	FIRST WHITE SPECKS	COLORADO GRP	

Table 2. Table of Formations of the Southern and Central Alberta Foothills and adjoining areas (modified from Rahmani and Lerbekmo, 1975).

B. Nomenclature

Literature reviews (McLean, 1971; Iwuagwu, 1979; Iwuagwu and Lerbekmo, 1982) show inconsistencies, ambiguities and duplication of names for this lithostratigraphic unit. McLean (1971) argued for dropping of the term Belly River for the American term Judith River for reasons of priority of usage. In the Southern and Central Foothills, as well as in the West-Central Alberta Plains, this lithostratigraphic unit is undivided and is traditionally called the Belly River Formation, or the Brazeau Formation in the absence of the Bearpaw Shale in the Central Foothills. Although the writer realizes the nomenclatural problem, he has no intention to dwell on it because it is not consequential to the present project. Rather, he will adopt the terminology and nomenclature most prevalent amongst geologists working on the Upper Cretaceous sediments of the Southern and Central Foothills of Alberta-the Belly River Formation/Brazeau Formation.

Rahmani and Lerbekmo (1975) and McLean (1971) have aptly summarized the stratigraphy of this lithostratigraphic unit as it is presently known. Table 2 modified from Rahmani and Lerbekmo (1975) shows the stratigraphic units in the study area and their lateral correlatives (equivalents) in the western United states, and the Southern and North-Central Plains of Alberta. Irrespective of the different formational names in various geographic areas, this lithostratigraphic interval is essentially made up of fine- to medium-grained, horizontal and cross-stratified sandstones, siltstones, mudstones, shales, coal seams and minor conglomerates.

In the study area, the lower contact of this unit with the Wapiabi marine shale is generally gradational and includes a transitional zone of interbedded shale and very fine grained sandstone which is conventionally known as the Wapiabi transition zone. Although most workers agree that the bulk of Belly River sediments are continental (fluvial), opinion is divided on the depositional environments of the Wapaibi transition zone and the basal part of the Belly River and Brazeau Formations in the study area. The resolution of this problem constitutes the major task of the present project.

For the purpose of this thesis, the term basal Belly River (informal name) is applied to the lowermost approximately 100 meters of the Belly River Formation and the underlying Wapiabi transition zone. It is equivalent to the Chungo (Highwood) and Nomad members of the Belly River Formation of the southern Foothills (Wall and Germundson, 1963; Stott, 1963) which are homotaxial with the Solomon and Chinook sandstones of the central and northern Foothills, respectively. Although it is safe to assume that the Chungo sandstone is equivalent to the Highwood sandstone, one would be hesitant to assume its isochronity with the Solomon and Chinook sandstones of the north.

III. LITHOFACIES ANALYSIS

A. Lithofacies Definitions and Descriptions

After careful inspection of sections (Appendix A), with awareness of the variabilities within each of the facies, the stratigraphic sections were subdivided into lithofacies (Figures 2,3). A facies is a unit of rock distinguished in the field by lithology,sedimentary structures, and organic features from adjacent facies, both vertically and laterally (deRaaf et al., 1965; Cant and Walker, 1976; Middleton, 1978).

On the bases of sedimentary structures, textures, minerology and paleontology nine lithofacies are recognized and defined in the Belly River Formation of the study area. These are as follows: Shale facies, Interstratified sandstone/shale facies (Heterolithic facies I), Bioturbated/distorted sandstone facies, Horizontal to low-angle cross-stratified sandstone facies, Coaly mudstone facies, Interstratified mudstone/sandstone facies (Heterolithic facies II), Scour-based high-angle cross-stratified sandstone facies, Load-structure-based cross-stratified sandstone facies and Scoured surface with mudclasts facies. For the sake of brevity these lithofacies are also given informal designations as A,B,C, D,E,F,G,H, and SS respectively.

Following standard facies analysis practices such as that proposed by Cant and Walker (1976), these lithofacies will be given depositional interpretation later (Chapter 1V) after their facies sequence has been established, so that the interpretation is based upon specific characteristics as well as overall relationship.

Evenly Laminated Fissile Shale Facies (A).

This facies consists dominantly of dark gray (N3) (and medium dark gray (N4)) silty shale; other shades of gray such as olive gray (5Y4/1), light olive gray (5Y6/1), greenish gray (5GY6/1), dark greenish gray (5GY4/1),olive black (5Y2/1), and grayish black (N2) are not uncommon. Despite minor color differences, shales of this facies are all fissile, though the fissility of an individual occurrence of this facies decreases upward with the incorporation of more silt sized particles, thereby rendering it more massive and mudstone-like in character. It is carbonaceous, sandy and concretionary (carbonate

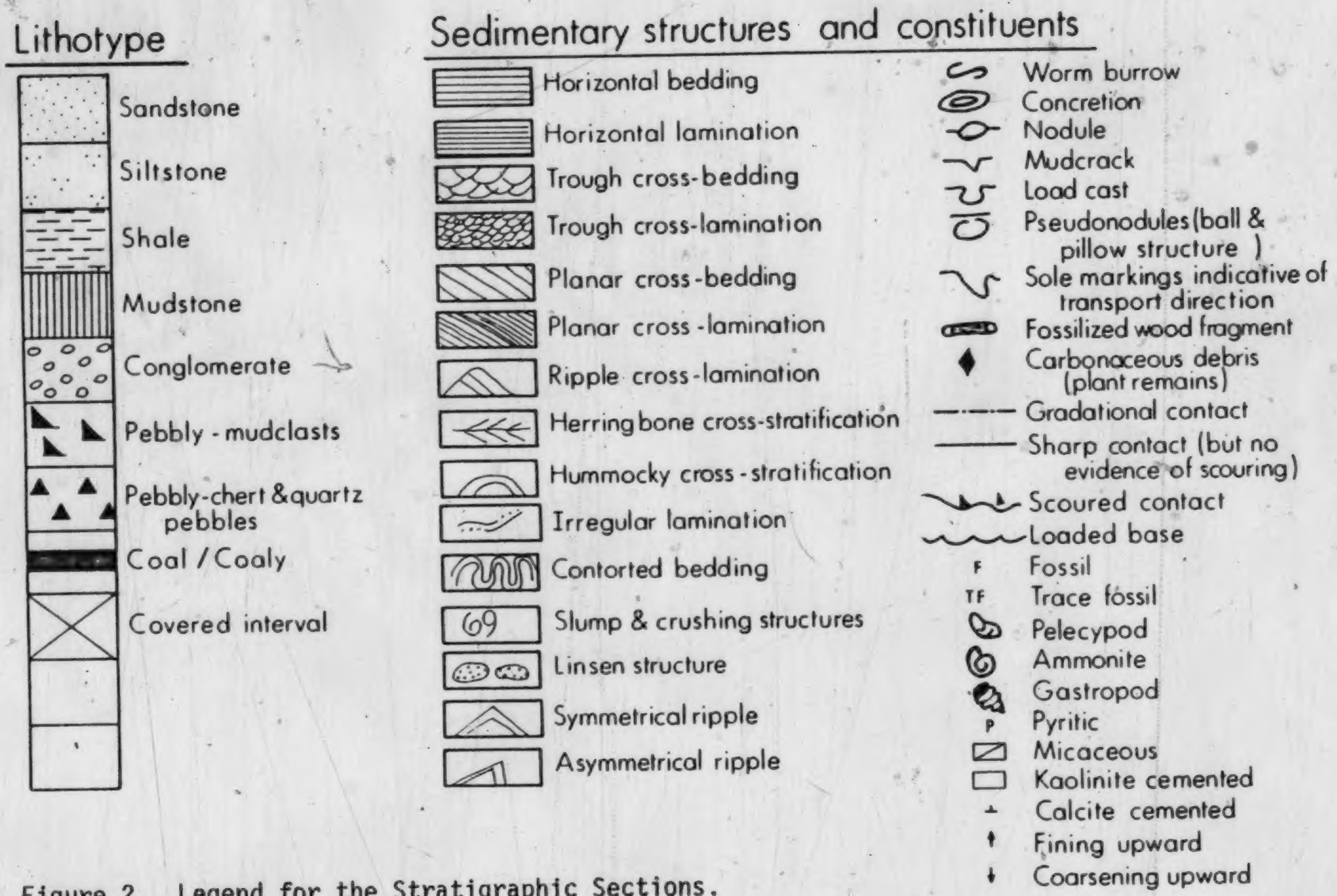
Lithotype
Sandstone
Siltstone
Shale
Mudstone
Conglomerate
Pebbly - mudclasts
Pebbly-chert & quartz pebbles
Coal / Coaly
Covered interval
Sedimentary structures and constituents
Horizontal bedding
Horizontal lamination
Trough cross-bedding
Trough cross-lamination
Planar cross-bedding
Planar cross-lamination
Ripple cross-lamination
Herringbone cross-stratification
Hummocky cross-stratification
Irregular lamination
Contorted bedding
69
Slump & crushing structures
Linsen structure
Symmetrical ripple
Asymmetrical ripple
Worm burrow
Concretion
Nodule
Mudcrack
Load cast
Pseudonodules (ball & pillow structure)
Sole markings indicative of transport direction
Fossilized wood fragment
Carbonaceous debris (plant remains)
Gradational contact
Sharp contact (but no evidence of scouring)
Scoured contact
Loaded base
F
Fossil
TF
Trace fossil
Pelecypod
Ammonite
Gastropod
P
Pyritic
Micaceous
Kaolinite cemented
Calcite cemented
Fining upward
Coarsening upward

Figure 2. Legend for the Stratigraphic Sections.

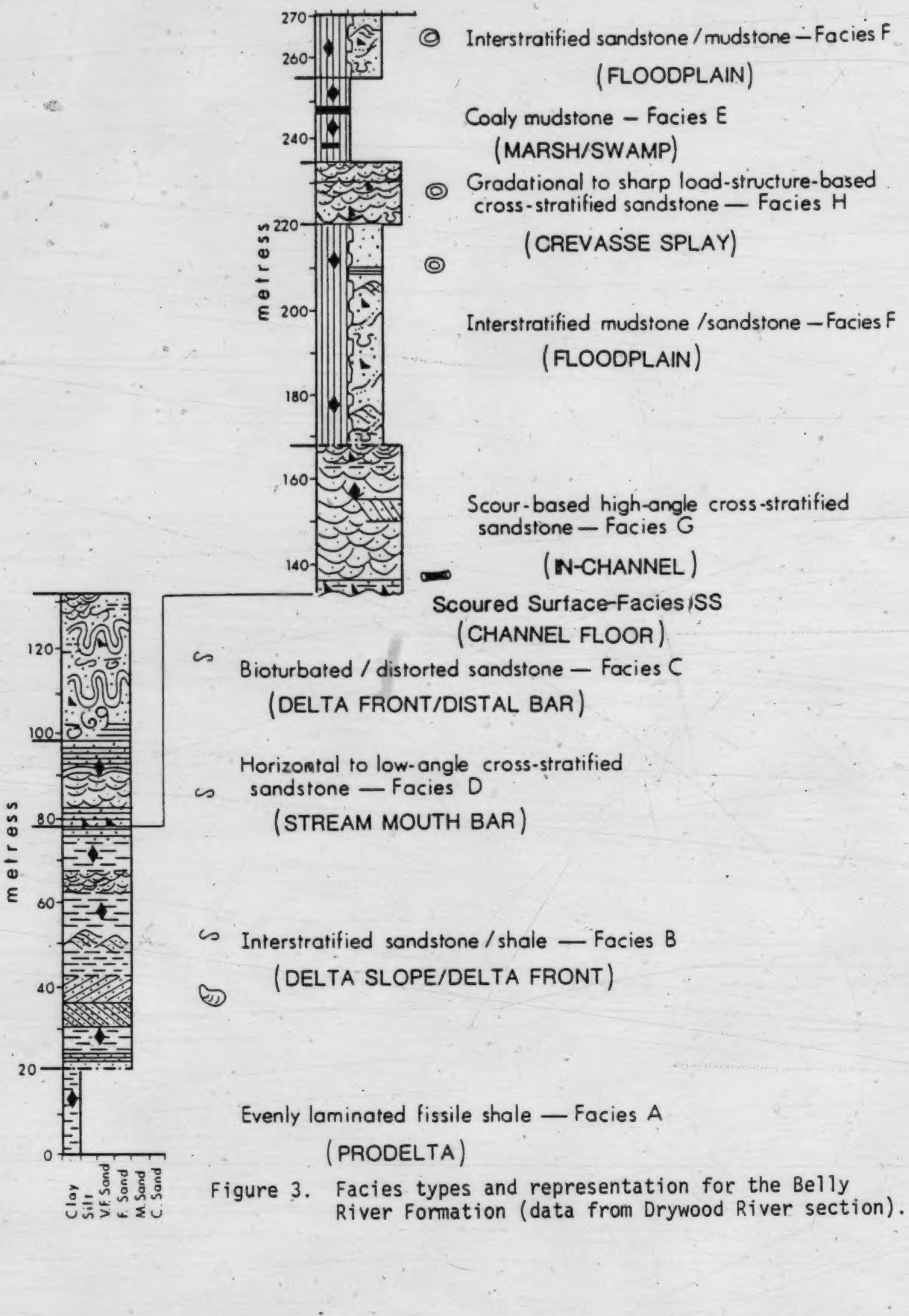
270
260
240
220
200
180
160
140
metress
Interstratified sandstone / mudstone — Facies F
(FLOODPLAIN)
Coaly mudstone — Facies E
(MARSH/SWAMP)
Gradational to sharp load-structure-based cross-stratified sandstone — Facies H
(CREVASSE SPLAY)
Interstratified mudstone /sandstone — Facies F
(FLOODPLAIN)
Scour-based high-angle cross-stratified sandstone — Facies G
(IN-CHANNEL)
Scoured Surface-Facies SS
(CHANNEL FLOOR)
120
100
80
60
40
20
0
metress
Bioturbated / distorted sandstone — Facies C
(DELTA FRONT/DISTAL BAR)
Horizontal to low-angle cross-stratified sandstone — Facies D
(STREAM MOUTH BAR)
Interstratified sandstone / shale — Facies B
(DELTA SLOPE/DELTA FRONT)
Evenly laminated fissile shale — Facies A
(PRODELTA)
Clay
Silt
V.F. Sand
F. Sand
M. Sand
C. Sand

Figure 3. Facies types and representation for the Belly River Formation (data from Drywood River section).

concretions) in places. It has a foraminiferal assemblage dominated by Haplophragmoides and Trochammina , as well as a few Ammobaculites and Eggerella .

This facies has mostly gradational lower and upper contacts (grading downward to the less silty marine Wapiabi Shale, and upward to the more sandy facies B but occasionally to facies H). In a few cases, the upper contacts of this facies are sharp but non-scoured, and are only a reflection of differences in color and grain size of the adjacent facies. It weathers papery to rubbly and crops out better than stratigraphically higher typical Belly River/Brazeau mudstones and shales of facies E and F.

Interstratified Sandstone/Shale Facies (B). (Heterolithic Facies I).

This facies consists of alternating strata of very fine- to fine-grained sandstones and shales (Figure 4). The sandstone layers are medium gray (N5) to medium light gray (N6) with occasional medium dark gray (N4), dark gray (N3), olive gray (5Y4/1), light olive gray (5Y6/1), light olive gray (5Y5/2) and greenish gray (5GY6/1) varieties. They are horizontally parallel laminated, trough cross-laminated, ripple cross-laminated, occasionally herringbone cross-laminated and irregularly (indistinctly) cross-laminated. In places ripples show well preserved surfaces (ripple marks) whereas in others the ripple marks are partially destroyed and coexist with a few non-discrete horizontal worm burrows and trails, or are completely destroyed by severe bioturbation. These sandstone units range in thickness from 2 to 40cm (average of 5 to 10cm) with the thicker ones more abundant upward through the facies occurrence. They are mostly tabular in form though lenticular and irregular shapes are also common, and in some places linsen structures (sand lenses in a shale matrix) are observed. They have sharp bases which are due to differences in grain sizes between the sandstones and the alternating shales. There are few instances of interstratification of bioturbated and non-bioturbated ripple cross-laminated sand layers. The sands are carbonaceous and sometimes the black organic matter is concentrated along lamination planes to form carbonaceous laminae; these and occasional shale partings show up the overall lamination of the sands. They are fair to poorly sorted (muddy), glauconitic, micaceous, and occasionally contain coal and wood fragments and shale clasts. They are carbonate cemented, well indurated , occasionally concretionary; mostly flaggy to platy

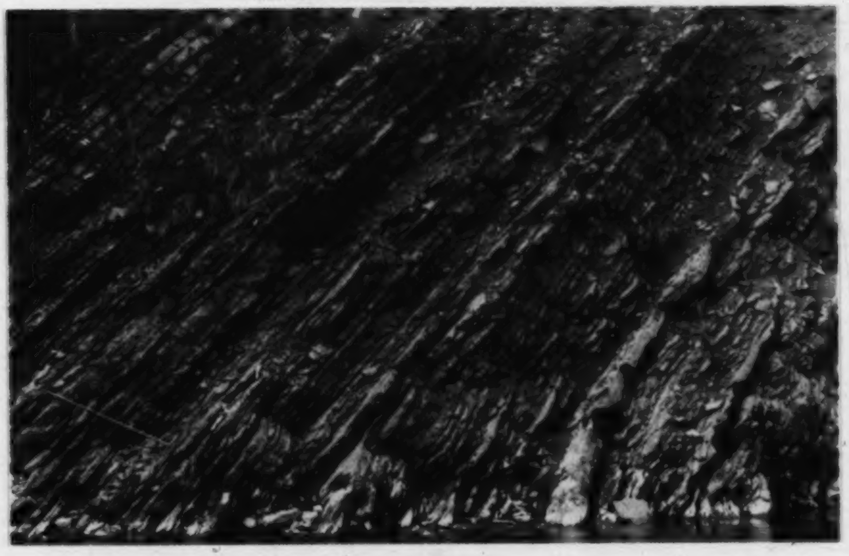

Figure 4. Interstratified sandstone/shale facies (B). Location: Unit 2 of Highwood River section.

weathering, though slabby and rubbly weathering in places.

The general sequence of sedimentary structures in the sandstone layers of facies B is distinct and is as follows: groove casts on the soles of the sand beds; horizontal lamination overlying a sharp but non-scoured base; minor trough cross-lamination; ripple cross-lamination; occasional indistinct (irregular) cross-lamination; an upper surface showing undulations and interference ripples and horizontal worm trails and burrows (Figure 5). There is pronounced repetition of structure types in definite sequences attributable to repetition of the depositional processes.

The interstratified shale of facies B is dominantly dark gray (N3) and medium dark gray (N4) to olive gray (5Y4/1), and occasionally greenish black (5GY2/1), grayish black (N2), light olive gray (5Y5/2), medium gray (N5), light olive gray (5Y6/1), dark greenish gray (5GY4/1) and olive black (5Y2/1). It is silty to slightly sandy, carbonaceous to very carbonaceous, micaceous and concretionary (carbonate concretions). The shale beds range in thickness from 2 to 25cm and decrease in thickness and importance upward through the facies. The sand/shale ratio in most occurrences ranges from about 30/70 at the base to 80/20 at the top.

A few pelecypod shells and fragments (Pleuromya?), drift wood fragments and comminuted plant debris form the body fossil component of this facies. Horizontal to slightly inclined worm burrows, especially Rhizocorallium (Figure 6), are common along bedding planes and in the upper parts of sand beds. These trace fossils were mainly sediment feeders; they belong to the Cruziana facies of Seilacher (1967) which indicates a littoral zone to wave base environment. Some vertical escape burrows passing through the sand beds were observed at the Crowsnest River (Lundbreck) section.

Individual occurrences of this facies range from 2 to 52 meters thick but most are in the range of 4 to 15 meters. They usually show coarsening upward characteristics in the form of increase in the thickness of sandstone layers, overall sand content, grain size and sorting (muddy and bioturbated at the base of some occurrences); some of the sand layers themselves show grading from fine to very fine sand and silt (a type of fining-upward gradient) within individual subunits. However, a few occurrences show upward decrease in sand layer thickness as a reflection of limited input of coarse detritus. They invariably have a lower gradational contact with facies A, and mostly a sharp upper

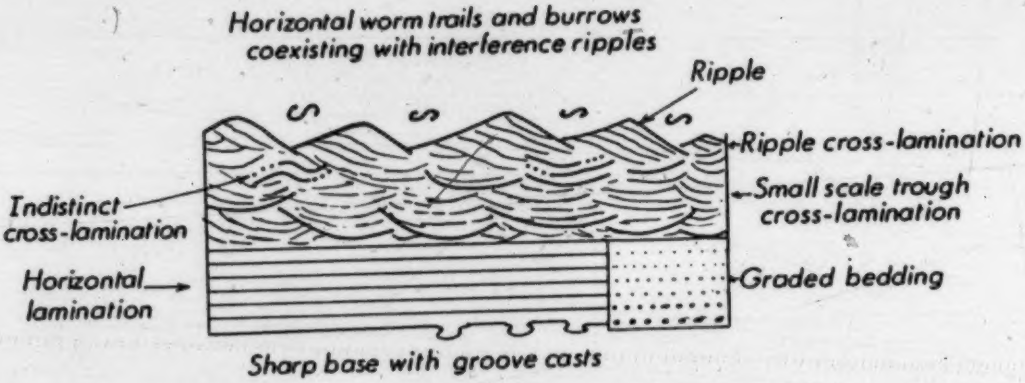
Horizontal worm trails and burrows coexisting with interference ripples
Ripple
Ripple cross-lamination
Small scale trough cross-lamination
Indistinct cross-lamination
Horizontal lamination
Graded bedding
Sharp base with groove casts

Figure 5a. Schematic generalized sequence of sedimentary structures typical of sandstone beds of facies B.

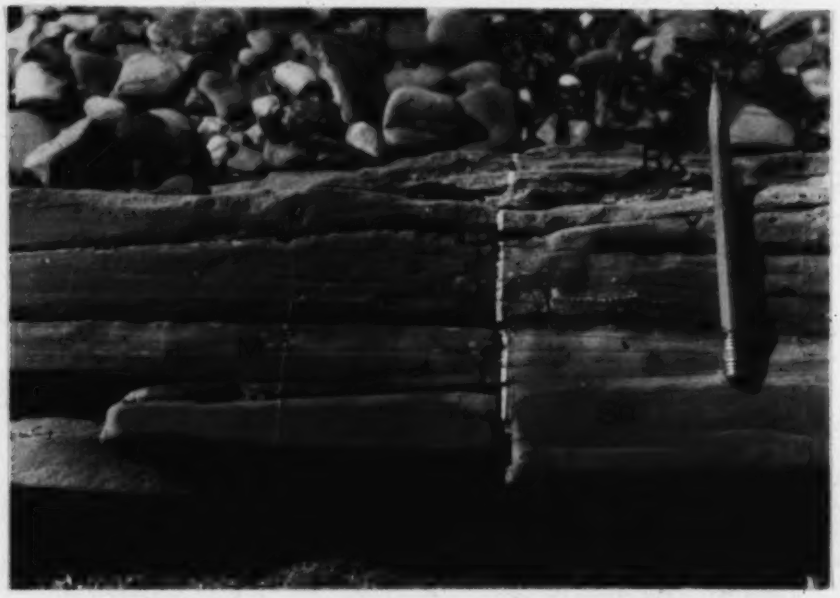

Figure 5b. Example of the sequence of sedimentary structures in the sandstones of facies B. Note the sharp base (arrow) between the shale (Sh) and the sandstone (Sd); horizontal lamination (M), low-angle cross-lamination (X) and ripple cross-lamination (RX). Location: Unit 7 of Drywood section.

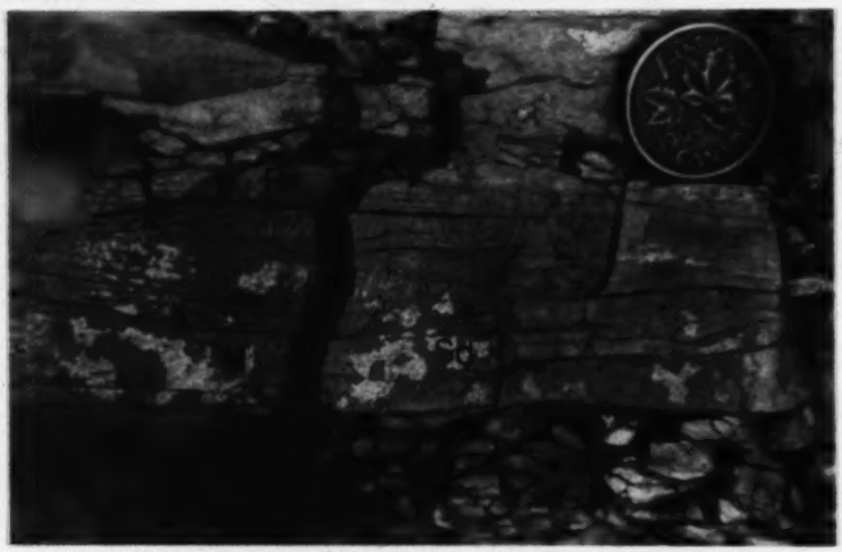

Figure 5c. Example of sequence of sedimentary structures in the sandstones of facies B. Note the sharp base (arrow) to the sandstone layer (sd), horizontal lamination (H), small scale low-angle cross-lamination (X) and ripple cross-lamination (RX). Black organic concentrations accentuated the laminations. Location: Unit 1 of Lundbreck section.

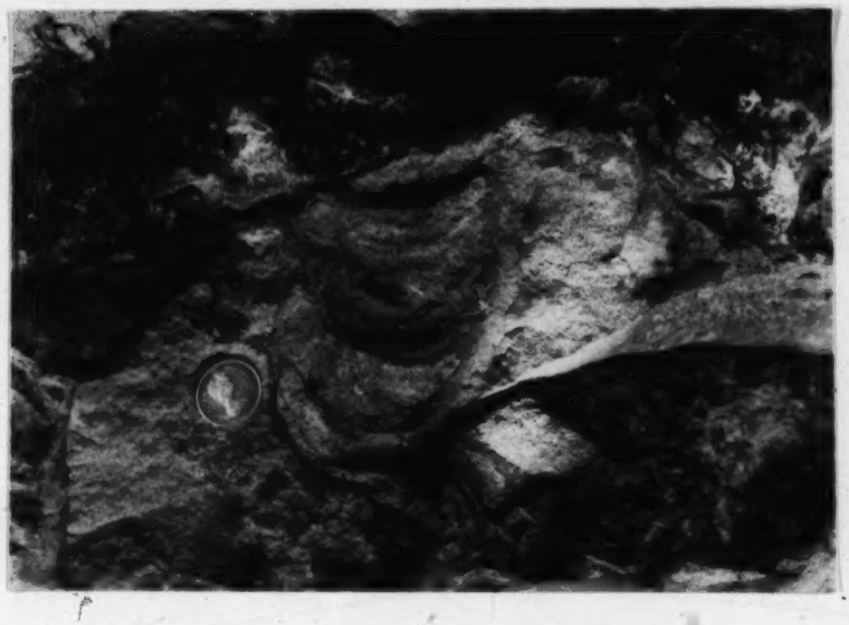

Figure 6. Rhizocorallium in sandstones of facies B.
Location: Unit 6 of Trap Creek section.

contact with facies D, H or G. Most of the sharp upper contacts with facies D and H are non-scoured and are due to differences in grain size, whereas those with facies G are scoured. However, some of the upper contacts of facies B are gradational to facies C.

Bioturbated/Distorted Sandstone Facies (C).

This facies consists of very fine- and fine- grained light gray (N7) and medium light gray (N6) to light olive gray (5Y6/1) sandstones whose primary sedimentary structures are partially or completely disturbed by either penecontemporaneous deformation or bioturbation or both (Figure 7). Following the definition proposed by Dott and Howard (1962) and used by Coleman and Gagliano (1965), the term distorted is used here in a purely descriptive sense, denoting all disturbed stratification, regardless of causal agent or agents. The sands are in general well sorted though in few places are muddy, especially at bases of occurrences; occasionally they are pebbly with mud and chert clasts, and grain sizes up to medium sand. They are carbonaceous with comminuted plant debris and coal fragments, and are micaceous. Slump structures, ball and pillow structures, load casts, turbated features, contorted lamination (especially near tops of occurrences), and bioturbation characterize these sands. Although most of the primary sedimentary structures are disturbed and at times completely destroyed, some of the sands still show some primary structures in the form of faint thick bedding to graded bedding and horizontal parallel lamination in their basal portions, and trough cross-lamination, minor trough cross-bedding, ripple cross-lamination and ripple marks (interference ripples). In some places there are intimate associations of distorted and undeformed layers, whereas in other cases there is interstratification of completely bioturbated homogenized sand layers and non-bioturbated horizontal laminated and ripple cross-laminated layers of 5 to 30cm thickness (Figure 8). These non-bioturbated sand layers show horizontal worm trails on their soles and tops, and a few very thin medium dark gray (N4) to olive gray (5Y4/1) carbonaceous shale partings and black carbonaceous laminae. They are mostly lenticular in form, though tabular shapes are common.

Individual occurrences range in thickness from 1.5 to 19 meters and may represent single episodes of deposition or a series of depositional episodes whose deposits are

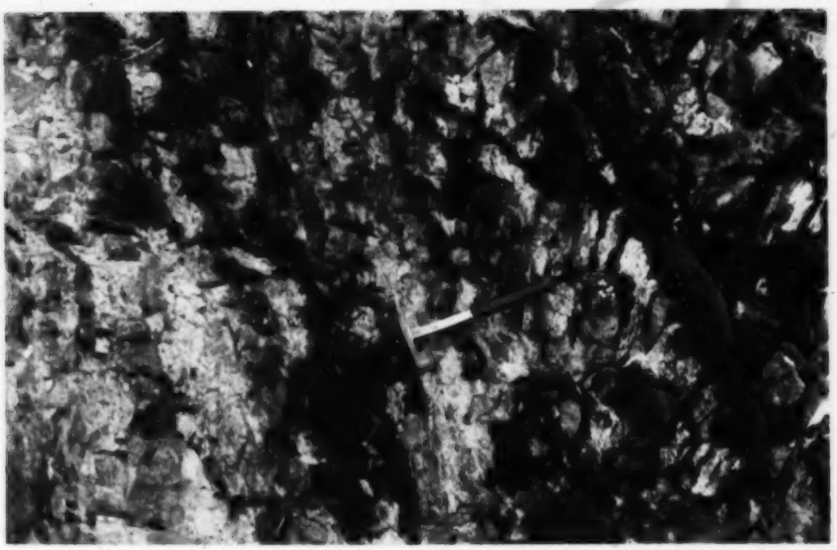

Figure 7a. Bioturbated sandstone of facies C; note the complete destruction of bedding. Location: Unit 10 of Oldman River section.

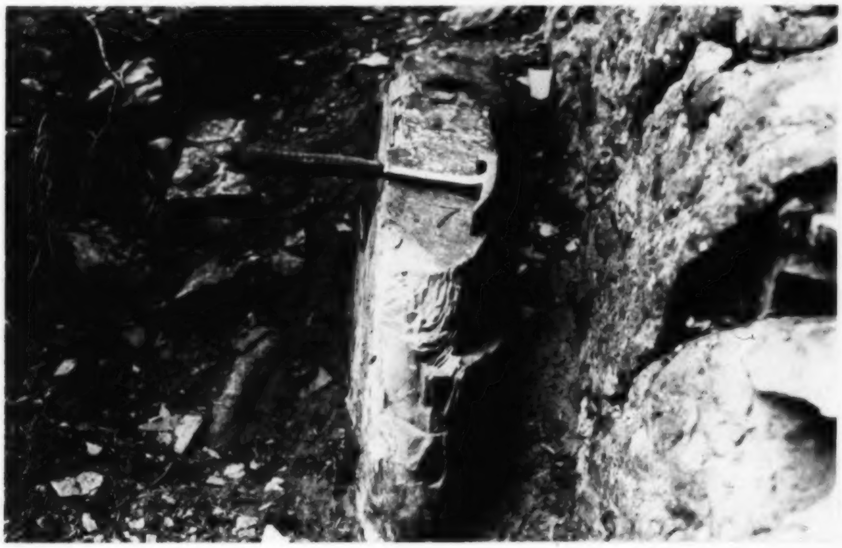

Figure 7b. Distorted sandstone of facies C; note the near horizontal fold axis of the intraformational recumbent fold. Location: Base of unit 7 of Trap Creek section.

Figure 7c. Deformed bedding common in facies C sandstones. Hammer for scale. Location: Within unit 7 of Trap Creek section.

Figure 8a. Interstratification of bioturbated homogenized (T) and non-bioturbated (N) sandstone layers of facies C. Note deformed bedding (arrow) at right which is common in facies C sandstones. Location: Unit 6 of Lundbreck section.

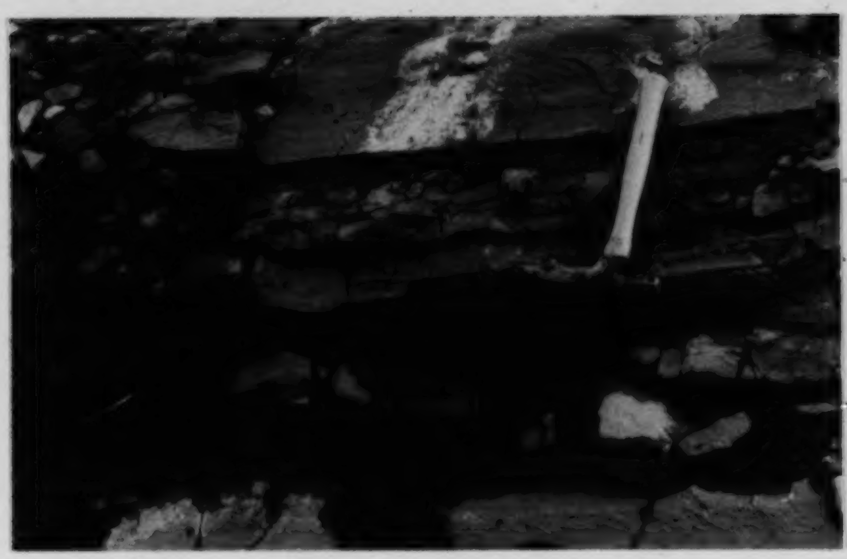

Figure 8b. Interstratification of bioturbated homogenized (T) and non-bioturbated (N) horizontal laminated sandstone layers of facies C. Note shallow scouring and troughing, and concentration of carbonaceous material (arrow).

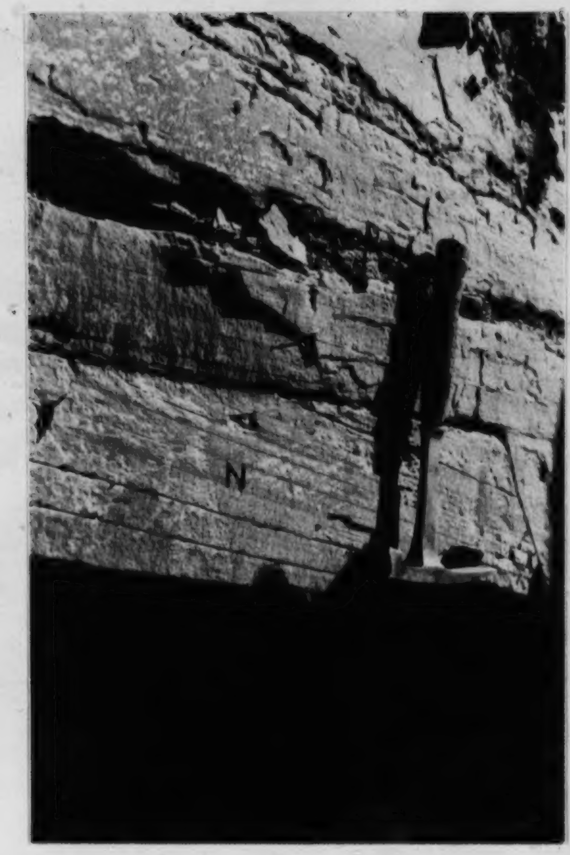

Figure 8c. Interstratification of bioturbated homogenized shaly sandstone layer (T) and non-bioturbated low-angle planar tabular cross-stratified sandstone layer (N) of facies C. Hammer for scale. Location: Unit 6 of Lundbreck section.

superimposed. The thinner (approximately 2 meters thick) occurrences show fining-upward characteristics and grading, sharp (sometimes scoured) lower contacts, usually gradational upper contacts and lenticular form. Preserved and recognizable sedimentary structures in these thinner occurrences are trough cross-lamination, ripple cross-lamination and a few low-angle cross-bedding in sets of 10 to 30cm thickness. These represent single episodes of deposition. The thicker occurrences (3 to 19 meters) are made up of superimposed subunits each of which, like the thinner occurrences, shows grading and fining-upward size gradient, becoming muddy (poorly sorted) in its upper portion. However, some of the subunits show coarsening-upward characteristics, being muddy and bioturbated in their basal portion, and better sorted and pebbly at the top with mud and chert clasts of up to 2.5cm maximum dimension; (e.g., unit 7 of the Trap Creek section). In other words, there are two levels of coarsening upward in some of these occurrences: the usual coarsening upward in the form of thicker sand layers upward in the occurrence; and increase in grain size and sorting upward within the subunits. Some of the sandstones are concretionary, especially at their top. Some have sharp, at times shallow scoured, lower contacts, though a few are gradational; usually gradational upper contacts with facies D or B; weathering is flaggy to slabby

The fossil assemblage includes Inoceramus fragments, Ammonites (Baculites) and Rhizocorallium.

It is pertinent to note that this facies is very variable in texture and sedimentary structures, and that these are a reflection of a combined effect of sedimentation processes and syndepositional deformation. Therefore, facies C does not strictly represent a sedimentation unit, but a combination of sedimentation and syndepositional deformation. The main differences between this facies (C) and facies B are:

1. more bioturbation in facies C than in facies B;
2. preponderance of syndepositional deformation structures in facies C; and
3. presence of a significant proportion of shale in facies B.

Horizontal to low-angle Cross-stratified Sandstone Facies (D).

This facies is composed of light olive gray (5Y6/1) to medium light gray (N6), very fine- and fine-grained horizontal to low-angle cross-stratified sandstones. Thicknesses range from 0.5 to 19.5 meters, with most of them in the range of 2 to 6 meters. They are mostly grossly lenticular and are in turn made up of lenticular horizontal lamina sets and low-angle cross-lamina and cross-bed sets of 2 to 50cm (usually 5 to 15cm) thickness separated by very thin carbonaceous shale partings. Most of the individual sand layers are characterized by sharp bases with or without sole marks and incipient load casts, horizontal lamination, low-angle trough cross-bedding and cross-lamination, abundant ripple cross-lamination, ripple marks (mostly linguoid ripples) and occasional hummocky cross-bedding and planar cross-lamination (Figure 9). Some of these sands are also graded. Horizontal worm trails are common on the soles and tops of these sands; a few beds show ball and pillow structures and contorted lamination, which is restricted to their bases. Interstratification of bioturbated and non-bioturbated sand layers with a few vertical escape worm burrows were observed in some instances, especially at the bases of the facies. The bioturbated sand layers are indicative of slow rates of deposition whereas the non-bioturbated layers with only a few vertical escape burrows indicate high rates of deposition. Although some of the thicker occurrences of this facies show coarsening-upward characteristics in the form of increases in the thickness of the sand layers and grain size (up to medium sand size) up through the occurrence, most show fining-upward characteristics in the form of decrease in sand bed thickness. But individual sand layers within both coarsening-upward and fining-upward occurrences typically show fining-upward size gradient, and are sometimes graded as well. In other words, there is an internal fining-upward characteristic of the sand layers irrespective of whether the entire occurrence is fining-upward or not. They are usually poorly sorted (muddy) in their upper portions, and at times pebbly (with chert and mud clasts) at their bases. The sandstones are carbonaceous with abundant black plant debris on the lamination planes, and with fossil wood fragments and impressions; also they are sparsely pyritic, micaceous, and usually calcite cemented.

The common sequence of sedimentary structures in the individual fining upward sand layers is: sharp base with or without sole marks; horizontal parallel lamination;

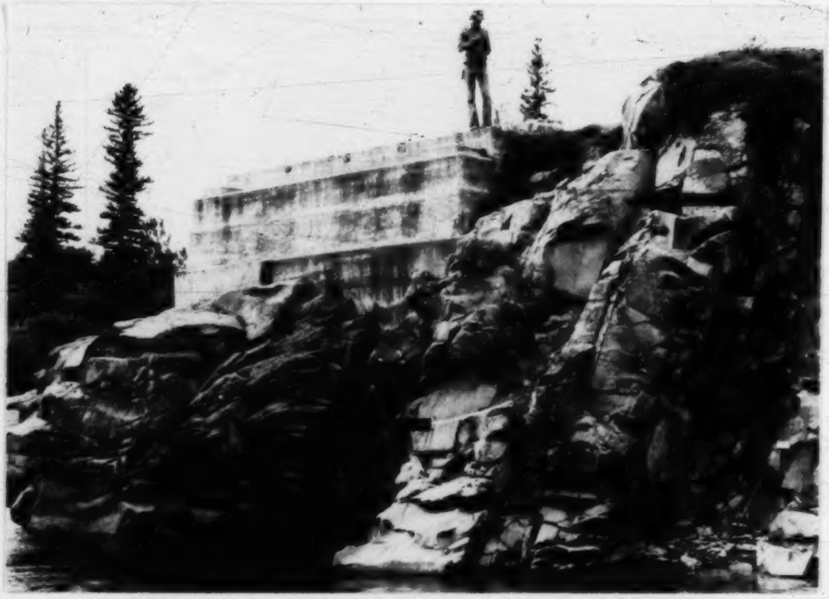

Figure 9a. Horizontal to low-angle cross-stratified sandstone facies (D). Note: 1) the lenticular form of the sand layers (arrows), 2) increase in sand layer thickness from bottom (right) to top (left), 3) sharp bases to the individual sand layers, 4) decrease to complete absence of shale partings (S) upward. Geologist is scale. Location: General view of Unit 9 of Trap Creek section.

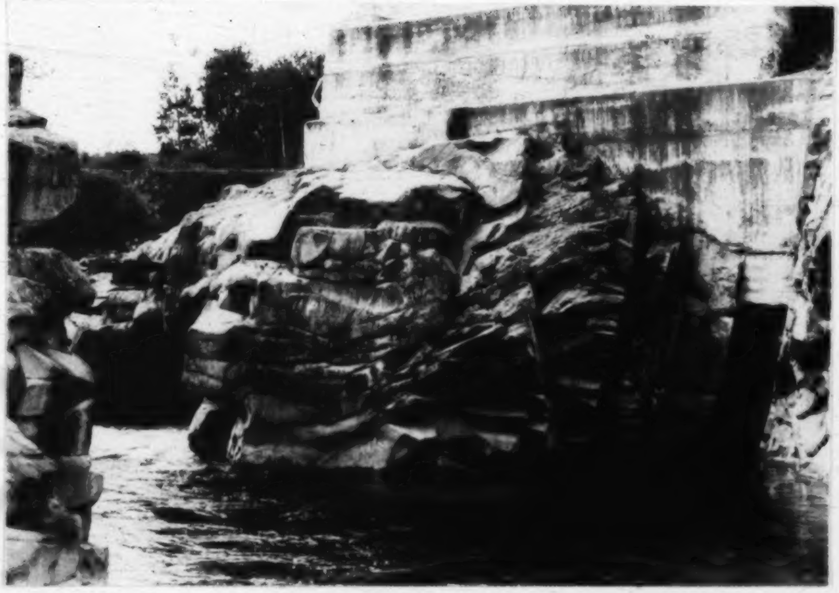

Figure 9b. Closeup of fig. 9a above. Note the lenticular form of the sand layers (arrows), and sequence of sedimentary structures as follows: sharp base, massive to horizontal bedding (M), low angle medium-to large scale cross-stratification (X), ball and pillow structure (P).

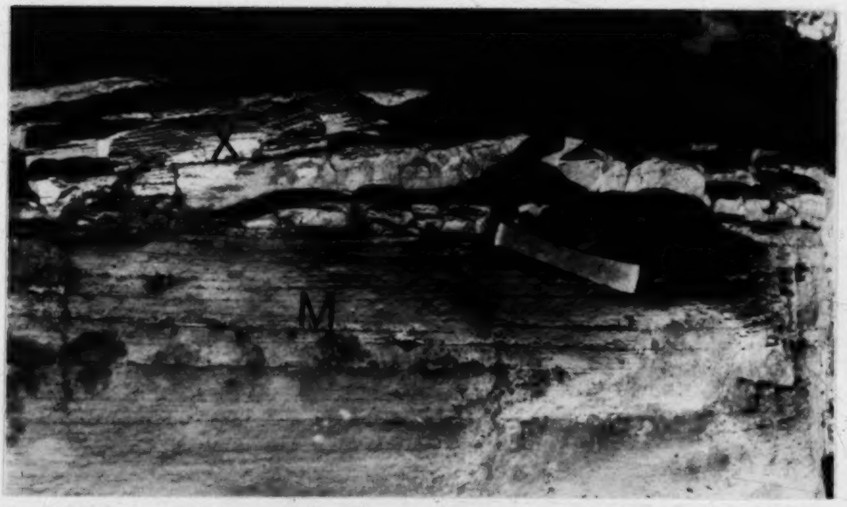

Figure 9c. Horizontal bedding (M) followed by low-angle cross-bedding (X) of facies D. Location: Approximately 12.5 m above base of Unit 9 of Trap Creek section.

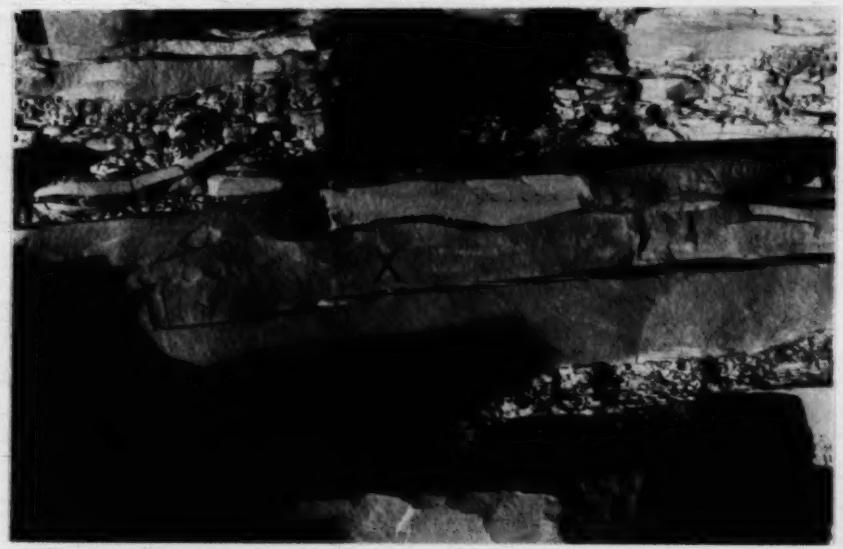

Figure 9d. Interstratification of clean horizontal laminated and ripple cross-laminated sandstone (X) and bioturbated shaly sandstone (T) layers of facies D. Location: Unit 2 of Lundbreck section.

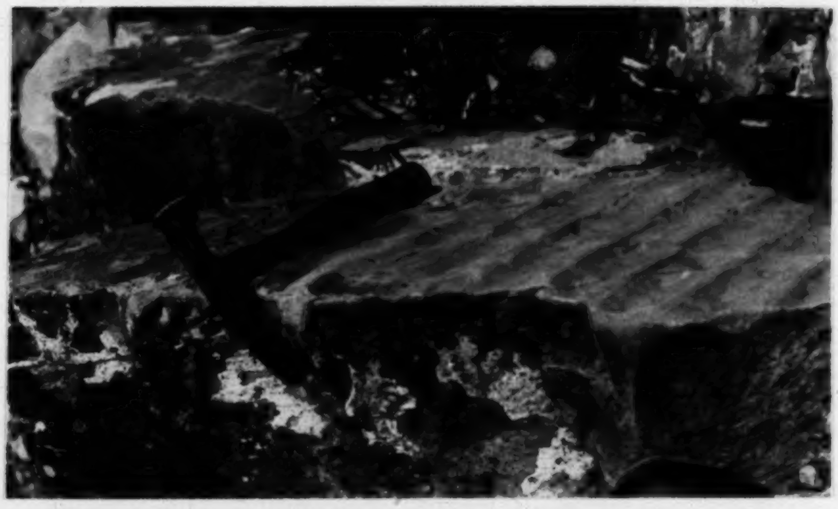

Figure 9e. Symmetrical straight crested ripples on the upper surface of a sandstone bed of facies D. Location: Approximately 1 m above base of Unit 9 of Trap Creek section.

Figure 9f. Interference ripples on a bedding plane of facies D sandstone. Arrow indicates direction of the lee side of ripple. Location: Approximately 1 m below top of Unit 9 of Trap Creek section.

low-angle small-scale trough cross-bedding and trough cross-lamination; ripple cross-lamination; indistinct (irregular) cross-lamination and ripple marks at the top of beds (Figure 10). Most of the sand layers of the thicker coarsening-upward occurrences have distorted "horizontal" laminated and loaded basal portions but well preserved small- to medium-scale low-angle trough cross-bedded and cross-laminated tops; they display a tabular form in outcrop in contrast to the lenticular sand layers of the upward-fining occurrences. They are usually coarser grained (medium to fine sand) with chert and mud clasts scattered throughout their lower portions or concentrated along definite bands of 3 to 5cm thickness, better sorted and have shallow-scoured lower contacts. The fossil assemblage of this facies includes an Ammonite (Baculites), Rhizocorallium, non-discrete horizontal burrows and trails and a few vertical escape burrows.

Most of the occurrences have sharp, non-scoured or gradational lower contacts and gradational upper contacts with facies B, C, or E, though scoured lower contacts are common among the coarser medium-grained sandstones.

Coaly Mudstone Facies (E).

This facies consists of coaly and carbonaceous olive gray (5Y4/1) to dark greenish gray (5GY4/1), and light olive gray (5Y6/1) to greenish gray (5GY6/1) mudstones. These are silt and clay sized, non-fissile massive rocks characterized by blocky and irregular fractures. Individual mudstones range from 0.5 to 19.0 meters thick but are mostly in the range of 1.5 to 10 meters, exhibit lenticular or tabular form in outcrop, and weather rubbly. They are sandy, and in few instances the sand forms irregular "lumps", lenses and very thin layers (15cm maximum). The mudstone is concretionary toward the top, with carbonate and iron oxide concretions of up to 30cm maximum diameter. Occasionally very thin coal beds (2 to 4cm thick) are encountered, especially near the less sandy tops. However, most of the time the carbonaceous plant material is disseminated throughout the mudstone giving it a darker color (medium dark gray (N4) to dark gray (N3)) and a more fissile shaly character; in contrast, lightening of color to greenish gray (5GY/1) and light olive gray (5Y6/1) is common in the soapy-feeling bentonitic varieties. Fossil wood fragments, carbonized rootlets and coal fragments are the main evidence of organic

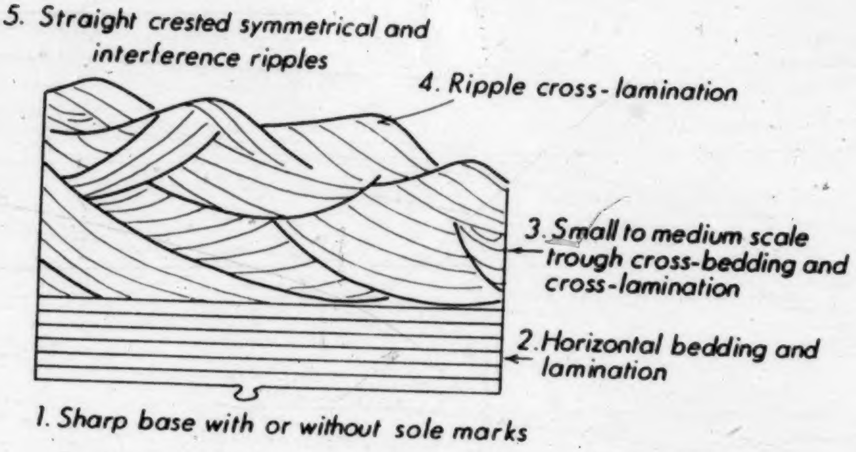
5. Straight crested symmetrical and interference ripples
4. Ripple cross-lamination
3. Small to medium scale trough cross-bedding and cross-lamination
2. Horizontal bedding and lamination
1. Sharp base with or without sole marks

Figure 10a. Schematic idealized sequence of sedimentary structures typical of sandstone beds of facies D.

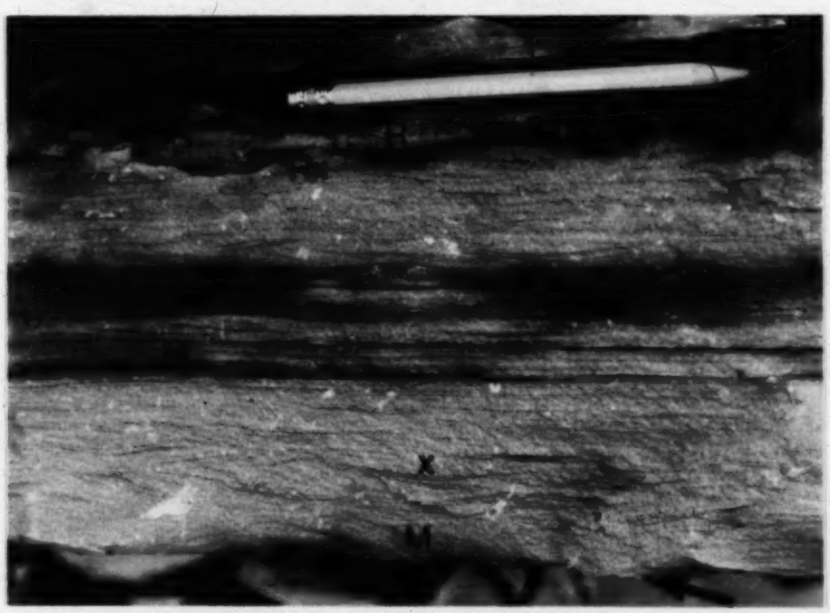

Figure 10b. Sequence of sedimentary structures common within sandstone beds of facies D. Note the sharp base (arrow), intimate association of small-scale trough cross-lamination (X), ripple cross-lamination (RX), horizontal lamination to massive bedding (M) and ripples (R).
Location: Unit 4 of Lundbreck section.

activity as the mudstone is rarely bioturbated.

Individual occurrences have gradational lower contacts with facies D, G, or H whereas their upper contacts with facies G or H are scoured and often irregular due to soft sediment deformation prevalent in the more concretionary upper parts; as well, gradational upper contacts with facies F are not uncommon.

Interstratified Mudstone/Sandstone Facies (F).

This facies is composed of interbedded very-fine and fine-grained sandstones and carbonaceous mudstones (Figure 11). Single occurrences range from 1 to 23 meters thick with most in the range of 1 to 10 meters.

The mudstones are olive gray (5Y4/1) to dark greenish gray (5GY4/1) and medium dark gray (N4) to dark gray (N3), though light olive gray (5Y6/1) and greenish gray (5GY6/1) are also common. They occur in beds of 10 to 50cm and constitute 40 to 80 percent of an individual facies occurrence. They are sandy (poorly sorted), bentonitic, concretionary and occasionally very carbonaceous to coaly with coal beds up to 10cm thick with carbonized rootlets. The mudstones are generally massive and structureless, though occasionally slightly fissile with a darkening in color due to increase in carbonaceous matter. They weather blocky to rubbly and are in most respects similar to mudstones of facies E.

The interstratified sandstone layers are 4cm to 0.75 meter thick, but mostly in the range of 5 to 30cm. They are horizontal parallel laminated, trough cross-laminated and ripple cross-laminated; occasionally planar cross-laminated, wavy laminated, and contorted laminated. They are characterized by sharp bases which may or may not be loaded, and are lenticular or tabular in form. In most cases, especially in the thinner (less than 30cm thick) tabular sand layers, the sharp bases are due to differences in grain size and color between the sand layers and the interstratified mudstones; they rarely show incipient load casts, which are common on the thicker (greater than 30cm thick) lenticular sand layers. Some of these thicker, lenticular sandstones also show very shallow scouring. In some instances, however, the sand components do not form distinct layers, rather they form irregular to lensoid sand masses chaotically distributed within the

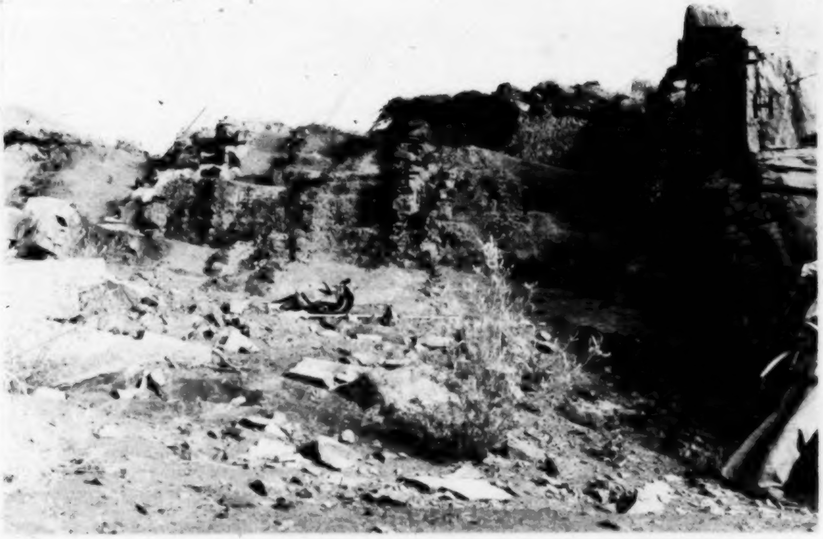

Figure 11a. Interstratified mudstone/sandstone facies (F). Note sharp, loaded upper contact with facies H (arrow) to the right. Location: Unit 13 of Sheep River section.

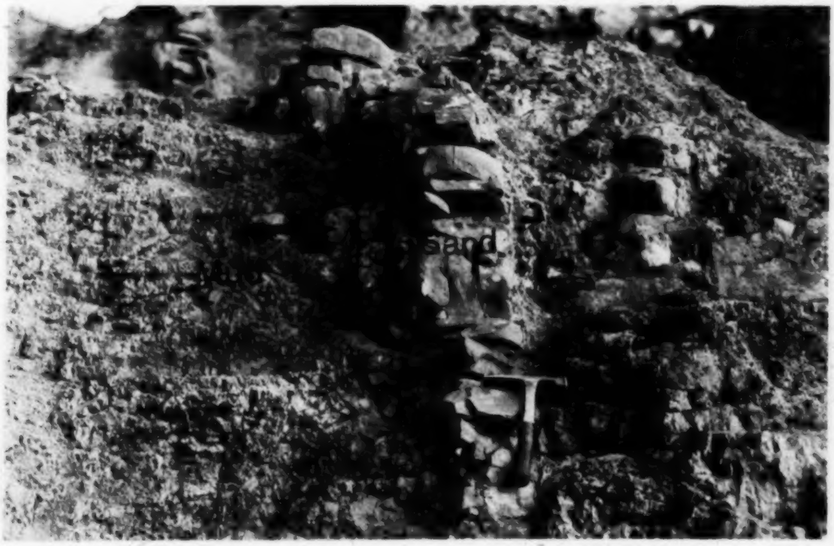

Figure 11b. Interstratified mudstone/sandstone facies (F). Closeup of figure 11a above. Note the loaded base (arrow) of the sandstone layer. Location: Unit 13 of Sheep River section.

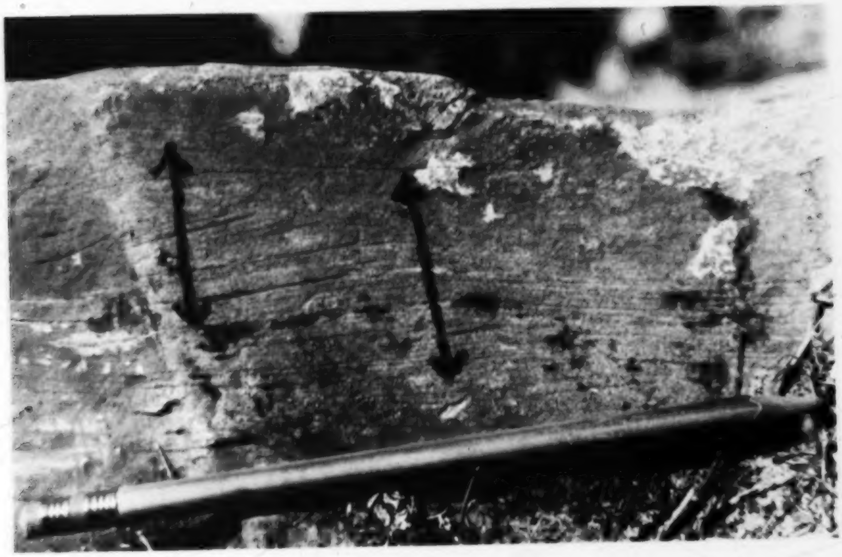

Figure 11c. Ripple cross-lamination common in facies F sandstones. Double arrows show axes of the ripples. Location: Top sandstone layer of Unit 22 of Trap Creek section.

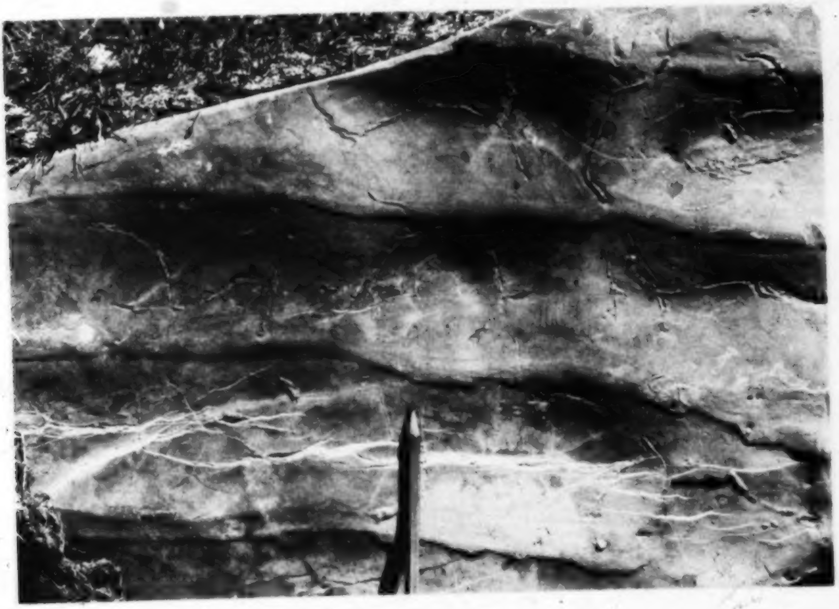

Figure 11d. Asymmetrical ripple marks on top of the top sandstone layer of Unit 22 of Trap Creek section (Fig. 11c). Note horizontal worm trails that have been partially replaced by calcite (arrow).

mudstone, resulting in a sort of linsen structure or lenticular bedding, i.e. sand lenses in a mudstone matrix . The sandstone layers are medium gray (N5) to dark greenish gray (5GY4/1), and light olive gray (5Y6/1) to greenish gray (5GY6/1), though other shades of gray are common. They are poorly sorted (muddy), carbonaceous with abundant plant debris and black organic laminae, micaceous, occasionally concretionary, and fine upward to the associated mudstones.

Large fossil wood fragments and impressions, and oysters found in one of the mudstone layers of the Drywood River section constitute the fossil component of this facies.

Whereas most of the occurrences are homogeneous with respect to the distribution of the mudstone and sandstone components, some show a coarsening-upward characteristic in the form of increase in the sand content and sand layer thickness. Still, a few occurrences exhibit some overall fining-upward characteristic, being sandier in the basal portions of the units than at their tops where they merge imperceptibly into facies E; these are probably more distal to the source of the coarse sediment input than the upward coarsening settings. Gradational basal contacts with facies G or H are usual, though sharp non-scoured lower contacts with facies E are common. Sharp and often scoured upper contacts with facies G or H is the rule, but occasionally facies F grades into facies E.

Scour-based High-angle Cross-stratified Sandstone Facies (G).

This facies consists of scour-based, medium- to large-scale, high-angle (greater than 10 degrees but mostly between 10 and 20 degrees), trough cross-bedded and cross-laminated, planar cross-bedded and cross-laminated, and ripple cross-laminated sandstones; and occasionally, massive sandstones (Figure 12). Individual occurrences range from 1 to 30 meters thick but are mostly in the range of 2 to 10 meters, and are lenticular in form. Cross-bed and cross-lamina sets ranging from 0.1 to 0.6 meter thick, and mostly wedge-shaped, are stacked on top of each other. In most cases, sets of cross-strata are separated by scours (upto 20cm deep) into lenticular cosets (subunits). These cosets range from 0.75 to 2.5 meters and average 1.5 meters (Figure 13). In a few

Figure 12. Scour-based high-angle cross-stratified sandstone facies (G). Note the scouring (SS) into facies E, minor shallow scouring (channelling) within facies G, and lenticular shape of the facies G sandstone. Geologist in foreground for scale. Location: James River section.

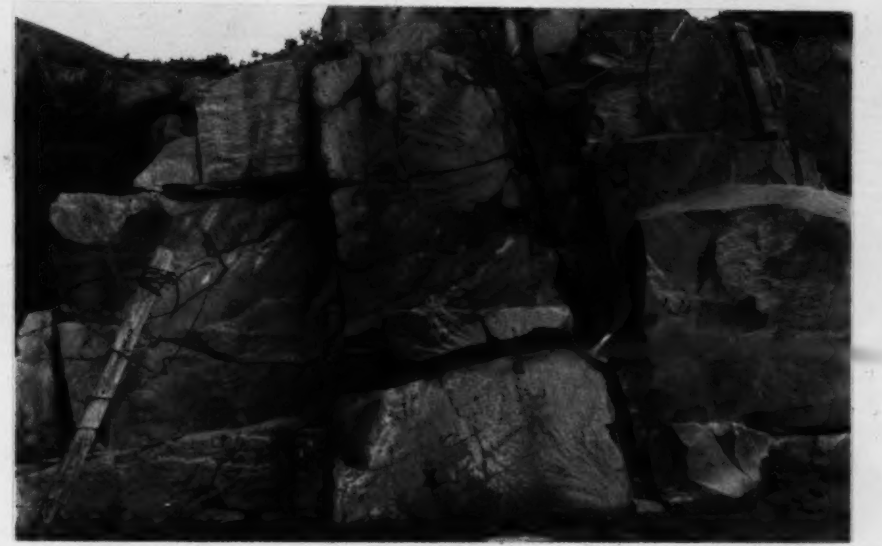

Figure 13. Multistorey channel sandstone with shallow minor channels (scours, S) within facies G sandstone. Note the lenticular form of each subunit and the trough cross-bedding (X) revealed by weathering of an otherwise massive to thick bedded sandstone. Location: Unit 10 of Sheep River section.

instances, however, occurrences consist only of single upward fining units. Horizontal lamination, ripple cross-lamination and rippled surfaces are common in the finer uppermost portions, whereas occasionally planar cross-stratification consisting mostly of single to a few isolated sets are sandwiched within the main body of the unit. Load casts, flute casts, and pseudonodules are not uncommon in some of the thick multiple cosets.

The definition of the cross-beds and cross-bed sets is variable from one occurrence to another and even within the same occurrence. It is dependent on the presence or absence of darker finer partings in the form of dark gray carbonaceous shale partings and black carbonaceous laminae. In some instances it is very clear whereas in others it is faint, especially in the basal portions of some occurrences, giving the casual observer the impression that the sandstone is completely massive. In most case, however, the cross-bed sets are separated by dark gray carbonaceous shale partings, and some of the individual cross-beds show internal lamination, thereby further improving their definition. There is usually a decrease in the scale of the sedimentary structures from base to top of each coset (subunit), but not necessarily from bottom to top of the whole unit. Hence, the cross-bed set thickness in most occurrences is similar, and decreases upward usually only in the uppermost coset.

The general sequence of sedimentary structures in a coset of strata typical of this facies is: coarse to pebbly, massive to faintly horizontal bedding and poorly defined trough cross-bedding overlying a scoured surface; well defined trough cross-bedding and cross-lamination; occasional planar cross-stratification; ripple cross-lamination, and ripple marks.

The sands are light gray (N7) to medium gray (N5), and light olive gray (5Y6/1) to greenish gray (5GY6/1) and dark greenish gray (5GY4/1), medium- to fine-grained, and occasionally coarse-grained. They are often pebbly with chert and mudclast pebbles of 1.5 cm maximum dimension. The pebbles are usually concentrated at the bases of the occurrences, on the scour surfaces and shallow channels that separate the cosets, and at bases of troughs, but are sometimes scattered throughout the basal massive to crudely horizontal and cross-bedded 0.5 meter. In a few instances, mud and chert pebble conglomeratic sandstones 20 to 30 cm thick, and thinner matrix-supported conglomerates, were observed. They are moderate to well sorted, carbonaceous with communited plant debris and coal fragments, micaceous, and mostly kaolinite cemented. Grain size and sorting slightly decrease upward in each coset, but decrease significantly in the uppermost, usually poorly sorted, coset of most occurrences. Thus there is an obvious fining upward size gradient in the uppermost coset of the multiple coset occurrences, and in the single coset occurrences. But within the cosets of multiple coset occurrences, fining upward size gradient is less distinct and at times non-existent; still, each coset is separated from the next by a thin (usually less than 15 cm) finer olive gray (5Y4/1) to dark greenish gray (5GY4/1) shale or mudstone parting. As a general rule, therefore, there are two levels of fining upward of grain size namely:

1. a subtle fining upward within each coset of beds (subunit), and
2. a more obvious one for each entire occurrence (unit).

The lower contacts are invariably scoured into facies E, and are occasionally associated with incipient load casts, large fossil wood fragments and impressions, and pseudonodules resulting from the foundering of sand layers into facies E mudstones. Their upper contacts are usually gradational, the coarse- to medium-grained well sorted sands grading through the muddy, often very carbonaceous and concretionary sands of the uppermost cosets to facies E or F.

Load-structure-based Cross-stratified Sandstone Facies (H).

This facies comprises load-structure-based, small- to medium-scale cross-stratified sandstones (Figure 14). Overall shape is lenticular or tabular ranging in thickness from 0.2 to 5.5 meters, but mostly in the range of 0.5 to 2.0 meters. Trough cross-bedding and cross-lamination, ripple cross-lamination, plus occasional horizontal and massive bedding characterize these sands. Occurrences are made up of single or multiple depositional units. The thicker (greater than 0.75 meter) lenticular units are composed of horizontal beds and wedge-shaped cross-bed and cross-lamina sets of 0.1 to 0.5 meter thickness separated by carbonaceous shale partings. In these thicker sand layers, cross-bed and cross-lamina set thicknesses decrease upward with an increase in their frequency and in carbonaceous shale partings. The thinner tabular (less than 0.75 meter) sand layers consist of horizontal lamina sets, and trough- and ripple cross-lamina

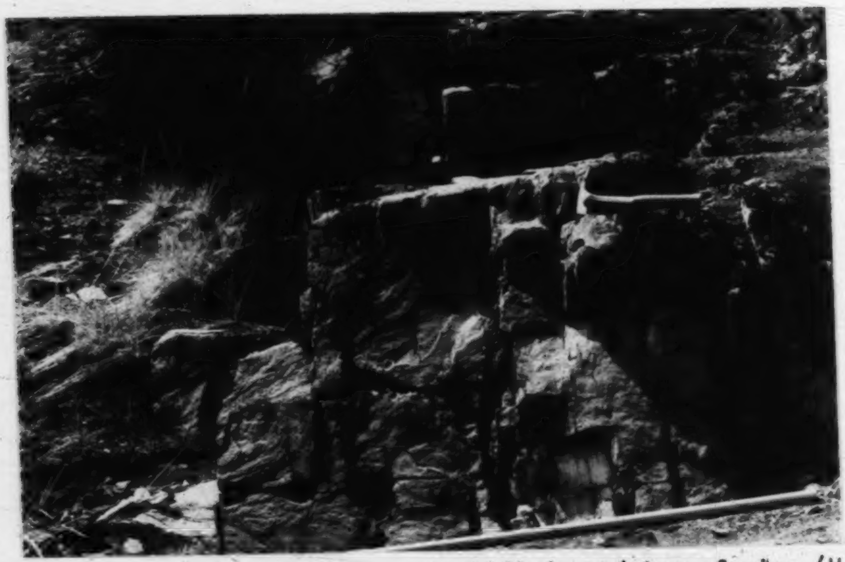

Figure 14a. Load-structure-based cross-stratified sandstone facies (H). Location: Unit 4 of Sheep River (Turner Valley) section.

Figure 14b. Typical base of facies H sandstone; note the large load cast and the crumpling of the underlying very carbonaceous mudstone of facies E. Location: Unit 6 of Sheep River section.

sets of 0.1 to 0.25 meter thickness separated by many carbonaceous shale and mudstone partings. In most instances, however, these thinner varieties are superimposed to form a thickness of up to 4 meters, just as a couple of the thicker lenticular varieties are superimposed to form thicknesses of up to 5 meters. The thicker varieties have a greater tendency to occur singly with individual thicknesses of up to 1.5 meters on the average. Contorted lamination, wavy to irregular laminations, flow structures, and large load casts are very common in the basal portions of the sandstones, though they are most spectacular in the thicker lenticular ones.

The general sequence of sedimentary structures in the thicker lenticular sand layers is as follows: loaded base in the form of undulating structures involving the sand and the underlying carbonaceous mudstone or shale, and large load casts that in some cases have diameters of up to 0.3 meter (Figure 14); horizontal bedding and lamination; trough cross-bedding and cross-lamination; ripple cross-lamination and ripple marks. The sequence in the thinner sand layers is: loaded base in the form of undulating structures and numerous small load casts; horizontal lamination; ripple cross-lamination and a few trough cross-laminations; ripple marks. It is pertinent to note that in some of the occurrences with thin tabular sand layers, the individual sands have sharp non-scoured bases which are due to grain size and color contrasts between them and the underlying mudstones, but show numerous flow structures. In some other cases, the sand layers are very much deformed into irregularly laminated lumpy masses.

The sands are medium light gray (N6) to dark gray (N3), and greenish gray (5GY6/1) to dark greenish gray (5GY4/1), fine- to very-fine grained, occasionally medium-grained and pebbly with mudclast pebbles. They are poorly sorted (muddy), carbonaceous, micaceous and concretionary, especially near their tops. They show fining upward size gradient especially in the thicker lenticular ones; in some instances two or more upward fining lenticular sand layers are superimposed on each other with about a 30 cm thick olive gray (5Y4/1) carbonaceous mudstone between them.

Large fossil wood fragments and impressions, comminuted plant debris, black organic laminae, coal fragments, rootlets and horizontal trails on the upper surfaces of the sands are very common in this facies. The facies usually has sharp non-scoured loaded bases and gradational upper contacts with facies E or F. Despite thickness and geometric variations of the individual sand layers within this facies, all occurrences are characterized by :

1. loaded base,
2. fining upward grain size and decreasing scale of cross strata within the sand layers (subunits),
3. poor sorting, and
4. significant numbers of flow structures.

Scoured Surface Facies (SS).

This facies consists of mudclast-strewn erosional surfaces that are invariably overlain by the high-angle cross-stratified sandstones of facies G (Figure 15). They occur at the bases of facies G, as well as within it. The maximum depth of erosion observed at the base of facies G was 2.0 meters; most is between 1.0 and 1.5 meters. Overlying the erosion surface, the mixture of pebble-sized mudclasts and coarse-grained, massive to faintly horizontally bedded sandstone reaches a maximum of 20 cm. The minor scoured surfaces within facies G are shallower in depth, usually less than 10 cm, and contain thinner deposits of mudclasts and coarse-grained massive to faintly horizontally bedded sandstone.

B. Facies Sequence: Markov Chain Analysis

Because some of the lithofacies defined in the field are liable to various interpretations when treated singly and in isolation (Walker, 1979), there is a need to incorporate their preferred stratigraphic sequence of occurrence in their interpretation. This was achieved by subjecting the lithofacies data of the fourteen measured and described stratigraphic sections of the Belly River Formation to "embedded" Markov chain analysis. The data of each stratigraphic section were analyzed separately, and then pooled and analyzed together.

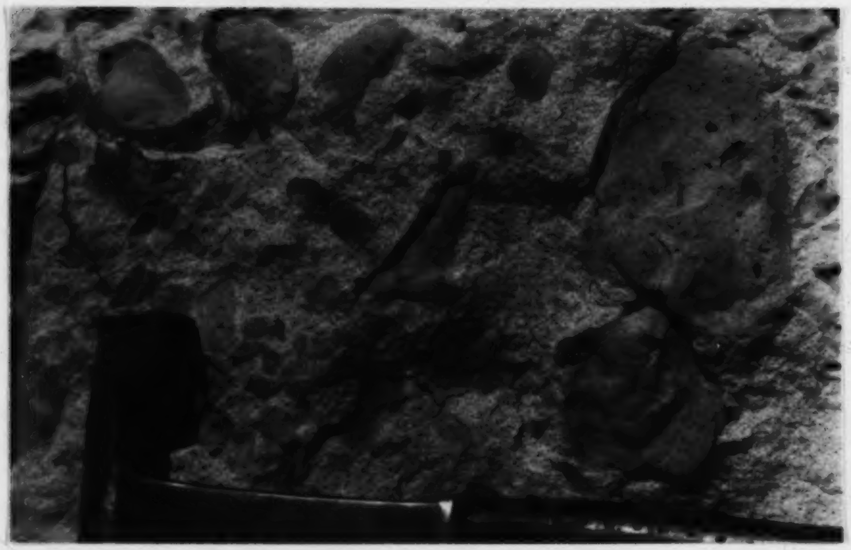

Figure 15. Plan view of scoured surface with mudclasts (facies SS). Location: Base of Unit 11 of Trap Creek section.

The rationale behind Markov chain analysis, especially as it is applied to stratigraphic studies, has been aptly expounded by Selley (1970), Miall (1973), Cant and Walker (1976) and Walker (1979). Earlier papers on Markov chain analysis include those of Anderson and Goodman (1957), Billingsley (1961), Krumbein (1967, 1968), Krumbein and Dacey (1969), Dacey and Krumbein (1970) and Gingerich (1969), among others. Selley (1970) described the technique of Markov chain analysis and applied it to four studies of sequence in sediments. He found that the probability of one lithology overlying another in a section is a function of their frequency (i.e., the number of times that they occur) and the 'memory' of the depositional process. Based on these studies, he, as well as Miall (1973) and Walker (1979), demonstrated that certain sedimentary successions such as the coal measure cyclothems and fluvial fining-upward cycles were laid down under the control of Markovian processes. A Markovian process is one 'in which the probability of the process being in a given state at a particular time may be deduced from knowledge of the immediate preceding state' (Harbaugh and Bonham-Carter, 1970, p.98).

Markov chain analysis therefore helps to describe the stratigraphic succession and hence the depositional process statistically. In essence, it consists of:

1. erection of a transition count matrix (a two-dimensional array of all possible vertical lithologic transitions),
2. tabulation of transition probability matrix,
3. tabulation of independent trial probability matrix,
4. erection of difference matrix, and
5. a test of significance of the resulting difference matrix (Selley, 1970; Walker, 1979).

This analytical technique helps to condense the stratigraphic section into a manageable size, i.e., it results in the simplification of the stratigraphic section and the facies relationships. It brings out the essentials of the section, detects cyclicity if present, and allows comparison of the section with established facies models. It helps to understand the vertical arrangement of facies in a sequence in an attempt to diagnose environments (Selley, 1970, p.558). In other words, it finally leads to a detailed and accurate interpretation of a sequence of lithologies (stratigraphic succession) in terms of depositional processes and environments.

In summary, Markov chain analysis objectively defines relationships in sediments, and detects facies transitions which occur more often than one would expect were they interbedded with one another at random. It is these transitions which are mostly considered when interpreting the sedimentary environments and processes responsible for the strata studied (Selley, 1970).

The approach used in the present study incorporates elements of those of Selley (1970), Miall (1973), Gingerich (1969), Cant and Walker (1976), Walker (1979), Moore (1979), and Hein (1979). Three matrices (observed transition probability, random probability and difference probability) were calculated from the transition count matrix using the following formulae:

1. $P_{ij} = f_{ij}/S_i$

   where P_{ij} is the observed transition probability of i being followed by j, f_{ij} is the number of transitions of i to j, S_i is the row total (Miall, 1973).

2. $r_{ij} = n_j/N - n_i$

   where r_{ij} is the random probability of transition from facies i to facies j, n_i and n_j are the number of occurrences of facies i and j respectively, and N is the total number of occurrences of all facies (Walker, 1979).

This formula is preferred to Miall's (1973) formula ($r_{ij} = S_j/t - s_i$) because most of the stratigraphic sections of the present study contain covered intervals.

3. $d_{ij} = P_{ij} - r_{ij}$

   where d_{ij} is the difference between observed probability (P_{ij}) and the random probability (r_{ij}) (Miall, 1973; Cant and Walker, 1976; Walker, 1979).

The transition count matrix records the observed and tallied upward transitions of the facies, i.e., the raw facies sequence; the observed probability matrix records the probabilities of the observed transitions whereas the random probability matrix records the probabilities assuming the facies were in a random sequence, i.e., assuming the same abundance of facies but in a random sequence. The difference matrix shows the observed minus random probability values; it highlights those facies transitions that have a higher or lower probability of occuring than if the sequence were random (Cant and Walker, 1976).

The transition count matrices, calculated observed transition probability matrices, random probability matrices and difference matrices, as well as the resultant Facies Relationship Diagrams (F.R.Ds) (Appendix B) for the individual stratigraphic sections were constructed . A composite transition count matrix is derived by combining all the transition counts from the fourteen stratigraphic sections (Table 3). It records a total of 406 transitions, and 434 states (Table 4). The data of this combined transition count matrix were subjected to Markov Chain analysis in a manner similar to those of the individual stratigraphic sections above. Tables 5, 6, 7, show the calculated observed transition probability matrix, random probability matrix, and difference matrix respectively.

Chi-square statistic, after Billingsley (1961), was applied to test the hypothesis that either the successive facies are the results of an independent (random) process or, if not resulting from an independent process, they could form a Markov chain. Chi-square value of 576.7 is significant at the 99.5 percent confidence level (Table 7b), indicating that the interbedded constituent facies of the basal Belly River sequence follow a Markovian rather than random order. Their deposition is therefore Markovian, i.e., due to a process with a 'memory'.

The difference matrix (Table 7) shows which transitions occur more, and which occur less frequently than if the facies were in a random sequence. In other words, it shows some values are relatively high-positive (transitions much more common than if facies were random) and others are high-negative (transitions much less common than random). The relatively high-positive values of the difference matrix is used to draw a simplified facies relationship diagram (F.R.D) (Figure 16) that shows the transitions that occur more frequently than random. This is in essence an idealized/generalized facies sequence (preferred facies sequence) and therefore a local summary for the Belly River Formation of the study area. A study of the individual FRDs (Appendix B) and the composite FRD (Figure 16) shows:

1. that the individual FRDs are similar to one another and to the composite FRD,
2. that the composite FRD shows two distinct major facies assemblages represented by (a) A,B,C,D and (b) SS, G, F,H,E; and four minor facies associations represented by A,B,C,D; SS; G; and F,H,E, and
3. that most of the FRDs of the individual stratigraphic sections (See Appendix B)

Table 3. Composite transition count matrix (observed number of transitions between facies) derived from all the fourteen stratigraphic sections combined.

	A	B	C	D	E	F	G	H	SS	Row Total
A		6	1	1	1	2		4		15
B	2		5	9	1	2		2	7	28
C		4		4		1			1	10
D	2	5	4		3	2			3	19
E	2					16	2	10	25	55
F		1		2	2		3	14	47	69
G	1	1		1	29	42		1	2	77
H	3	2			21	6			2	34
SS			2	1			91	5		99
Column Total	10	19	12	18	57	71	96	36	87	
Grand Total										406

Table 4. Summary statistics of the number of occurrences of the different lithofacies in all the fourteen stratigraphic sections combined.

Lithofacies	Total number of occurrences
A	17
B	27
C	12
D	22
E	55
F	72
G	92
H	39
SS	98
Total occurrrences (states) of the various facies	434

Table 5. Observed transition probability matrix (observed transition probabilities).

	A	B	C	D	E	F	G	H	SS
A		0.4	0.07	0.07	0.07	0.13		0.27	
B	0.07		0.18	0.32	0.04	0.07		0.07	0.25
C		0.4		0.4		0.1			0.1
D	0.11	0.27	0.21		0.16	0.11			0.16
E	0.04					0.29	0.04	0.18	0.46
F		0.02		0.03	0.03		0.04	0.20	0.68
G	0.01	0.01		0.01	0.38	0.55		0.01	0.03
H	0.09	0.06			0.62	0.18			0.06
SS			0.02	0.01			0.92	0.05	

Table 6. Random probability matrix (transition probabilities for random sequence).

	A	B	C	D	E	F	G	H	SS
A		0.07	0.03	0.05	0.13	0.17		0.09	
B	0.04		0.03	0.05	0.14	0.18		0.10	0.24
C		0.06		0.05		0.17			0.23
D	0.04	0.07	0.3		0.13	0.18			0.24
E	0.05					0.19	0.24	0.10	0.26
F		0.08		0.06	0.15		0.25	0.11	0.27
G	0.05	0.08		0.06	0.16	0.21		0.11	0.29
H	0.04	0.07			0.14	0.18			0.25
SS			0.04	0.07			0.27	0.12	

Table 7a. Difference probalility matrix (observed minus random transition probabilities).

	A	B	C	D	E	F	G	H	SS
A		0.33	0.04	0.02	-0.06	-0.04		0.18	
B	0.03		0.15	0.27	-0.1	-0.11		-0.03	0.01
C		0.34		0.35		-0.07			-0.13
D	0.07	0.20	-0.09		0.03	-0.07			-0.08
E	-0.01					0.1	-0.2	0.08	0.2
F		-0.06		-0.03	-0.12		-0.21	0.09	0.41
G	-0.04	-0.07		-0.05	0.22	0.34		-0.1	-0.26
H	0.05	-0.01			0.48				-0.19
SS			-0.02	-0.06			0.65	-0.07	

Table 7b. Chi-square statistics to test the significance of facies transitions.

Test equation	X^2	Degrees of freedom	Limiting value at 99.5%
Billingsley (1961)	576.7	41	66.8

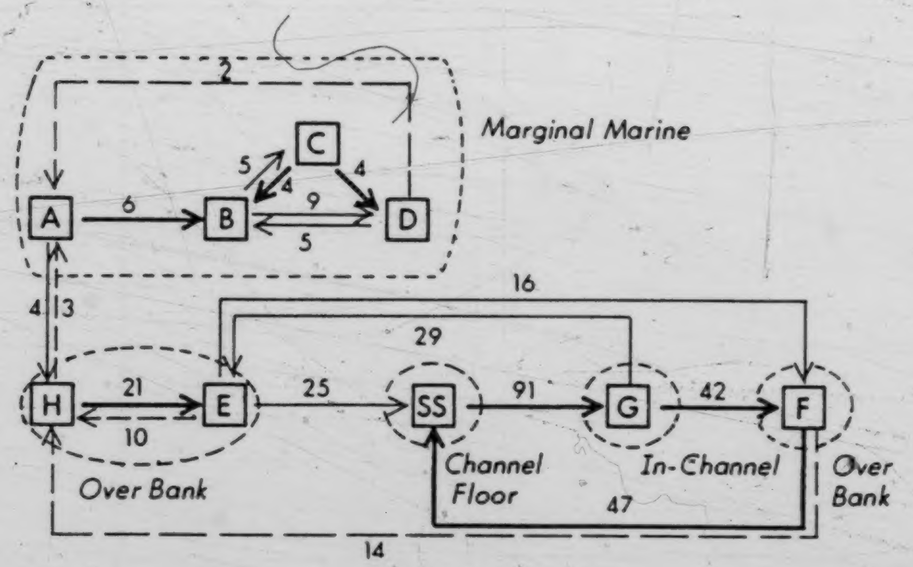
Marginal Marine
A
B
C
D
2
6
5
4
4
9
5
4
3
16
29
H
E
SS
G
F
21
10
25
91
42
47
14
Over Bank
Channel Floor
In-Channel
Over Bank

Figure 16a. Composite simplified facies relationship diagram for the basal Belly River Formation. Diagram is based on transitions that occur more commonly than random and show only transitions whose observed-minus-predicted (random) transition probabilities exceed 0.05. Thin, dashed arrows show probabilities in the range 0.05 to 0.10; thin unbroken arrows, 0.10 to 0.30; thick arrows, >0.3. Numbers above or beside the arrows indicate the number of transitions observed. Four facies associations have been recognized, interpreted and circled on the diagram.

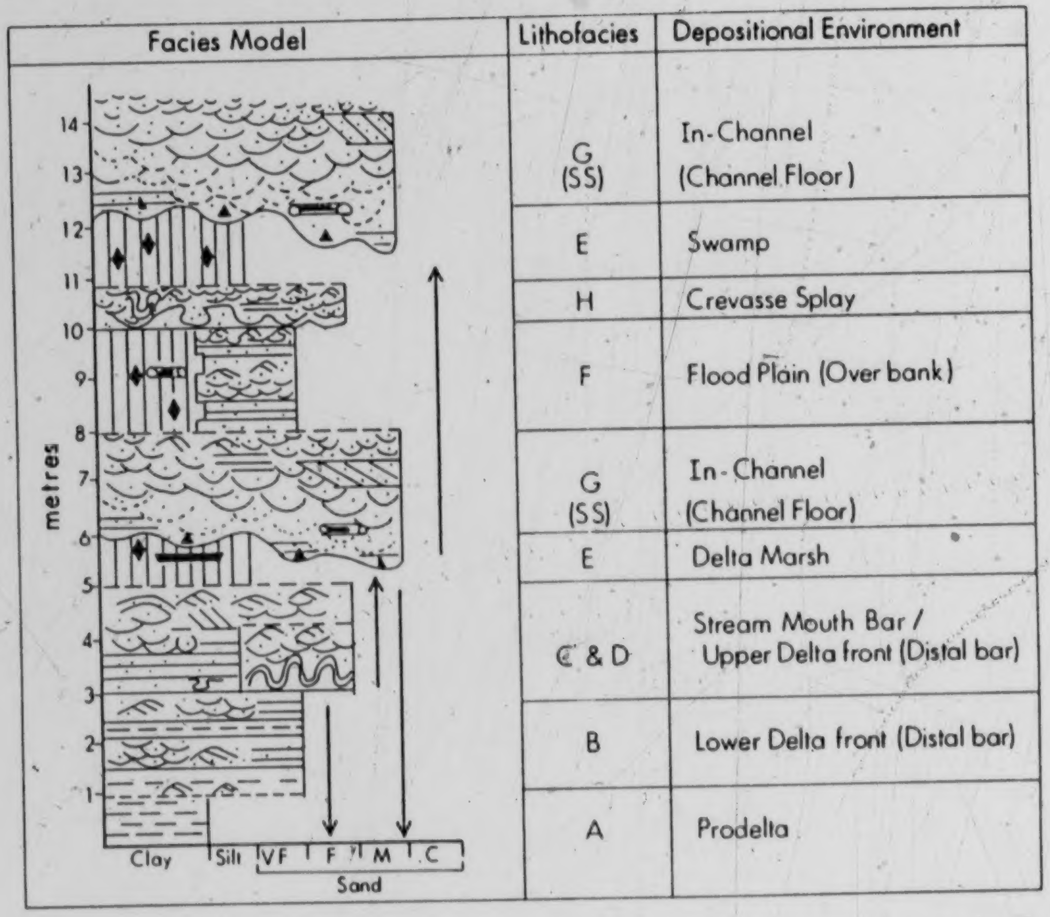
Facies Model
Lithofacies
Depositional Environment
metres
14
13
12
11
10
9
8
7
6
5
4
3
2
1
Clay
Silt
VF
F
M
C
Sand
G
(SS)
In-Channel
(Channel Floor)
E
Swamp
H
Crevasse Splay
F
Flood Plain (Over bank)
G
(SS)
In-Channel
(Channel Floor)
E
Delta Marsh
C & D
Stream Mouth Bar /
Upper Delta front (Distal bar)
B
Lower Delta front (Distal bar)
A
Prodelta

Figure 16b. A local facies model for basal Belly River sequence based on Markov diagram (Figure 16a).

similarly show two broad facies assemblages and four minor facies associations. These two major facies assemblages and the four minor facies associations will be given environmental interpretation in Chapter 1V.

IV. FACIES AND FACIES SEQUENCE : DEPOSITIONAL ENVIRONMENTAL INTERPRETATION

Having defined the nine lithofacies and established their preferred sequence, it is now appropriate to proceed with an interpretation of their depositional environments. This entails the interpretation of the individual FRDs (Appendix B) and the composite FRD (Figure 16) along with the interpretation of individual lithofacies based on their dominant physical (lithology, sedimentary structures and textures) and biological features, as well as comparison with possible recent analogs. The resultant overall interpretation is finally compared with well documented facies models to buttress the inferred depositional interpretation.

Most of the individual FRDs and the composite FRD show two major facies assemblages:

(a) a basal assemblage made up of facies A, B, C and D, and

(b) an upper assemblage of facies E, F, G, H and SS. These two major lithofacies assemblages represent two major depositional environments, namely:

1. Deltaic (marginal-marine), and
2. Continental (fluvial channel and its flood plain) environments.

In other words, the basal association (A, B, C, D) is interpreted as deltaic (delta front), whereas the upper assemblage (E, F, G, H, SS) is fluvial in origin. To put the above environments and their subsequent subenvironments into proper perspective and avoid ambiguities ordinarily associated with terminologies, I have adopted the subenvironmental definitions of Coleman and Gagliano (1965) (Figure 17) as follows:

1. Shelf environment: an environment of slow accumulation of fine muds generally removed from areas of deltaic progradation and usually less than 120 meters water depth.
2. Prodelta environment: the area of deposition of clays, associated with a specific prograding delta system; it is transitional into the shelf environment.
3. Delta Front environment: a complex of associated subenvironments in an advancing locus of active deposition of a prograding fluvial dominated delta. This consists of the following subenvironments:

   (a) Distal bar–the seaward margin of the advancing delta front complex with high

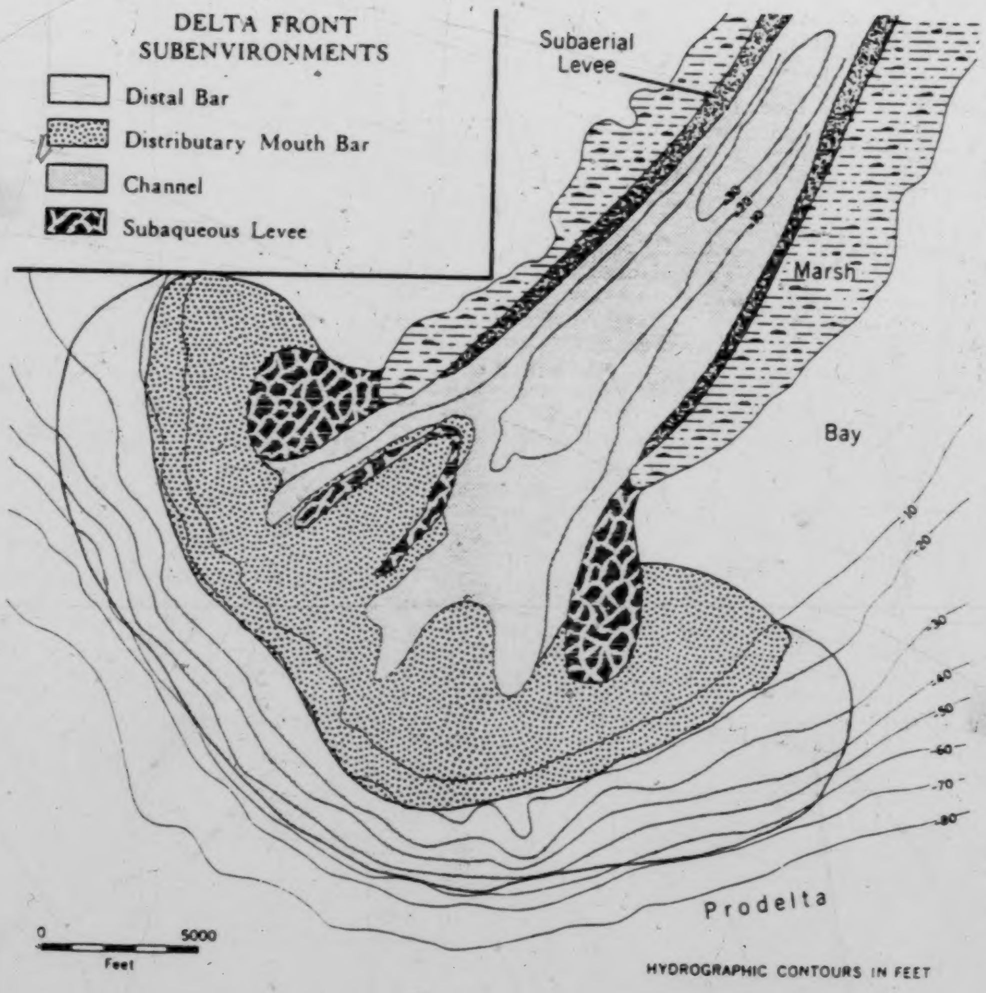
DELTA FRONT SUBENVIRONMENTS
Distal Bar
Distributary Mouth Bar
Channel
Subaqueous Levee
Subaerial Levee
Marsh
Bay
-10
-20
-30
-40
-50
-60
-70
-80
Prodelta
0
5000
Feet
HYDROGRAPHIC CONTOURS IN FEET

Figure 17. Delta front subenvironments (after Coleman and Gagliano, 1965).

sedimentation rates, and current and wave processes.

(b) Distributary Mouth bar- an area of shoaling associated with the seaward terminus of a channel mouth with an accumulation rate higher than in any other delta front environment. The sediments are constantly subjected to reworking by stream currents and waves generated in open water beyond the channel mouth.

(c) Distributary channel- a lower extension of the trunk system which accomodates and directs a portion of the discharge and transported sediment from the parent river system. It broadens, shoals, bifurcates, and loses its identity within the delta front especially as the stream mouth bar is approached.

4. Marsh environment: low tract of periodically inundated land supporting non-woody grasses, reeds, and rushes; its surface approximates mean high tide level and could be fresh, brackish or salt.
5. Swamp environment: low, flat areas periodically covered or saturated with water and supporting a cover of woody vegetation with or without an undergrowth of shrubs; mostly developed in fresh water basins of the upper delta, though smaller patches are common in small isolated basins within the active delta.
6. Interdistributary Bay environment: areas of shallow open water (rarely exceeding 3.5 meters in depth) within the active delta which may be completely surrounded by marsh or distributary levees, but which more often are partially open to the sea or connected to it by tidal channels.

The silty shale facies (A) is preferentially overlain by the interstratified sandstone/shale facies (B); though occasionally overlain by the load-structure-based cross-stratified sandstone facies (H). Considering its overall stratigraphic position, the presence of carbonaceous detritus, very little bioturbation, and the presence of a shallow marine foraminiferal suite dominated by Haplophragmoides and Trochammina , with only a few Eggerella and Ammobaculites , this facies is interpreted as a prodelta to shallow marine shelf deposit. The foraminiferal assemblage indicates deposition in water depth of about 80 meters of estuarine nature, and therefore places the basal Belly River sediments in the inner shelf (25-80 m) to outer shelf (80-180 m) environments (Stelck,C.R., 1982; personal communication). It is pertinent to recall that Ogunyomi and Hills(1977), who studied the more marine equivalent of the basal Belly River beds (Foremost Formation) further east in the Milk River area recorded a similar microfaunal assemblage dominated by Haplophragmoides and Trochammina. They interpreted the associated beds as of marginal-marine shoreline origin.

The interstratified sandstone/shale facies (B) generally overlies facies A and therefore is more continental than facies A. The interstratified sandstone/shale facies is interpreted as deposits of the lower delta front (distal bar) to nearshore environment with a considerable marine process influence. The fluvial system flushes abundant clay to fine sand onto the delta front. These fine sediments in all probability are reworked by marine processes of a moderate wave energy. The sedimentary structures (sharp base, horizontal lamination, minor trough cross-lamination followed by ripple cross-lamination and interference ripples) and the textural variation within the sand layers (grading of some of the sands resulting in internal fining upward) indicate the formation of the sandstone beds of this facies by single depositional episodes related to a waning current. Storm waves are envisaged to be responsible for the suspension, transportation and deposition of these sediments. That storm wave currents are capable of reworking fluvially flushed in clay to fine sand has been documented by Ager (1973), Goldring and Bridges (1973), Kelling and Mullin (1975), Kumar and Sanders (1976), Hayes (1967), Reineck et al. (1967) and Gadow and Reineck (1969). Coleman and Gagliano's (1965) study of the modern Mississippi delta sediments also documents a similar lithology (laminated silts and clays) and suite of sedimentary structures for the distal bar environment. Vos (1977) in his study of Upper Devonian and Lower Carboniferous deposits of the Tindouf Basin, southern Morocco, described a facies similar to facies B of the present study and interpreted it to be storm wave formed. He attributed the sandstone beds to storm wave surge currents; individual beds probably recording a single event of storm turbulence with resuspension of sand-sized material from the shelf floor. After resuspension at maximum storm wave energy, settling of the suspended material results in grading observed in some of the sandstone beds, and wave surge currents cause ripple cross-lamination. He also pointed out that since deposition probably occurs as wave surge velocities decrease, sedimentary structures record a waning current, whereas the upward decrease in the thickness of finer grained interbedded shale through the facies, as well as the upward increase in abundance of thicker sandstone beds, indicate a shallowing environment. These two conclusions are equally applicable to facies B of the present study. The approach of the distributary mouth also results in the sand layers becoming thicker at the expense of the interbedded shale layers, whereas the pronounced repetition of structure types in a definite sequence is attributed to a repetition of the depositional processes of fluvial currents and wave reworking. Coleman and Gagliano (1965) observed this type of repetition of sequences of structures in the distal bar environment of the Mississippi River delta and attributed it to depositional processes which vary in intensity and are repeated periodically; these result in structure types repeated again and again in the same order.

A turbidity current mechanism of deposition for facies B is discounted on the basis of:

1. absence of deep-water foraminifers in the interbedded shales,
2. presence of a low diversity fauna due to low salinity of the water,
3. limited amount of bioturbation, also due to low salinity of the water in the delta front environment,
4. dominance of laminated plant debris in the sand layers and disseminated carbonaceous material in the associated shales,
5. predominance of trough- and ripple cross-laminations,
6. presence of significant numbers of starved ripples, and
7. the mimicing of some turbidite characteristics by storm reworked deltaic deposits (Nelson, 1982).

Nelson (1982) states that the graded sand layers off the modern Yukon delta are deposits of storm surges in a shallow shelf environment. He proposes that they are the product of storm-associated bottom currents combined with storm-wave liquefaction processes (Clukey et al., 1980), and do not require significant change in water depth or generation of density currents to produce a sequence of turbidite-like deposits over a flat shallow shelf, as opposed to the turbidity current interpretation of Hamblin and Walker (1979). It is pertinent to note that there is a strong similarity in sedimentary structure sequence and textures between facies B of the present study and the shallow-water, graded, storm-sand beds of Nelson (1982). I believe the depositional setting and processes that operated during basal Belly River time may have been similar to those operating off the modern Yukon River delta.

The bioturbated and distorted sandstone facies (C) usually overlies facies B and underlies facies D. The bioturbated and distorted sandstone facies is interpreted as an upper delta front/distal bar deposit. Deformed bedding in the form of load casts, ball and pillow structures, slumped structures and contorted lamination prevalent in the upper portions of the facies are indicative of rapid sedimentation (Reineck, 1961; Allen, 1963; Walker, 1963; Mckee, 1965). The presence of Inoceramus , Baculites and Rhizocorallium indicate a shallow marine environment. The preserved minor trough cross-bedding and cross-lamination probably reflect stronger currents during flood stages. The interstratification of bioturbated and non-bioturbated sandstone beds in this facies is an indication of fluctuating rates of sediment influx; the bioturbated sandstone beds represent occasional periods of slow deposition rates and the absence of strong reworking by waves and currents, whereas the non-bioturbated and often deformed beds represent rapid deposition. Ball and pillow structures are rheomorphic syndepositional deformation features which result from the sudden deposition of sand over a hydro-plastic muddy layer (Vos, 1977).

The similarity of this facies to the sediments of the delta front sequences as documented by Coleman and Gagliano (1965) in a recent delta, Erxleben (1973) and Vos (1977) in ancient deltas, and its stratigraphic position in the measured sections, support a delta front interpretation. The main differences between the environment of deposition of this facies and that of the interstratified sandstone/shale facies (B) are

(a) the greater effectiveness of the marine processes in reworking the sediments of facies B, and

(b) the possible proximity of facies C to the axis of sediment input resulting in its deformed characteristics.

The stratigraphic position, lithology (moderately to well sorted sandstone with only occasional shaly sandstone), and suite of sedimentary structures of facies D strongly suggest its deposition in the stream mouth bar environment. It has the coarsest size grade of the detrital lens that represents the delta front environment, and the individual beds are thicker than any other beds of the delta front deposit, faithfully recording the approach of the main sediment sources (distributaries) and the resultant shoaling of the environment. This is in accord with observations from modern delta fronts. Coleman and Gagliano

(1964) noted that the bulk of coarse deposition takes place within the immediate vicinity of the distributary mouths of the active delta front of the Mississippi River delta. Facies D is usually underlain by facies B or C; occasionally by facies H. The suite of sedimentary structures, consisting of horizontal bedding and lamination, trough cross-bedding and cross-lamination, ripple cross-lamination, and occasional wedge-shaped cross-bedding, hummocky cross-bedding and herringbone cross-lamination, attest to the dynamic nature of its environment of deposition with both current and wave processes. The occasional thin layers of quartz and chert pebble conglomerate, concentrations of mudclasts in definite horizons and grading of some of the sand beds are evidence of storm wave activity, especially during delta lobe abandonment and reworking. Similar characteristics have been noted in studies of modern stream mouth bar sediments (Coleman and Gagliano, 1965; Nelson, 1982). The variation in the thickness of this facies as recorded in different stratigraphic sections is a reflection of the lateral proximity or remoteness of the section to a sediment source (distributary channel).

The coaly and carbonaceous mudstone facies (E) is interpreted as marsh and swamp deposit on account of its stratigraphic position (usually overlying facies D, H or G), high organic content, and similarity to modern delta marsh deposits (Coleman and Gagliano, 1965; Gould, 1970). The abundance of plant debris in the form of thin coal beds and fragments, disseminated plant debris, carbonized rootlets and fossil wood fragments shows this facies is a shoreline to continental deposit. The seaward margin of the deltaic plain remains at or near sea level during most of deltaic sedimentation and is covered by marsh and swamp vegetation. During floods, these environments receive large volumes of the fine constituents (silt and clay) carried across the levees. The combined accumulations of the organic remains of the luxuriant marsh and swamp vegetation and the floods of fine inorganic detritus account for the considerable thickness of marsh deposits (Gould, 1970). The lowest facies E occurrence in a stratigraphic section invariably overlies facies D and therefore may represent the delta abandonment facies that forms the essentially non-detrital top sediments of a normal delta sequence (Coleman and Gagliano, 1964), whereas the higher occurrences of this facies are likely to be fresh water backswamp deposits of the fluvial environment.

The interstratified mudstone/sandstone facies (F) is interpreted as a flood plain deposit. The term flood plain deposit is used here as a general one to denote the sediments deposited during overbank flow; this results in muddy sediments as well as abundant sand deposition (Reineck and Singh, 1975, p.252; Friedman and Sanders, 1978, p.220). This is equivalent to Allen's (1965) undivided top-stratum deposits. They characterize rivers that shift their position rapidly and therefore do not have well-developed natural levees and flood basins (Reineck and Singh, 1975). Leopold and Wolman (1957) noted that in rivers with rapidly changing channels, velocities of overbank flows are rather rapid, and very commonly current velocities of up to 40 or 50 cm/sec are achieved. The result is that overbank flooding deposits consist of mud and sand, and cannot be differentiated easily from similar looking levee and crevasse splay deposits.

The FRDs, generalized and individual ones alike, show facies F occurring most consistently above facies G (scour-based high angle cross-stratified sandstone) and occasionally above facies E (coaly mudstone facies) and followed by the scoured surface facies (SS). The alternation of horizontal and cross-laminated fine- to very fine- grained sandstones with carbonaceous mudstone suggests vertical accretion in the overbank area of a fluvial system (Cant and Walker, 1976). The mudstone layers are the result of deposition from suspension whereas the cross-stratified sands require some form of traction transportation producing lower flow regime bedforms such as ripples. The presence of trough cross-bedding and cross-lamination and occasional planar cross-lamination are due to unusually high stage overbank flooding resulting in higher than normal current velocities; in contrast, the load features observed in the thicker sandstone layers (>0.3 meter) are due to rapid deposition of sand on hydroplastic mud during this unusually high stage overbank flooding. Some of these thicker sandstone layers can in fact be crevasse splay deposits in the normal finer flood plain mudstones (Reineck and Singh, 1975, p.248). (See also facies H interpretation for more detailed discussion). The couplet of a basal sandstone and an upper mudstone may represent a single flooding episode or just a part of such an event. In other words, more than one coarser and one finer unit may be deposited during a single flood event, indicating fluctuations during the flood (Reineck and Singh, 1975). The assemblage of sedimentary structures, texture and general lithology of this facies is very similar to that documentated in modern flood plain deposits such as those of Bigeon Creek, Colorado (Mckee et al., 1967), and the Indus River (Mckee, 1966).

Stratigraphic position (invariably above facies SS), predominance of trough cross-bedding which results from unidirectional migration of dunes, occasional planar cross-bedding which is a product of movement of larger bedforms (sand waves) and abundant carbonized plant debris in the form of fossil logs, strongly suggest the deposition of facies G within an active channel (Leopold and Wolman, 1957; Allen, 1963, 1964, 1970; Cant and Walker, 1976; Jackson, 1976, 1978; Walker and Cant, 1979; Blatt et al., 1972; Collinson, 1978; Reineck and Singh, 1975; Friedman and Sanders, 1978). It represents the lateral accretion component of the fluvial deposits of the Belly River Formation.

Although detailed and extensive scientific research has been carried out on modern streams (Fisk, 1944, 1947; Sundborg, 1956; Bernard and Major, 1963; Bernard et al., 1970; Bluck, 1971; Jackson, 1976, 1978; Shepherd, 1976; etc.) with the aim of establishing the relationship between channel pattern and sediment characteristics, a consensus has not been reached. The geologic application of these studies in deciphering the channel patterns of ancient fluvial systems based on their sediment characteristics is therefore fraught with problems. (A more detailed discussion of this topic is deferred to Chapter V). But considering the predominance of trough cross-bedding in facies G (Harms et al., 1963), the high diversity of the paleocurrent data (Chapter V), the distinct separation of the relatively coarse-grained bedload deposits of the channel and the relatively fine-grained overbank deposits, the overall dominance of the fine component (mudstones) (Friedman and Sanders, 1978, p.219) of the studied sections, and the undifferentiated nature of the flood plain (overbank) deposits, the writer is inclined to interpret the the channel pattern of the lower Belly River streams as a variety of meandering river pattern with relatively rapidly shifting channels.

The load-based cross-stratified sandstone (H) facies is interpreted as a crevasse splay deposit. A crevasse splay is a breach in the "natural levee" resulting in the formation of a system of distributary channels on the levee slope when water escapes through the low section (Gregory and Walling, 1977, p.263). Although the adoption of this terminology (crevasse splay) may appear to contradict the usage of the term flood plain in the interpretation of facies F above, it is used here to designate a probable origin for discrete thicker, flood plain sand layers. In other words, these thicker overbank sand layers may be only better developed members of the interstratified sand layers of facies F.

The texture (very fine- to fine-grained, poorly to moderately sorted sandstones), sedimentary structures, stratigraphic position (usually sandwiched between finer muddy sediments of the flood plain proper, facies F and E), and the thin average thickness (approximately 1.0 m) form the bases for a crevasse splay interpretation for this facies. The loaded bases of the sand layers are indicative of the sudden dumping of the sand on the underlying finer grained mudstones of facies E and F during crevassing, whereas the small-scale cross-bedding and cross-lamination indicate the presence of lower-flow regime bedforms (ripples) during deposition. The deformed internal nature of some of the layers resulted from the interplay among the depositing current, the substrate over which the current moved, and the sediment being deposited (Friedman and Sanders, 1978, p.234), and the high sedimentation rate, which does not allow adequate time for compaction of the sands and the attendant escape of the entrapped fluids.

Although the characteristics of modern crevasse splays are not adequately documented, the few criteria for their recognition given by Coleman (1969) for the modern Brahmaputra River, and the compilations by Reineck and Singh (1975), Collinson (1978), and Friedman and Sanders (1978) are similar to those observed in facies H of the present study and therefore buttress the above interpretation.

The scoured surface facies (SS) represents the erosion and establishment of an active channel followed by the deposition of the channel lag (a lining of the channel floor with pebble-sized mudclasts); this in turn is followed by the other in-channel coarse deposits. It is the fluvial channel floor. The subordinate, shallower scoured surfaces within multistory facies G are minor truncation surfaces of the channel deposit resulting from periodic increases in velocity during floods. During these flood periods, some of the finer grained top portion of the previous in-channel deposit is eroded before the re-establishment of another depositional phase. This process has been documented in the modern meandering Brazos River by Bernard et al., (1970).

Based on the lithologic sequence and associations (Figure 16), sedimentary structures and textures of the individual lithofacies, biological features, and a comparison of the overall lithology with deposits of modern environments (facies models) (see Chapter V for a detailed discussion), one can conclude:

1. The Belly River Formation in the study area represents the deposit of a progradational shoreline which grades from a marine deltaic environment to a continental fluvial environment; it clearly forms a characteristic coarsening-upward sequence.
2. The basal assemblage of A, B, C, and D facies represents the deposits of the delta front environment and is equivalent to the portion of this lithostratigraphic unit traditionally known as the basal Belly River Sandstone.
3. The basal Belly River delta was a wave-influenced, river-dominated one.
4. The lithofacies assemblage consisting of SS, G, E, F and H represents the continental fluvial environment, with facies SS as the channel floor, G as the in-channel deposit, and facies E, F and H as the overbank deposits (see Chapter V for a more detailed discussion).

Based on the Markov diagram (Fig. 16) and taking into consideration average thickness of each facies, a local facies model (Fig. 16b) is erected and sums up the writer's environmental interpretation of the basal Belly River Formation. This local facies model compares favorably with the idealized deltaic sequences compiled by Selley (1970) and Miall (1979) and therefore corroborates the inferred deltaic-fluvial origin of the basal Belly River Formation in the study area.

V. DEPOSITIONAL HISTORY AND PALEOGEOGRAPHY OF THE WESTERN ALBERTA SHORELINE DURING BELLY RIVER TIME.

A. Sedimentation History

The general characteristics of deltaic sediments compiled by Miall (1979) were used as a basis of comparison in the interpretation of the lithofacies of the present study, especially for the the basal assemblage of A, B, C and D. According to Miall (1979):

1. Deltaic deposits tend to be thick.
2. They contain a considerable volume of sand and/or silt.
3. Coal beds are commonly present.
4. The faunal content of interbedded units may indicate marine, brackish, and fresh water depositional environments.
5. The sedimentary structures indicate shallow water deposition by traction- rather than turbidity currents, and
6. They show a traceable gradation into finer-grained clastic deposits of offshore origin.

Whereas the general lithology and sequence of the Belly River Formation of the study area compare very closely with those of a generalized deltaic deposit as outlined by Miall (1979), which corroborates a deltaic interpretation, the establishment of the delta type for the basal Belly River delta/deltas is more problematic. Workers on both modern and ancient deltas acknowledge these problems which stem from the variable nature of the factors which influence and control deltaic sedimentation. These factors include among others : river regime, coastal processes, structural behavior, and climate (Morgan, 1970; Coleman and Wright, 1975; Galloway, 1975). But these difficulties have not deterred workers in the field of deltaic sedimentation from making attempts at classification of deltas, as shown by Coleman (1975), Coleman and Wright (1975), Galloway (1975), and Scott and Fisher (1969), while still realizing that no two deltas are identical (Selley, 1979).

Delta Type

Having established a deltaic origin for the basal Belly River sediments in the southern and central Foothills of Alberta, an attempt is made to decipher the nature of its depositional history and therefore reconstruct the paleogeography of the western shoreline during Belly River time. As has been stated by Selley (1979), no two deltas are identical and therefore it is not to be expected that the depositional history of the Belly River delta system would be identical to that of any single modern delta. After a review of available delta classifications and models (Coleman and Wright, 1975; Galloway, 1975), the writer decided to adopt the classification of Galloway (1975; Figure 18) in the present study. This classification is based on the relative strengths of the fluvial and marine processes in the depocenter, and therefore reflects the variations in transportation patterns on the delta. The establishment of the delta type for the basal Belly River hinges on the comparison of the deltiac sediments of the present study with the specific characteristics of the three end-members of the deltaic facies models of Galloway (1975). Studies of modern deltaic sediments and their resultant facies models reveal that no one delta model could be formulated to be used as a basis for predicting vertical sequences in all ancient deltas, hence the formulation of the six-fold facies model of Coleman and Wright (1975), and the three-fold facies models of Galloway (1975) and Scott and Fisher (1969). Miall (1979), in his summary of the state of the art of delta classification and models, stated that there are at least three distinct delta models or "norms" to choose from in interpreting ancient rocks, and that many deltas are combinations of all three. All delta classifications, however, recognize and emphasize the interplay of fluvial and coastal marine processes, since they mostly determine the distribution of the sediments within the depositional basin, and hence the delta type.

A study of the FRDs (facies relationship diagrams), individual and composite alike and the raw stratigraphic columns, show that the Belly River sediments form a characteristic coarsening-upward sequence. Also the basal assemblage of lithofacies A, B, C, and D of most stratigraphic sections shows repeated coarsening-upward cycles. Each complete coarsening-upward cycle in this basal assemblage commences with an evenly laminated fissile shale (A) of prodelta origin which grades upward into interstratified sandstones and shales (B). These sandstones are essentially horizontally- and

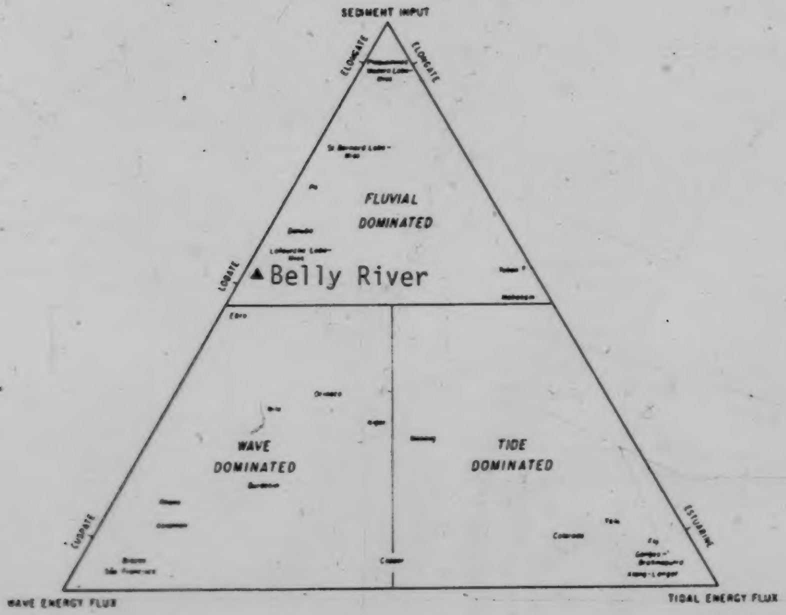
SEDIMENT INPUT
ELONGATE
ELONGATE
FLUVIAL DOMINATED
LOBATE
▲Belly River
Ebro
Orinoco
WAVE DOMINATED
TIDE DOMINATED
CUSPATE
ESTUARINE
Colorado
Fly
Copper
WAVE ENERGY FLUX
TIDAL ENERGY FLUX

Figure 18. Suspected position of Belly River delta on a schematic diagram illustrating the threefold division of deltas into fluvial-dominated, wave-dominated, and tide-dominated types (after Galloway, Fig. 3, in Broussard, 1975).

cross-laminated. The interstratified sandstones and shales grade up through bioturbated and distorted sandstones (C) to horizontal and low-angle cross-stratified sandstones (D), though the interstratified sandstones and shales do in some cases grade directly into the horizontal and low-angle cross-stratified sandstones, thereby bypassing the bioturbated and distorted sandstones. The low-angle cross-stratified sandstones, which are interpreted as distributary mouth sheet sands, form the coarsest member of the cycle. They are characterized by trough and planar crossbeds, and ripple marks. The top of the cycle is formed by delta marsh sediments of coal and coaly mudstones, but in some cases by channel sands. These are akin to the sediment characteristics which Miall (1979) stated are indicative of river-dominated deltas. It is in situations where wave and tidal processes are overpowered by fluvial processes that the clearly characteristic coarsening-upward cycles as observed in the present study are developed. The presence of sharp non-scour based graded sandstone layers and hummocky cross-bedding in some of the facies B sandstones indicate some influence of wave activity in the basal Belly River delta system. As a logical corollary, the basal Belly River delta is interpreted as a wave-influenced river-dominated one; it is similar to Galloway's (1975) fluvial-dominated wave-modified deltas.

Having established the fluvial-dominated nature of the basal Belly river delta, one is left with two possible alternatives regarding its geometry (Galloway, 1975). These alternatives are:

1. Elongate
2. Lobate.

Considering that:

1. All the measured stratigraphic sections in the southern portion of the study area contain considerable amounts of distributary mouth sheet sand,
2. There is a basal sandstone (the basal Belly River sandstone) in most of the boreholes that penetrated this lithostratigraphic unit in the immediate vicinity of the Foothills (as shown by electric logs), attesting to the 'lateral continuity' of this basal sandstone,
3. There are wave formed structures in this basal sandstone, and therefore there is possible wave redistribution of the distributary mouth bars into sheet sands,

the writer suspects a lobate shape for the basal Belly River deltas.

The thickness of basal Belly River deltaic sediments (subaqueous deposits – lithofacies A, B, C, and D) ranges from 3.7 to 165 meters (Table 8, Appendix A). The occurrence of these subaqueous lithofacies are confined to the basal portion of measured stratigraphic sections. They do not recur in the higher portions of the sections. Considering the thinness , relative position, and widespread nature of the subaqueous deltaic lithofacies (A, B, C and D), one can conclude that :

1. Structural effects were minimal during the deposition of Belly River sediments;
2. Rate of sediment supply was high and therefore the fluvial processes overpowered marine processes and subsidence;
3. The depositional basin was relatively shallow, and most of the deposition took place at or above sea–level (hence the thinness of the subaqueous deltaic lithofacies, and the preponderance of subaerial lithofacies of the upper Belly River Formation);
4. The widespread occurrence of the subaqueous lithofacies was mainly due to the frequent choking of the channel outlets in the delta front region by its own sediment load resulting in a complex of laterally shifting channels. These in turn resulted in a complex of laterally displaced and overlapping delta lobes which record the pronounced effect of the river regime during progradation. The process envisaged here is similar to that which was operating in the Recent Mississippi delta, resulting in the formation of subdeltas and partially overlapping lobes (Coleman and Gagliano, 1964; Kolb and Van Lopik, 1966), but modified by moderate wave activity (Figure 19).

Channel Pattern

The channel pattern of the Belly River system is inferred to be meandering based on the sediment characteristics (grain size, sedimentary structures, vertical facies sequence) and paleocurrent data [with due regard for the problems of determining channel pattern from sediment characteristics (Allen, 1963, 1964, 1970; Bluck, 1971; Leopold and Wolman, 1957; Shepherd, 1976; Rust, 1978, 1979; Bernard and Major, 1963; Bernard et al., 1970; Walker and Cant, 1979; Jackson, 1976, 1978)]. The literature clearly demonstrates the controversy over channel pattern and sediment characteristics. Jackson (1978) pointed out the inappropriateness of assuming close correspondence between

Table 8. Total thickness of facies A, B, C, and D (the subaqueous deltic lithofacies) in the various sections.

Section	Thickness (meters)
Drywood River	165.1
Crowsnest River (Lundbreck)	74.3
Oldman River	87.7
Highwood River	91.0
Trap Creek	65.1
Sheep River (Turner Valley)	
Jumpingpound (A)	21.0
Jumpingpound (B)	21.0
Bow River (Morley)	3.7
Little Red Deer River	25.4
South Burnt Timber Creek	18.0
James River	84.4
Ram River	47.3
Cripple Creek	116.4*

* Assumes that the covered intervals in the lower portion of the section are of delta front origin.

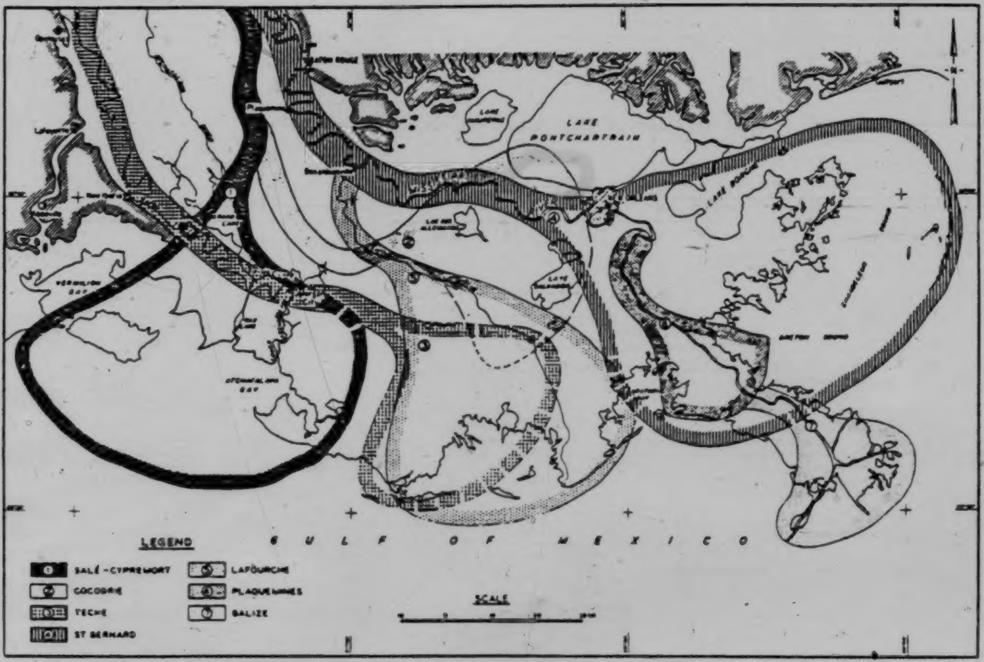
LAKE PONTCHARTRAIN
LAKE BORGNE
VERMILION BAY
GULF OF MEXICO
LEGEND
SALÉ-CYPREMORT
COCODRIE
TECHE
ST BERNARD
LAFOURCHE
PLAQUEMINES
BALIZE
SCALE

Figure 19. The seven partially overlapping lobes of the Mississippi delta which have developed during the last 5000 years (from Kolb and Van Lopik, Fig. 2, in Shirley, 1966).

channel pattern and lithofacies, and summarized the state of the art of meandering stream research. He outlined the characteristics (criteria) which lead to better determinations of the channel pattern of ancient meandering streams. These characteristics include:

1. Fining-upward cycles of grain size and sedimentary structures,
2. Presence of appreciable thickness of the fine member,
3. Presence of only small amounts of gravel (large clasts) in the coarse member,
4. Large dispersion of current indicators (often greater than 180 degrees),
5. Presence of exhumed meander belt (in proper sections),
6. Great continuity of sand and gravel beds (in the coarse member) with little lateral change in texture.

However, Jackson (1978) points out that with the exception of the presence of a exhumed meander belt (which consists of the accretionary ridge-and-swale topography), all the other criteria are inconclusive, since some of them may be lacking in some meandering streams whereas others may be present in non-meandering streams as well. This raises the philosophic questions of necessity and sufficiency.

There are at least four meandering stream lithofacies models (which form a continuum) to consider in the interpretation of ancient fluvial deposits. These are : the standard fining-upward cycle (Allen, 1963, 1970), Endrick River model (Bluck, 1971), Lower Wabash River model (Jackson, 1976) and Rio Puerco River model (Shepherd, 1976). Whereas the writer appreciates the problems of inferring a paleochannel pattern from sedimentological characteristics of ancient deposits, he favors a meandering pattern for the Belly River channel for the following reasons :

1. A high suspended load/bed load ratio in the Belly River sediments of the study area as shown by high proportions of mudstones in all the measured stratigraphic sections (Appendix A). Fine materials (silt and clay) serve as cohesive bank materials and therefore tend to reduce the rate of channel migration (Leopold and Wolman, 1957; Friedman and Sanders, 1978, p.228).
2. Similarity of facies F (Heterolithic facies II) of the present study to Jackson's (1976) upper Heterolithic facies (homogeneous sand-mud, and sand lens in mud).
3. The fact that whereas it has been documented that meandering streams can be characterized by mud to gravel size grades (Jackson, 1978), the deposits of braided

streams consist mostly of sand and gravel; muds are subordinate or absent. This absence of shales generally distinguishes the ancient deposits of braided streams from those of meandering streams (Friedman and Sanders, 1978, p.219).

4. The large dispersion in paleocurrent directions (Table 9; Figure 20). A study of Table 9 and Figure 20 shows that there is a large dispersion between the sections as well as within them. This is in accord with a meandering stream current pattern (Jackson, 1978).

After comparison of the above outlined meandering stream characteristics of the Belly River system with the above listed four available meandering stream lithofacies models, the writer believes that the basal Belly River channel pattern fits most closely with Allen's (1963, 1970) fining-upward model and Jackson's (1976) Lower Wabash River model. It also falls within Jackson's (1978) class of sand-bed streams with modest thickness of fine member characterized by upward fining of coarse member. This is basically a lithofacies classification of meandering streams based on textural attributes of grain size and sedimentary structures. The streams in question therefore were sand-bed meandering streams.

Within the upper portion of the Belly River Formation there are repeated sequences or cycles. Each cycle commences with the scoured surface (SS) which can be regarded as the fundamental boundary between cycles. The scoured surface therefore divides the stratigraphic sections into similar cycles which ideally consist of scoured surface (SS), high-angle cross-stratified sandstone (G) and interstratified mudstone/sandstone (F), or load-structure-based cross-stratified sandstone (H) and coaly mudstone (E). The upper portion of the Belly River Formation therefore clearly shows a cyclic pattern of sedimentation typical of fluvial systems.

B. Paleogeography

The use of the composite Facies Relationship Diagram (Figure 16) as a local model with which each individual stratigraphic section is compared reveals some interesting differences. These differences are especially obvious in the basal subaqueous deltaic portion of lithofacies A, B, C, and D. Whereas some of the stratigraphic sections show a large percentage of this basal subaqueous deltaic portion, others barely contain it. This is

Table 9. Summary of paleocurrent data.

Section	Unit no.	No. of readings	Dip direction of rotated cross bed (mean)	Dip of rotated cross bed (mean)
Drywood River	13	1	187.7	23.4
Drywood River	15	2	94.3	6.8
Drywood River	17	2	191.1	9.1
Drywood River	26	2	273.3	17.6
Drywood River	27	1	236.1	26.0
Drywood River	28	1	231.6	23.0
Drywood River	34	1	281.1	8.0
Drywood River	37	4	236.6	20.0
Crowsnest River	10	2	346.4	8.6
Crowsnest River	12	31	64.3	7.7
Oldman River	12	44	223.4	18.1
Oldman River	14	34	254.9	5.9
Highwood River	4	11	71.0	5.4
Highwood River	6	31	93.2	5.7
Trap Creek	9	20	151.1	35.1
Trap Creek	17	12	29.9	13.4
Trap Creek	24	25	80.1	12.5
Sheep River	2	2	38.7	20.7

Sheep River	22	6	128.9	12.9
Sheep River	24	12	161.1	8.2
Sheep River	26	12	129.0	16.6
Sheep River	32	26	166.0	12.7
Sheep River	34	4	113.1	15.9
Sheep River	36	8	75.1	13.5
Sheep River	38	7	130.1	23.6
Jumpingpound (1)	4	2	199.7	4.7
Jumpingpound (1)	20	2	217.5	18.5
Jumpingpound (2)	32	9	147.7	6.3
Jumpingpound (XX)		29	165.1	13.0
Bow River	5	4	251.7	15.1
Bow River	18	12	157.5	8.5
Bow River	25	2	136.6	10.1
Bow River	26	3	246.6	1.3
Bow River	27	16	155.9	18.8
Little Red Deer	2	6	288.8	26.6
Little Red Deer	9	7	282.2	18.2
Burnt Timber Creek	2	2	276.0	17.0
Burnt Timber Creek	31	3	287.6	16.3
Burnt Timber Creek	38	6	285.3	16.6
James River	3	1	225.2	7.3

James River	7	4	208.0	8.9
James River	9	4	196.4	7.2
James River	26	4	254.0	12.4
James River	28	2	201.1	13.1
James River	38	6	214.3	5.6
James River	42	2	272.2	3.4
James River	44	2	327.1	9.6
James River	48	2	231.3	24.3
James River	52	3	223.2	13.9
James River	54	2	281.5	11.3
Ram River	13	8	6.8	3.4
Cripple Creek	21	6	308.7	10.5
Cripple Creek	35	2	282.1	2.8
Mean Value			190 degrees	
Standard Deviation			82 degrees	
Variance			6735	

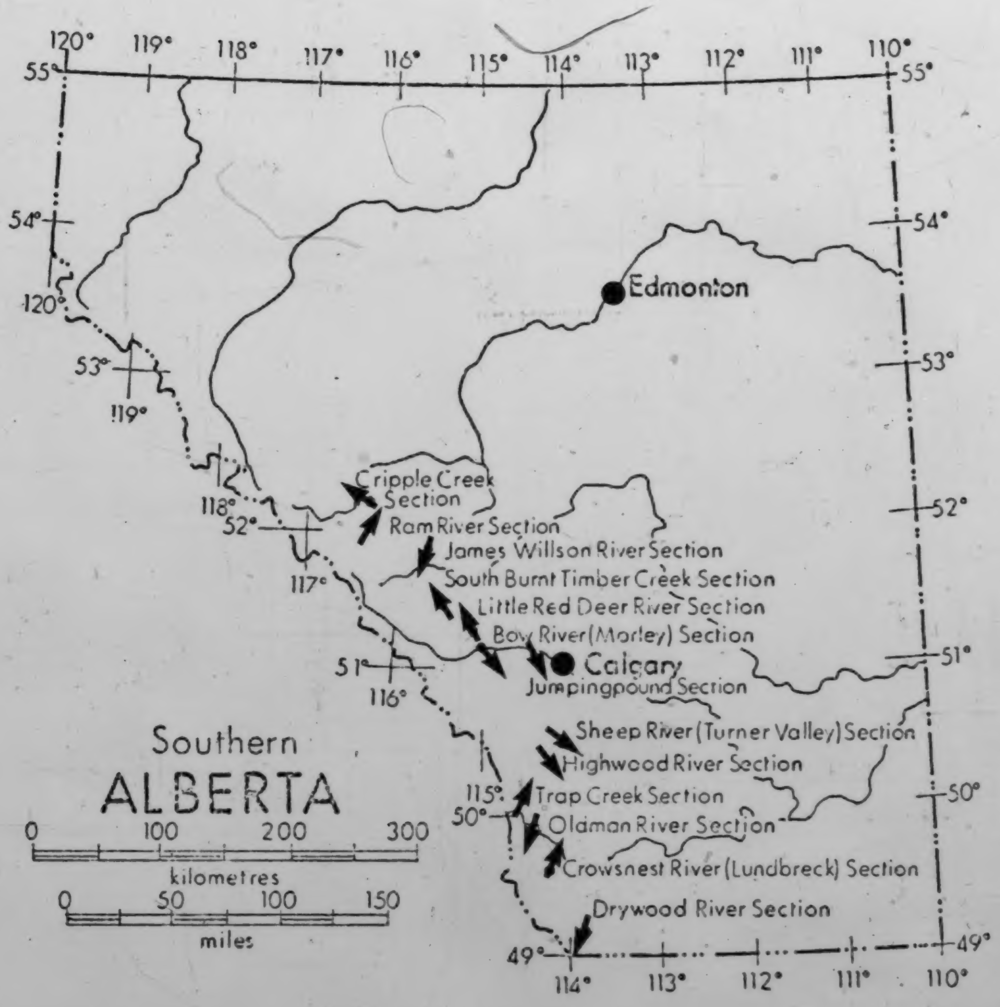

120°
119°
118°
117°
116°
115°
114°
113°
112°
111°
110°
55°
54°
53°
52°
51°
50°
49°
Edmonton
Calgary
Cripple Creek Section
Ram River Section
James Willson River Section
South Burnt Timber Creek Section
Little Red Deer River Section
Bow River (Morley) Section
Jumpingpound Section
Sheep River (Turner Valley) Section
Highwood River Section
Trap Creek Section
Oldman River Section
Crowsnest River (Lundbreck) Section
Drywood River Section
Southern
ALBERTA
0
100
200
300
kilometres
0
50
100
150
miles

Figure 20. Dominant paleocurrent directions at measured outcrop sections.

well demonstrated when one compares the Drywood River, Bow River and Cripple Creek sections (Figure 2.1). Whereas the Drywood River section shows ten facies transitions within this interval, the Bow River and Cripple Creek sections show only five and three transitions respectively. When this is considered in terms of the geographic positions of these sections, one may conclude that the transition of the Wapiabi marine shale to the Belly River Formation was more abrupt in the north than in the south. One may also conclude:

1. That the western paleoshoreline in basal Belly River time was variable from south to north as shown by the variation in the nature of the transitional beds (lithofacies A, B, C, and D) of the measured sections; and
2. That the retreat of the Cretaceous seaway during basal Belly River time probably began in the north and was more rapid in the north than in the south.

Provenance of Belly River Sediments

The detrital composition of the basal Belly River sandstones (see Chapter V.1) indicates that the source terrain was composed of sedimentary, metamorphic, plutonic, and volcanic rocks. The abundance of sedimentary rock fragments (over 40 percent of the essential detrital components) in the form of mudrock fragments, carbonates, and chert indicate a major contribution by the sedimentary rocks in the source area. The presence of rounded and subrounded quartz, chert and zircon grains is a further indication of contribution of detritus by a sedimentary terrain. The variation in the proportion of some of the sedimentary components, especially the carbonate fraction, is an indication of the variability within the source area, or that there were a number of source areas with different compositions. Most of the sections in the southern Foothills show significant proportions of detrital carbonate whereas most of those of the central Foothills show but a trace of it. This is probably due to differences in the source areas of the southern and central sections, and not simply a variation within a single source terrain (see paleocurrent data).

The presence of metamorphic rock fragments in the form of argillites, metasiltstone, and low-grade schists (quartz, micas, chlorite, albite), quartzite rock fragments (polycrystalline mega-quartz), strongly undulose metamorphic quartz grains,

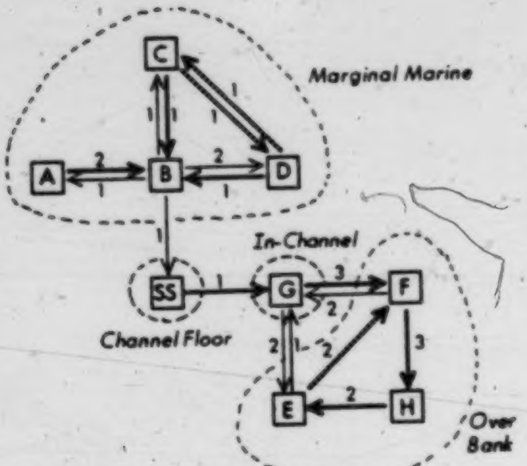
Marginal Marine
C
A
B
D
1
1
1
1
2
1
2
1
1
In-Channel
SS
G
F
1
3
2
Channel Floor
2
1
2
3
E
H
2
Over
Bank

A. Drywood River section.

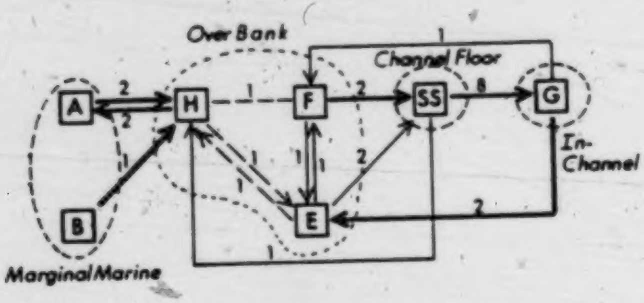
Over Bank
1
Channel Floor
A
H
F
SS
G
2
2
1
2
8
1
1
1
2
1
1
In-
Channel
B
E
2
1
Marginal Marine

B. Bow River (Morley) section.

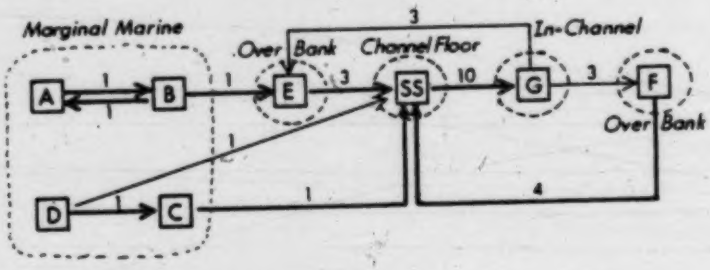
Marginal Marine
3
In-Channel
Over Bank
Channel Floor
A
B
E
SS
G
F
1
1
1
3
10
3
Over Bank
1
D
C
1
1
4

C. Cripple Creek section.

Figure 21. Comparison of Drywood River, Bow River and Cripple Creek section FRDs.

chlorite and epidote grains, especially in the central Foothills sections, show the presence of metamorphic rocks in the source terrain of the basal Belly River sediments. The presence of volcanic rock fragments with characteristic trachytic texture, detrital quartz grains with well-developed non-diagenetic crystal faces and zoned plagioclase feldspars show some contribution of detritus by either a volcanic terrain or contemporaneous volcanism or both. The presence of bentonites, and bentonitic shales in the basal Belly River sediments is a direct evidence of contemporaneous volcanism during basal Belly River time.

Plutonic rock fragments (quartz, orthoclase, micas), abundant common quartz grains, fresh orthoclase feldspar, micas, a few microcline feldspar crystals and occasional tourmaline crystals indicate some contribution of detritus by plutonic igneous terrains.

The location of the source area/areas of the basal Belly River sediments, based on their mineralogical composition, is more difficult than its identification. Considering the regional paleogeography of the Upper Cretaceous of North America, the location of terrains with comparable lithologic assemblage to those indicated by the detrital composition of basal Belly River sandstone lie in the west half of the compass and in all probability fall within the Cordillera.

During Late Cretaceous time, the interior of western Canada was occupied by a broad, epeiric sea connecting the Gulf of Mexico in the south with the Arctic Ocean in the north (Williams and Burk, 1964). It was bordered on the west by the tectonic highlands uplifted by the Columbian orogeny (the Cordillera) and on the east by the low lying Canadian Shield. Invariably, the uplifted highlands in the west shed enormous amounts of clastic detritus to the western margin of this epicontinental sea, resulting in a series of regressions of the shoreline and deposition of a thick sediment pile of which the Belly River Formation is a part (Williams and Burke, 1964; Weimer, 1960; Nelson and Glaister, 1975). This series of regressions was punctuated by minor transgressions of the sea, but there is no evidence to show the penetration of the sea as far west as the present day Foothills (Figure 22) during Belly River time (Williams and Burk, 1964; Ogunyomi and Hills, 1977).

The late Precambrian Belt Series and Mississippian and Pennsylvanian formations of Western Canada have been suggested by Ogunyomi and Hills (1977) and Rapson (1965) as

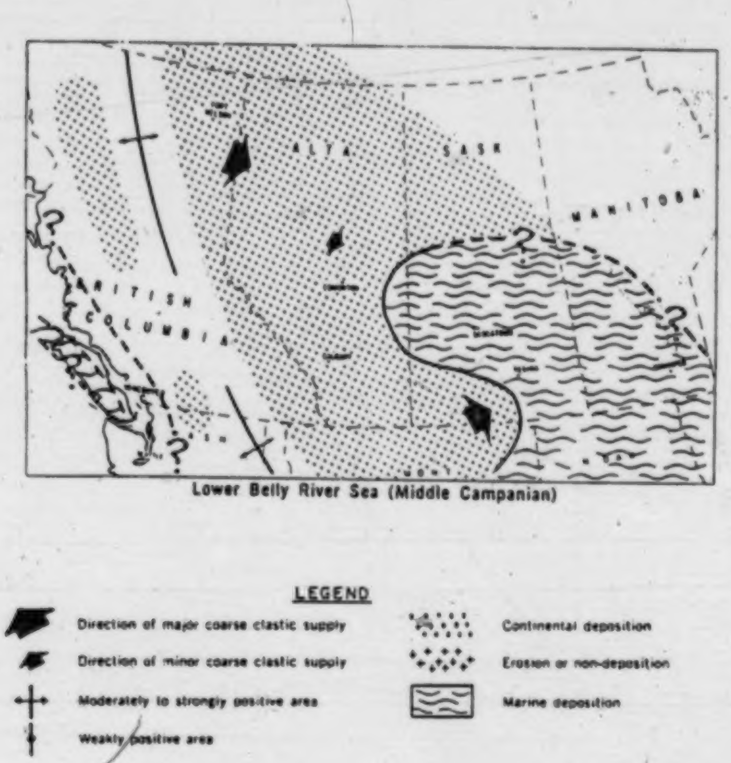
ALTA
SASK
MANITOBA
BRITISH COLUMBIA
?
Lower Belly River Sea (Middle Campanian)
LEGEND
Direction of major coarse clastic supply
Direction of minor coarse clastic supply
Moderately to strongly positive area
Weakly positive area
Continental deposition
Erosion or non-deposition
Marine deposition

Figure 22. Paleogeographic map of Western Canada for Belly River time (after Williams and Burk, 1964; Ogunyomi and Hills, 1977).

the likely sources of the basal Belly River sedimentary detritus. They also suggested that 'younger' sedimentary formations such as Pakowki/Wapiabi could have contributed some of the detrital mudrock fragments. Lerbekmo (1963) and Ogunyomi and Hills (1977) also believe that the metamorphosed phases of the Belt Series in contact with Mesozoic intrusives is the source of the metamorphic material present in Belly River sediments. The Belt Series is exposed in western Montana, northern Idaho and southeastern British Columbia (Ogumyomi and Hills, 1977) and could have been exposed during Campanian time. Contemporaneous Cretaceous volcanic rocks of west-central Montana, as well as older volcanic rocks, appear to have contributed detritus to the Belly River sediments, especially to those of the southern Foothills (Lerbekmo, 1963). Lerbekmo argued that, on the basis of prevalence of bentonites in the Upper Cretaceous Alberta sediments and a grain size study of one of the bentonites in the Drywood River section, the volcano contributing to the southern Belly River sediments could have existed within 100 miles of the Drywood River section and would now be covered by the overthrust belt of the present Rocky Mountains. Ogunyomi and Hills (1977), who worked on the Foremost and Oldman Formations of Milk River area further east, believed that the Cretaceous Elkhorn Mountain volcanics in west-central Montana probably supplied most of the volcanic detritus. The location of the volcanic source area for the central Foothills' Belly River sediments is less certain as volcanic rocks of Cretaceous age are rare in British Columbia (Lerbekmo, 1963). The writer thinks it likely that volcanic centers similar to that postulated by Lerbekmo (1963) for the southern Belly River sediments in the overthrust belt of the Rocky Mountains could have existed in the region of the central and northern Rocky Mountains. This suggestion is supported by significant proportions and indeed an increase in the proportion of the volcanic rock fragments in the sandstones of the central Foothill sections as revealed by the present study (see Chapter V1). Rahmani and Lerbekmo (1975) also stated that contemporaneous volcanism in British Columbia and western Montana supplied large volumes of detritus during Late Cretaceous time.

Although most workers on Belly River sediments agree on the scarcity or rarity of microcline feldspar in Belly River sandstones and therefore doubt an interpretation favoring a major batholithic contribution, there is enough indirect evidence to believe that plutonic igneous terrains contributed to the basal Belly River Sediments. This includes :

1. the realization that orthoclase rather than microcline is the normal potash feldspar of some batholiths, for example, the Coast Range batholith of southern British Columbia (K.C. McTaggart, 1961 as cited by Lerbekmo, 1963),
2. comparable radiometric K/Ar ages of 110 Ma and 107 Ma for the Nelson batholith orthoclase and Belly River sandstone orthoclase, respectively. The close correspondence of the age of the Belly River sandstone with that of the Nelson batholith orthoclase convinced Lerbekmo (1963) to favor an interpretation of origin from a Mesozoic batholithic pluton for the Belly River orthoclase. This therefore strongly suggests contribution of detritus by plutonic rocks to the basal Belly River sediments despite the absence or scarcity of microcline feldspar. Lerbekmo (1963) favored the Nelson batholith of south-central British Columbia and the Idaho batholith as the main western Mesozoic plutons that contributed to Belly River sediments, for the following reasons: (a) both have orthoclase apparently dominating microcline, and in the Nelson batholith, at least, this orthoclase is largely sodic with smaller than normal optic angle, and (b) the Idaho batholith has phases particularly rich in allanite.

Rahmani and Lerbekmo (1975), based on their K-Ar dates of detrital hornblende, also believe that the Mesozoic crystalline rocks of the northern Omineca geanticline (Cassiar Mountains) were major contributors to the Upper Cretaceous sediments. Nelson and Glaister (1975) favor the Central Cordillera of south-central British Columbia as a major contributor of basal Belly River clastics, based on detrital composition analysis and some paleocurrent data from the basal Belly River sandstone exposure at Trap Creek.

It is pertinent to note that Rahmani and Lerbekmo (1975), who carried out a more regional study of the provenance of the Upper Cretaceous sediments in the southern, central, and northern Foothills of Alberta based on heavy mineral analysis, recognized and emphasized the contribution of detritus to the Belly River depositional area by distributive provinces to the north/northwest of the study area in British Columbia (the eastern Cordillera – Omineca geanticline). They believe that the Proterozic and Lower Cambrian clastic sedimentary rocks (e.g., Atan Group) and the Upper Palaeozoic eugeosynclinal rocks such as the Carboniferous-Permian Cache Creek Group equivalents in central British Columbian contributed most of the sedimentary detritus. The low- to high-grade metamorphic rocks found along the length of the Omineca geanticline of the eastern Cordillera (Monger and Hutchison, 1971, as cited by Rahmani and Lerbekmo, 1975), probably contributed most of the metamorphic detritus. They also believe that contemporaneous volcanism in British Columbia and probably western Montana, as well as older volcanics in the interior of British Columbia, made an appreciable contribution to the terrigenous detrital clastics of the Belly River Group. They suggested that Late Cretaceous volcanics (rhyolite, rhyodacite, and dacite ash-flow and ignimbrite) in the western Cordillera in British Columbia, may well have contributed the bulk of the volcanic material to the Upper Cretaceous sediments.

Paleocurrent Analysis and the Dispersal Pattern of Basal Belly River Sediments.

Although there is considerable agreement on the identification and location of possible source terrains of the basal Belly River sediments based on comparative studies of the light- and heavy-mineral assemblages (Lerbekmo, 1963; Rahmani and Lerbekmo, 1975; McLean, 1971; Ogunyomi and Hills, 1977; Nelson and Glaister, 1975), the question of dispersal pattern is controversial. Part of the problem arises from the relatively limited nature of the study areas, concentration of the studies in southern Alberta and southwestern Saskatchwan, and the existence of possible source rocks in the south, west and north of the Belly River depositional basin. The only exception to limited study areas is the regional study by Rahmani and Lerbekmo (1975), which embraced most of the geographic areas covered by the other authors and therefore has the advantage of viewing the problems of provenance and dispersal of the Belly River sediments regionally, especially with regard to the south, central and northern Foothills.

In the present regional study, paleocurrent measurements were made at fourteen outcrop sections (Figure 20). Directional structures measured were cross-stratification (medium and large scale trough cross-bedding) and a few sole marks in the form of flute casts (Figure 23). The paleocurrent measurements (Table 9, Figure 20) show that transport directions were rather variable across the study area during basal Belly River deposition. A study of the paleocurrent data (Table 9, Figure 20) reveals that most of the stratigraphic sections south of Bow River indicate a dominant north to south transport direction. The only exceptions to this are the Crowsnest River (Lundbreck) and Trap Creek sections with

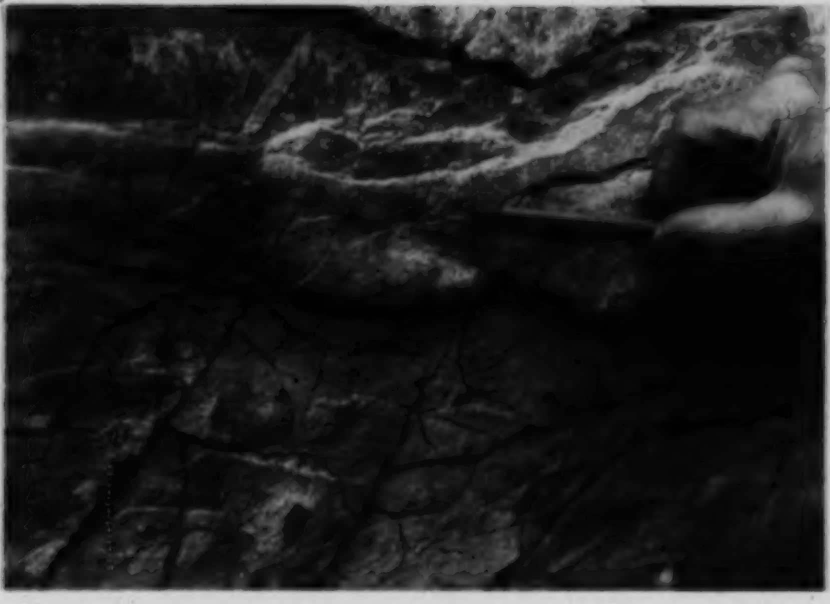

Figure 23. Flute casts on the sole of Unit 5 high-angle cross-stratified sandstone facies (G) at Morley.

dominant south to north transport direction. The sections north of the Bow River, on the other hand, show a dominant south to north (mostly southeast to northwest) transport direction, with the exception of the James River section which shows a dominant north to south direction like the southern sections.

A southeast to northwest transport direction indicated by the paleocurrent data of most of the northern sections seems anomalous when considered in the light of the overall paleogeography of North America during the Upper Cretaceous and Early Tertiary time. But when one considers the fact that most stream deposits show cross-bedding variance of up to 90 or 120 degrees, and that in deltas and littoral deposits cross-bedding is even more variable, commonly lying within a 180 to 220 degree sector (Jungst, 1938, as cited by Potter and Pettijohn, 1977, p.109), one realizes how dangerous reliance on paleocurrent data for dispersal pattern can be. Potter and Pettijohn (1977, p. 103-111) in their discussion of the principles of interpretation of cross-bedding data and inference of paleoslope emphasized the importance of integrating a cross-bedding study with other geologic evidence such as lateral variations in grain size, formation thickess, and proportion of marine sediment and so on. They recommend the evaluation of the direction of sediment transport indicated by the sedimentary structures along with other available characteristics of the deposit. They stated that in most cases there is a good agreement between cross-bedding direction and these other sedimentary properties, whereas in some other cases agreement is lacking.

The writer discounts the likelihood of a general southeast to northwest transport direction as indicated by the available cross-bedding directions in most of the northern sections on the basis of the known paleogeography of western North America during basal Belly River time. He thinks this direction could be a local phenomenon reflecting some local structure in the basin or its immediate vicinity rather than a general paleoslope effect, or a reflection of bias in outcrop pattern affecting exposure of measurable cross-stratification. As Potter and Pettijohn (1977, p. 111) have aptly suggested, a qualitative appraisal of paleocurrent data rather than a more precise statistical evaluation is more realistic. The writer infers a major north to south transport direction during basal Belly River deposition. Minor south to north, and west to east dispersals, especially in the southern Foothills of Alberta, are also indicated. This is based on:

1. the detrital composition of the basal Belly River sandstone and its similarity to most of the rocks of the Omineca geanticline,
2. the more marine nature of the southern sections,
3. the more abrupt nature of the Wapiabi/Belly River Formation transition of the northern stratigraphic sections, and
4. the dominant north to south transport direction indicated by the cross-bed data of the southern sections.

This direction is in accord with some of the earlier paleocurrent inferences for Belly River sediments such as those of Williams and Burk (1964), Rahmani and Lerbekmo (1975), and Shawa and Lee (1975). But it is at variance with the paleocurrent direction inferred for the Belly River sediments by McLean (1971), Ogunyomi and Hills (1977), Nelson and Glaister (1975), and Dodson (1971). These authors inferred a dominant south to north/northeast paleocurrent direction for Belly River sediments. Their studies, however, have two main limitations :

1. they are confined to the southern portion of Belly River deposits and therefore overemphasized the south to north component of the paleocurrent data ; a close look at their paleocurrent data shows that a significant proportion of their measurements also indicate a north to south transport direction,
2. some of these studies lack detailed information from actual measurements of directional structures and therefore based their paleocurrent direction solely or mainly on the similarity of the detrital composition of the Belly River sediments to those of a possible provenance.

From the foregoing discussion, a more general picture of provenance and dispersal pattern for the basal Belly River Formation only emerges when one considers all available evidence, from both the present study and previously published data. These include :

1. detrital composition of the basal Belly River sandstones,
2. regional paleocurrent data,
3. the more abrupt nature of the Wapiabi/Belly River Formation transition of the northern stratigraphic sections,
4. the more marine nature of the southern sections indicating a longer period of marine

conditions/residency in the south during basal Belly River deposition,

5. the greater thickness of recognizable Belly River sediments or their equivalent in the south [800 m. (Lerbekmo, 1963) as compared to 250 m. of the lower Brazeau Formation (Belly River Formation equivalent) of the northern Foothills (Rahmani and Lerbekmo, 1975)],
6. radiometric age determinations of Lerbekmo (1963), and Rahmani and Lerbekmo (1975),
7. the general tectonic evolution of the Western Canadian Cordillera.

The above considerations favor a major north to south sediment transport direction with possible minor east to west, and south to north transport directions during basal Belly River deposition.

In summary, with increased tectonic uplift in the Cordillera during Middle Campanian time and the consequent withdrawal of the Wapiabi/Lea Park sea, many rivers contributed detritus to the shoreline of this Upper Cretaceous epicontinental sea, flowing mostly from the north/northwest to south/southeast. This resulted in the formation of a series of deltas that constitute the basal Belly River deltaic deposit. In all probability, some of the rivers also flowed directly eastward from the rising ancestral Rocky Mountains. Continued shoreline progradation in a south/southeast direction resulted in the deposition of the fluvio-deltaic Belly River Formation over the marine Wapiabi Shale.

VI. MINERALOGICAL COMPOSITION AND CLASSIFICATION

Classification

The basal Belly River sandstone in the study area is composed mainly of rock fragments (38–90%), quartz (2–44%) and feldspars (7–34%), averaging 53.1, 25.4 and 21.5%, respectively (Table 10). All thirty analysed samples are classified as lithic sandstone according to the scheme of Chen (1968) (Figure 24). Two observations are worth noting:

1. All the samples are low in quartz content, which rarely exceeds, 40 percent of the essential components.
2. There is some interenvironmental (lithofacies) variation among the samples, with the coarser facies G samples being richer in quartz and chert grains, whereas the finer-grained facies F and H samples, and some facies B and D samples, are rich in volcanic and mudrock fragments. There is, however, some compositional overlap between facies G and some of the "coarser" (fine grained variety) facies H sandstones.

This variation in detrital composition appears to be grain size related which in turn is related to the depositional environment.

Quartz

On the bases of the type and amount of inclusions, crystal outline and extinction character, four quasi-genetic types of quartz, as defined by Folk (1959), plus quartzite (polycrystalline quartz) grains, were identified in the samples (Table 11). The most abundant type observed is "common" quartz which makes up from 1 to 36% of the rock and averages 17.1%. It is characterized by irregular outline, a few inclusions in the form of bubbles, and only moderately undulose extinction (Plate 1A,B). These characteristics are suggestive of plutonic origin but the possibility of other origins, such as metamorphic and vein, cannot be ruled out (Folk, 1959; Blatt et al., 1980; Iwuagwu and Lerbekmo, 1982).

The second most abundant quartz type is the schistose metamorphic variety. It makes up from less than 1 to 8% of the sample and averages 3.4%. Strong undulose extinction and inclusions of metamorphic minerals such as micas characterize these quartz

Table 10. Essential components (recalculated to 100%).

Serial No.	Sample No.	Depositional Environment	Quartz (%)	Feldspar (%)	Rock Fragments (%)
1	D1	Distal bar	32.0	25.0	43.0
2	D2	Stream mouth bar	27.8	33.9	38.3
3	D15B	Stream mouth bar	24.2	25.2	50.6
4	D17B	Stream mouth bar	36.7	22.6	40.7
5	D18	Crevasse splay	28.3	28.7	43.0
6	D23	Crevasse splay	32.1	29.4	38.5
7	D24B	Fluvial channel	27.4	29.1	43.5
8	D26B	Fluvial channel	40.0	21.5	38.6
9	D27(ii)	Crevasse splay	44.3	19.3	36.3
10	D30B	Crevasse splay	34.7	24.8	40.5
11	D34B	Fluvial channel	44.0	12.0	43.8
12	D37B	Fluvial channel	33.3	11.0	55.7
13	D47	Crevasse splay	18.6	15.9	65.5
14	D48B	Crevasse splay	23.3	22.5	54.2
15	M2	Crevasse splay	7.8	22.4	69.8
16	M3	Crevasse splay	21.8	24.0	54.2
17	M5	Crevasse splay	18.7	19.2	62.1
18	M6	Fluvial channel	24.3	11.4	64.2
19	M8	Crevasse splay	25.0	22.8	52.2

20	M10	Crevasse splay	19.3	22.6	58.1
21	M12	Crevasse splay	28.4	21.9	49.7
22	M21B	Fluvial channel	27.1	14.7	58.2
23	M26B	Fluvial channel	23.4	22.8	53.8
24	M30B	Fluvial channel	17.9	21.9	60.2
25	S4/3-36	Stream mouth bar	21.4	26.6	52.0
26	S6/3-36	Stream mouth bar	20.7	24.1	55.2
27	S10/3-36	Stream mouth bar	2.4	7.0	90.6
28	S11/3-36	Stream mouth bar	17.9	22.1	60
29	S18/3-36	Crevasse splay	13.1	29.6	57.3
30	S21/3-36	Fluvial channel	25.1	11.1	63.8

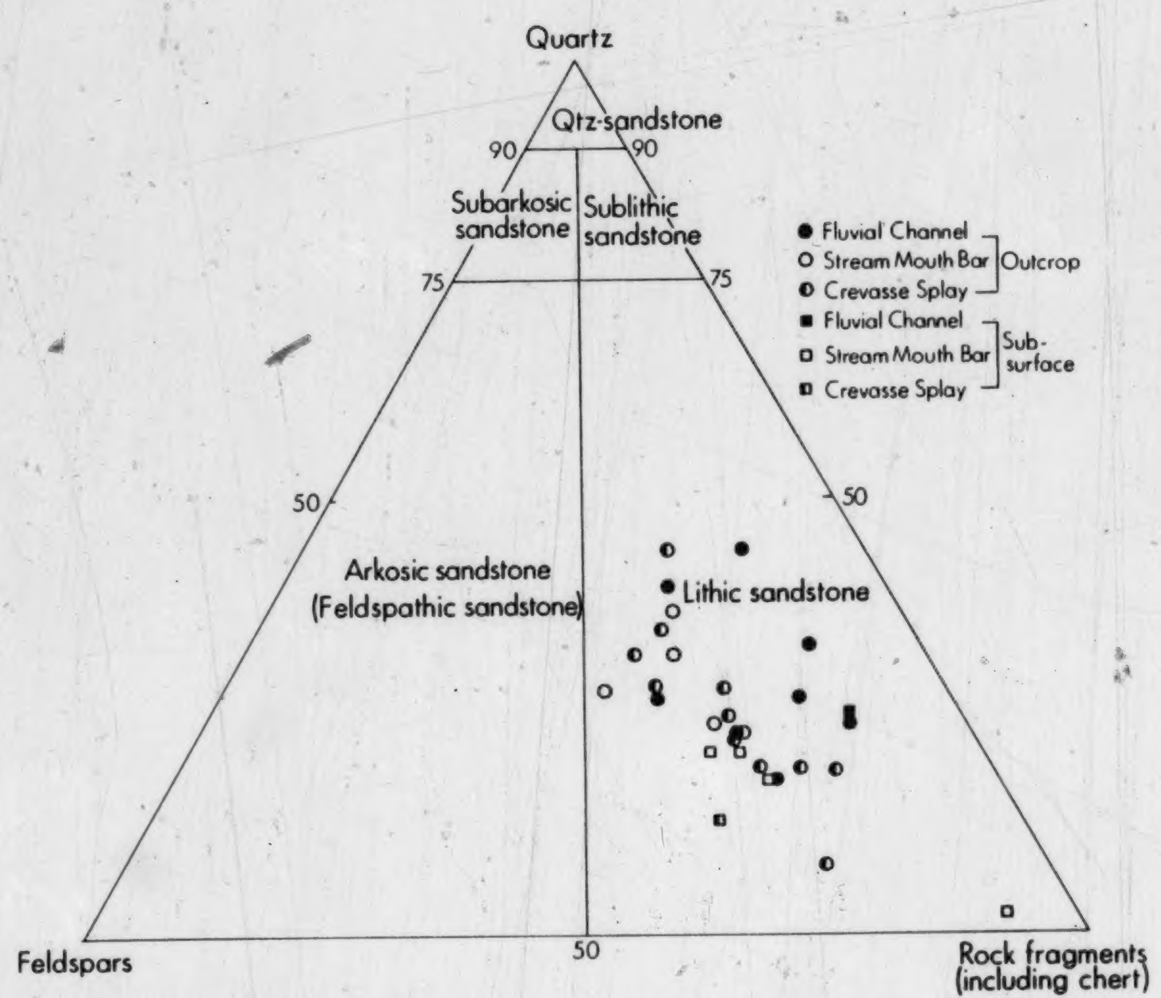

Figure 24. Detrital composition of basal Belly River sandstone in the study area.

Table 11. Quartz types as percentage of total essential components.

Ser.No	S.No.	Env.	Med.	C	M	V	S	QF
1	D1	DB	3.4 (0.1mm)	26.0	5.1	Trace	0.2	0.6
2	D2	SMB	3.0 (0.13mm)	22.8	3.7	Trace	Trace	1.4
3	D15B	SMB	3.8 (0.07mm)	17.6	3.1	Trace	Trace	3.6
4	D17B	SMB	3.5 (0.09mm)	28.5	4.2	0.2	Trace	3.8
5	D18	CS	3.6 (0.08mm)	20.8	4.2	0.2	0.4	2.6
6	D23	CS	3.2 (0.11mm)	21.5	6.8	0.2	0.4	3.1
7	D24B	FC	3.1 (0.12mm)	21.9	4.7	Trace	Trace	0.8
8	D26B	FC	2.3 (0.2mm)	29.5	2.8	0.2	2.1	5.4
9	D27(ii)	CS	2.5 (0.18mm)	36.1	2.8	0.5	0.7	4.2
10	D30B	CS	2.5 (0.18mm)	20.9	8.0	0.2	1.0	4.6
11	D34B	FC	2.3 (0.2mm)	30.7	5.2	Trace	1.0	7.1

12	D37B	FC	1.8 (0.29mm)	25.7	3.6	0.2	1.1	2.4
13	D47	CS	3.8 (0.07mm)	16.3	1.0	Trace	Trace	1.3
14	D48B	CS	3.8 (0.07mm)	20.6	0.4	Trace	Trace	2.3
15	M2	CS	–	6.4	1.1	Trace	Trace	0.4
16	M3	CS	3.4 (0.1mm)	14.7	1.3	Trace	0.2	5.6
17	M5	CS	3.3 (0.1mm)	12.5	3.0	Trace	Trace	3.2
18	M6	FC	2.15 (0.23mm)	12.5	2.1	Trace	Trace	9.7
19	M8	CS	3.1 (0.12mm)	13.3	6.1	Trace	0.4	5.3
20	M10	CS	3.4 (0.1mm)	12.6	3.4	Trace	0.2	3.2
21	M12	CS	2.9 (0.13mm)	18.8	4.5	0.2	Trace	4.9
22	M21B	FC	2.2 (0.22mm)	10.3	4.4	Trace	Trace	12.4
23	M26B	FC	2.3 (0.2mm)	10.3	3.3	Trace	0.4	9.4
24	M30B	FC	2.2 (0.22mm)	9.6	3.2	Trace	0.6	8.6
25	S4/3	SMB	3.4	14.3	4.0	Trace	0.2	3.0

26	S6/3	SMB	3.3	13.0	3.3	0.2	0.2	4.1
27	S10/3	SMB	2.8	1.1	0.4	0.2	Trace	0.7
28	S11/3	SMB	3.4	8.4	2.6	Trace	Trace	7.0
29	S18/3	CS	3.7	10.4	0.9	Trace	0.2	1.6
30	S21/3	FC	2.5	11.1	1.9	Trace	0.4	11.7
		Average		17.14	3.37	0.08	0.32	4.6

Env.= depositional environment; DB= distal bar; SMB= stream mouth bar; CS= crevasse splay; FC= fluvial channel; Med.= thin section median (phi); C= "common"; M= metamorphic; V= volcanic; S= sedimentary; QF= quartzite rock fragments; Ser.No= serial number; S.No= sample number.

Plate 1. Photomicrographs of thin sections of basal Belly River sandstones.

A. Channel sandstone showing "common" quartz (q), polycrystalline quartz (pq), carbonate rock fragment (cf), mudrock fragment (m), detrital chlorite (cl) and corrensite pore filling cement (arrows). Plane light. X40.

B. Same as A, but between crossed polarizers. X40.

C. Fragmental volcanic quartz (q), without many inclusions, being partially replaced by calcite cement (c) giving a sawtooth contact; detrital carbonate fragment (cf). Crossed polarizers. X40.

D. Quartzite (pq) rock fragment with inclusions of mica; metamorphic quartz (mq) and mudrock fragment (m). Plane light. X40.

E. Same as D, but between crossed polarizers. X40.

F. Unaltered potassic feldspar (o) with Carlsbad twinning; mudrock fragment (m). Crossed polarizers. X40.

G. Partially altered microcline feldspar (mi), common quartz (q), chert rock fragment (ch) and pore (P) crossed polarizers. X40.

H. Volcanic rock fragment with feldspar microlites (V); partially altered plagioclase feldspar showing polysynthetic twinning (pf); chert rock fragment (ch). Crossed polarizers. X40.

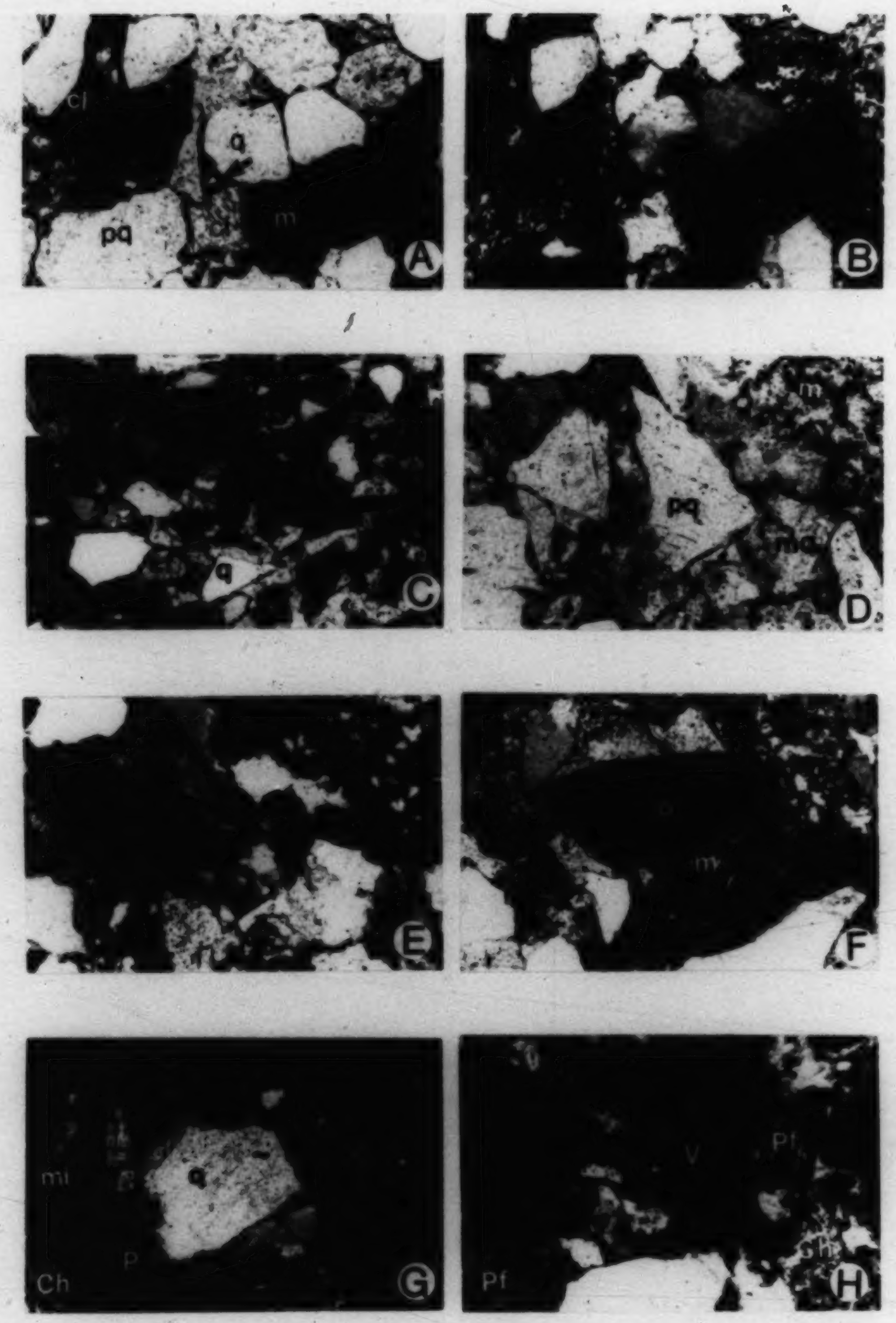
cl
q
pq
m
A
B
q
C
m
pq
mq
D
E
m
F
mi
q
P
Ch
G
V
Pf
Pf
sh
H

PLATE 1

grains.

Sedimentary quartz (up to 2%) is next in abundance, averaging 0.3%. Quartz grains included in this variety are characterized by appreciable rounding, but as Thiel (1940) showed, quartz grains of medium sand size require much transport to produce noticeable rounding; hence the apparent counts of up to 2% are almost certainly too low. It is likely that many first cycle sedimentary quartz grains have been mistakenly included in other varieties.

Quartz identified as volcanic in origin is the least abundant of the quartz types (less than 1% in all cases) and averages 0.1%. It is characterized by one or more well-developed nondiagenetic crystal faces and a lack of inclusions. In the case of fragmented volcanic quartz grains without preserved crystal faces, the absence of inclusions (Plate 1C) alone was used as a basis for identification.

Quartzite rock fragments (polycrystalline quartz grains) form up to 12% of the sandstones and average 4.6%. The individual quartz crystals within the composite grain show strong undulose extinction, characteristic of metamorphic quartz. The presence of metamorphic minerals such as muscovite is also common within the grains (Plate 1A, B, D, E).

Feldspars

The feldspars were classified into potassic and plagioclase types (Table 12). To facilitate the identification of the potassic feldspars, they were stained yellow with sodium cobaltinitrite. The potassic feldspars are commonly fresh in appearance (Plate 1F) and constitute less than 1 to more that 8% of the detrital grains averaging 2.5%. They are mostly orthoclase, though a few microcline crystals were observed (Plate 1G). The plagioclase feldspars form 6 to 26% (19% average) of the sandstone and, in contrast to the potassic feldspars, most are altered (Plate 1H).

Rock Fragments

Sedimentary, metamorphic and volcanic rock fragments are all common constituents of the basal Belly River sandstone (Table 13). Sedimentary rock fragments are the most abundant and consist of mudrocks, carbonates, and cherts. The mudrock

Table 12. Feldspar types as percentage of total essential components.

Serial No.	Sample No.	Depostional Environment	Median Grain Size (Phi)	Potassic Feldspar	Plagioclase Feldspar
1	D1	Distal Bar	3.4 (0.1mm)	4.2	20.8
2	D2	Stream Mouth Bar	3.0 (0.13mm)	8.9	25.0
3	D15B	Stream Mouth Bar	3.8 (0.07mm)	3.1	22.1
4	D17B	Stream Mouth Bar	3.5 (0.09mm)	5.9	16.7
5	D18	Crevasse Splay	3.6 (0.08mm)	4.8	23.9
6	D23	Crevasse Splay	3.2 (0.11mm)	6.0	23.4
7	D24B	Fluvial Channel	3.1 (0.12mm)	6.2	22.9
8	D26B	Fluvial Channel	2.3 (0.2mm)	6.8	14.7
9	D27(ii)	Crevasse Splay	2.5 (0.18mm)	6.8	12.5
10	D30B	Crevasse Splay	2.5 (0.18mm)	1.2	23.6
11	D34B	Fluvial Channel	2.3 (0.2mm)	2.3	9.7
12	D37B	Fluvial Channel	1.8 (0.29mm)	2.4	8.6
13	D47	Crevasse Splay	3.8 (0.07mm)	3.3	12.7
14	D48B	Crevasse Splay	3.8 (0.07mm)	3.8	18.7
15	M2	Crevasse Splay	-	Trace	22.4
16	M3	Crevasse Splay	3.4 (0.1mm)	Trace	24.0
17	M5	Crevasse Splay	3.3 (0.1mm)	0.9	18.4
18	M6	Fluvial Channel	2.2 (0.23mm)	Trace	11.4
19	M8	Crevasse Splay	3.1 (0.12mm)	Trace	22.8

20	M10	Crevasse Splay	3.4 (0.1mm)	0.8	21.9
21	M12	Crevasse Splay	2.9 (0.13mm)	1.2	20.7
22	M21B	Fluvial Channel	2.2 (0.22mm)	Trace	14.7
23	M26B	Fluvial Channel	2.3 (0.2mm)	0.2	22.6
24	M30B	Fluvial Channel	2.2 (0.22mm)	0.6	21.3
25	S4/3-36	Stream Mouth Bar	3.4 (0.1mm)	Trace	26.6
26	S6/3-36	Stream Mouth Bar	3.3 (0.1mm)	Trace	24.1
27	S10/3-36	Stream Mouth Bar	2.8 (0.14mm)	0.2	6.7
28	S11/3-36	Stream Mouth Bar	3.4 (0.1mm)	Trace	22.1
29	S18/3-36	Crevasse Splay	3.7 (0.08mm)	6.5	23.1
30	S21/3-36	Fluvial Channel	2.5 (0.18mm)	0.2	10.9
		Average		2.5	19.0

Table 13. Rock Fragments as Percentage of Total Essential Components.

S.No.	Environ.	Median	Carb	Ch	Mr	Meta	Vr	OC	G	B	M	Chl	E	Z
D1	DB	3.4	17.0	1.9	16.5	4.0	3.6	0.5	T	2.3	0.8	0.3		T
D2	SMB	3.0	9.1	0.9	25.0	2.5	0.7	0.8		2.2		1.3		T
D15B	SMB	3.8	25.2	2.4	21.1	0.7	1.2	0.5	0.3	1.3		0.2		
D17B	SMB	3.5	13.4	3.3	15.1	6.6	2.4	1.5	0.2	1.2	0.3	0.7		0.2
D18	CS	3.6	6.1	2.9	27.0	4.4	2.6	0.3	T	1.0	0.2	0.2		
D23	CS	3.2	12.4	2.1	18.0	3.3	2.7	1.5	T	2.0	0.3	1.2		0.2
D24B	FC	3.1	11.9	2.5	17.6	5.0	6.5	0.3		0.8	0.2	4.0		T
D26B	FC	2.3	4.7	6.8	12.6	10.3	4.2	0.3		2.0		0.5		T
D27(ii)	CS	2.5	6.8	7.3	12.3	7.1	2.8	0.8		0.8		1.0		T
D30B	CS	2.5	14.8	6.8	9.5	6.3	3.2			1.2		0.3		T
D34B	FC	2.3	6.9	12.7	8.8	11.1	4.4	0.2		1.7	0.2	0.5	T	T
D37B	FC	1.8	6.9	20.5	15.8	7.3	5.2	0.2		2.3	0.2	0.2		
D47	CS	3.8	10.0	2.1	47.1	2.5	3.8	0.7	T	0.7	0.3	1.2		T
D48B	CS	3.8	21.0	1.9	26.9	2.1	2.3	1.2	T	0.3	0.7	0.7		
M2	CS		T	3.2	60.8	0.9	5.0	1.7		0.3	0.7	2.7		
M3	CS	3.4	T	7.1	39.6	1.3	6.2	1.7		0.2	0.2	2.3		T
M5	CS	3.3	T	6.6	46.4	3.6	5.5	1.0		0.5	0.3	1.2		T
M6	FC	2.2	T	23.6	20.2	11.8	8.6	0.8				0.2		T
M8	CS	3.1	0.2	5.1	29.8	6.1	11.0	0.7		0.3		2.0		T
M10	CS	3.4	T	3.6	37.0	8.8	8.8	1.3		1.7	0.5	2.8		

M12	CS	2.9	T	6.1	28.4	5.7	9.4	1.2		0.5		0.5		T
M21B	FC	2.2	T	14.5	25.4	9.5	8.8	1.2		0.7		0.5		
M26B	FC	2.3	T	10.5	17.1	19.7	5.9	1.2		0.3	0.2		0.5	
M30B	FC	2.2	T	13.1	23.4	16.7	7.0	1.0		1.8	0.2	0.5	0.2	
S4/3	SMB	3.4	1.2	2.6	30.8	6.2	11.3	2.5		0.5		1.2	T	
S6/3	SMB	3.3	1.4	3.3	35.5	4.3	10.8	1.6		0.3	0.2	0.5		
S10/3	SMB	2.8	59.5	2.2	26.8	1.1	1.1	1.5		2.3	0.7	0.2		
S11/3	SMB	3.4	1.6	4.4	39.5	12.7	1.8	2.8	T	1.0	0.2	0.8		
S18/3	CS	3.7	0.4	3.2	47.8	1.1	4.9	3.8	T	0.7	0.8			
S21/3	FC	2.5	T	17.5	28.4	11.9	6.0	0.8		0.3	0.2	0.3		
	Av.	=	7.7	6.7	27.0	6.5	5.3	1.12		1.04	0.25	0.96		

Environ.= depositional environment; S.No.= sample number; DB= distal bar; SMB= stream mouth bar; CS= crevasse splay; FC= fluvial channel; T.S= thin section; Median= thin section median in phi; Carb= carbonate; Ch= chert, Mr= mudrock fragment, Meta= metamorphic rock fragment, Vr= volcanic rock fragment, T= trace, OC= opaque and carbonaceous material, G= glauconite, B= biotite, M= muscovite, Chl= chlorite, E= epidote, Z= zircon. * Means as a percentage of the total detrital components.

fragments are the most plentiful of the sedimentary rock fragments, constituting an average of 27%. Included are essentially all fine, detrital silicate rocks of silt and clay sizes (Plate 1A, B, E, F; 2A, B). Carbonate rock fragments are the second most abundant and average 7.7% of the sandstone. They are fine-grained limestone, dolomite or sideritic fragments, as well as coarse single crystals (Plate 2C, D, E). Chert fragments (cryptocrystalline siliceous rock fragments) average 6.7% of the sandstones (Plate 1H; 2A, B). Both colorless and pale brown varieties are common.

Low-grade metamorphic rock fragments in the form of argillite and metasiltstone are abundant in all samples and average 6.5%. Argillite, a metamorphic equivalent of mudrock, is characterized by slight recrystallization of fine phyllosilicates into coarser metamorphic minerals such as sericite, and a fairly homogeneous texture. Metasiltstone, the metamorphic equivalent of siltstone, consists essentially of silt-size quartz grains and micas (Plate 2C, D).

Fine-grained silicic volcanic rock fragments average 5.3% of the sandstones. Many are characterized by the presence of aligned plagioclase feldspar microlites giving them a trachytic texture (Plate 1H).

Carbonaceous and other opaque materials of uncertain affinity are present in almost all the samples, but do not constitute a significant proportion (less than 1.2% average). Some of the carbonaceous materials show some cell structures and are very likely carbonized leaf and stem fragments.

Varietal/Accessory Minerals

Biotite, muscovite, chlorite, zircon, epidote, glauconite, apatite and tourmaline form the varietal and accessory mineral suite recognized in thin section. Biotite and chlorite are the most prevalent, averaging 1% each of the detrital composition of the sandstone. The biotite grains are mostly brown to reddish brown in color and are probably in part iron-rich metamorphic varieties. Muscovite occurs in nearly all samples but rarely constitutes 0.5% of the sandstones. "Glauconite" (deep green and light green microcrystalline pellets), zircon, epidote, apatite and tourmaline were sparingly encountered in some samples.

Plate 2. Photomicrographs of thin sections of basal Belly River sandstone.

A. Mudrock fragment (m), polycrystalline quartz (pq), chert rock fragment (ch), and kaolinite cement completely plugging a pore (k). Plane light X40.

B. Same as A, but between crossed polarizers. X40.

C. Metasiltstone (ms), coarse grained composite dolomite rock fragment (d), partially leached volcanic rock fragment with intraparticle porosity (v) and paritally leached mudrock fragment (m). Plane light X40.

D. Same as C, but between crossed polarizers. X40.

E. Carbonate rock fragment (cf) probably of algal origin or algal affected. Note also a siderite rich mudrock fragment (m), and calcite replacement cement (c); calcite replaces the interstitial matrix between (m) and (cf). Plane light. X40.

F. Kaolinite pore fill (k), calcite pore fill (c), and quartz overgrowth (qo). Note also thin clay lining (arrow) and significant proportion of detrital quartz (q) which characterizes channel sandstones. Plane light X64.

G. Same as F, but between crossed polarizers. X64.

H. Fibrous corrensite cement (co) occluding a pore. Note also "common" quartz. Plane light. X200.

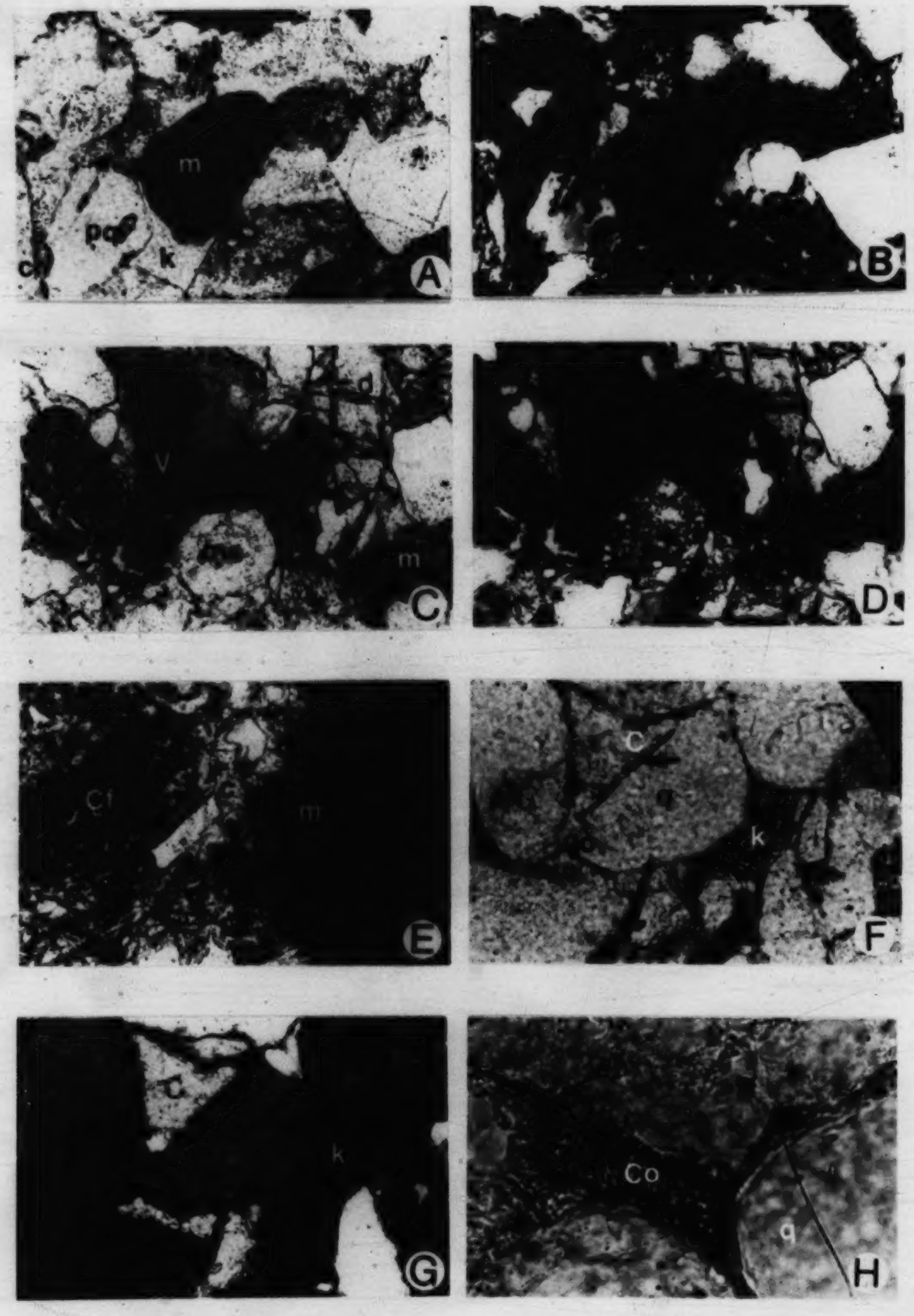
m
pa
c
k
A
B
d
v
m
C
D
Cl
m
E
c
q
k
F
c
k
G
Co
q
H

PLATE 2

The general uneven distribution of these varietal and accessory minerals is a reflection of differences in provenance of the detritus, depositional environment and the hydraulic sorting of the sediments. Zircon and apatite are most common in samples from sections south of Bow River, whereas epidote and tourmaline were only observed in samples from Bow River and sections north of it. This is due to differences in the provenance and dispersal pattern of the southern and northern section sediments. The micas (biotite, muscovite) and chlorite are most abundant in the crevasse splay and stream mouth bar sandstones and are due to some hydraulic sorting of the sediments. There is a preferential settling out of these micas in the 'quieter' depositional milieu of delta front and crevasse splay. On the other hand, glauconite was only observed in lower delta front, stream mouth bar and some crevasse splay sandstones, with the deep green variety most common in the lower delta front and stream mouth bar sandstones. The restriction of this mineral to these sandstones is due to the chemistry of the depositional environment. Marine waters usually produce deeper colored glauconite than brackish to fresh waters.

VII. TEXTURE: GRANULOMETRIC ANALYSIS

A. Size Frequency Distribution

The raw data obtained from the grain size analyses using thin sections and a Humphries' micrometer eyepiece are presented in Appendix C. The results of these analyses were plotted as cumulative curves using a probability scale ordinate to show the size frequency distribution of the samples (Figure 25 and Appendix D). These log-probability plots show the percentage frequency greater than a particular value and facilitate visual comparison of the samples. The cumulative frequency percent-probability is believed to be meaningful with regard to depositional processes (Visher, 1969) and will be discussed in greater detail later. The raw data were also plotted as bar graphs (histograms) which represent frequency by area; these further characterize the samples and aid their visual comparison (Figure 26 and Appendix E).

Parameters

From the cumulative curves, descriptive statistical measures of average size (mode, median, graphic mean) and sorting or uniformity (inclusive graphic standard deviation) were obtained. Folk's (1959) formulae were used for the computation of these graphic statistics. Arithmetic means and standard deviations were also computed for these samples by the method of moments (Iwuagwu, 1979). The calculated thin section statistics were converted to their sieve equivalent values by using Adams' (1977) formulae.

Table 14 summarizes these derived and converted descriptive statistical parameters. The samples have sieve median diameters that range from 2.2 phi to 4.7 phi (0.22mm to 0.04mm) (fine sand to coarse silt). Sieve inclusive graphic standard deviations of 0.15 phi to 0.65 phi were computed for the samples, though most are in the range of 0.20 phi to 0.50 phi. According to Folk's (1959) classification scale for sorting, these samples are very well sorted (standard deviation under 0.35 phi) to well-sorted (standard deviation = 0.35 to 0.50 phi). The samples are therefore characterized as fine-to very fine-grained, well to very well sorted sandstones and coarse siltstones.

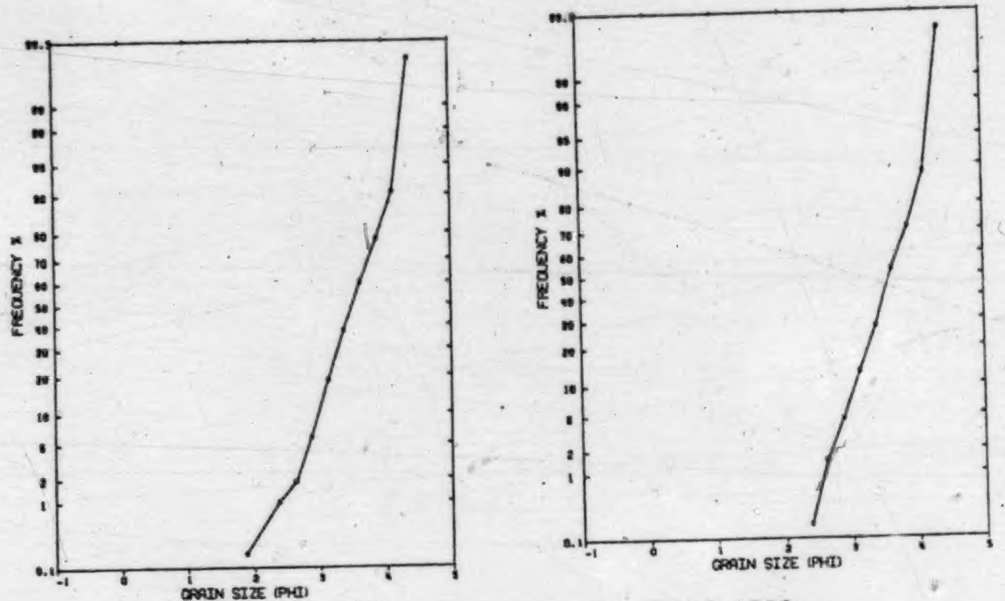

A. Sample D1

B. Sample D18

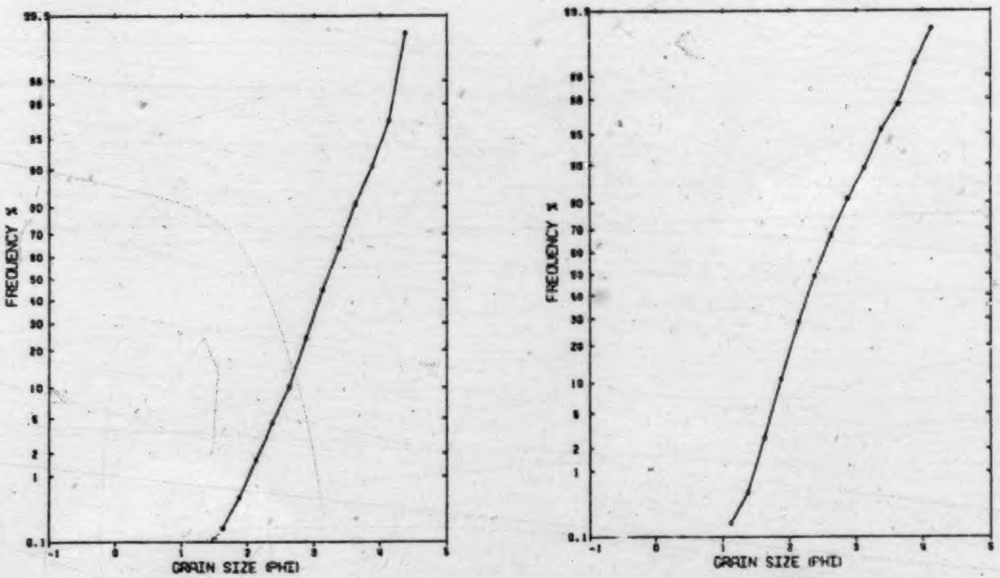

C. Sample D24B

D. Sample D34B

Figure 25. Size frequency of representative basal Belly River sandstones in the study area, determined by thin section analysis. A, B, C and D illustrate distal bar, crevasse splay, channel sandstone with some fine fraction and channel sandstone without fine fraction respectively.

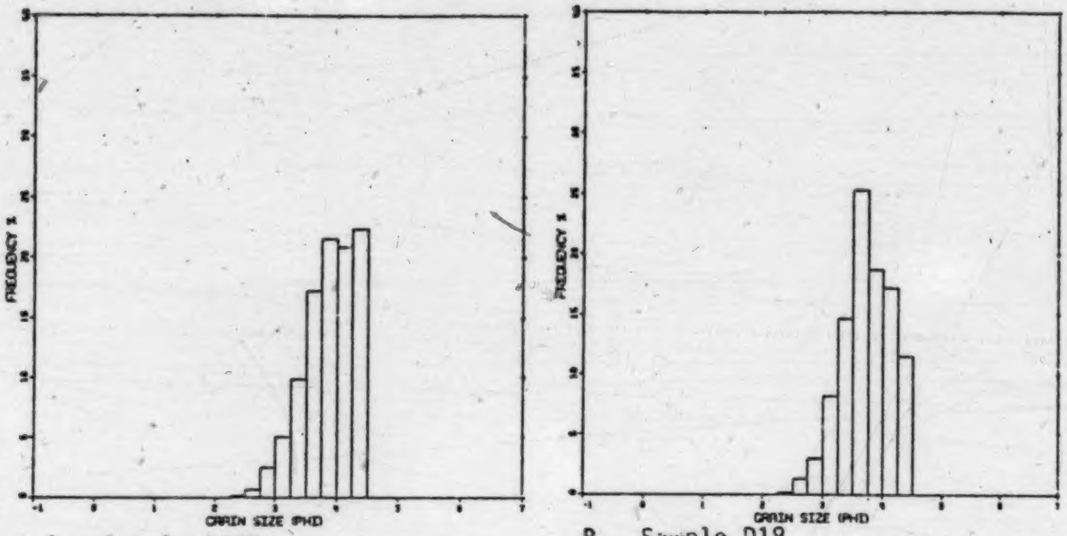

A. Sample D15B

B. Sample D18

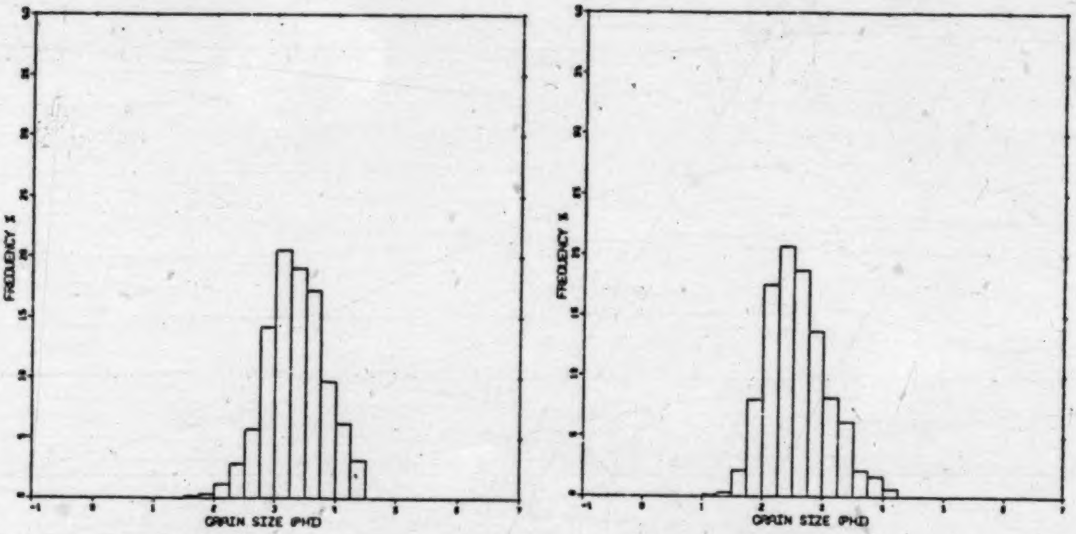

C. Sample D24B

D. Sample D34B

Figure 26. Histograms of samples representative of basal Belly River sandstones in the study area. A, B, C and D illustrate negatively skewed stream mouth bar, negatively skewed crevasse splay, symmetrical channel sandstone and positively skewed channel sandstone respectively.

Table 14.Summary statistics of the granulometric analyses (phi units) of basal Belly River sandstones.

S.No	Env.	Mod.	Med.	S.Med	TSGM	SGM	TSAM	SAM	TSIGSD	SIGSD	ASD	%F
D1	DB	3.63	3.4	3.9	3.5	4.0	3.64	4.1	0.44	0.31	0.43	15.0
D2	SMB	3.13	3.0	3.5	3.1	3.5	3.24	3.67	0.56	0.42	0.51	4.5
D15B	SMB	4.38	3.8	4.4	3.8	4.3	3.9	4.38	0.42	0.30	0.42	30.0
D17B	SMB	3.63	3.5	4.0	3.6	4.1	3.7	4.17	0.41	0.29	0.43	15.0
D18	CS	3.63	3.6	4.1	3.6	4.1	3.64	4.1	0.42	0.3	0.42	18.0
D23	CS	3.13	3.2	3.7	3.2	3.7	3.29	3.73	0.55	0.41	0.53	6.0
D24B	FC	3.13	3.1	3.6	3.2	3.7	3.33	3.77	0.49	0.36	0.49	5.0
D26B	FC	2.38	2.3	2.7	2.4	2.8	2.49	2.87	0.57	0.43	0.54	0.1
D27II	CS	2.63	2.5	2.9	2.5	2.9	2.6	2.99	0.6	0.46	0.57	0.7
D30B	CS	2.63	2.5	2.9	2.5	2.9	2.66	3.05	0.52	0.39	0.52	0.2
D34B	FC	2.38	2.3	2.7	2.4	2.8	2.57	2.95	0.48	0.35	0.51	0.3
D37B	FC	1.88	1.8	2.2	1.9	2.3	2.01	2.35	0.66	0.51	0.63	0.1
D47	CS	3.63	3.8	4.4	3.7	4.2	3.79	4.26	0.45	0.32	0.42	24.0
D48B	CS	3.88	3.8	4.4	3.8	4.3	3.82	4.29	0.45	0.32	0.45	28.0
M2	CS											
M3	CS	3.38	3.4	3.9	3.6	3.9	3.46	3.91	0.64	0.49	0.63	17.0
M5	CS	3.38	3.3	3.8	3.3	3.8	3.47	3.92	0.53	0.40	0.51	10.0
M6	FC	2.13	2.2	2.6	2.2	2.6	2.32	2.69	0.56	0.42	0.58	0.3
M8	CS	2.88	3.1	3.6	3.2	3.7	3.21	3.64	0.49	0.36	0.49	3.5
M10	CS	3.38	3.4	3.9	3.5	4.0	3.53	3.98	0.56	0.42	0.54	15.0

M12	CS	2.88	2.9	3.4	2.9	3.3	2.91	3.32	0.53	0.40	0.56	3.0
M21B	FC	2.38	2.2	2.6	2.3	2.7	2.42	2.79	0.51	0.38	0.51	0.2
M26B	FC	2.38	2.3	2.7	2.3	2.7	2.47	2.85	0.52	0.39	0.49	0.1
M30B	FC	2.13	2.2	2.6	2.3	2.7	2.39	2.76	0.51	0.38	0.53	0.3
S4/3	SMB	3.63	3.4	3.9	3.4	3.9	3.44	3.89	0.57	0.43	0.55	12.0
S6/3	SMB	3.13	3.3	3.8	3.3	3.8	3.34	3.78	0.48	0.35	0.49	6.0
S10/3	SMB	2.63	2.8	3.3	2.8	3.2	2.87	3.28	0.82	0.65	0.81	5.0
S11/3	SMB	3.63	3.4	3.9	3.4	3.9	3.45	3.90	0.53	0.39	0.51	8.0
S18/3	CS	3.88	3.7	4.3	3.7	4.2	3.78	4.25	0.50	0.37	0.47	25.0
S21/3	FC	2.38	2.5	2.9	2.5	2.9	2.57	2.95	0.64	0.49	0.61	0.4
M14	CS	3.88	3.7	4.3	3.7	4.2	3.75	4.22	0.48	0.35	0.43	22.0
M15	CS	3.88	3.8	4.4	3.7	4.2	3.77	4.24	0.46	0.33	0.44	22.0
M18B	CS	2.88	2.7	3.2	2.7	3.1	2.77	3.17	0.55	0.41	0.54	0.6
M21T	FC	2.63	2.5	2.9	2.5	2.9	2.61	3.0	0.48	0.35	0.48	0.6
M22B	FC	1.88	1.9	2.3	2.0	2.4	2.1	2.45	0.55	0.41	0.54	0.1
M22T	FC	3.13	3.1	3.6	3.1	3.5	3.20	3.63	0.57	0.43	0.51	5.0
M24B	FC	3.38	3.2	3.7	3.2	3.7	3.36	3.8	0.44	0.31	0.45	4.0
M26T	FC	2.13	2.1	2.5	2.2	2.6	2.27	2.63	0.47	0.34	0.49	0.3
M30T	FC	2.63	2.5	2.9	2.6	3.0	2.69	3.08	0.45	0.32	0.46	0.3
OR3B	DB	4.38	4.0	4.6	3.9	4.4	4.06	4.6	0.34	0.23	0.37	54.0
OR3T	DB	4.38	3.9	4.5	3.8	4.3	3.92	4.4	0.14	0.29	0.41	35.0
OR4T	DB	4.38	4.1	4.7	4.0	4.5	4.14	4.64	0.25	0.15	0.31	62.0

OR5B	DB	4.38	3.9	4.5	3.8	4.3	3.95	4.43	0.38	0.26	0.39	38.0
OR5T	DB	4.38	4.0	4.6	3.9	4.4	4.0	4.49	0.38	0.26	0.41	50.0
OR6B	SMB	4.38	4.0	4.6	3.9	4.4	3.95	4.43	0.30	0.19	0.37	52.0
OR6T	SMB	4.38	3.9	4.5	3.8	4.3	3.94	4.42	0.41	0.29	0.42	20.0
OR8B	SMB	4.38	4.0	4.6	3.9	4.4	4.01	4.5	0.34	0.23	0.41	48.0
OR8T	SMB	3.63	3.5	4.0	3.5	4.0	3.64	4.1	0.49	0.36	0.49	18.0
OR10B	SMB	4.38	3.8	4.4	3.8	4.3	3.85	4.33	0.42	0.30	0.43	28.0
OR10T	SMB	3.63	3.4	3.9	3.4	3.9	3.52	4.0	0.56	0.42	0.53	15.0
OR11B	SMB	3.38	3.3	3.8	3.3	3.8	3.43	3.88	0.48	0.35	0.45	7.0
OR11T	SMB	3.38	3.3	3.8	3.3	3.8	3.4	3.84	0.51	0.38	0.47	7.0
OR12B	FC	3.38	3.3	3.8	3.3	3.8	3.4	3.84	0.49	0.36	0.5	7.0
OR12T	FC	2.63	2.5	2.9	2.6	3.0	2.75	3.15	0.59	0.45	0.59	3.7
OR14B1	CS	2.88	2.9	3.4	2.9	3.3	3.01	3.43	0.56	0.42	0.55	4.6
OR14T1	CS	4.38	4.1	4.7	4.0	4.5	4.1	4.6	0.29	0.18	0.34	58.0
OR14B2	CS	2.88	2.7	3.2	2.7	3.1	2.81	3.21	0.60	0.46	0.61	1.8
OR14B3	CS	2.63	2.4	2.8	2.4	2.8	2.6	3.0	0.55	0.41	0.55	0.6
OR14T3	CS	2.63	2.5	2.9	2.6	3.0	2.71	3.10	0.61	0.47	0.58	1.2

S.No.=sample number; Mod.=thin section mode; Med.=thin section median; S.Med.= sieve median; TSMG=thin section graphic mean; SGM=sieve graphic mean; TSAM=thin section arithmetic mean; SAM=sieve arithmetic mean; TSIGSD=thin section inclusive graphic standard deviation; SIGSD=sieve inclusive graphic standard deviation; ASD=arithmetic standard deviation; %F=Percent finer than 4 phi; DB=distal bar; SMB=stream mouth bar;CS=crevasse splay; FC=fluvial channel; Env.=depositional environment.

Textural Maturity

As a corollary to the sorting of these samples, this sandstone unit is classified as texturally mature, since with the exception of one sample, all the standard deviations are under 0.50 phi and the detrital grains are still not rounded (Folk, 1959). (See following for the discussion of roundness). It is pertinent to note that size sorting is dependent on various factors whose individual effects are difficult to assess. Such factors include size range of available particles, current characteristics, type of deposition and rate of supply of detritus compared with efficiency of the sorting agent (Folk, 1959).

B. Other Textural Attributes

The textural attributes of shape and fabric were also studied in the course of the granulometric analysis. Roundness, an element of shape, was studied by visual comparison of grains with standard images of grains of known roundness. According to Power's (1953) scale of roundness, the grains are very angular, especially in the very fine-grained crevasse splay sandstones, to subrounded in the coarser fluvial channel sandstones; these correspond to Folk's (1955) rho values of 0 to 4. Experimental studies indicate that roundness is related to the degree of abrasion or wear suffered by the particle during transport and therefore should be related to the type and length of transport or reworking (Blatt et al., 1972, p.65). The very angular character of most of the facies F and H sandstones is a reflection of their suspension mode of transport in which the grains are provided with a cushioning effect by the transporting medium (water) and therefore are less abraded. The more rounded (subrounded) nature of the coarser facies G sandstones is due to significant abrasion that results from the grains rubbing against one another during transport (attrition effect). The better rounding of the facies G samples therefore indicates traction and saltation modes of transport for these. Discussion of the fabric of these samples is deferred till Chapter VIII.

C. Paleohydraulics : Interpretation of the Grain Size Curves

As Folk (1959) has aptly stated, it is difficult to deduce precise information about any/all of the factors that influence size sorting of sediments. However, the following is an attempt to deduce what the current characteristics, mechanisms of transport and deposition, and rate of suppply of detritus were like during the deposition of these sands and silts. It is an attempt to reconstruct from the grain size distribution the physical forces that produced these sandstones and siltstones.

An inspection of the cumulative frequency curves of the studied samples (Figure 25 and Appendix D) shows that:

1. Most of the curves contain two or three more or less straight line segments (subdivisions);
2. Most of the samples have breaks in slope at about 4 phi; in some cases a second break exists between 2 and 3 phi;
3. The segment of the curve above the 4 phi break, which represents the percent of silt and clay present in a sample, is quite variable. It ranges from less than 1 to 62 percent;
4. Most of the samples have maximum grain diameter of about 2 phi (0.25mm), i.e., around the medium/fine sand boundary; only a few samples have a maximum grain diameter of 1 phi (0.5mm) or greater, i.e., coarse sand size.

The problem of predicting the competence of flows, or of inferring the properties of a flow from the largest size of particle in a given sedimentary deposit is of interest to both geologists and engineers (Blatt et al., 1972, p. 90; Visher, 1969). Shields (1936, as cited by Blatt et al., 1972) provided a fairly simplified, reasonably satisfactory solution to the problem; he related the grain size (diameter) to shear stress (tangential force per unit area of surface), among other things. For sand and gravel, the critical shear stress is roughly proportional to quartz size (Blatt et al., 1972, p. 91). Using Shields' diagram and considering that the average maximum diameter of the basal Belly River sandstones is 0.5mm and that these grains are of quartz composition, the required critical bottom shear-stress for initiation of movement of the coarsest grains is only about 3 dynes/sq cm or a shear velocity of 1.73cm/sec. This translates to a critical velocity of about 20cm/sec for grains of about 0.5mm in the older Hjulstrom diagram which expresses competency in terms of a critical velocity. The above figures should at best be regarded as approximations since ripples and other irregularities on the bed cause local variations in shear stress and consequently reduce the average bottom shear stress needed to start movement of the grains. In the region of grain sizes smaller than sand sizes, finer sizes require larger velocities for movement, especially if they are more cohesive than sand (Blatt et al., 1972, p. 90-94).

The similarity within groups of log-probability curves (consistency of the position of inflection points, slopes of the segments etc.) suggest meaningful relationships regarding the depositional process and possibly environments of the studied samples. Studies in hydraulics of stream transport (fluid mechamics concepts) have established the three modes of sediment transport as traction (sliding and rolling), saltation, and suspension and relate grain size distribution of the resultlant depositis to their mode of transport and deposition (Moss, 1962, 1963 as cited by Visher, 1969). If one accepts the concept that each mode of transport is capable of generating a specific type of deposit, it is reasonable to suggest that each segment of a log-probabiliity curve (subpopulation) represents a deposit from a specific transport/deposition mechanism. But the interpretation of which part of the curve (segment) represents which mechanism, especially traction and saltation mechanisms, is somewhat conjectural and needs more field and laboratory data. However, Visher (1969) attempted to relate the subpopulations and their possible transport mechanisms to specific depositional environments. He states that the points of inflection (breaks in slope) divide the samples into subpopulations each of which represents a different sediment transport mechanism. These mechanisms are related to the depositional environments. He further classified the log-probability curves, based upon their overall shape, into specific environments such as shallow marine, beach, distributary channel, fluvial channel, and turbidity current. Whereas I agree with Visher's (1969) suggestion that each segment of a log-probability curve may represent a specific mode of transport, supplementary information is probably necessary to confidently relate the curves to depositional environments. However, one can at least use the textural information to infer the dominance of a given transportation/deposition processes in a given depositional environment. A further use can be made of such textural information in the characterization of the different sandstone lithofacies of the present study. This allows the application of knowledge gained from a widespread outcrop study to the domain of the subsurface where only a limited data base is available. See Chapter X for more detailed discussion of the possible use of textural information in the subsurface.

Based on the above data and discussion, one can conclude that:

1. Facies B, D, F and the very fine variety of H sandstones were deposited mainly from suspension, saltation and traction being subordinate; hence their high percentages of fine fraction.
2. The facies G sandstones and some of the coarser facies H sandstones were mainly transported and deposited by a process or processes other than suspension, notably by saltation and traction mechanisms; hence their low contents of fine fraction.
3. The very well to well sorted nature of facies B, D, F and some H sandstones are due to hydraulic sorting of the sediment during transportation prior to deposition, whereas the well sorted nature of the facies G sandstones is due to winnowing of the sediments in their depositional milieu by relatively strong currents.

D. Textural Characterization of Basal Belly River Sandstone Lithofacies

A further textural characterization and refinement of basal Belly River sandstone lithofacies involves a more detailed examination and classification of their log-probabiliity curves and histograms. Study of these reveals interesting groupings of curves and histograms which correspond to definite lithofacies. Two main groups of log-probability curves are common, namely:

1. A group with high percentage of fine fraction (15 to 62 percent finer than 4 phi) and
2. A group with low percentage of fine fraction (generally less than 5 percent finer than 4 phi).

The group with high percentage of fine fraction is further divisible into two: (a) those with two points of inflection - one at about 4 phi and the other between 2 and 3 phi; this group mostly characterizes the facies B and D sandstones; (b) those with only one point of inflection at about 4 phi; this is characteristic of the facies F and H sandstones. Likewise the group with low percentage of fine fraction is divisible into two: (a) those with a single point of inflection at about 4 phi and (b) those that have no conspicuous point of inflection and plot essentially as a straight line. These two last classes of curves characterize the facies G sandstones.

E. Textural Summary

In summary, a detailed textural analysis of basal Belly River sandstone lithofacies reveals some differences among them. These include differences in overall shape of the log-probability curves, symmetry/asymmetry of the histograms, sorting and percentage of the fine fraction (less than 4 phi).

1. Facies B and D samples generate log-probability curves that tend to have three segments (Fig. 25A), whereas the facies F and H samples usually have two segment curves (Fig. 25B). Facies G samples, on the other hand, generate either two segment log-probability curves or curves without any point of inflection at all (Fig. 25C, D). Although facies F and H samples generate two segment cumulative curves like facies G samples, facies F and H invariably do not contain grains larger than 1 phi; only facies G samples contain such grains and on the average have the largest median diameter.
2. These differences in size grading are also easily discernable from their histograms (Fig.26). Facies B, D, F and H samples are usually negatively skewed (with coarse tail); facies G samples are either symmetrical or positively skewed (with fine tail). However, some of the coarser facies H samples, which are very likely channel portions of crevasse splays, tend to mimic the facies G histograms by being either symmetrical or positively skewed.
3. The amount of fine fraction present in some of the lithofacies appears to be diagnostic. Facies G samples invariably contain less than 5 percent of fine fraction, whereas facies B, D, F and H usually contain significant amounts of fines (Fig. 27; Table 14). Facies B and D samples contain 5 to 62 percent of these fines; facies F and H samples contain 1 to 58 percent of fines but mostly in the range of 15 to 30%. The occasional low-fine-fraction variety of facies H does not however contain grains up to 1 phi; its largest grains average 2.0 phi.
4. Facies B and D samples have sieve median sizes of 3.3-4.7 phi, whereas facies G samples have sieve median diameters of 2.2-3.8 phi. Facies F and H samples on the hand have median sizes in between the extremes represented by facies B and D, and

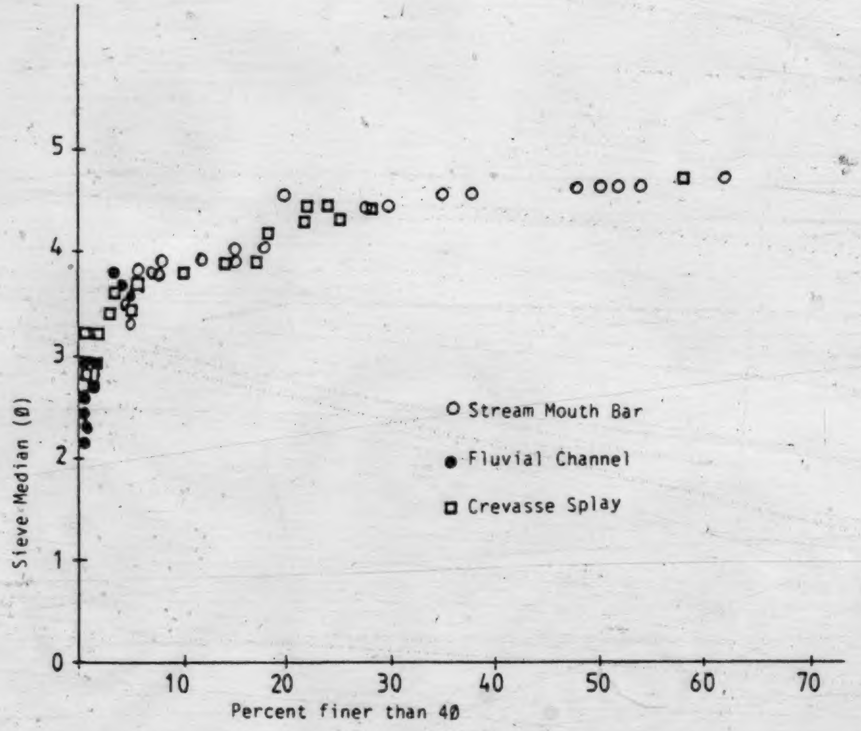

Figure 27. Sieve Median Diameter vs. Percent Finer than 40 of basal Belly River sandstones.

facies G. They have sieve median sizes of 2.8–4.7 phi.

5. The sieve inclusive graphic standard deviation values range from 0.15–0.43 phi for facies B and D samples, through 0.18–0.49 phi for facies F and H samples to 0.31–0.50 phi for facies G samples. Facies B and D samples are on the average the best sorted, whereas facies G samples are the most poorly sorted. The data for facies F and H samples are, as usual, in betweeen the two extremes.

A plot of the sieve median diameter versus sieve inclusive graphic standard deviation shows that the finest samples, mostly facies B and D samples, are the best sorted, whereas the coarsest samples, mostly facies G samples, are the most poorly sorted. Sorting improves with decrease in median diameter, probably reflecting a single dominant deposistional mechanism, likely suspension. The poorer sorting of the coarser samples is indicative of operation of more than a single transport/depositional mechanism.

VIII. DIAGENESIS

Most of the diagenetic features observed in the present study are similar to those described by Iwuagwu (1979), Iwuagwu and Lerbekmo (1981, 1982). However, differences exist in the magnitude of the various diagenetic processes in the different sandstone lithofacies of the present study. The net effect of diagenesis in all cases is the reduction of the initial porosity and probably permeability of these sandstones. Diagenetic processes responsible for pore space reduction in these sandstones can be divided into three categories: mechanical compaction, authigenic cementation, and to a less extent replacement. The fourth diagenetic process of solution has resulted in the enhancement of porosity of some of the lithofacies by the dissolution of some of the volcanic and mudrock fragments, as well as feldspars, resulting in moldic secondary porosity.

The type and magnitude of diagenetic alterations are to a large extent dependent on particle size and mineralogical composition of the detrital components, the depositional environment and the postdepositional temperature, pressure, hydrologic and chemical regimes of the diagenetic environment (Krumbein, 1942; Mankiewicz and Steidtmann, 1979). Some of the diagenetic processes and effects are more prominent in some lithofacies than in others. In the present study, a detailed study of the diagenetic features in the various sandstone lithofacies shows a variation in diagenetic patterns. These variations are strongly related to the texture and mineralogic composition. The particle size and sorting of the detrital components as well as the mineralogy are to a large extent different in the different lithofacies (see Chapters VI and VII). For example, whereas facies B, D, F and some H samples are very-fine grained and rich in volcanic and mudrock fragments, facies G samples are coarser (fine- to medium grained) and rich in quartz and chert fragments. These variations in texture and detrital composition are dependent on the depositional processes and environments. The particle size and detrital composition, and therefore indirectly the depositional environment, controlled the diagenetic history of the sandstones by determining the type of diagenetic process or processes and the degree to which they operated in the basal Belly River Sandstone.

Four broad facies related diagenetic patterns are observed in the present study. These are:

1. Early calcite cementation of facies B sandstones.

2. Compaction and authigenic clay cementation of facies D sandstones.
3. Mechanical compaction, and occasional cementation (calcite and authigenic clays) of facies F and H sandstones.
4. Extensive authigenic clay cementation of facies G sandstones.

A. Diagenesis of Facies B Sandstones

Lithofacies B sandstones (distal bar sandstones) are characterized by calcite plugging of their original porosity. The "open" packing (low packing proximity) of the grains (appearing to "float" in a groundmass of calcite cement (Plate 7A,B)) and the absence of other types of cement or grain alteration in these samples indicate the early origin of calcite cementation in these sands. It is very likely that the cementing calcite had a local source, possibly in the detrital components, since some of the facies B sandstones contain considerable amounts of very fine-grained carbonate rock fragments and single crystals of calcite and dolomite. Only in a few instances were some of the detrital components partially replaced by the cementing calcite; the grains appear to have been sealed in the calcite cement early in their diagenetic history and without much subsequent diagenetic alteration.

B. Diagenesis of Facies D Sandstones

Stream mouth bar samples are characterized by considerable mechanical compaction and authigenic clay cementation (Plate 3C,D; 7E,F). An evaluation of their cement-free porosity (Fig. 28) shows values of 10 to 25 percent which indicate considerable mechanical compaction. In most cases they have moderate (30 to 50 percent) packing proximity. Clay cementation is the next diagenetic process that affected stream mouth bar samples. Clay cements account for as much as 11 percent of some of the samples but range down to 3 percent (Table 15). In some cases, however, calcite cement tends to be more abundant than clay cement and the diagenetic pattern tends to mimic that of facies B sandstone (Plate 7C,D). However, other differences exist between these calcite cemented facies D samples and facies B samples in that these facies D samples have closer packing than facies B samples, and there is also a coexistence of their calcite cement with considerable authigenic clay. In these facies D samples too, the calcite

Plate 3. Photomicrographs of thin sections and SEM photomicrographs of basal Belly River sandstone.

A. Same as plate 2,H, but between crossed polarizers. X200.

B. Photomicrograph showing paragenetic sequence of the cements. Chlorite rim cement (arrow) followed by corrensite (co) which is in turn followed by kaolinite (k). Note same remaining unoccluded pore (p). Plane light. X250.

C. Subsurface sample of a stream mouth bar sandstone with extensive development of authigenic clay (ac) cement. Note also a slightly recrystallized mudrock fragment (m) and secondary pore (p) resulting from the solution of a detrital grain of which a remnant (r) is still present. Plane light. X64.

D. Same as C, but between crossed polarizers. X64.

E. SEM photomicrograph showing the relationship of a detrital grain (g) and pore fill corrensite (Co) in a channel sandstone from outcrop. Note also the submicroscopic porosity of the corrensite, e.g., (p).

F. Higher magnification of a part of E, showing exclusively the corrensite cement. Note the honey-comb (box-like) structure, stubby nature of the plates, and submicroscopic pores.

G. SEM photomicrograph showing relationship between a detrital quartz grain (q) and corrensite (Co) pore filler. Note the wispy nature of the corrensite in this location. X100.

H. Higher magnification of part of G, showing only the corrensite cement; note the submicroscopic pores, e.g., (p). X3500.

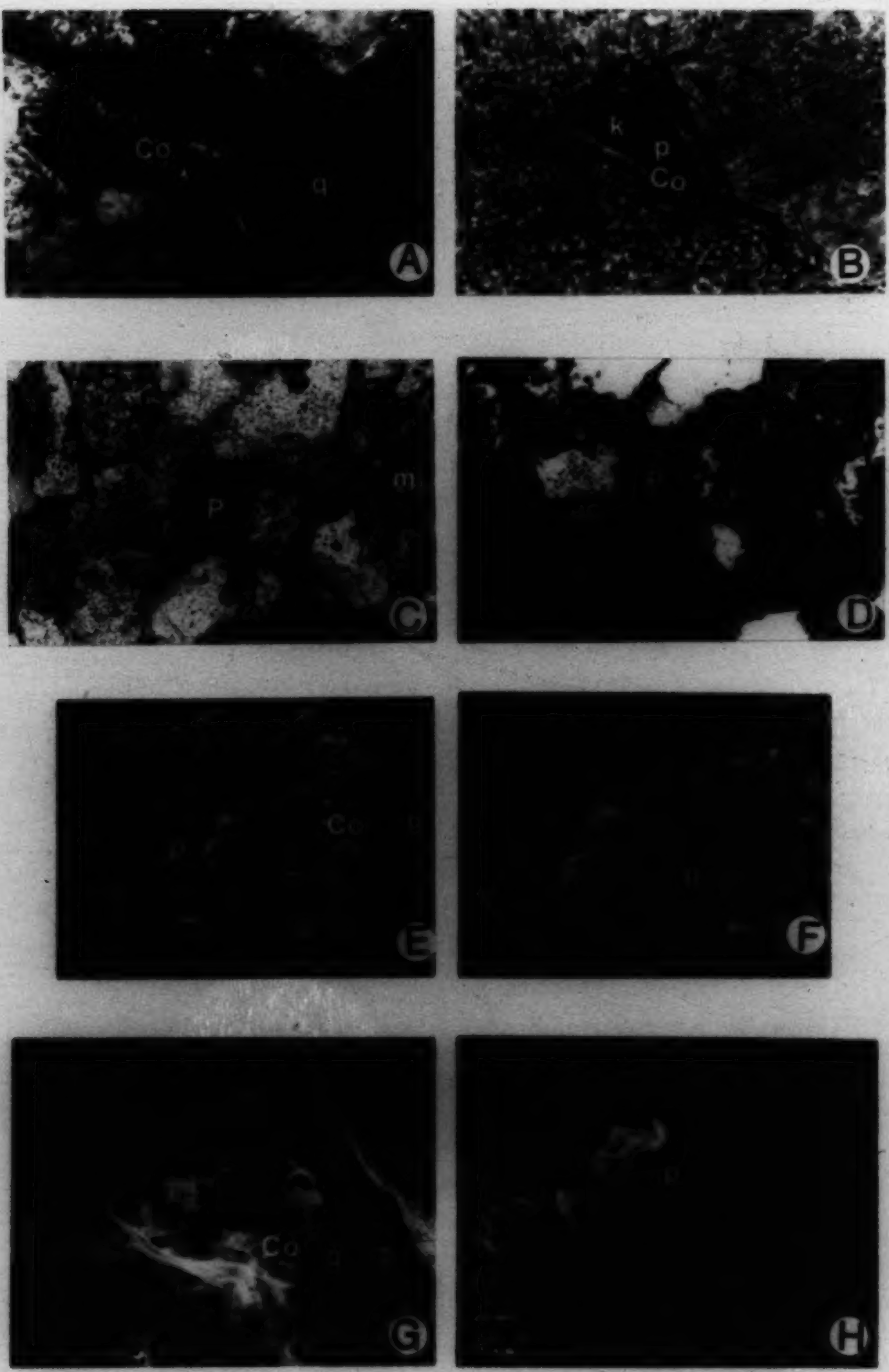
Co
q
A
k
p
Co
B
P
m
C
D
p
Co
E
F
Co
G
p
H

PLATE 3

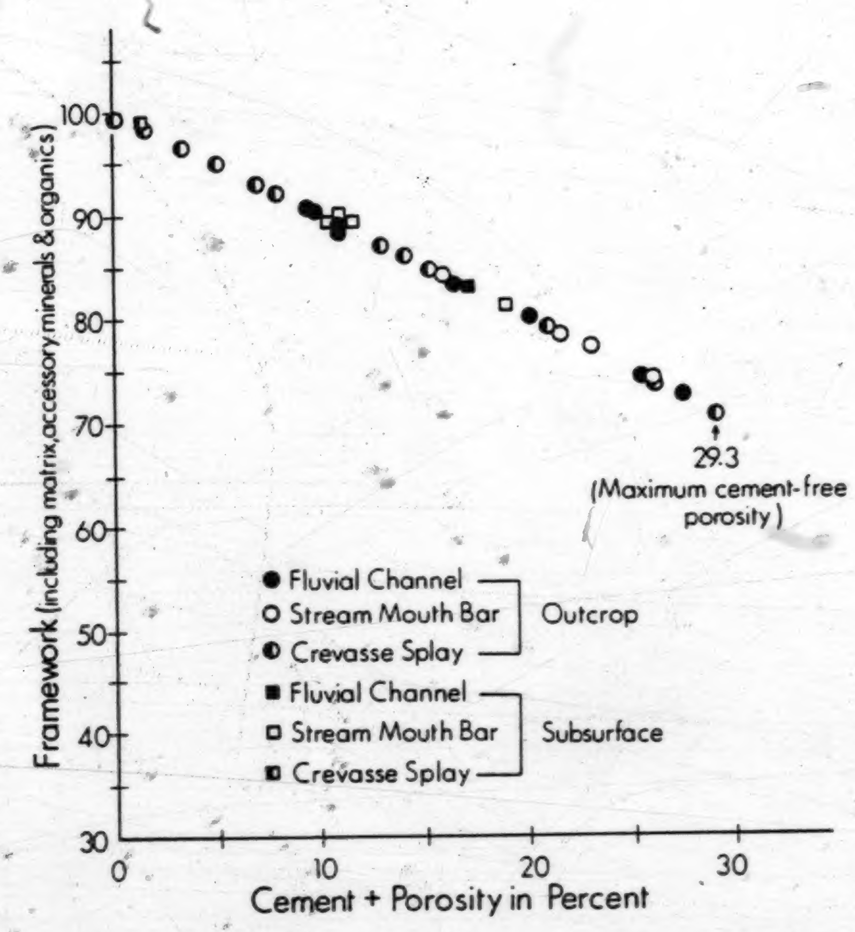

Figure 28. Framework vs. cement-free porosity (a measure of degree of compaction before cementation).

Table 15.Cement types and percentages.

S.No.	Environ	Median	Cements	Carb	Clays	Quartz	Feld	Chert	Iron
D1	DB	3.4	16.0	15.8	0.2				
D2	SMB	3.0	21.5	18.5	3.0				
D15B	SMB	3.8	25.7	20.2	5.5				
D17B	SMB	3.5	21.8	9.5	11.7	0.3			0.3
D18	CS	3.6	21.0	17.7	3.0				0.3
D23	CS	3.2	12.2	6.3	5.5				0.3
D24B	FC	3.1	27.5	26.3	1.2				
D26B	FC	2.3	23.0	21.0	2.0				
D27(II)	CS	2.5	26.3	22.3	3.7				0.3
D30B	CS	2.5	29.0	27.3	1.3		0.3		
D34B	FC	2.3	15.3	5.7	8.2				0.2
D37B	FC	1.8	19.8	18.3	1.3				0.2
D47	CS	3.8	8.0	5.3	2.5	0.2			
D48B	CS	3.8	14.0	10.7	2.8	0.3	0.2		
M2	CS		0.3	0.3					
M3	CS	3.4	5.2	0.2	4.6	0.2	0.2		
M5	CS	3.3	1.8		1.8				
M6	FC	2.2	5.2		3.3	0.2			
M8	CS	3.1	6.8	0.5	5.6			0.5	
M10	CS	3.4	3.5	0.5	2.8	0.2			

M12	CS	2.9	15.0	13.5	1.3				
M21B	FC	2.2	7.5		7.2	0.3			
M26B	FC	2.3	6.7	0.3	5.7		0.3		0.3
M30B	FC	2.2	10.3	5.0	5.0				0.3
S4/3	SMB	3.4	9.7	1.3	8.3				
S6/3	SMB	2.3	9.8	1.7	8.0	0.2			
S10/3	SMB	2.8	16.3	16.3					
S11/3	SMB	3.4	8.8	0.3	8.3	0.2			
S18/3	CS	3.7	1.5	1.2	0.3				
S21/3	FC	2.5	16.8		16.5			0.2	0.2
	Ave		13.5	8.9	4.4				

S.No.=sample number; Environ=depositional environment;Median=thin section median in phi;Cements=total cements;Carb=carbonate;Clays=authigenic clay; Feld=feldspar;Iron=iron oxide;DB=distal bar;CS=crevasse splay; FC=fluvial channel;Ave=average.

cement is mostly replacement calcite as indicated by detectable detrital component ghosts (Plate 2E).

The identification of the authigenic clay minerals is by thin section petrography, scanning electron microscopy and elemental spectral analysis. Based on optical data, the authigenic clay cement consists mainly of kaolin group mineral though illite/montmorillonite mixed-layer clay and chlorite are common (Plate 4E,F,G; 6A). They occur as pore fillings, as well as pore linings and coatings.

Simple solution is the latest diagenetic process which affected facies D samples. The very fine-grained volcanic rock fragments of these samples are partially to completely dissolved resulting in moldic secondary porosity (Plate 7E,F; 8E).

C. Diagenesis of Facies F and H Sandstones

Mechanical compaction is the most important diagenetic process that affected facies F and H sandstones. The mechanically labile components (especially shale fragments) are squeezed between the more physically stable components and into the former pores resulting in a pseudomatrix-rich texture (Plate 8A,B,H). These samples are characterized by high packing proximity, usually in excess of 70 percent, and low cement-free porosity (Fig. 28). In the fine-grained variety of facies H, thin linings and coatings of illite/montmorillonite, and calcite pore fillings are common (Plate 8C,D; 5A,B; 6C).

D. Diagenesis of Facies G Sandstones

Facies G samples are characterized by extensive development of authigenic clay cements which, in some cases, are accompanied by considerable calcite cement (Plate 2F,G,H; 3A,B). Clay cements range from less than 2 percent in the calcite-rich facies G samples to more than 16 percent in the exclusively authigenic clay cemented samples (Table 15). The authigenic clays are mostly kaolin group mineral and chlorite/montmorillonite mixed-layer clay (Plate 3E,F,G,H; 4A; 5C,D). Chlorite is present as pore-linings and coatings, though in small amounts (Plate 4B; 5E). It is pale green in color. Kaolin and chlorite/montmorillonite mixed-layer clay occur mainly as pore fillings; kaolin is characterized by first order grey birefringence (Plate 2G; 3D) and pseudohexagonal crystal

Plate 4. SEM photomicrographs of authigenic clays of the basal Belly River sandstone.

A. Kaolinite pore filling cement from a channel sandstone. Outcrop.

B. Chlorite pore fill cement from a channel sandstone. Outcrop. Note submicroscopic pores, e.g., (p).

C. Illite/montmorillonite (IM) cement bridging a pore (p).

D. Higher magnification of C. Note the submicroscopic pores (p).

E. Illite/montmorillonite (IM) and kaolinite (k) occurring in the same pore of a subsurface stream mouth bar sandstone.

F. Higher magnification of a part of E, showing exclusively the kaolinite cement (k).

G. Higher magnification of part of E, showing the illite/montmorillonite cement (IM).

H. Illite/montmorillonite from a crevasse splay sandstone. Note the honey-comb structure, and submicroscopic pores, e.g., (p). Outcrop sample.

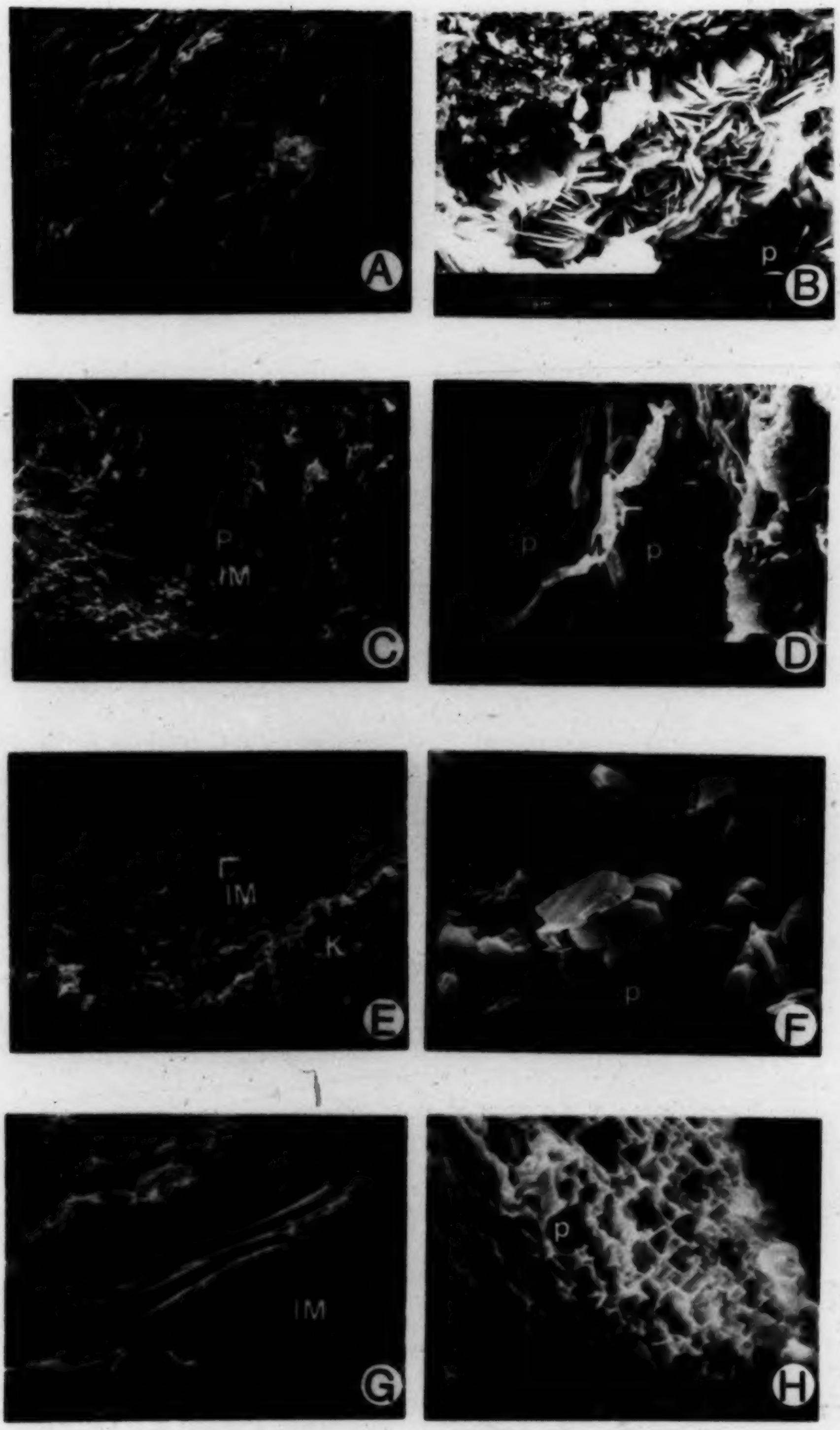
A
p
B
P
IM
C
p
p
D
IM
K
E
p
F
IM
G
p
H

PLATE 4

Plate 5. SEM photomicrograph and spectral profiles of authigenic clays of the basal Belly River sandstone.

A. Illite/montmorillonite cement from crevasse splay. Higher magnification of plate 4,H. Outcrop sample.

B. Compositional spectrum of A (illite/montmorillonite cement).

C. Compositional spectrum of 3F (corrensite).

D. Compositional spectrum of 3H (corrensite).

E. Compositional spectrum of 4B (chlorite).

F. Compositional spectrum of illite/montmorillonite mixed layer clay from a surface channel sandstone.

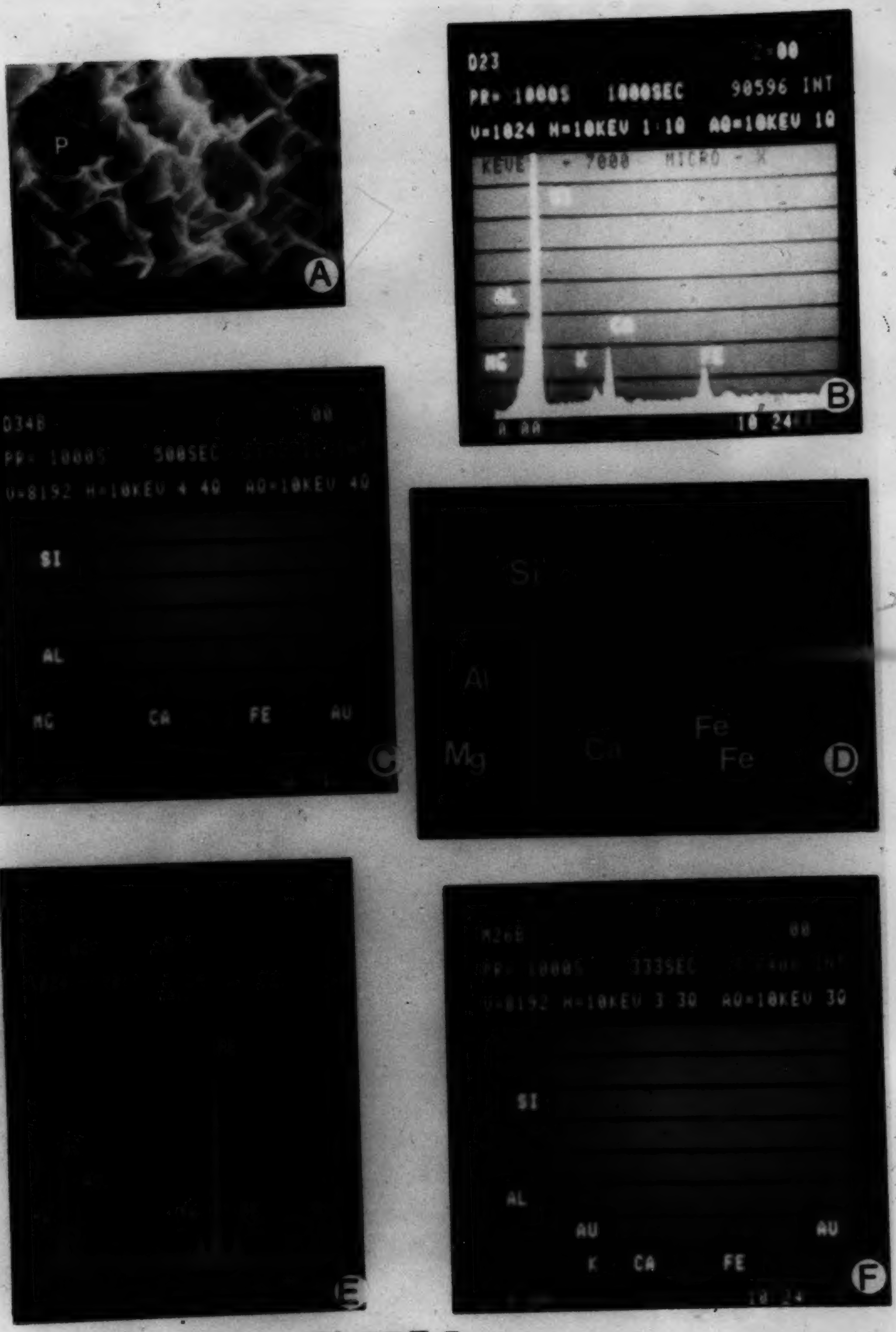
P
A
D23
PR= 1000S 1000SEC 90596 INT
V=1024 H=10KEV 1:10 AQ=10KEV 10
KEVE 7000 MICRO - X
SI
AL
CA
MG
K
FE
0.00
10.24
B
D34B
PR= 1000S 500SEC
V=8192 H=10KEV 4:40 AQ=10KEV 40
SI
AL
MG
CA
FE
AU
C
Si
Al
Mg
Ca
Fe
Fe
D
E
M26B
00
PR= 1000S 333SEC
V=8192 H=10KEV 3:30 AQ=10KEV 30
SI
AL
AU
AU
K
CA
FE
10.24
F

PLATE 5

Plate 6. Composition of authigenic clay cements of basal Belly River sandstone as displayed by the energy-dispersive X-ray spectrometer.

A. Compositional spectrum of 4G (illite/montmorillonite, and chlorite), from a subsurface sample of a stream mouth bar sandstone.

B. Compositional spectrum of kaolinite cement from a subsurface sample of a channel sandstone.

C. Compositional spectrum of illite/montmorillonite clay from an outcrop sample of a crevasse splay sandstone.

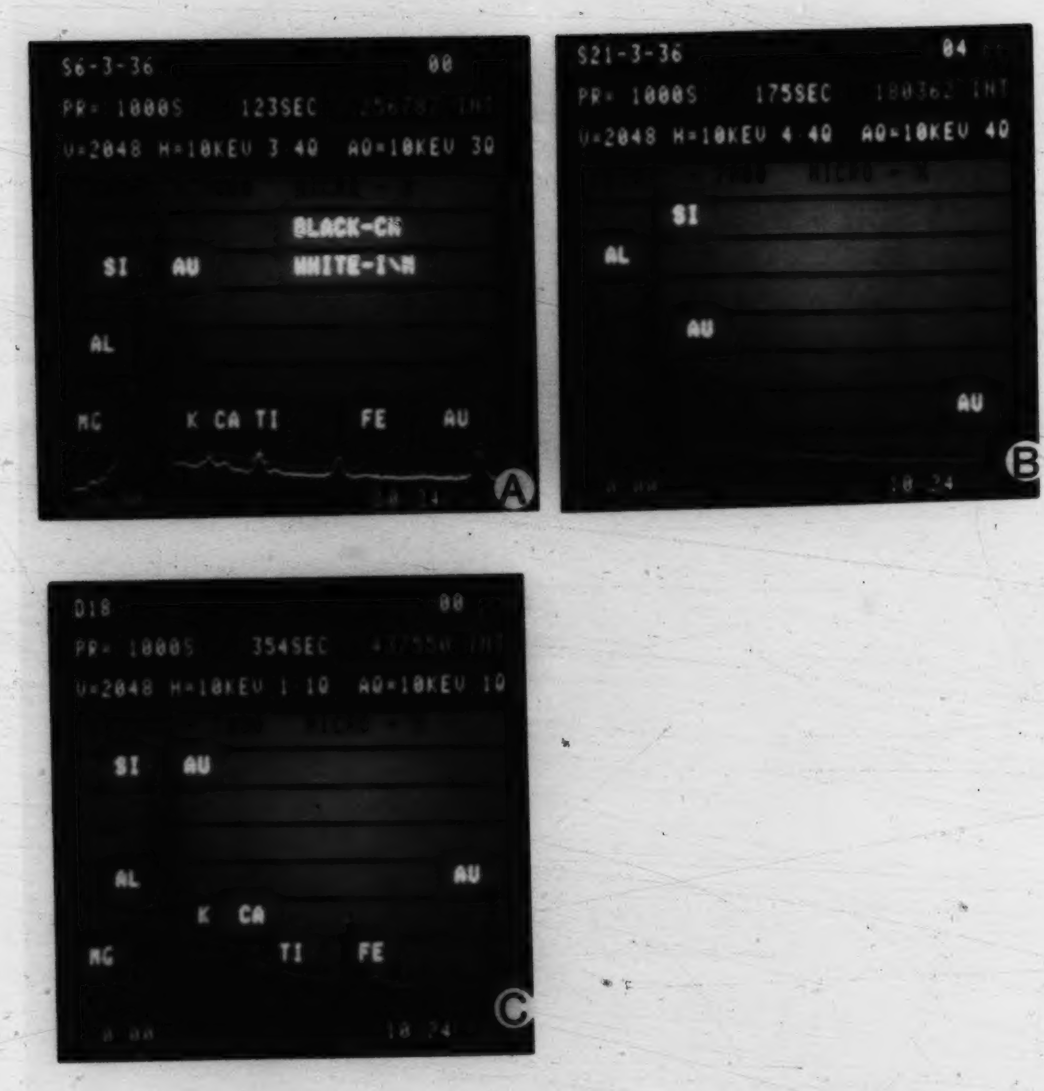

```
S6-3-36                        00
PR= 1000S     123SEC   [illegible] INT
V=2048 H=10KEV 3 40   AQ=10KEV 30
```

```
S21-3-36                       04
PR= 1000S     175SEC   180362 INT
V=2048 H=10KEV 4 40   AQ=10KEV 40
```

```
D18                            00
PR= 1000S     354SEC   [illegible] INT
V=2048 H=10KEV 1 10   AQ=10KEV 10
```

PLATE 6

outline (Plate 4A), whereas chlorite/montmorillonite is characterized by a greenish yellow color, slightly higher birefringence (first order yellow), fibrous texture under petrographic microscope (Plate 2H; 3A,B) and box-like (honey-comb) texture under the SEM (Plate 3E,F,G,H; 5C,D).

In most cases all three authigenic clays (kaolin, chlorite/montmorillonite mixed-layer clay and chlorite) coexist in a single pore (Plate 3B). Their sequence of occurence is as follows:

1. a thin chlorite lining/coating,
2. fibrous chlorite/montmorillonite pore-filling, and finally,
3. random , poorly crystalline kaolin group mineral.

In some cases, the authigenic mineral suite completely occludes the pore (Plate 2F,G,H; 3A), whereas in others a portion of the pore remains open (Plate 3B). When calcite cement occurs with the authigenic clay minerals, it is the last pore-filling. It is likely that some of the calcite cement of the facies G samples is a replacement of earlier clay cements. Stable isotope studies of the Belly River sandstones by Longstaffe (1983) indicate early diagenetic origin of the chlorite cements from connate fluids, and later origin of the kaolinite and calcite cements from fluids containing a significant fraction of meteoric water. This isotope information supports the diagenetic sequence arrived at by textural considerations of the cements.

E. Discussion

From the foregoing observations, the diagenesis of the basal Belly River sandstones in the study area has been accomplished by mechanical compaction, authigenic cementation, replacement and solution. The primary textural and detrital composition variations which are functions of depositional environments controlled the type and degree of diagenesis of the different lithofacies. Because of this relationship between primary texture, detrital composition and depositional environment of the basal Belly River sandstones, it is possible to achieve some degree of predictability of diagenetic patterns and therefore of reservoir quality of the different lithofacies. In other words, the diagenetic pattern is related to depositional environment.

Mechanical compaction and deformation of softer detrital grains along with authigenesis (cementation) are the two main diagenetic processes responsible for loss of intergranular porosity in the basal Belly River sandstone. Mudrock and volcanic rock fragments, as well as micas, have all been subjected to mechanical compaction and deformation in all the sandstone facies but most drastically in the very-fine grained matrix-rich samples. In these samples, mechanical compaction and deformation of detrital grains are the main or sole processes responsible for the occlusion of the primary intergranular porosity. As a consequence, they have high packing proximity in the range of 70-90 percent and are devoid of secondary cement and porosity.

With the exception of the very calcareous facies B sandstone samples (with less than 10 percent packing proximity), most of the studied samples are medium to closely packed with 30 to 90 percent packing proximity. An evaluation of cement-free porosity shows a maximum of 29 percent (Fig. 28) which is far less than the estimated average initial porosity of 40 percent for sandstones (Pryor, 1968). This cement-free porosity value therefore gives a compaction factor of at least 10 percent before the initiation of cementation. Mechanical compaction, like other diagenetic processes, affected the different sandstone lithofacies of the basal Belly River Formation to varying degrees. The very fine-grained sandstones of facies F and H are the most affected; most of them have packing proximity values of 50 percent and above. Most of the facies B, D and G samples are less affected by mechanical compaction. The least affected very calcareous facies B and D samples have very "open" packing (low packing proximity); this "open" packing texture is partly due to replacement of some of the detrital components by secondary calcite (Plate 2E). In all cases, however, the overall effect of mechanical compaction is the reduction of initial porosity and permeability, as in facies D and G, or complete obliteration of porosity and permeability as in facies F and H. Mechanical compaction has the most irreversible damaging effect on porosity and permeability as it forms a permanent and effective seal to subsequent diagenetic alterations by shutting off all circulation of pore fluids fairly early in the diagenetic history of the samples. Most diagenetic changes that take place in a sedimentary rock, such as cementation and dissolution, result from reactions between moving aqueous solutions and the rock itself, and the ability of the rock to transmit these fluids governs the rate and intensity of diagenesis (Blatt, et al., 1972, p.323-373). A hinderance to circulation of pore fluids by any diagenetic process, such as mechanical compaction, prevents further textural and compositional changes in the rock (Mankiewicz and Steidtmann, 1979); hence the virtual absence of cements and secondary moldic porosity in facies F and very fine-grained facies H samples of the present study.

Chemical cements constitute a significant proportion of most of the samples, averaging 13.5 percent of the total rock and ranging up to 29 percent in some samples (Table 15). Six types of cement are recognized and include carbonate, authigenic clays (phyllosilicates), silica, feldspar, iron oxide and zeolite. The most common types are authigenic clays, carbonate and silica; feldspar, iron oxide and zeolite are less abundant (Table 15) and in all cases constitute less than 0.5 percent of the sample.

Calcite pore-fill cement averages 8.9 percent of all studied samples and ranges widely from sample to sample, from 0 to over 27 percent. It is present in all sandstone facies but is most abundant in facies B, D and the fine-grained variety of facies H. It occurs in the form of coarse mosaic sparite, though chemical staining of the carbonate cement with Alizarin red S shows the calcite to be ferroan. It is usually the last pore filler following authigenic clay pore linings and fillings, whenever these other phases are present.

Authigenic clay cement constitutes a significant proportion of some of the samples, ranging from less than 1 percent to over 16 percent. It averages 4.4 percent over all the studied samples but is most abundant in facies G and some facies D samples. Monomineralic as well as mixed-layer type are present, although the most common varieties are kaolin, chlorite/montmorillonite, chlorite and illite/montmorillonite. They occur in a variety of habits including well-crystallized flakes and plates oriented perpendicular to their substrates as in the case of fibrous chlorite/montmorillonite (Plate 3A,B,E,F,G,H) and some kaolinite, unoriented microcrystalline aggregates as in the case of most of the kaolinite (Plate 2F,G; 3B; 4F) and as clay coats and linings that have particles unoriented relative to the substrate as in the illite/montmorillonite and chlorite rims (Plate 2F). Kaolinite is very abundant in facies G and some facies D samples and in all cases occurs as either euhedral or subhedral pore filling. Rarely the kaolinite is pale green but in most cases it is colorless, clear and uniform in appearance making it easy to identify and differentiate from detrital matrix under the petrographic microscope.

Chlorite/montmorillonite on the other hand usually has a greenish tinge to it and is characterized by fibrous texture under a petrographic microscope. It too, like the kaolinite, is abundant in facies G and occurs mostly as pore-filling cement. Authigenic chlorite cement, though common in facies D and G samples as pore linings and coatings, is on the whole quantitatively insignificant. It is characterized by very low birefringence, but rarely exhibits its characteristic rosette form. Elemental spectral analysis confirms its presence in some of the samples (Plate 5E). It is usually early and separates the chlorite/montmorillonite of facies G from framework grains. Illite/montmorillonite, like chlorite, occurs mainly as pore linings and coatings, though in some cases it forms bridges across large pores (Plate 4D,G). It is common in facies D and the fine-grained variety of facies H, and is characterized by bright birefringence (first order yellow), and irregular lath-like projections as seen in the SEM (Plate 5A). Quantitatively, it is insignificant in all cases.

Silica cement is present in minor amounts and in all cases less than 1 percent (Table 15). It is present primarily as quartz and "chert" overgrowths. The quartz overgrowths are usually delimited from the detrital nuclei by some "dustlines" which are, in reality, largely minute liquid inclusions, whereas the "chert" overgrowths occur as coarser, cleaner cryptocrystalline aggregates on detrital chert grains; they at times fill micro-fractures in the detrital grains.

Authigenic feldspar cement is observed in few samples, mostly facies H samples, and in all instances is less than 0.5 percent (Table 15). It occurs as aggregates of minute laths of feldspar and possibly represents recrystallized clay matrix.

Iron oxide cement occurs as a reddish brown to dark brown coating on some of the larger quartz and chert grains, but amounts to less than 0.5 percent. In some cases, it masks the color of the matrix giving it a brownish color, whereas in the case of clay cements it colors them light greenish brown; for example, kaolinite of sample S6-3-36.

Zeolite pore-fill cement is common in most of the fine- to medium grained facies G (channel sandstones) and D (stream mouth bar) samples, but is volumetrically insignificant. A coarse pseudohexagonal habit, lack of color, good cleavage, negative relief (lower than quartz) and low birefringence (first order grey) characterize this zeolite, which is probably heulandite.

Replacement of detrital components is restricted to feldspars and very fine-grained volcanic and mudrock fragments. It is most prevalent in the calcite-cemented samples, irrespective of their lithofacies, and involves the replacement of the labile detrital components such as feldspars and very fine-grained rock fragments by calcite. In the case of an incompletely replaced detrital component such as a feldspar grain, a worm-eaten appearance is imparted to it (Plate 1G). In the case of a completely calcite replaced grain, the only indication of the original grain is a tell-tale boundary between the ghost and the cementing/replacing calcite, which is usually marked by dark brown siderite blebs and iron oxide concentrations. The replacing calcite is usually observed as a single large crystal. Few instances of calcite replacement of the more resistant grains, e.g., quartz, were observed. In these instances, the replacement is piecemeal, with a complex irregular crystal outline to the remnant quartz grain (Plate 1C); the replacing calcite merges imperceptibly with the calcite cement without a delimiting boundary.

Solution, unlike the above discussed diagenetic processes, tends to restore and enhance the porosity and permeability of the sandstones. Selective solution of some of the very fine-grained volcanic and mudrock fragments and feldspars is common in facies D and G samples, and accounts for a significant proportion of their porosity. Complete dissolution and leaching of some of the unstable detrital components of these samples results in moldic secondary porosity (Plate 7E,F; 8F,G). In the case of partial dissolution of the detrital grain, intraparticle porosity is developed (Plate 7G,H; 8E); this is common in the volcanic and mudrock fragments.

It is noteworthy that the general diagenetic features and sequence observed in the present study are akin to those reported by Galloway (1974) and Burns and Ethridge (1979). The early calcite cementation of the facies B sandstones corresponds very well to Galloway (1974) and Burns and Ethridge (1979) stage 1 calcite porefill cement which they interpreted to form locally very early in the burial history of the sandstone. The chlorite and illite/montmorillonite rim cements of facies G, D, and H respectively correspond to their stage 2 authigenic clay coats and rims which they interpreted to have formed as depth of burial increased and higher temperatures and pressure became the controlling factors in the geochemical environment. The chlorite/montmorillonite, kaolinite, zeolite

Plate 7. Photomicrographs of thin sections of basal Belly River sandstone.

A. General texture of distal bar sandstone. Note the general absence of pores and significant development of calcite cement (c). Outcrop sample. Plane light. X40.

B. Same as A, but between crossed polarizers. The calcite cement (c) stands out because of its bright birefringence. X40.

C. General texture of stream mouth bar sandstone. Note the presence of considerable calcite (c) cement as well as authigenic clay (arrows). Note also plagioclase feldspar (pf), volcanic rock fragment (v), mudrock fragment (M), carbonate rock fragment (cf) and a small remnant quartz grain (q) engulfed by replacing calcite cement (c). This sample is slightly coarser and better sorted than the sample shown in A. Outcrop sample. Plane light. X40.

D. Same as C, but between crossed polarizers. It shows better the replacement of the quartz grain (q) by calcite cement (c).

E. General characteristics of stream mouth bar sandstone. Note the general absence of calcite cement and extensive development of authigenic clay (arrows); very fine grained volcanic rock fragments with intraparticle pores (v); intergranular pores (p), and mudrock fragment (m). Plane light. X40.

F. Same as E, but between crossed polarizers. X40.

G. General characteristics of channel sandstone. Note its coarser grain size, abundance of quartz (q), polycrystalline quartz (pq), chert (Ch) and authigenic clays (corrensite and kaolinite) (arrows). Note also detrital chlorite (cl), mudrock fragments (m) and carbonate fragment (cf). Outcrop sample. Plane light. X40.

H. Same as G, but between crossed polarizers. X40.

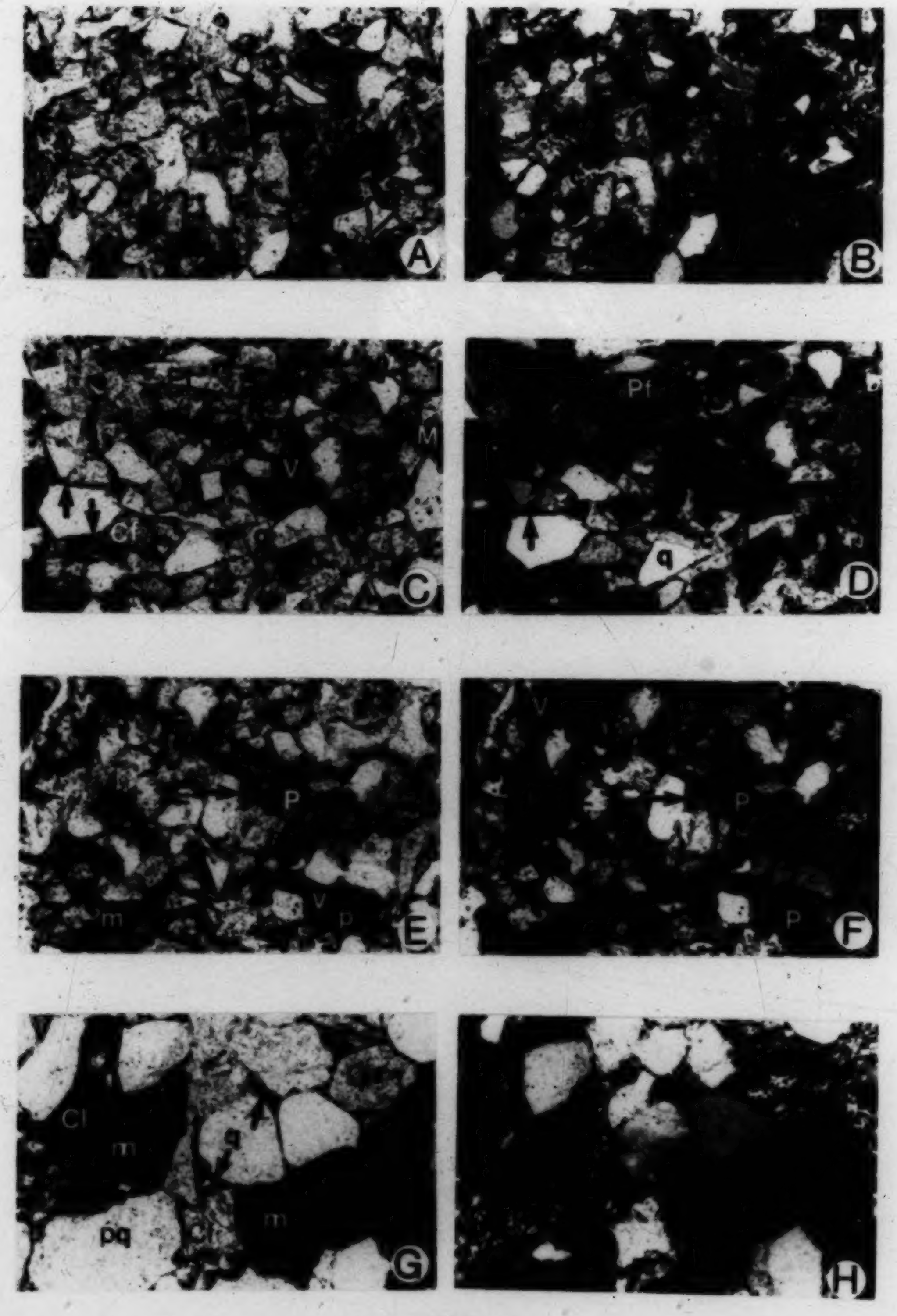
A
B
M
V
Cf
C
Pf
q
D
P
m
v
p
E
V
P
P
F
Cl
m
q
pq
Cl
m
G
H

PLATE 7

Plate 8. Photomicrographs of thin sections of basal Belly River sandstones.

A. General textural characteristics of a very fine grained crevasse splay sandstone (Facies F). Note the dominance of mudrock fragments (m), angularity of the more resistant fragments such as quartz (q), general poor sorting of the sand, little distinction between clay matrix and squeezed mudrock fragments and complete absence of recognizable cement and porosity. Outcrop sample. Plane light. X40.

B. Same as A, but between crossed polarizers.

C. General textural characteristics of a fine grained crevasse splay sandstone (Facies H). Note the dominance of mudrock fragments (m) as in A and B, but better sorting and some replacement cement (arrow). Note also the general absence of porosity. Outcrop sample. Plane light. X40.

D. Same as C, but between crossed polarizers. Calcite cement (arrow) is marked by its high birefringence. X40.

E. Photomicrograph showing the general characteristics of a typical subsurface stream mouth bar. Note the extensive leaching of the fine grained volcanic rock fragments (V) resulting in moldic porosity (p). Plane light. X40.

F. Photomicrograph showing the general characteristics of a typical subsurface channel sandstone. Note the presence of intergranular pore (p), common quartz (q), chert (Ch), microcline feldspar (mi), mudrock fragment (m) and kaolinite cement (k). Plane light. X40.

G. Same as F, but between crossed polarizers. X40.

H. Photomicrograph showing general characteristic of a typical subsurface crevasse splay sandstone. Note the dominance of mudrock fragment (m), angularity of the resistant quartz, e.g., (q), and general absence of recognizable cement and pores. Crossed polarizers. X40. (Plate 7A–H and 8A–H are of the same magnification, X40, so as to aid visual comparison of the thin sections).

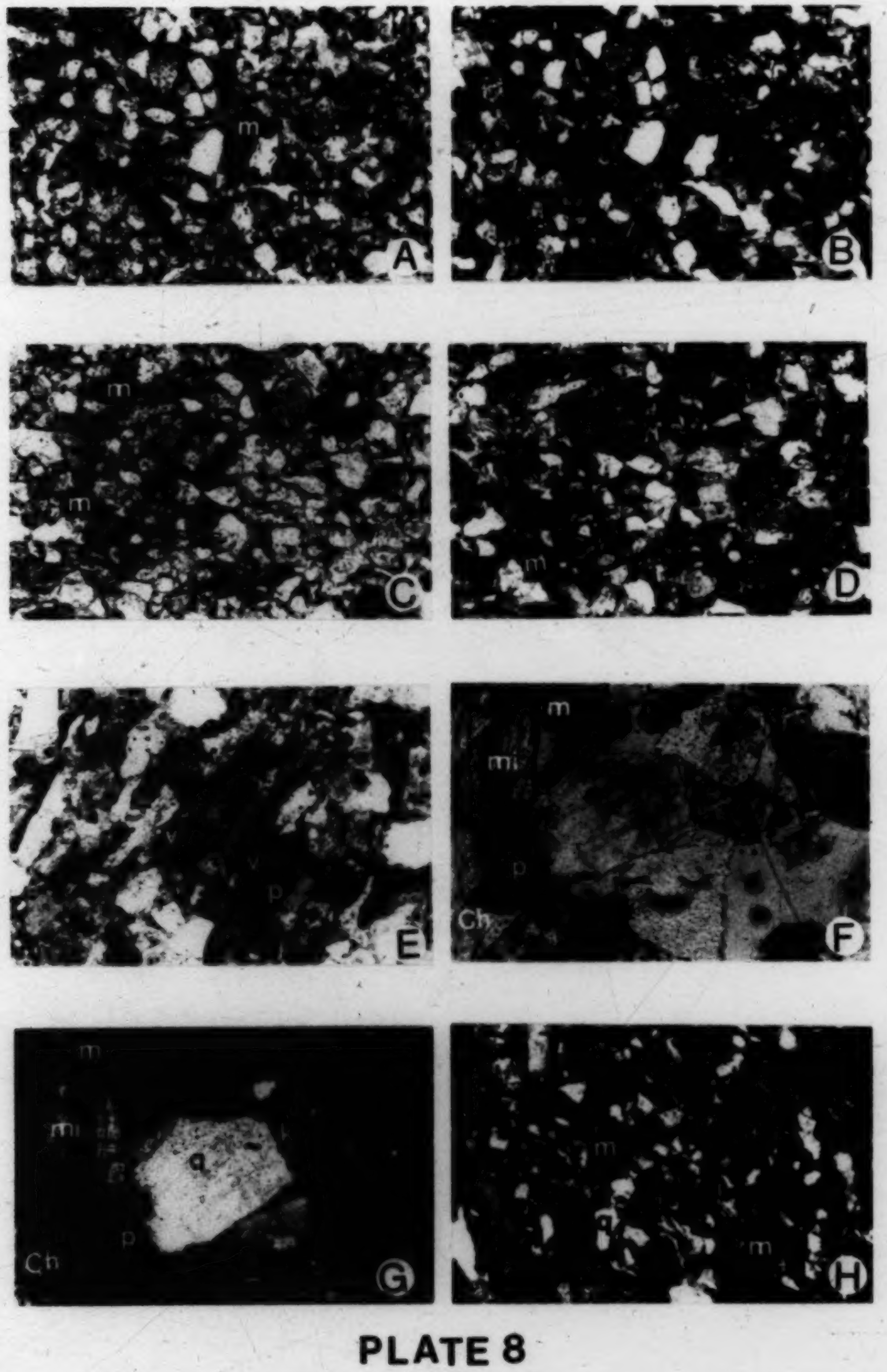
m
A
B
m
m
C
m
D
v
v
p
E
m
mi
p
Ch
F
m
mi
q
p
Ch
G
m
q
m
H

PLATE 8

and late stage calcite pore filling cements of facies G samples correspond to their stage 3 of diagenetic events (well-crystallized phyllosilicate or zeolite cements). The only difference between the diagenetic stages observed in the present study and those of Burns and Ethridge is that in the basal Belly River sandstone, the well-crystallized phyllosilicate (corrensite) and zeolite (heulandite?) coexist, whereas in the Umpqua Formation studied by Burns and Ethridge these cements are mutually exclusive.

The presence of zeolite cement in both the outcrop and subsurface samples of the basal Belly River sandstone indicates that the sediments were subjected to burial (maximum) depths sufficient to encounter temperatures and pressures necessary for zeolite facies development (Coombs, 1961; Lerbekmo, 1963; Turner, 1968; Burns and Ethridge, 1979). A second inference that stems from the above is that the presence of zeolite in the basal Belly River sandstone along with other authigenic minerals (corrensite, illite/montmorillonite, chlorite and calcite) indicates that the total diagenesis of this sandstone is not simply a present day groundwater effect; it supports Lerbekmo's (1963) conclusion that the Belly River sandstone diagenesis is within the zeolite facies range. The similarity of diagenetic assemblages in the surface and subsurface samples in the study area indicates that these diagenetic mineral assemblages are rather stable under both surface and subsurface conditions. As a logical corollary to the above, it indicates that the present day physio-chemical conditions have not substantially affected the rock. This therefore helps to predict the most likely exploration targets based on the primary depositional textural characteristics. (See Chapter X for a more detailed discussion).

In summary, the diagenetic features observed in the basal Belly River formation include phyllosilicate, calcite, silica, iron oxide and zeolite cements; compacted and deformed fine-grained rock fragments; some replacement fabrics; and solution of detrital grains. The phyllosilicate cements occur in three varieties: clay coats and rims on detrital framework grains, fibrous corrensite pore-fillings, and unoriented kaolinite aggregate pore-fillings. Based on petrographic observations, the general order of formation (paragenesis) of the diagenetic features in facies G and D samples is interpreted as follows:

1. Some mechanical compaction,
2. Early development of chlorite and illite/montmorillonite clay coats and iron oxide

rims around framework grains,

3. Precipitation of radiating and fibrous pore-fill corrensite, and unoriented aggregates of kaolinite; precipitation of silica overgrowths may follow the iron oxide rim cement,
4. Precipitation of calcite cement in the center of pores not completely filled by corrensite or kaolinite; in some cases however, stage 3 is absent and the second stage clay coats and iron oxide rims are directly followed by calcite precipitation, and finally
5. Zeolite formation in the presence of volcanic rock fragments where some remaining intergranular porosity coupled with long residence time allows migration of formation fluids under adequate temperature and pressure conditions; zeolite is the last pore filler wherever it occurs.

The paragenesis of the authigenic cements in facies G and D sandstones (in chronological order) is: iron oxide, quartz, chlorite/montmorillonite or illite/montmorillonite, kaolin group mineral, calcite and zeolite. This sequence is similar to a portion of the diagenetic sequence observed by Walgenwit et al., (1981) for the sandstones of the Belly River Formation. In facies F and the very fine-grained variety of facies H, the presence of large amounts of detrital matrix, reduced porosity and mechanical compaction preclude the development of pore-fill corrensite and kaolinite cement. Early calcite cementation is common in the fine-grained variety of facies H; in facies B sandstones, early calcite cementation and complete loss of primary intergranular porosity is the rule.

F. Reservoir Quality

A plot of framework, cement and observed porosity values of the studied samples is shown in Fig. 29 (Table 16). It shows:

1. A cluster of all the facies F and H samples (crevasse splay sands) close to zero porosity line,
2. That all facies G and D samples have porosity values above 1 percent but less than 5 percent.

The inference from the above observations is that the basal Belly River sandstone is a tight reservoir, but when one considers the submicroscopic porosity of its authigenic clays it

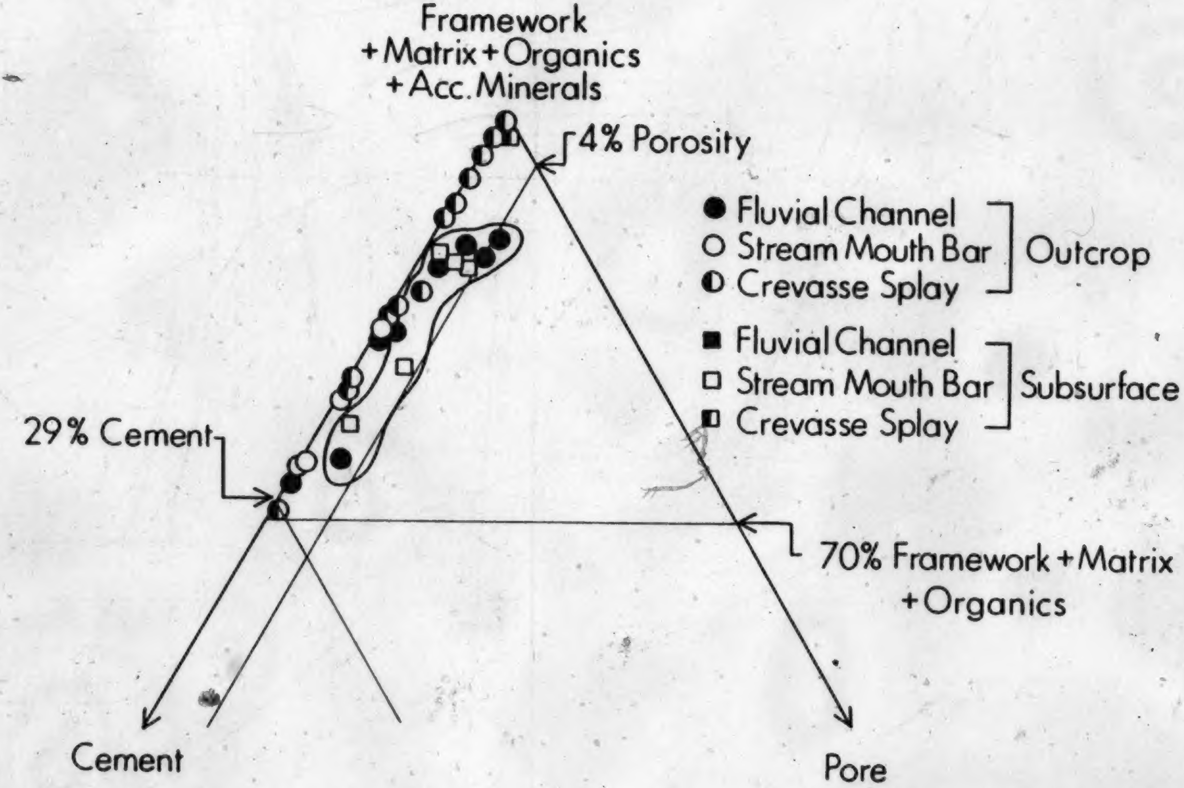

Figure 29. Framework, cement and porosity characteristics of the different sandstone lithofacies.

Table 16. Total cement, thin section porosity, cement+ porosity, framework, matrix, accessory minerals, opaques, and framework+matrix+accessory minerals+opaques as percentage of total components.

S.No.	Environ	Median	Cements	Pore	C+P	F	M	A	O	F+M+A+O
D1	DB	3.4	16.0	0	16.0	78.7	1.3	3.5	0.5	84.0
D2	SMB	3.0	21.5	0	21.5	73.2	1.0	3.5	0.8	78.5
D15B	SMB	3.8	25.7	0.2	25.9	70.2	1.7	1.8	0.3	74.0
D17B	SMB	3.5	21.8	1.2	23.0	70.8	2.2	2.5	1.5	77.0
D18	CS	3.6	21.0	0	21.0	76.0	1.3	1.3	0.3	78.9
D23	CS	3.2	12.2	1.0	13.2	80.5	1.3	3.5	1.5	86.8
D24B	FC	3.1	27.5	0	27.5	67.0	0.2	5.0	0.3	72.5
D26B	FC	2.3	23.0	2.5	25.5	71.3	0.3	2.5	0.3	74.4
D27(ii)	CS	2.5	26.3	0	26.3	70.4	0.3	1.8	0.8	73.6
D30B	CS	2.5	29.0	0.3	29.3	68.7	0.5	1.5	0	70.7
D34B	FC	2.3	15.3	1.2	16.5	80.0	1.0	2.3	0.2	83.5
D37B	FC	1.8	19.8	0.2	20.0	77.2	0	2.7	0.2	80.1
D47	CS	3.8	8.0	0	8.0	86.8	2.3	2.2	0.7	92.0
D48B	CS	3.8	14.0	0.2	14.2	79.3	3.8	1.8	1.2	85.8
M2	CS		0.3	0	0.3	94.3	0*	3.7	1.7	99.7
M3	CS	3.4	5.2	0	5.2	88.8	1.7	2.7	1.7	94.9
M5	CS	3.3	1.8	0	1.8	93.7	1.3	2.2	1.0	98.2
M6	FC	2.2	5.2	4.2	9.4	89.0	0.5	0.3	0.8	90.6
M8	CS	3.1	6.8	0	6.8	87.8	2.2	2.5	0.7	93.2

M10	CS	3.4	3.5	0	3.5	89.2	1.0	5.0	1.3	96.5
M12	CS	2.9	15.0	0.2	15.2	81.5	1.2	1.0	1.0	84.9
M21B	FC	2.2	7.5	2.2	9.7	87.3	0.7	1.2	1.2	90.4
M26B	FC	2.3	6.7	4.0	10.7	85.5	1.0	1.7	1.2	89.4
M30B	FC	2.2	10.3	1.2	11.5	83.8	1.0	2.7	1.0	88.5
S4/3	SMB	3.4	9.7	1.5	11.2	84.0	0.7	1.7	2.5	88.9
S6/3	SMB	3.3	9.8	0.7	10.5	86.3	0.7	1.0	1.5	89.5
S10/3	SMB	2.8	16.3	2.5	18.7	76.5	0	3.2	1.5	81.2
S11/3	SMB	3.4	8.8	2.3	11.1	83.8	0.2	2.0	2.8	88.8
S18/3	CS	3.7	1.5	0	1.6	92.8	0.3*	1.5	3.8	98.5
S21/3	FC	2.5	16.8	0.2	17.0	80.0	0.3	0.8	0.8	82.9

S.No.=sample number; Eviron=depositional environment; DB=distal bar; SMB=stream mouth bar; CS=crevasse splay; FC=fluvial channel; Median=thin section median diameter in phi; Cements=total cement; Pore=observed thin section porosity; C+P=cement+porosity; F=framework; M=matrix; A=accessory minerals; O=opaques; * indicates apparent absence of fines due to very fineness of the median grain size and the inclusion of the matrix in the mudrock fragment fraction, replacement by calcite, or recrystallization.

becomes somewhat more interesting as a possible petroleum reservoir. Whereas poor sorting, resulting in the presence of substantial amounts of detrital matrix, and the presence of soft lithic fragments which under compaction formed pseudomatrix, eliminated pores in facies F and H samples and whereas early calcite cementation occluded pores of facies B samples, facies G and D sandstones had their pores partially filled by relatively less damaging authigenic clays. The authigenic clays characteristically have submicroscopic porosity (Plate 3E,F,G,H; 4D,F,G,H) which in most cases is about 50 percent of their bulk volume (Iwuagwu, 1979; Iwuagwu and Lerbekmo, 1981). When one considers that only facies G and D samples have observable thin section porosity of 1 to 5 percent, and that some of the facies G and D samples have authigenic clay content of up to 16 percent (4.4 percent average), the total porosity of these samples may be double the observed value, thereby increasing their reservoir quality. Based on these observations, facies G and D sandstones (channel and stream mouth bar sands) are believed to be the best exploration targets since they are the most porous and probably most permeable basal Belly River sands. But, the presence of these authigenic clays may cause some undesirable formation damage due to: (a) swelling of the mixed-layer illite/montmorillonite and corrensite clays, (b) migration of kaolinite "booklets" within the pore system, and (c) secondary mineral precipitation, such as gelatinous ferric hydroxide [$Fe(OH)_3$] from chlorite (Almon and Davies, 1981; Iwuagwu and Lerbekmo, 1981).

IX. SUBSURFACE DATA FROM THE BASAL BELLY RIVER FORMATION IN THE STUDY AREA.

A search of more than 1000 wells east of the outcrop sections (west of Range 22 W4M in the south, and Range 5 W5M in the north), turned up only five wells with cores of the Belly River Formation. Of these, only three wells had more than 10 feet of continuously recovered full diameter core (Table 1), and only one well (3-36-40-9W5) cored the basal Belly River/Wapiabi transition. This scarcity of core of Belly River sediments results from the fact that many of the Belly River tests were drilled as Cardium zone commitments and reached total depth another 1,000 feet below the basal Belly River (Oilweek, October 26/64).

The core from well 3-36-40-9W5 was slabbed and polished for detailed study, whereas the study of the other two wells (4-27-40-8W5 and 12-31-40-8W5) was done on unslabbed core . Following slabbing and polishing of the core from well 3-36-40-9W5, the core slabs were photographed (Plate 9) and logged (Figs. 30, 31). The unslabbed core from wells 4-27-40-8W5 and 12-31-40-8W5 was also logged and described (Figs.32,33). Major depositional units (lithofacies) were recognized and designated in accordance with those described earlier from the outcrop (Fig. 3, Chapter III). Recognition of individual units was based on lithology (texture, sedimentary structure associations), and depositional environment was inferred by considering lithologic characteristics, vertical sequence and comparison with the local facies model (Fig. 16b, Chapter 1V).

Figs. 30, 32 and 33 show electric log characteristics, facies description and depositional environmental interpretation of the studied cores. Core depths are indicated on the electrical logs; only minor depth adjustments were made to match the lithology (cores) with the electrical log responses.

A. Core description (lithofacies)

Of the nine lithofacies recognized in outcrop, only six are present in the studied cores. These include:

1. Interstratified sandstone/shale (Facies B),
2. Horizontal to low angle cross-stratified sandstone (Facies D),

Plate 9. Photographs of core slab typical of the basal Belly River Formation. (Well: 3-36-40-9W5).

A. Photograph shows coaly mudstone (M) (Facies E) at base and scour-based high-angle cross-stratified sandstone (Facies G). Note sharp (probably scoured) contact (arrow) between coaly mudstone and Facies G; cross-bedding (C) in facies G, siderite pebble (P), carbonized rootlet (R) in facies E, and mudclast strewn scoured surface at the base of one of the channel sands (double arrow).

B. Photograph shows muddy, deformed/loaded facies H sandstone at base which grades into overlying coaly mudstone (M) (Facies E). Note flow structure/load structure (L) near base of the sand.

C. Photograph shows facies H sandstone sandwiched within facies E. Note flow structure (pencil tip) within the sandstone, and a 4 cm thick coal (arrow) at top of coaly mudstone. Note also the loaded base (L) of the sand, wavy to horizontal lamination, and ripple-to trough cross-lamination of the sandstone, and incorporation of shale clasts (Sh).

D. Similar to C with facies H sandstone sandwiched within coaly mudstone. Note siderite concretion (arrow) above which is a syndepositional flow structure (L).

E. Horizontal to low-angle cross-stratified sandstone (Facies D). Note shallow scour (small arrow), mudclast-rich layer (bold arrow) and shale parting, which characterize facies D sandstone.

F. Photograph shows mostly interstratified sandstone/shale (Facies B) and horizontal to low angle cross-stratified sandstone (Facies D) at top. Note sharp non-scoured base (arrow) of facies D sandstone on underlying facies B, and minor scour and truncation (ST) of laminae within facies D.

C
A
Top
F
Bottom
E
D

PLATE 9

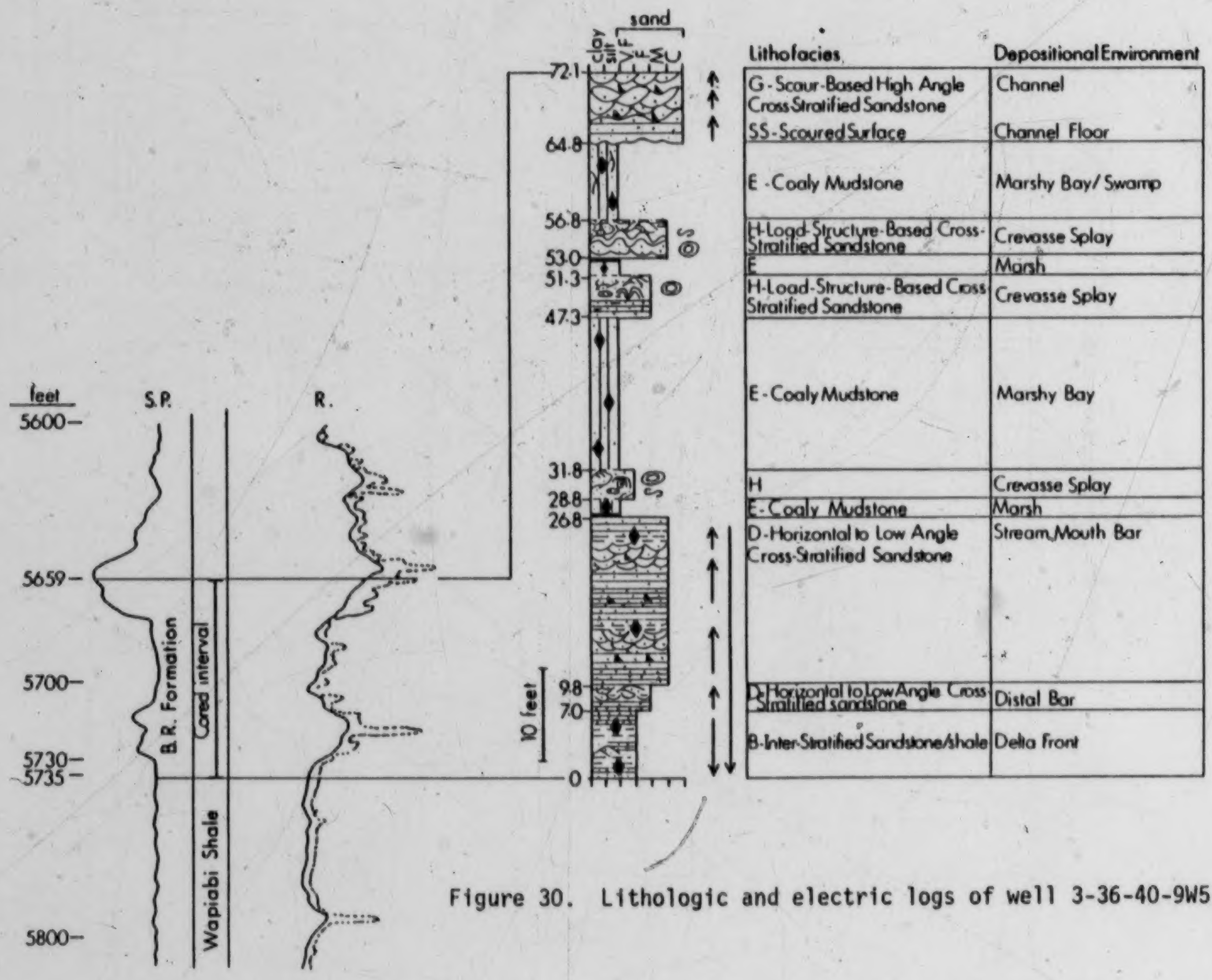
feet
5600–
5659–
5700–
5730–
5735–
5800–
S.P.
R.
B.R. Formation
Cored interval
Wapiabi Shale
10 feet
clay
silt
sand
VF
F
M
C
72.1
64.8
56.8
53.0
51.3
47.3
31.8
28.8
26.8
9.8
7.0
0
Lithofacies
Depositional Environment
G - Scour-Based High Angle Cross-Stratified Sandstone
Channel
SS - Scoured Surface
Channel Floor
E - Coaly Mudstone
Marshy Bay/ Swamp
H-Load-Structure-Based Cross-Stratified Sandstone
Crevasse Splay
E
Marsh
H-Load-Structure-Based Cross Stratified Sandstone
Crevasse Splay
E - Coaly Mudstone
Marshy Bay
H
Crevasse Splay
E-Coaly Mudstone
Marsh
D-Horizontal to Low Angle Cross-Stratified Sandstone
Stream,Mouth Bar
D-Horizontal to Low Angle Cross-Stratified sandstone
Distal Bar
B-Inter-Stratified Sandstone/shale
Delta Front

Figure 30. Lithologic and electric logs of well 3-36-40-9W5.

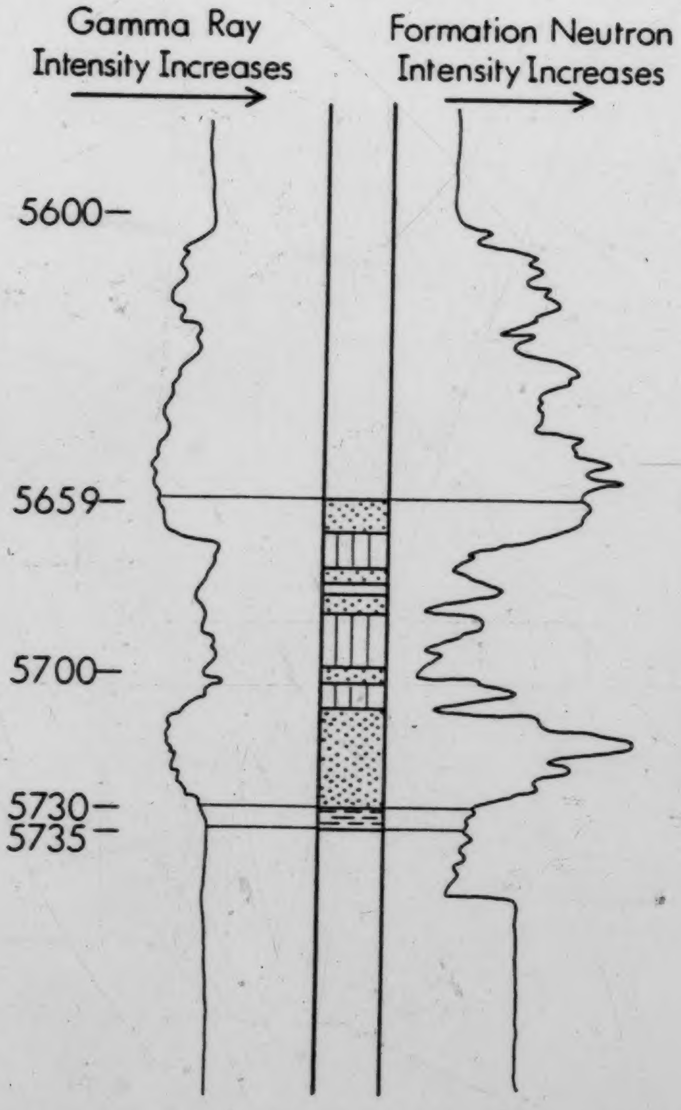

Figure 31. Gamma ray-neutron and lithologic logs of well 3-36-40-9W5.

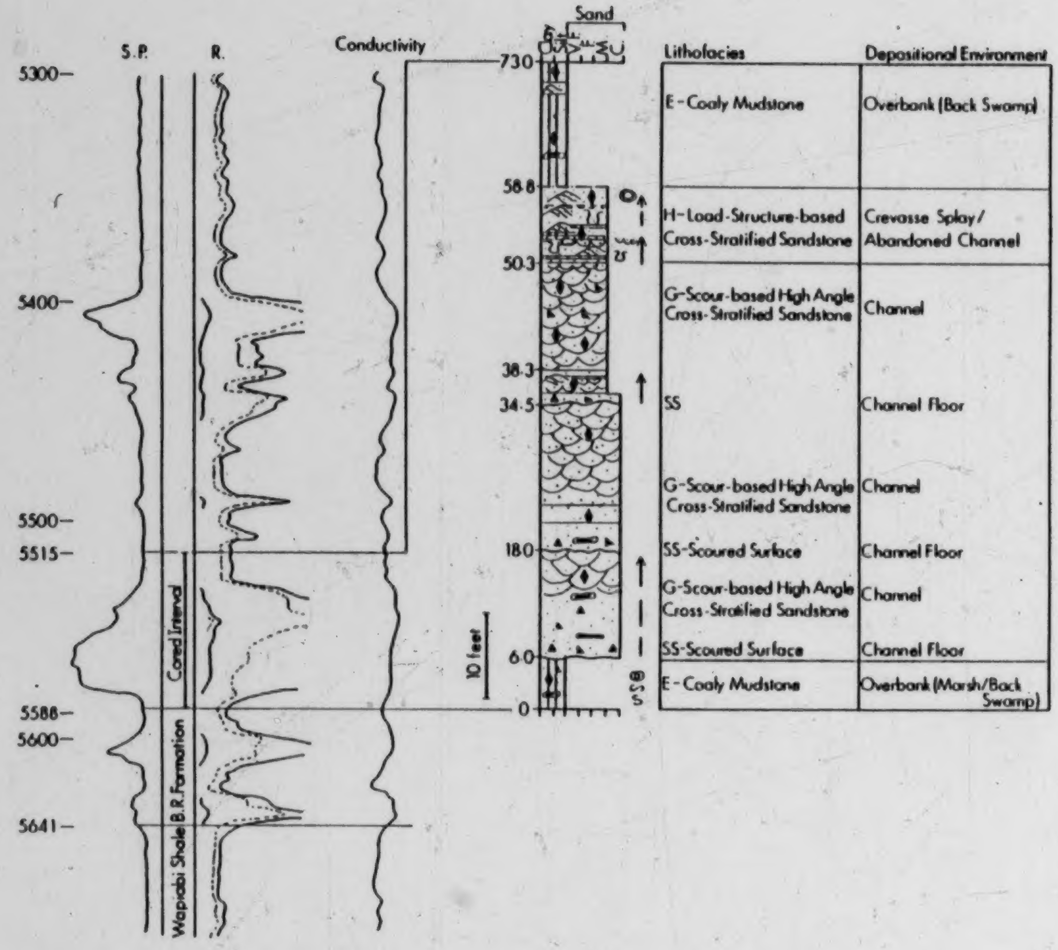

Figure 32. Lithologic and electric logs of well 4-27-40-8W5.

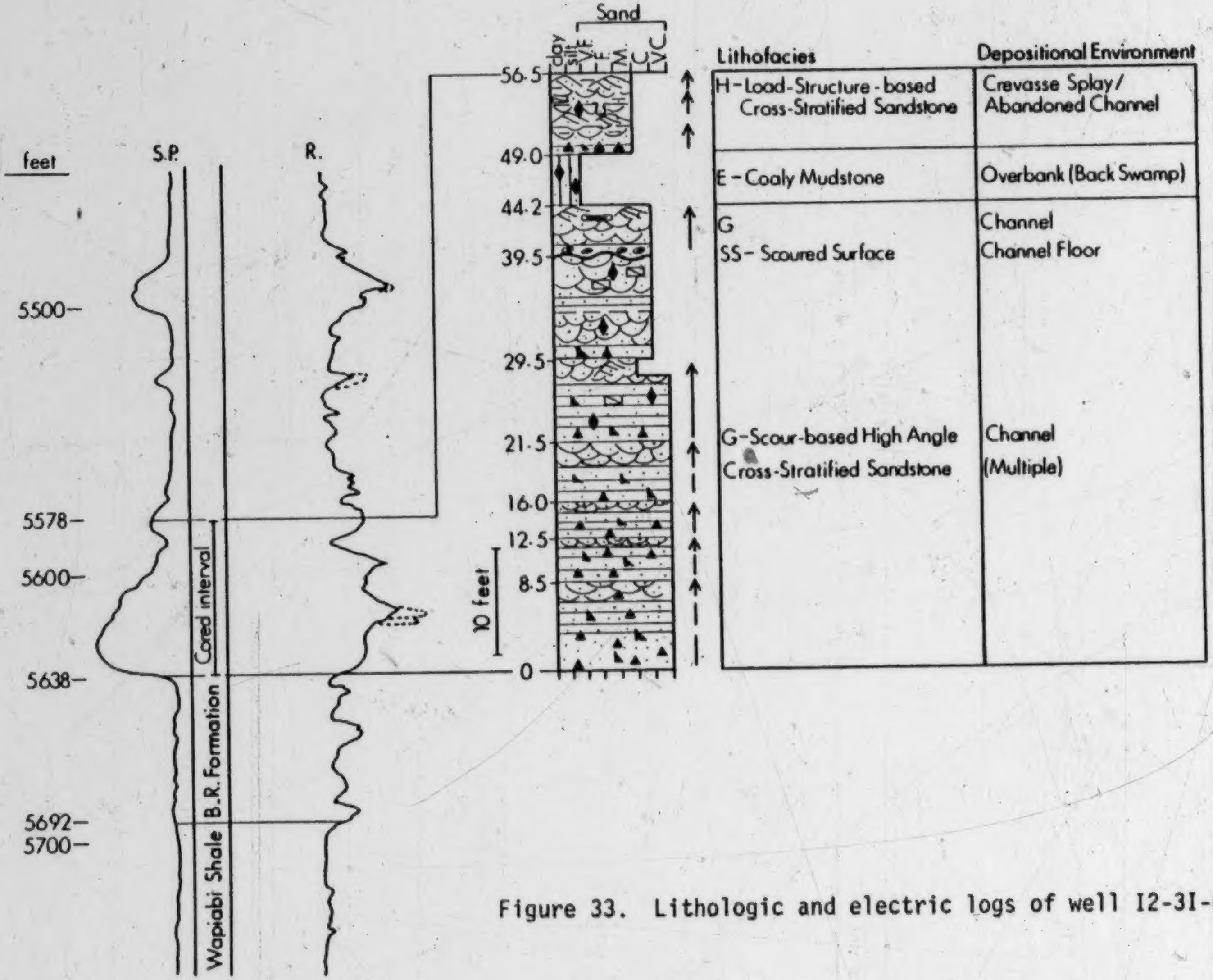
feet
5500
5578
5600
5638
5692
5700
S.P.
R.
Cored interval
B.R. Formation
Wapiabi Shale
10 feet
56.5
49.0
44.2
39.5
29.5
21.5
16.0
12.5
8.5
0
clay
silt
Sand
VF
F
M
C
VC
Lithofacies
Depositional Environment
H - Load-Structure-based Cross-Stratified Sandstone
Crevasse Splay/ Abandoned Channel
E - Coaly Mudstone
Overbank (Back Swamp)
G
SS - Scoured Surface
Channel
Channel Floor
G-Scour-based High Angle Cross-Stratified Sandstone
Channel (Multiple)

Figure 33. Lithologic and electric logs of well 12-31-40-8W5.

3. Coaly mudstone (Facies E),
4. Load-structure-based cross-stratified sandstone (Facies H),
5. Scour-based high-angle cross-stratified sandstone (Facies G) and
6. Scoured surface (Facies SS).

Interstratified sandstone/shale (Facies B)

This facies consists of interbedded very fine-grained sandstone and shale (Plate 9F). The sands are laminated and ripple cross-laminated in sets of 0.5 to 4 cm. The shale is dark gray, carbonaceous and sandy. It has a gradational lower contact with facies A (marine Wapiabi Shale).

Horizontal to low-angle cross-stratified sandstone (Facies D)

Horizontal bedding and lamination, and low angle cross-stratification characterize this facies (Plate 9E). Minor shallow scours (Plate 9F,E) and mudclast rich layers (Plate 9E), and thin carbonaceous and shale partings are common in this facies. The sand is very fine-to fine-grained (occasionally medium grained); some sand layers are graded (fining upward into shale partings). It has gradational lower and upper contacts with facies B and E respectively.

Coaly mudstone (Facies E)

This facies comprises coaly and carbonaceous mudstone (Plate 9B,C,D). It is sandy and concretionary (with siderite concretions and nodules, e.g., Plate 9D). It occasionally becomes very carbonaceous and even contains thin coal beds (maximum thickness of about 4 cm) (Plate 9C). Carbonized rootlets (Plate 9A) are common.

Scour-based high-angle cross-stratified sandstone (Facies G)

This facies consists of scour-based high-angle cross-stratified sandstones (Plate 9A). It is occasionally pebbly, massive and faintly horizontal bedded; mostly trough cross-bedded. Most of the siderite, chert and mudclast pebbles (Plate 9A) are concentrated at the bases of the individual sedimentation units (channel deposits), though some of the pebbles are scattered within the units themselves. The scour-based sedimentation units are stacked one on top of the other to form a multistory unit. It is fine to medium grained, occasionally coarse grained, well sorted and mostly authigenic clay cemented.

Load-structure-based cross-stratified sandstone (Facies H)

This facies comprises load-structure-based muddy sandstones (Plate 9B,C,D), usually encased in facies E. It is characterized by loaded, syndepositionally deformed bases that pass upward to less deformed massive to faintly horizontal and wavy laminated, and indistinctly trough and ripple cross-laminated intervals. Flow structure (Plate 9C, pencil tip), black carbonaceous laminae, shale breaks and mudclasts are common. It is very fine-to medium-grained, poorly sorted (muddy) and carbonaceous (contains abundant disseminated plant material and coal fragments).

Scoured surface (Facies SS)

This consists of erosional surfaces strewn with mudclasts and chert pebbles (Plate 9A). It usually forms the erosional base of facies G sandstones.

B. Mechanical log characteristics

A study of available mechanical logs of the above-mentioned wells shows that:

1. The basal Belly River sediments have characteristic recognizable log responses, and
2. Most of the lithofacies can be recognized on mechanical logs (Figs. 30,32,33).

The basal Belly River sandstone units usually show as negative deflections from the shale base-line on the spontaneous potential curve, though their deflection are reduced where they contain calcite-cemented zones, mudstone and siltstone lenses or shaly partings. The two lowest sandstone units, part or all of which are cored, are usually easily recognizable on SP-logs, though in some cases the lower of the two (the basal upward coarsening sandy sequence) does not show up, e.g., well 12-31-40-8W5 (Fig.33). This may be due to channel down-cutting, thereby eroding the basal sands, sudden channel switching into a shallow bay, or tight calcite cementation of the sands. The writer favors an interpretation of calcite cementation for the non-indication of the basal upward coarsening sandy sequence in some of these SP-logs for the following reasons:

1. In all instances there is a 50-60 feet sediment interval (as indicated by the SP-log) between the Wapiabi/Belly River contact and the first obvious fining upward channel sand.
2. There are some relatively more resistive zones within this 50-60 feet interval as indicated by the resistivity log (Fig.33).

Therefore, caution must be exercised in interpreting this entire basal interval as shale or mudstone rather than the usual shale/sandstone interstratification. The sandstone units are usually indicated on resistivity logs as relatively more resistive beds than the mudstones and shales. On the gamma ray log, the sandstone units show up as low gamma ray counts, whereas on the neutron log, they are indicated as high neutron counts; the mudstone and shale units, on the other hand, show up on the gamma ray and neutron logs as high gamma and low neutron counts respectively (Fig.31).

Mechanical logs of the basal Belly River sediments show that they develop recognizable characteristic log patterns and therefore can be easily mapped in the subsurface where mechanical logs and cores are available. The lower gradational contact of the Belly River Formation with the Wapiabi strata, the basal upward coarsening sandy sequence, and the scour-based upward fining channel sandstone units seen in cores are well reflected in the mechanical logs.

In summary, in core the rock sequence clearly coarsens upwards, commencing at the base with dark gray shales and sandy shales, and passing through interstratified shale and sandstone to horizontal and low angle cross-stratified sandstones capped by coaly mudstone. This basal sequence passes upwards rapidly into a scour-based massive to thick bedded and distinctly high angle cross-bedded and cross-laminated sands which, in turn, grade upward into interstratified carbonaceous mudstone and very fine grained sandstones. There is a gradual and continuous upward coarsening trend. However, in detail several shaly and muddy intervals tend to break this overall coarsening upward progression. The five lithofacies recognized in cores reflect a shoreline (littoral) depositional setting which includes shallow marine (prodelta), delta front, delta marsh and continental fluvial environments. These lithologic characteristics (facies and sequence) are recognizable on the available mechanical logs (electrical, gamma ray-neutron). The basic vertical sequence of facies encountered in all the cored wells compares very favorably with the local facies model for the basal Belly River Formation (Fig. 16b).

X. COMPARATIVE EVALUATION OF OUTCROP AND SUBSURFACE DATA : POSSIBLE APPLICATION OF OUTCROP INFORMATION TO SUBSURFACE EXPLORATION OF THE BASAL BELLY RIVER SANDSTONE RESERVOIR.

This chapter considers the possibility of recognition of the different sandstone lithofacies at various levels – outcrop, full diameter core, sidewall core and drill–cuttings. A comparison of outcrop and subsurface data from the basal Belly River Formation shows good agreement and therefore indicates a possible extension of the local facies model (Fig. 16b) into the subsurface. It also indicates the possibility of recognition of the different sandstone lithofacies at various scales – outcrop, core and drill–cuttings.

Lithofacies analysis of fourteen outcrop sections resulted in the recognition of nine lithofacies (Fig. 3) and erection of a local facies model (Fig. 16b). Belly River cores from wells east of the outcrop belt (Fig. 30,32,33) compare favorably with this local facies model. Both (local model and subsurface data) in essence consist of an upward coarsening sequence which grades from prodelta marine shale through delta front shale/sandstone interbeds to fluvial channel sandstones and coaly mudstones. But because most of the earlier wells (drilled in the 1960s), and even some of the recent ones, that penetrated the Belly River Formation did not core the Belly River Formation interval, the local model would have limited application in the subsurface if it required core. To overcome this problem and enhance the utility of the model, detailed thin section petrography was carried out with the aim of deriving information that can help identify the different facies even at the drill–cutting level.

Samples from known outcrop sandstone facies and environments as well as those from the subsurface were selected for comparative petrographic analysis. Grain size analyses resulted in the generation and recognition of log–probability curves, sieve median size and sorting characteristics of distal bar/stream mouth bar, crevasse splay and channel sands irrespective of their present surface or subsurface position (Fig. 34,35). Distal bar and stream mouth bar sands are characterized by two or three segment log–probability curves, high fine fraction (5–62%), 3.3–4.7 phi (0.1–0.04 mm) sieve median diameter and very well sorting (with sieve inclusive graphic standard deviation values of 0.15–0.43 phi). The crevasse splay sands are characterized by two segment log–probability curves, modest fine fraction (mostly in the range of 15–30%), 2.8–4.7 phi (0.14–0.04 mm) sieve

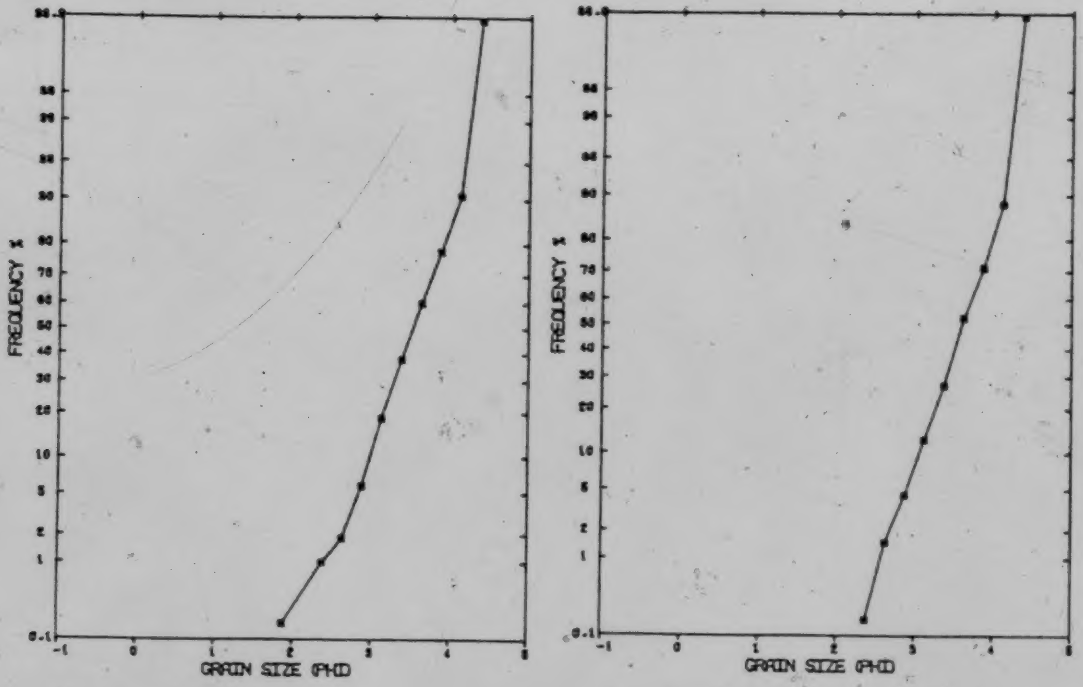

A. Sample D1 B. Sample D18

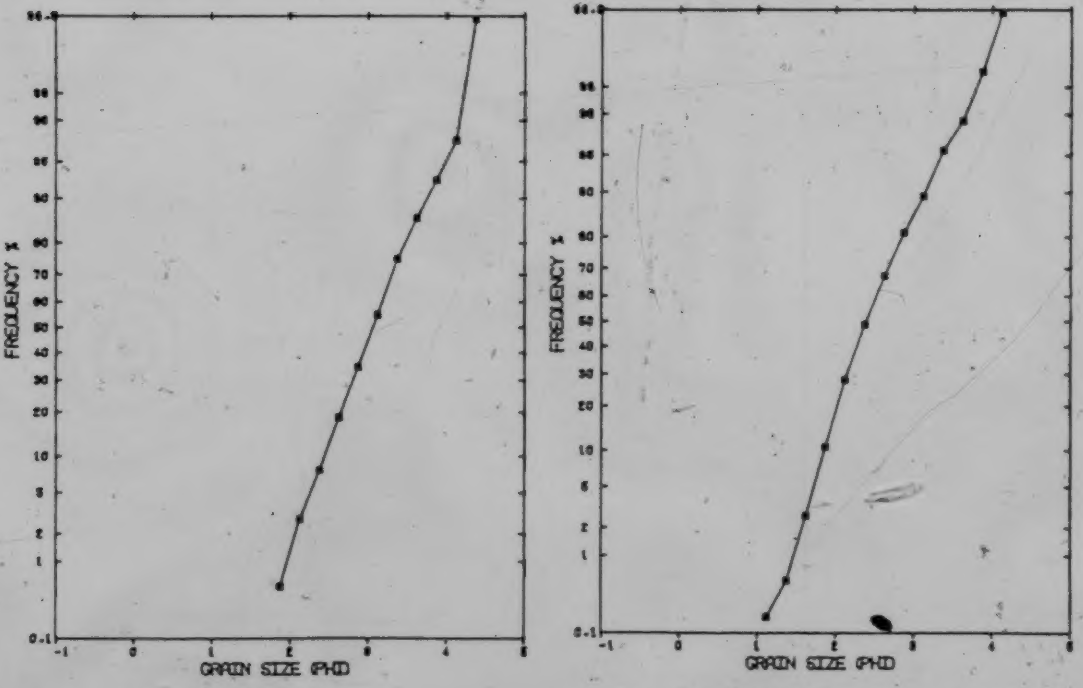

C. Sample M22T D. Sample D34B

Figure 34. Log-probability curves representative of outcrop sandstone samples of the basal Belly River sandstone. A, B, C, and D illustrate a three segment curve distal bar, a two segment crevasse splay curve, a two segment curve channel sand and a one segment curve channel sand respectively.

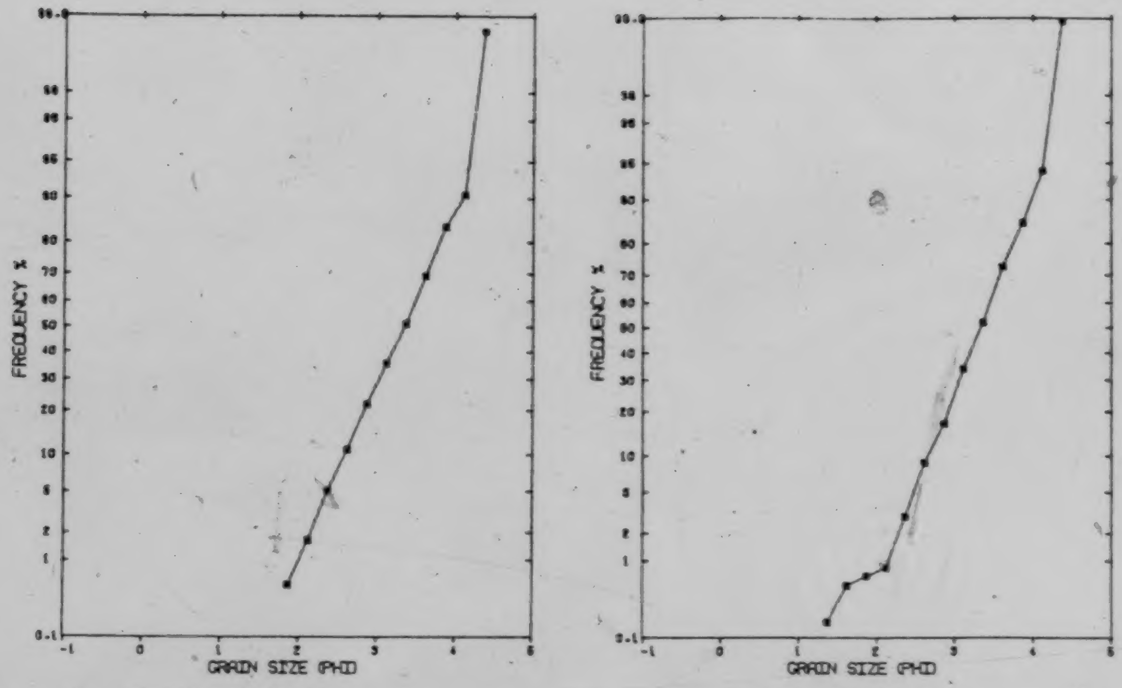

A. Sample S4/3-36 B. Sample S11/3-36

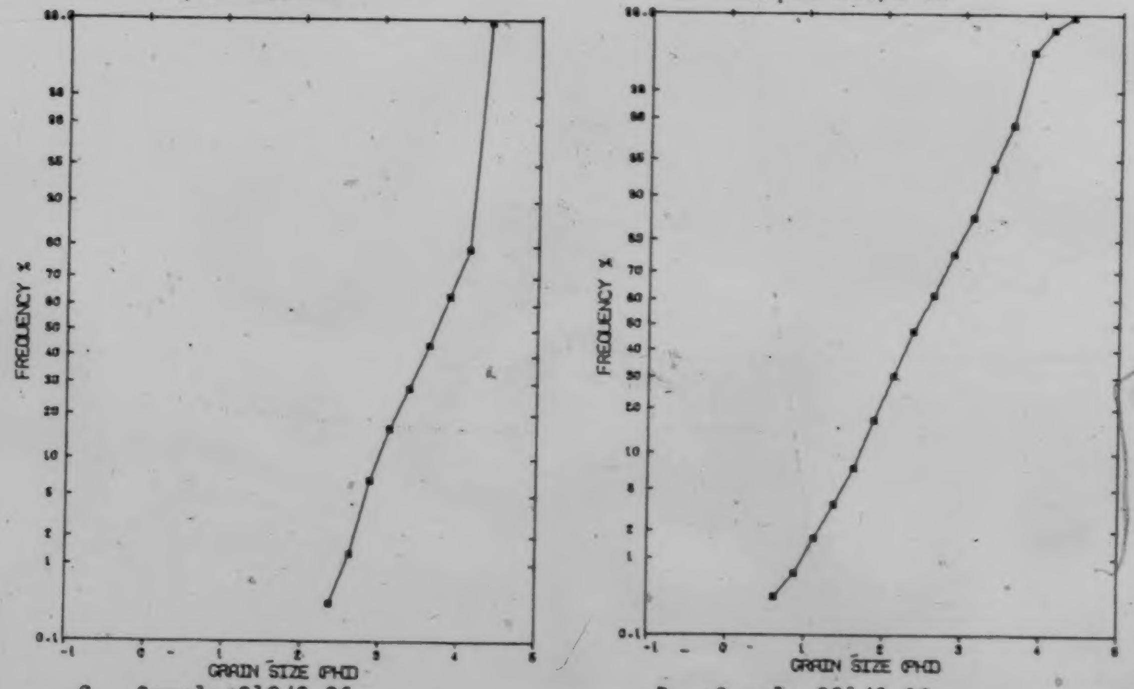

C. Sample S18/3-36 D. Sample S21/3-36

Figure 35. Log-probability curves representative of subsurface sandstone samples of the basal Belly River sandstone. A, B, C and D illustrate a two segment curve stream mouth bar, a three segment curve stream mouth bar, a two segment crevasse splay sand and a two segment curve channel sand respectively.

median diameter and very well to well sorting (with sieve inclusive graphic standard deviation values of 0.18–0.49 phi). The channel sandstones, on the other hand, exhibit two or one segment log-probability curves, very low fine fraction value (always less than 5%), 2.2–3.8 phi (0.22–0.07 mm) sieve median diameter and are well to moderately well sorted (with sieve inclusive graphic standard deviation values of 0.31–0.65 phi). Only channel sandstones have grain diameters greater than 1.0 phi (0.5 mm); the fine grained variety of crevasse splay sandstones which have low fine fraction rarely have grains up to 0.5 mm. With the exception of channel sandstones, most samples have maximum grain diameter of 2.0 phi (0.25 mm) (medium/fine sand boundary).

Detrital composition analysis show that distal bar and stream mouth bar sandstones are rich in volcanic and mudrock fragments (Plate 7E,F; 8E), and that crevasse splay sands are rich in mudrock fragments (Plate 8A,B,C,D,H); the channel sandstones are rich in quartz and chert fragments (Plate 7G,H; 8F,G). These variations in detrital composition are grain size dependent (Chapters VI, VII).

The dominant diagenetic processes and features are also different for the different sandstone facies. Distal bars are characterized by early calcite cementation, whereas stream mouth bar sandstones underwent considerable compaction before authigenic clay cementation; kaolinite and calcite are the main pore fillers, with illite/montmorillonite and chlorite as subordinates. Mechanical compaction and complete loss of porosity characterize crevasse splay sands; occasional carbonate pore filling and illite/montmorillonite pore lining are present in the fine grained variety of facies H. Authigenic clay cementation with kaolinite and chlorite/montmorillonite cements and occasional calcite cement form the diagenetic features of facies G sandstones (Chapter VIII).

Based on the above generalities, a nine-point check list (Table 17) results which, if used judiciously, allows identification of the sandstone lithofacies at various levels. The table consists of the dominant sedimentary structures, grain size distribution curves, percent finer than 4 phi (fine tail), sieve median size, sieve inclusive graphic standard deviation (sorting), relative abundant detrital component, dominant diagenetic features and processes, dominant cements and presence or absence of porosity in the different sandstone facies.

Table 17. Check list of sediment properties for the differentiation of the basal Belly River sandstone lithofacies.

Properties	Distal and stream mouth bar sands	Crevasse splay sandstones	Channel sandstones
1. Dominant sedimentary structures	Sharp base; horiz. lam., trough cross- and ripple cross-lam., syndep. structure.	Loaded base; flow structure, horiz. lam., trough cross-and ripple cross-lamination.	Scoured base; med. to large scale, high angle trough cross-bedding and cross-lamination.
2. Grain size distr. curve	Two or more curve segments.	Two curve segments.	One or two curve segments.
3. Percent finer than 4 phi (fine tail).	High in silt and clay (suspension population) (5-62%).	High in silt and clay (1-58% but mostly in the range of 15-30%).	Very low in silt and clay; generally less than 5%.
4. Sieve median size	3.3-4.7 phi (0.1-0.04 mm).	2.8-4.7 phi (0.14-04 mm).	2.2-3.8 phi (0.22-0.07 mm).
5. Sieve inclusive graphic standard deviation (sorting)	0.15-0.43 phi; best sorted of all on the average.	0.18-0.49 phi.	0.31-0.50 phi; relatively most poorly sorted.

6. Abundant detrital component (relative)	Rich in volcanic and mudrock fragments.	Rich in mudrock fragments.	Rich in quartz and chert fragments.
7. Dominant diagenetic features/processes	Early calcite cementation in distal bar; compaction and authigenic clay cementation in stream mouth bar.	Mechanical compaction; subordinate carbonate cementation.	Authigenic clay cementation.
8. Dominant cements	Carbonate cement in distal bar sands; kaolinite and calcite cements in the stream mouth bar sands. Illite/mont. clay and chlorite are common.	Absent in the very fine grained variety; present in the fine grained variety in the form of thin linings and coatings of illite/montmorillonite and calcite.	Kaolinite and corrensite cements; subordinate calcite cements.
9. Porosity	Absent in the very fine grained distal bar sands due to calcite cementation; present in the stream	Generally absent especially in the matrix rich very fine grained variety.	Present in both the microscopic and submicroscopic (within the authigenic clays) forms, but

mouth bar sands, mostly as solution secondary porosity; but significantly reduced by cementation.	is significantly reduced by cementation.

In summary, on the basis of facies sequence, variations in detrital composition, texture, sedimentary structures and diagenesis, the sandstone lithofacies of the basal Belly River Formation can be differentiated at various scales – namely outcrop, full diameter core , sidewall core and drill–cuttings.

XI. SUMMARY AND CONCLUSIONS

Lithofacies and petrographic analyses of the basal Belly River Formation in the Southern and Central Foothills of Alberta show that:

1. This lithostratigraphic unit forms a coarsening-upward sequence commencing at the base with dark gray shales and sandy shales, and passing through interbedded shale and sandstone to horizontal and low-angle cross-stratified sandstones capped by coaly mudstone or scoured into by fluvial channels.
2. It represents the deposit of a progradational shoreline which grades from a marine deltaic environment to a continental fluvial environment.
3. The basal Belly River delta(s) was wave-influenced but river-dominated and the channel pattern of the Belly River fluvial system was meandering.
4. The western paleoshoreline was variable in character from south to north and the retreat of the seaway at this time probably began in the north and was more rapid there than in the south.
5. The source area of the Belly River sediments lie to the west, probably within the Cordillera and the major sediment dispersal was from north to south.
6. Although all the sandstone lithofacies of the basal Belly River are lithic in composition, there are some interenvironmental variation amongst them with the coarser channel sandstones being richer in quartz and chert grains, whereas the finer-grained crevasse splay, distal bar and stream mouth bar sandstones are rich in volcanic and mudrock fragments. This variation in detrital composition appears to be grain size related which in turn is related to the depositional environment.
7. Texturally, they are fine-to very fine-grained, well to very well sorted mature sandstones.
8. The diagenesis of the sandstones is environment specific; it has been accomplished by compaction, authigenesis, replacement and solution, and is within the zeolite facies range.
9. Four broad facies related diagenetic patterns are observed in the basal Belly River sandstones. These are: (i) Early calcite cementation of the distal bar sandstones. (ii) Compaction and authigenic clay cementation of stream mouth bar sandstones. (iii) Mechanical compaction, and occasional cementation (calcite and authigenic clays), of

the crevasse splay sandstones, and (iv) Extensive authigenic clay cementation of the channel sandstones.

10. Present day physico-chemical conditions have not substantially affected the Belly River sediments in outcrop and therefore it is possible to predict the most likely subsurface exploration targets based on outcrop information.
11. The channel and stream mouth bar sandstones are the most porous (1 to 5 percent observable thin section porosity, and 2 to 10 percent total porosity) and probably the most permeable lithofacies, and therefore the best petroleum resevoir.
12. The different Belly River sandstone lithofacies, irrespective of their present day position, can be differentiated at various levels - outcrop, core and drill-cuttings - based on facies sequence, variations in detrital composition, texture, sedimentary structures and diagenesis.

REFERENCES CITED

Adams, J., 1977. Sieve size statistics from grain measurement. Journal of Geology, v. 85, p. 209–227.

Ager, D.V., 1973. The nature of the stratigraphical record. Macmillan, London, 114 p.

Allen, J.R.L., 1963. Henry Clifton Sorby and the sedimentary structures of sands and sandstones in relation to flow conditions. Geologie en Mijnbouw, v. 42, p. 223–228.

Allen, J.R.L., 1964. Studies in Fluvial Sedimentation: Six cyclothems from the Lower Old Red Sandstone, Anglo-Welsh Basin. Sedimentology, v. 3, p. 163–198.

Allen, J.R.L., 1965. Fining-upward cycles in alluvial successions. Geology Journal, v. 4, p. 229–246.

Allen, J.R.L., 1970. Studies in Fluvial Sedimentation: A comparison of fining-upward cyclothems, with special reference to coarse-member composition and interpretation. Journal of Sedimentary Petrology, v. 40, p. 298–323.

Almon, W.R. and Davies, D.K., 1981. Formation damage and the crystal chemistry of clays, in Longstaffe, F.J. ed., Short Course in Clays and the Resource Geologist. Mineralogical Association of Canada, p. 81–103.

Anderson, T.W. and Goodman, L.A., 1957. Statistical inference about Markov chains. Ann. Math. Statist. v. 28, p. 89–110.

Bernard, H.A. and Major, C.F., 1963. Recent meandering belt of the Brazos River: An alluvial "sand" model (abs.). American Association of Petroleum Geologists Bulletin, v. 47, p. 350.

Bernard, H.A., Major, C.F. Jr., Parrot, B.S. and Leblanc, R.J. Sr., 1970. Recent Sediments of Southeast Texas. Bureau of Economic Geology, University of Texas, Guidebook II.

Billingsley, P., 1961. Statistical methods in Markov chains. Ann. Math. Statist. v.32, p. 12–40.

Blatt, H., Middleton, G. and Murray, R., 1980. Origin of Sedimentary Rocks. 2nd. ed. Prentice-Hall, Inc. 782p.

Bluck, B.J., 1971. Sedimentation in the meandering River Endrick. Scottish Journal of Geology, v. 7, p. 93–138.

Burns, L.K., and Ethridge, F.G., 1979. Petrology and diagenetic effects of lithic sandstones: Paleocene and Eocene Umpqua Formation, Southwest Oragon. In Scholle, P.A. and Schluger, P.R. (ed.), Aspects of Diagenesis. Society of Economic Paleontologists and Mineralogists, Special Publication No. 26, p. 307-317.

Cant, D.J. and Walker, R.G., 1976. Development of a braided-fluvial facies model for the Devonian Battery Point Sandstone, Quebec. Canadian Journal of Earth Science, v. 13, p. 102-119.

Chen, P.Y., 1968. A modification of sandstone classification. Journal of Sedimentary Petrology, v. 38, p. 54-60.

Clukey, E., Cacchione, D.A., and Nelson, C.H., 1980. Liquefaction potential of the Yukon prodelta, Bering Sea: Proc. Offshore Technology Conference, Houston, v. 1 paper 3773, p. 315-325.

Coleman, J.M., 1969. Brahmaputra River: channel processes and sedimentation. Sedimentary Geology, v. 3 p. 129-239.

Coleman, J.M. and Gagliano, S.M., 1964. Cyclic sedimentation in the Mississippi River deltaic plain. Gulf Coast Association Geological Society Transactions, v. 14, p. 67-80.

Coleman, J.M., and Gagliano, S.M., 1965. Sedimentary structures: Mississippi River deltaic plain. In Middleton, G.V. (ed.), Primary sedimentary structures and their hydrodynamic interpretation. Society of Economic Paleontologists and Mineralogists Special Publication No. 12, p. 133-148.

Coleman, J.M. and Wright, L.D., 1975. Modern River deltas: Variability of processes and sand bodies. In Broussard, M.L. (ed.), Deltas, 2nd ed. Houston Geological Society, Houston, Texas, p. 99-150.

Collinson, J.D., 1978. Alluvial Sediments. In H.G. Reading, (ed.), Sedimentary Environments and facies, p. 15-60.

Coombs, D.S., 1961. Some recent work on the lower grades of metamorphism. Australian Journal of Science, v.24, p. 203-215.

Darcey, M.F. and Krumbein, W.C., 1970. Markovian models in stratigraphic analysis. Journal of International Association of Mathematical Geologists, v. 2, p. 175-191.

De Raaf, J.F.M., Reading, H.G. and Walker, R.G., 1965. Cyclic sedimentation in the Lower Westphalian of north Devon. Sedimentology, v. 4, p. 1-52.

Dodson, P.,, 1971. Sedimentology and Taphonomy of the Oldman Formation (Campanian), Dinosaur Provincial Park, Alberta (Canada). Palaeogeography, Palaeoclimatology, Palaeoecology, v. 10. p. 21-74.

Eisbacher, G.H., Carrigy, M.A. and Campbell, R.B., 1974. Paleodrainage pattern and late-orogenic basins of the Canadian Cordillera. In: Dickinson (ed.), Tectonics and Sedimentation. Society of Economic Paleontologists and Mineralogists Special Publication 22, p. 143-166.

Erxleben, A.W., 1973. Depositional systems in the Pennsylvanian Canyon Group of North-Central Texas. Bureau of Economic Geology, Guidebook No. 14, p. 43-56.

Fisk, H.N., 1944. Geological investigation of the alluvial valley of the lower Mississippi River : U.S. Army Corps of Engineers, Mississippi River Commission, Vicksburg, Mississippi.

Fisk, H.N., 1947. Fine-grained alluvial deposits and their effects on Mississippi River activity. Mississippi River Commission, Corps of Engineers, U.S. Army, Vicksburg, Mississippi.

Folk, R.L., 1955. Student operator error in determination of roundness, sphericity and grain size. Journal of Sedimentary Petrology, v. 25, p. 297-301.

Folk, R.L., 1959. Petrology of Sedimentary Rocks. Hemphill Publishing Co., 154p.

Friedman, G.M. and Sanders, J.E., 1978. Principles of Sedimentology. John Wiley and Sons, Toronton, 792p.

Gadow, S. and Reineck, H.E., 1969. Ablandiger Sandstransport bei Sturmfluten: Senckenbergiana Marit., v. 1, p. 63-78.

Galloway, W.E., 1974. Deposition and diagenetic alteration of sandstones in Northeast Pacific arc-related basins : Implications for graywacke genesis. Geological Society of America Bulletin, v. 85, p. 379-390.

Galloway, W.E., 1975. Process framework for describing the morphological and stratigraphic evolution of deltaic depositional systems. In Broussard, M.L. (ed.), Deltas, 2nd: Houston Geological Society, Houston, Texas, p. 87-98.

Gingerich, P.D., 1969. Markov analysis of cyclic alluvial sediments. Journal of Sedimentary Petrology, v. 39,330-332.

Goldring, R. and Bridges P., 1973. Sublittoral Sheet sandstones. Journal of Sedimentary Petrology, v. 43, p. 736-747.

Gould, H.R., 1970. The Mississippi Delta complex. In Morgan, J.P. (ed.), Deltaic Sedimentation: Society of Economic Paleontologists and Mineralogists Special Publication No. 15, p. 3-30.

Gregory, K.J. and Walling, D.E., 1979. Drainage basin form and process - a geomorphological approach. Edward arnold, 458p.

Hamblin, A.P. and Walker, R.G., 1979. Storm-dominated marine deposits : The Fernie-Kootenay (Jurassic) transition, Southern Rocky Mountains. Canadian Journal of Earth Science, v. 16, p. 1673-1690.

Harbaugh, J.W. and Bonham-Carter, G., 1970. Computer Simulation in Geology. Wiley-Interscience, New York.

Harms, J.C., Mackenzie, D.B. and McCubbin, D.G., !963. Stratification in modern sands of the Red River, Louisiana. Journal of Geology, v. 71, p. 566-580.

Hays, M.O., 1967. Hurricanes as geological agents : case studies of hurricanes Carlas, 1961, and Cindy, 1963 : Report of Investigation No. 61, Bureau of Economic Geology, Austin, Texas, 54p.

Hein, F.J., 1979. Deep sea Valley-fill Sediments: Cap Enrage Formation, Quebec. Unpublished Ph.D thesis, McMaster University, 514p.

Iwuagwu, C.J., 1979, Diagenesis of the basal Belly River Sandstone Reservoir, Pembina Field, Alberta, Canada. Unpublished M.Sc. thesis, The University of Alberta, 175p.

Iwuagwu, C.J., and Lerbekmo, J.F., 1981. The role of authigenic clays in some reservoir characteristics of the basal Belly River sandstone, Pembina Field, Alberta. Bulletin of Canadian Petroleum Geology, v. 29, p. 479-491.

Iwuagwu, C.J., and Lerbekmo, J.F., 1982. The petrology of the basal Belly River sandstone reservoir, Pembina Field, Alberta. Bulletin of Canadian Petroleum Geology, v. 30, p. 187-207.

Jackson, R.G.II, 1976. Depositional model of point bars in the Lower Wabash River. Journal of Sedimentary Petrology, v. 46, p. 579-594.

Jackson, R.G.II, 1978. Preliminary evaluation of lithofacies models for meandering alluvial streams. Society of Petroleum Geologists, Memoir 5, p. 543-576.

Jeletzky, J.A. 1971. Marine Cretaceous biotic provinces and paleogeography of western and Arctic Canada illustrated by a detailed study of ammonites: Geological Survey Canada Paper 70-22, 92 p.

Kelling, G. and Mullin, P., 1975. Graded limestones and Limestone-quartzite couplets: possible storm deposits from the Moroccan Carboniferous. Sedimentary Geology, v. 13, p. 161-190.

Kolb, C.R. and Van Lopik, J.R., 1966. Depositional environments of the Mississippi River delta plain - southeastern Louisiana. In Shirley, M.L., (ed.), Deltas in their geological framework. Houston Geological Society.

Krumbein, W.C., 1942. Physical and chemical changes in sediments after deposition. Journal of Sedimentary Petrology, v. 12, p. 111-117.

Krumbein, W.C. 1967. Fortran IV computer programs for Markov Chain experiments in Geology. Computer Contribution, Geological Survey, Kansas, 13, 38.

Krumbein, W.C., 1968. Fortran IV computer program for simulation of transgression and regression with continuous time Markov models. Computer Contribution Geological Survey, Kansas, 26,38p.

Krumbein, W.C. and Dacey, M.F., 1969. Markov chains and embedded chains in geology. Journal of International Association of Mathematical Geologists, v. 1, p. 79-96.

Kumar, N. and Sanders, J.E., 1976. Characteristics of shoreface storm deposits: Modern and ancient examples. Journal of Sedimentary Petrology, v. 46, p. 145-162.

Leopold, L.B. and Wolman, M.G., 1957. River channel patterns: Braided, Meandering and Straight. U.S. Geological Survey Professional Paper 282-B, p. 39-85.

Lerand, M.M. and Oliver, T.A., 1975. Stratigraphy and Sedimentology of the Lundbreck section. In M.S. Shawa (ed.), Guidebook to selected sedimentary environments in southwestern Alberta, Canada. Calgary, Canadian Society of Petroleum Geologists Field Conference.

Lerbekmo, J.F., 1963. Petrology of the Belly River Formation, southern Alberta Foothills. Sedimentology, v. 2, p. 54-86.

Longstaffe, F.J., 1983. Stable isotope studies of diagenesis in clastic rocks. Geoscience Canada (in press).

Mankiewicz, D. and Steidtmann, J.R., 1979. Depositional environments and diagenesis of the Tensleep Sandstone, Eastern Big Horn Basin, Wyoming. In Scholle, P.A. and Schluger, P.R. (ed.), Aspects of Diagenesis. Society of Economic Paleontologists and Mineralogists, Special Publication No. 26, p. 319-336.

McKee, E.D., 1965. Experiments on ripple lamination. In Middleton, G.V. (ed.), Primary sedimentary structures and their hydrodynamic interpretation. Society of Economic Paleontologists and Mineralogists Special Publication No. 12, p. 66-83.

McKee, E.D., 1966. Significance of climbing-ripple structure. U.S. Geological Survey Professional Papers, 550-D, D94-D, 103p.

McKee, E.D., Crosby, E.J., and Berryhill, H.L., 1967. Flood deposits, Bijou Creek, Colorado. Journal of Sedimentary Petrology, v. 37, p. 829-851.

McLean, J.R., 1971 Stratigraphy of the Upper Cretaceous Judith River Formation in the Canadian Great Plains. Saskatchewan Research Council, Geology Division, Report 11, 96 p.

Miall, A.D., 1973. Markov chain analysis applied to an ancient alluvial plain succession. Sedimentology, v. 20, p. 347-364.

Miall, A.D., 1979. Facies Models 5. Deltas. In R.G. Walker, (ed.), Geoscience Canada Reprint Series 1, p. 43-56.

Middleton, G.V., 1978. Facies. The Encyclopedia of Sedimentology. In Fairbridge, R.W. and Bourgeois, J. (ed.), Encyclopedia of Earth Sciences Series, v. VI, p. 323-325.

Monger, J.W.H. and Hutchison, W.W., 1971. Metamorphic Map of the Canadian Cordillera. Geological Survey Canada, Paper 70-33.

Moore, P.S., 1979. Deltaic sedimentation - Cambrian of south Australia. Journal of Sedimentary Petrology, v. 49, p. 1229-1244.

Morgan, J.P., 1970. Depositional processes and products in the deltaic environment. In Morgan, J.P., (ed.), Deltaic Sedimentation - modern and ancient. Society of Economic Paleologists and Mineralogists Special Publication No. 15, p.31-47.

Moss, A.J., 1962. The physical nature of common sandy and pebbly deposits. Part 1. American Journal of Science, v. 260; p. 337-373.

Moss, A.J., 1963. The physical nature of common sandy and pebbly deposits. Part II. American Journal of Science, v. 261, p. 297-343.

Nelson, C.H., 1982. Modern shallow-water graded sand layers from storm surges, Bering Shelf: A mimic of Bouma sequences and turbidite systems. Journal of Sedimentary Petrology, v. 52, p. 537-545.

Nelson, H.W. and Glaister, R.P., 1975. Trap Creek Belly River section; a deltaic progradational sequence. In Shawa, M.S. (ed.), Guidebook to Selected Sedimentary Environments of Southwestern Alberta. Calgary, Canadian Society of Petroleum Geologists, p. 41-53.

Ogunyomi, O. and Hills, L.V., 1977. Depositional environments, Foremost Formation (Late Cretaceous), Milk River area, southern Alberta. Bulletin of Canadian Petroleum Geology, v. 25, p. 929-968.

Oilweek, October 26, 1964.

Potter, P.E. and Pettijohn, F.J., 1977. Paleocurrents and Basin Analysis. Berlin, Sspringer-Verlag, 425p.

Power, M.C., 1953. A new roundness scale for sedimentary particles. Journal of Sedimentary Petrology, v. 23, p. 117-119.

Pryor, W.A., 1968. Reservoir inhomogeneities of Recent sandstones. Final Report, American Petroleum Institute Research Project 91-B, American Petroleum Institute.

Rahmani, R.A. and Lerbekmo, J.F., 1975. Heavy mineral analysis of Upper Cretaceous and Paleocene sandstones in Alberta and adjacent areas of Saskatchewan. In Caldwell, W.G.E. (ed.), Geological Association of Canada Special Paper No. 13, p. 607-632.

Rapson, J.E., 1965. Petrography and derivation of JurassicCretaceous clastic rocks, southern Rocky Mountains, Canada. American Association of Petroleum Geologists Bulletin, v. 49, p. 1426-1452.

Reineck, H.E., 1961. Sedimentbewegungen an Kleinripplen im Watt : Seckenbergiana Lethaea, v. 42, p. 51-61.

Reineck, H.E., Guttmann, W.F. and Hertweck, G., 1967. Das Schlickgebeit sudlich Helgoland als Beispeil rezenter Schelfablagerungen. Senckenbergiana Lethaea, v. 48, p. 219275.

Reineck, H.E. and Singh, I.B., 1975. Depositional Sedimentary Environments. 1st ed. Springer-Verlag, New York, 439p.

Rosenthal, L., 1982. Depositional environments and paleogeography of the Upper Cretaceous Wapiabi and Belly River Formations in Southwestern Alberta, Canada (abs.). Eleventh International Congress on Sedimentology, p. 159.

Russel, L.S. and Landes, R.W., 1940. Geology of the southern Alberta plains. Geological Survey of Canada, Memoir 221, 223 p.

Rust, B.R., 1978. Classification of alluvial channel systems. Canadian Society of Petroleum Geologists Memoir 5, p. 187-198.

Rust, B.R., 1979. Facies Models 2: Coarse Alluvial Deposits. In R.G. Walker, ed., Geoscience Canada, Reprint Series 1, p 9-21.

Seilacher, A., 1967. Bathymetry of trace fossils. Marine Geology, 5, p 413-428.

Selley, R.C., 1970. Studies of sequence in sediments using a simple mathematical device. Quarterly Journal of the Geological Society of London, v. 125, p. 557-581.

Selley, R.C., 1970b. Ancient Sedimentary Environments. New York, Ithaca, 237p.

Selley, R.C., 1979. Concepts and methods of subsurface facies analysis. American Association of Petroleum Geologists, Continuing Education Course Note Series No. 9, p. 33-46.

Shawa, M.S. and Lee, P.J., 1975. Depositional environment of the Belly River section. In: Shawa, M.S. (ed.), Guidebook to Selected Sedimentary Environments in Southwestern Alberta. Calgary, Canadian Society of Petroleum Geologists, p. 34-40.

Shepherd, R.G., 1976. Sedimentary processes and structures of ephemeral-stream point-bars, Rio Puerco near Albuquerque, New Mexico. Geological Society of America Abstracts Program (Annual Meeting), v. 8, p. 1103.

Stelck, C.R., 1982. Personal Communication.

Stott, D.F., 1963. The Cretaceous Alberta Group and equivalent rocks, Rocky Mountain Foothills, Alberta. Geological Survey of Canada, Memoir 317, 306p.

Sundborg, A., 1956. The River Klaralven, a Study in Fluvial Processes. Geografiska Annaler, 38, p. 125-316.

Thiel, G.A., 1940. The relative resistance to abrasion of mineral grains of sand size. Journal of Sedimentary Petrology, v. 10, p. 103-124.

Turner, F.J., 1968. Metamorphic petrology. New York, McGraw-Hall Book Co., 403p.

Visher, G.S., 1969. Grain size distributions and depositional processes. Journal of Sedimentary Petrology, v. 39, p. 1074-1106.

Vos, R.G., 1977. Sedimentology of an Upper Paleozoic River, wave and tide influenced delta system in southern Morocco. Journal of Sedimentary Petrology, v. 47, p. 1242-1260.

Walgenwitz, F., Thomas, M. and Porthault, B., 1981. Example of diagenesis in a substatic hydrologic environment in the Belly River Formation sandstones, Alberta, Canada. Soc. Nat. Elf Aquitaine (Production), F-64018 Pau CEDEX, p. 137-150.

Walker, R.G., 1963. Distinctive types of ripple-drift cross-lamination. Sedimentology 2, 173.

Walker, R.G., 1979. Facies and Facies Models 1: General Introduction. In R.G. Walker, ed., Geoscience Canada Reprint Series 1, p. 1-7.

Walker, R.G. and Cant, D.J., 1979. Facies models 3: Sandy fluvial systems. In R.G. Walker, ed., Geoscience Canada Reprint Series 1, p. 23-31.

Wall, J.H. and Germundson, R.K., 1963. Microfaunas, megafaunas, and rock-stratigraphic units in the Alberta Group (Cretaceous) of the Rocky Mountain Foothills. Bulletin of Canadian Petroleum Geology, v. 11, p. 327-349.

Weimer, R.J., 1960. Upper Cretaceous stratigraphy, Rocky Mountains area. Bulletin of American Association of Petroleum Geologists, v. 44, p. 1-20.

Williams, G.D. and Burk, C.F. Jr., 1964. Upper Cretaceous. In Geological History of Western Canada. Calgary, Alberta Society of Petroleum Geologists, p. 169-189.

APPENDIX A: STRATIGRAPHIC SECTIONS

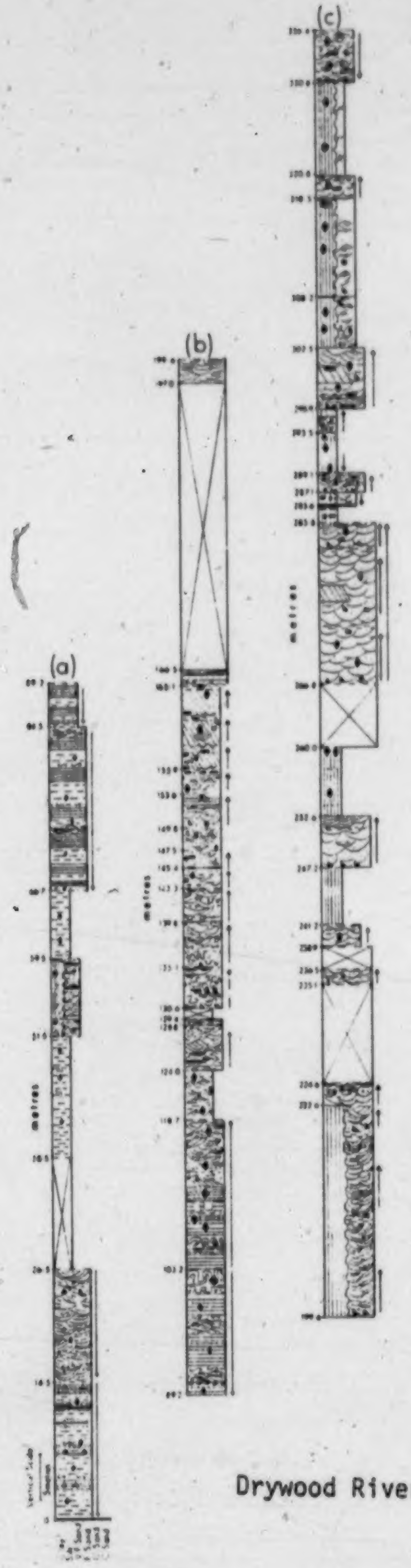
(a)
(b)
(c)
metres
metres
metres
Vertical Scale

Drywood River Section

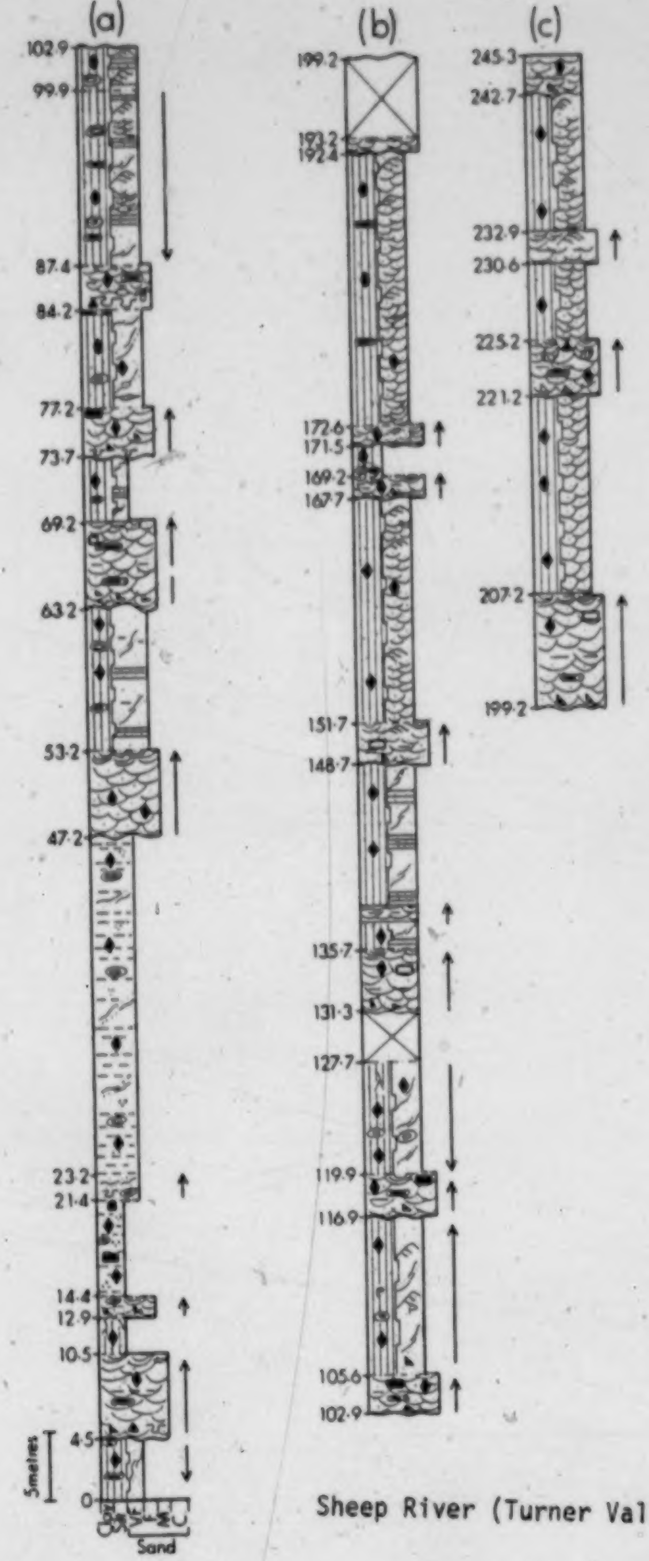
(a)
102.9
99.9
87·4
84·2
77·2
73·7
69·2
63·2
53·2
47·2
23·2
21·4
14·4
12·9
10·5
4·5
0
5metres
Sand
(b)
199·2
193·2
192·4
172·6
171·5
169·2
167·7
151·7
148·7
135·7
131·3
127·7
119·9
116·9
105·6
102·9
(c)
245·3
242·7
232·9
230·6
225·2
221·2
207·2
199·2

Sheep River (Turner Valley) section

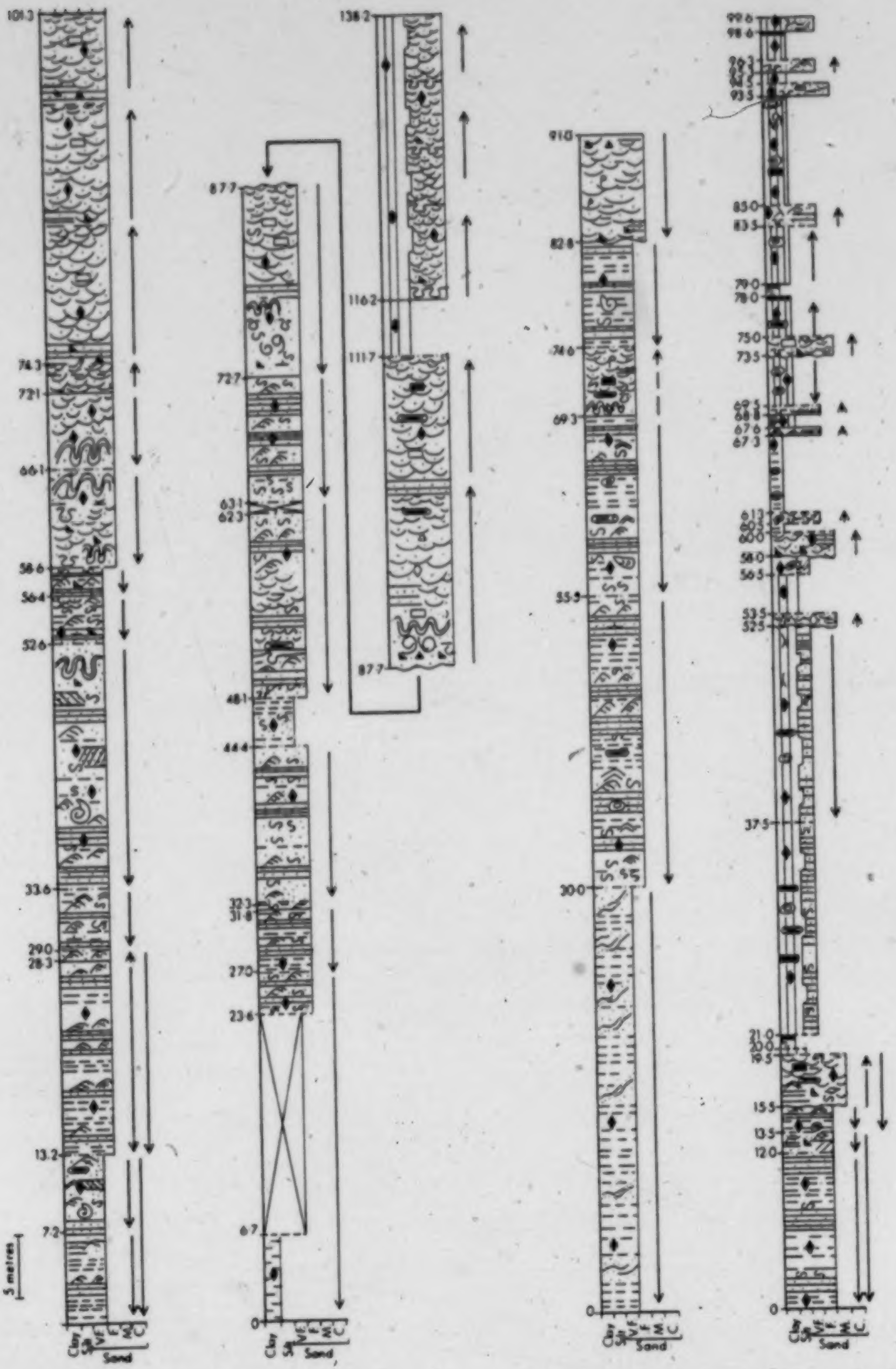
101.3
74.3
72.1
66.1
58.6
56.4
52.6
33.6
29.0
28.3
13.2
7.2
5 metres
Clay
Silt
Vf
F
M
C
Sand
87.7
72.7
63.1
62.3
48.1
44.4
32.3
31.8
27.0
23.6
6.7
0
138.2
116.2
111.7
87.7
91.0
82.8
74.6
69.3
55.5
30.0
0
99.6
98.6
96.3
93.5
85.0
83.5
79.0
78.0
75.0
73.5
69.5
68.8
67.6
67.3
61.3
60.0
58.0
56.5
53.5
52.5
37.5
21.0
20.0
19.5
15.5
13.5
12.0
0

Crowsnest River Oldman River Highwood River Jumpingpound (J1)

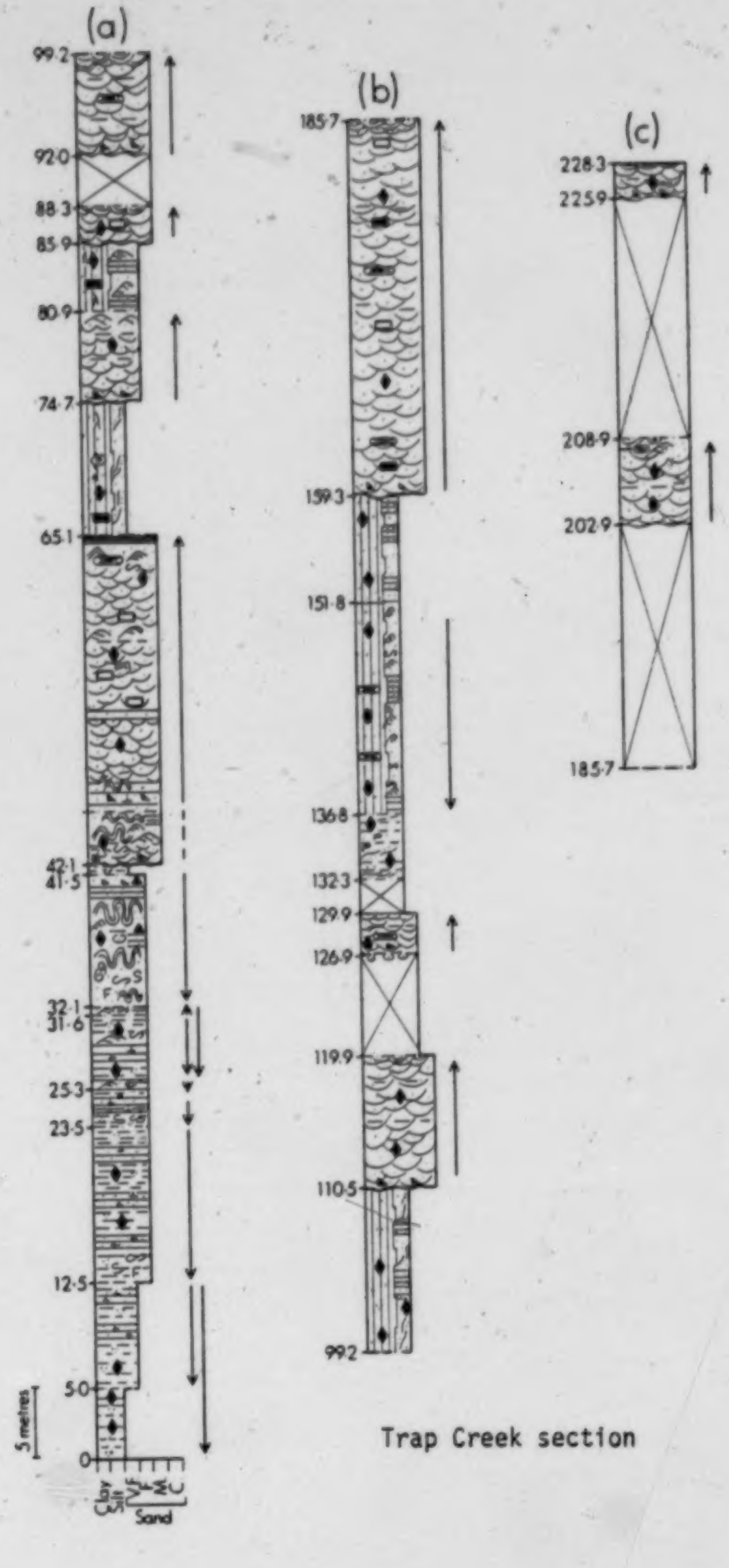
(a)
99·2
92·0
88·3
85·9
80·9
74·7
65·1
42·1
41·5
32·1
31·6
25·3
23·5
12·5
5·0
0
5 metres
Clay
Silt
VF
F
M
C
Sand
(b)
185·7
159·3
151·8
136·8
132·3
129·9
126·9
119·9
110·5
99·2
(c)
228·3
225·9
208·9
202·9
185·7

Trap Creek section

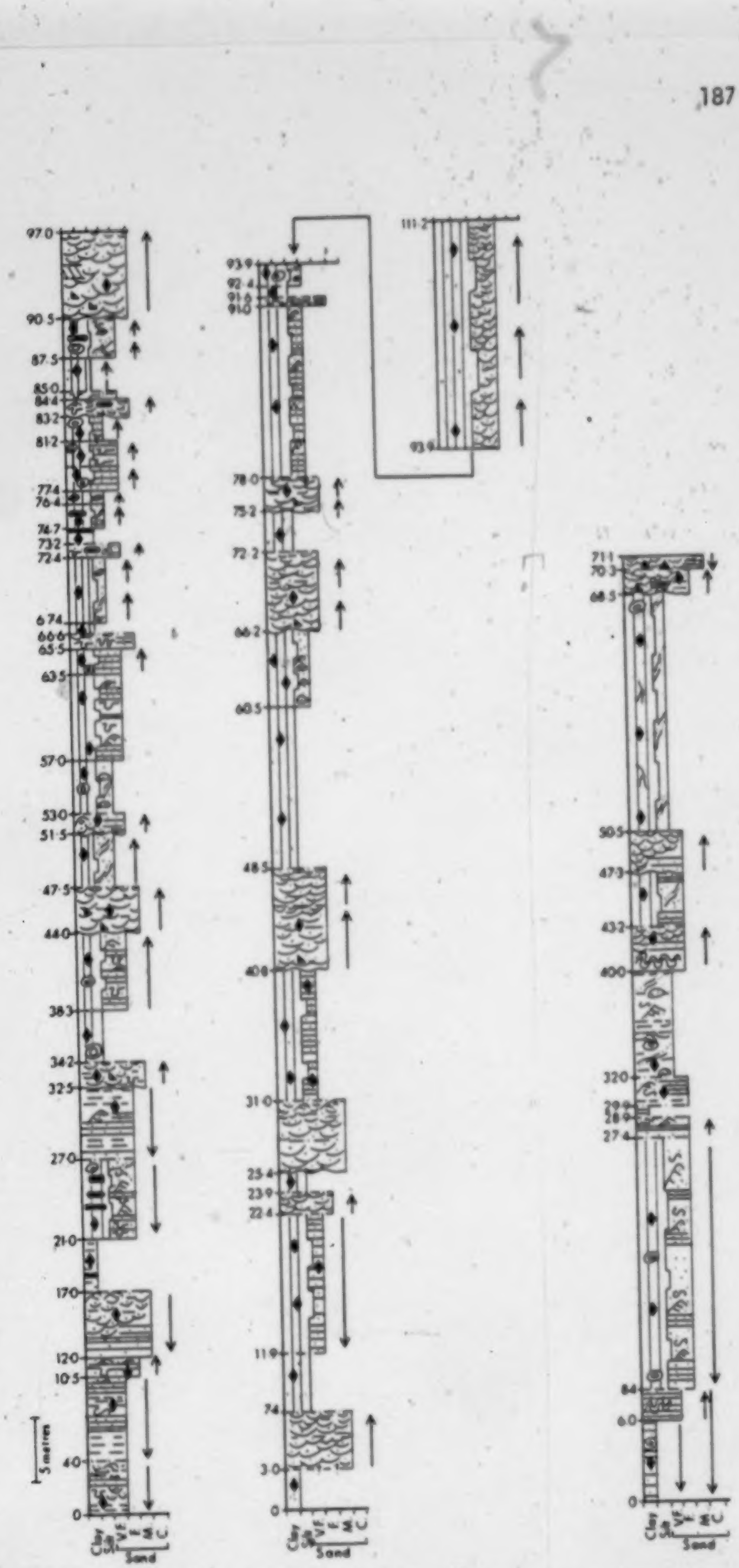
97.0
90.5
87.5
85.0
84.4
83.2
81.2
77.4
76.4
74.7
73.2
72.4
67.4
66.6
65.5
63.5
57.0
53.0
51.5
47.5
44.0
38.3
34.2
32.5
27.0
21.0
17.0
12.0
10.5
4.0
0
5 metres
111.2
93.9
93.9
92.4
91.6
91.0
78.0
75.2
72.2
66.2
60.5
48.5
40.8
31.0
25.4
23.9
22.4
11.9
7.4
3.0
0
71.1
70.3
68.5
50.5
47.3
43.2
40.0
32.0
29.9
28.9
27.4
8.4
6.0
0
Clay
Silt
VF
F
M
C
Sand

Jumpingpound (J2) Little Red Deer River Ram River

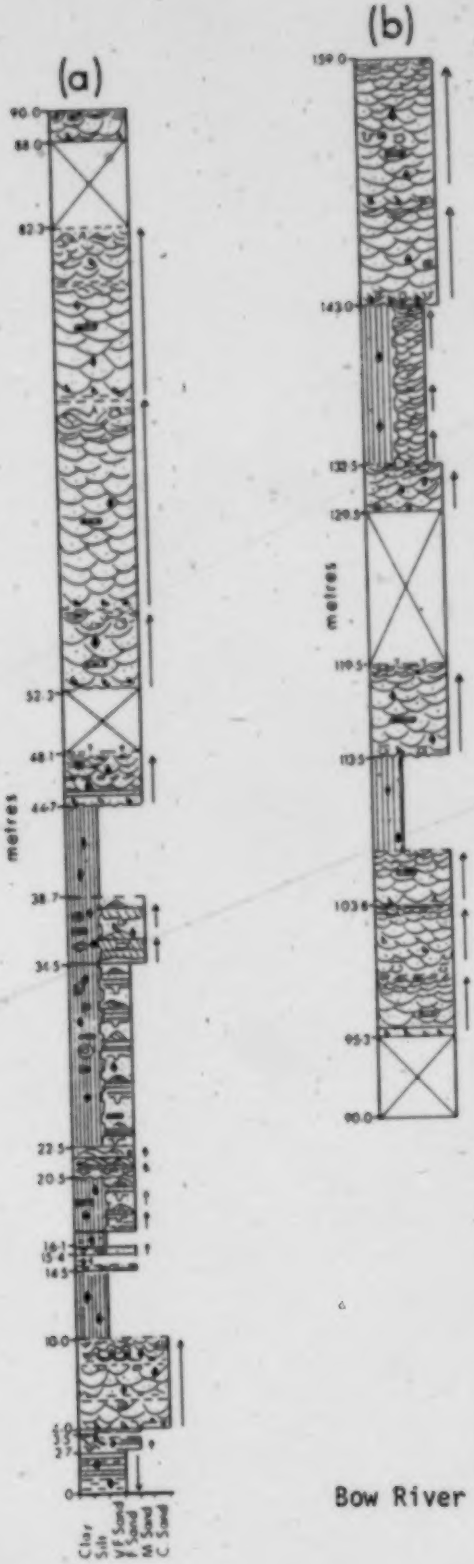
(b)
(a)
159.0
143.0
132.5
129.5
metres
119.5
113.5
103.6
95.3
90.0
90.0
88.0
82.3
52.3
48.1
46.7
metres
38.7
34.5
22.5
20.5
16.1
15.4
14.5
10.0
4.0
3.3
2.7
0
Clay
Silt
VF Sand
F Sand
M Sand
C Sand

Bow River (Morley) section

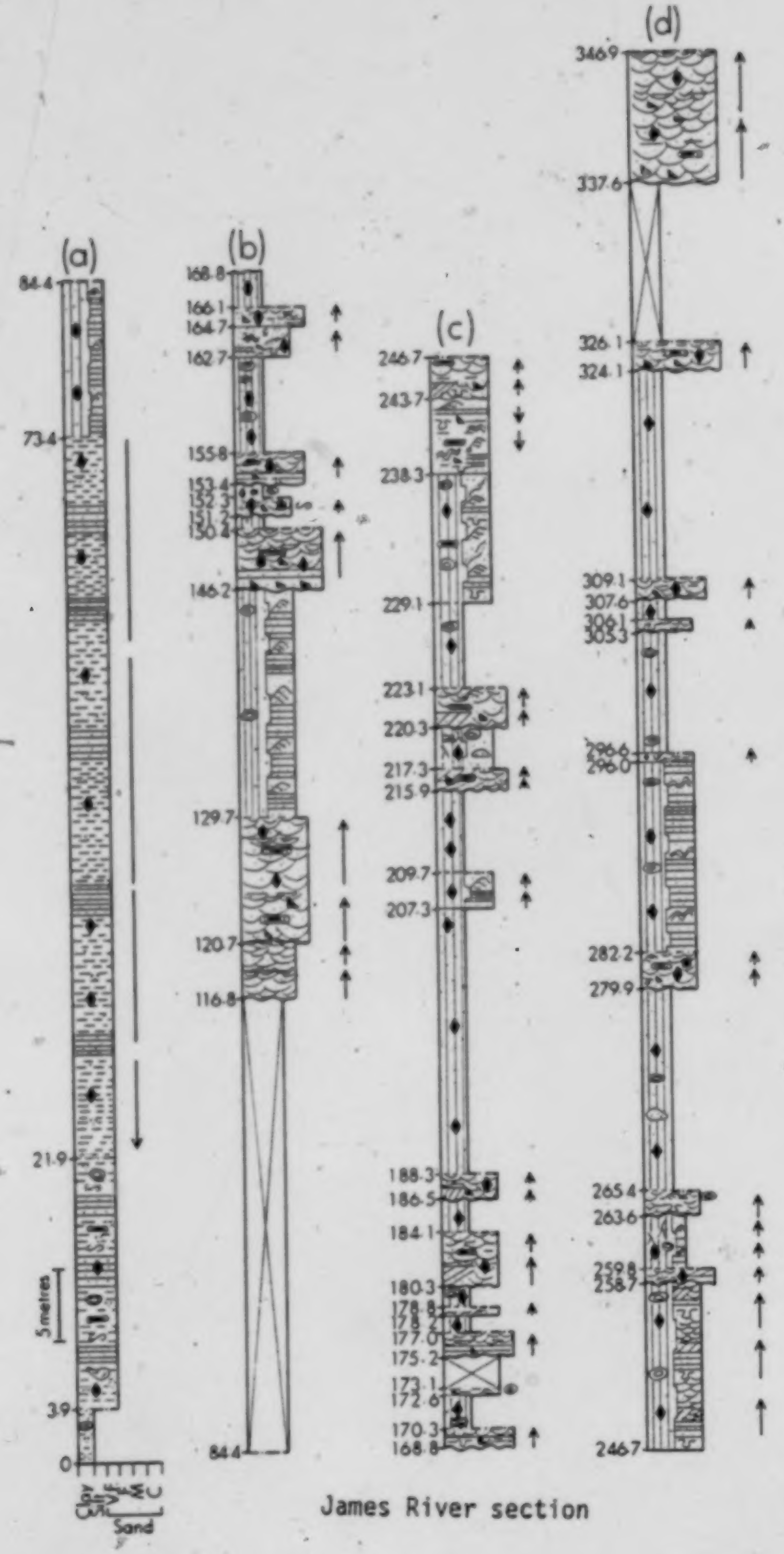
(a)
84.4
73.4
21.9
3.9
0
5 metres
Sand
(b)
168.8
166.1
164.7
162.7
155.8
153.4
152.3
151.2
150.4
146.2
129.7
120.7
116.8
84.4
(c)
246.7
243.7
238.3
229.1
223.1
220.3
217.3
215.9
209.7
207.3
188.3
186.5
184.1
180.3
178.8
178.2
177.0
175.2
173.1
172.6
170.3
168.8
(d)
346.9
337.6
326.1
324.1
309.1
307.6
306.1
305.3
296.6
296.0
282.2
279.9
265.4
263.6
259.8
258.7
246.7

James River section

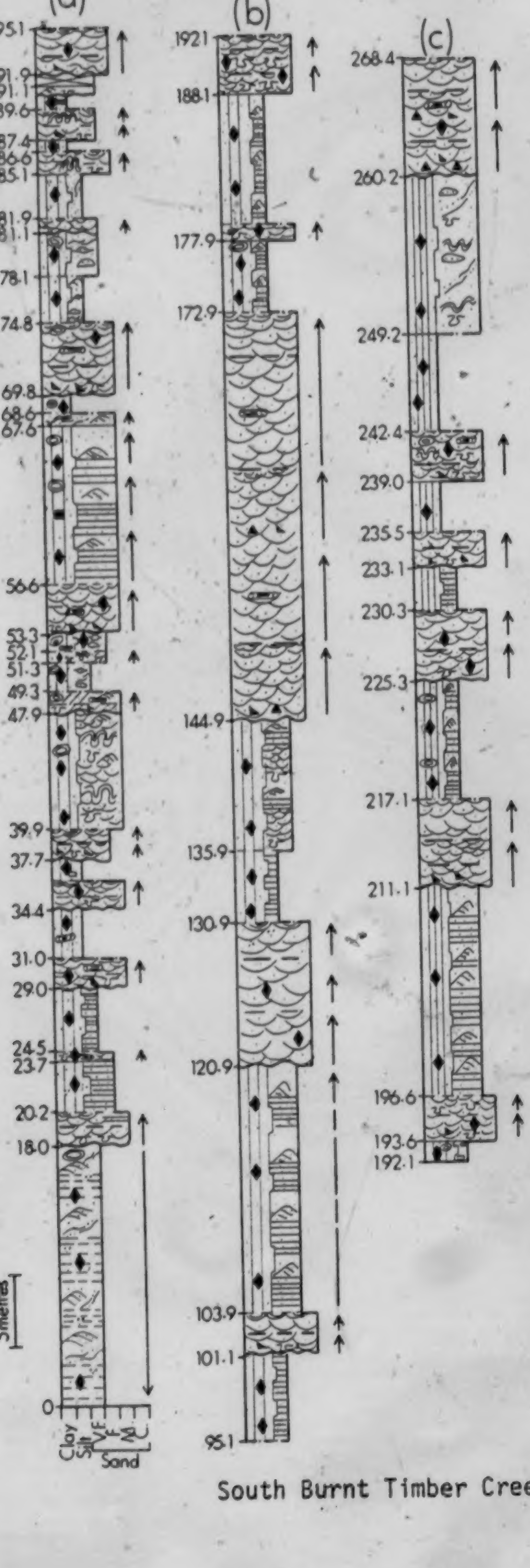
(a)
95.1
91.9
91.1
89.6
87.4
86.6
85.1
81.9
81.1
78.1
74.8
69.8
68.6
67.6
56.6
53.3
52.1
51.3
49.3
47.9
39.9
37.7
34.4
31.0
29.0
24.5
23.7
20.2
18.0
5metres
0
Clay
Silt
VF
F
M
Sand
(b)
192.1
188.1
177.9
172.9
144.9
135.9
130.9
120.9
103.9
101.1
95.1
(c)
268.4
260.2
249.2
242.4
239.0
235.5
233.1
230.3
225.3
217.1
211.1
196.6
193.6
192.1

South Burnt Timber Creek section

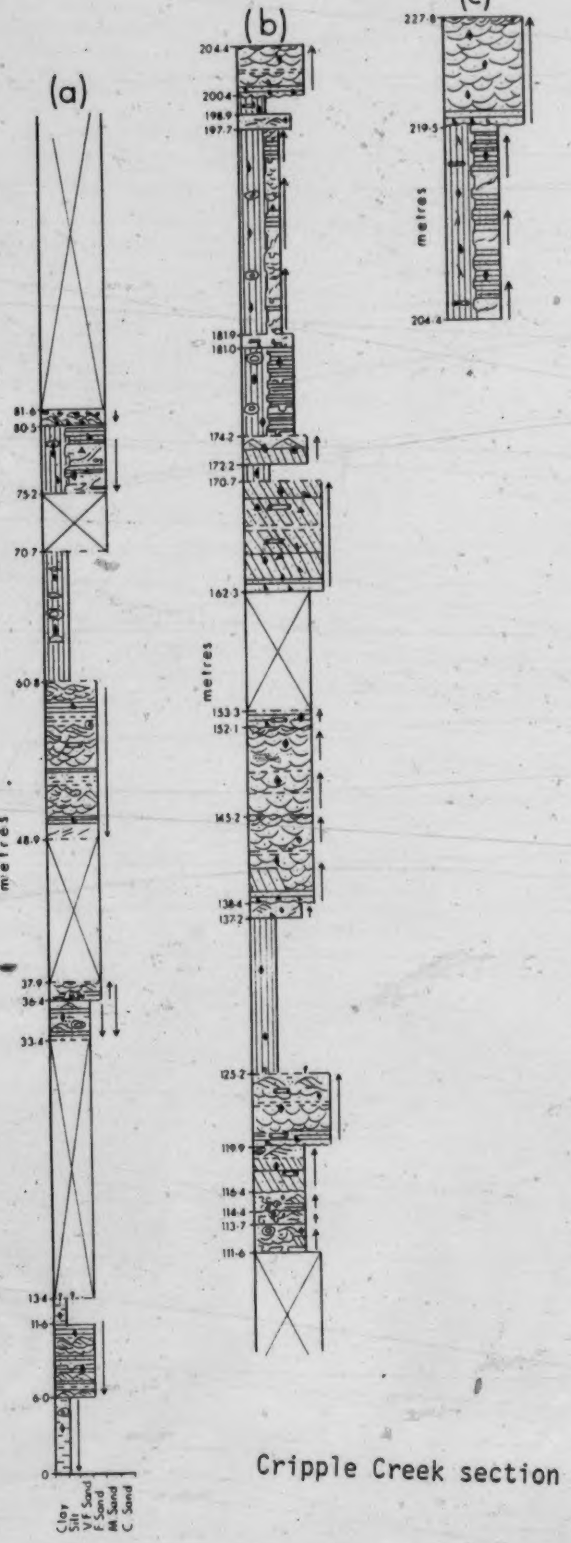
(a)
81.6
80.5
75.2
70.7
60.8
48.9
37.9
36.4
33.4
13.4
11.6
6.0
0
metres
Clay
Silt
VF Sand
F Sand
M Sand
C Sand
(b)
204.4
200.4
198.9
197.7
181.9
181.0
174.2
172.2
170.7
162.3
metres
153.3
152.1
145.2
138.4
137.2
125.2
119.9
116.4
114.4
113.7
111.6
(c)
227.8
219.5
metres
204.4

Cripple Creek section

APPENDIX B: FACIES RELATIONSHIP DIAGRAMS (FRDS) FOR THE INDIVIDUAL STRATIGRAPHIC SECTIONS.

Diagrams are based on transitions that occur more commonly than random and show only transitions whose observed-minus-predicted (random) transition probabilities exceed 0.05. Thin, dashed arrows show probabilities in the range 0.05 to 0.10; thin unbroken arrows, 0.1 to 0.30; thick arrows, >0.30. Numbers above or beside the arrows indicate the actual difference probability values. Four facies associations have been interpreted and circled on the diagrams.

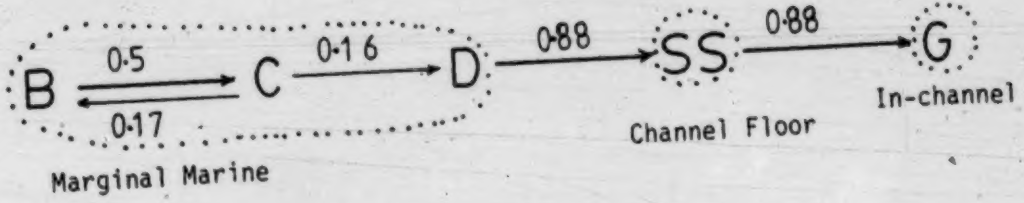
B
0·5
0·17
C
0·1 6
D
0·88
SS
0·88
G
In-channel
Channel Floor
Marginal Marine

Crowsnest (Lundbreck) River Section

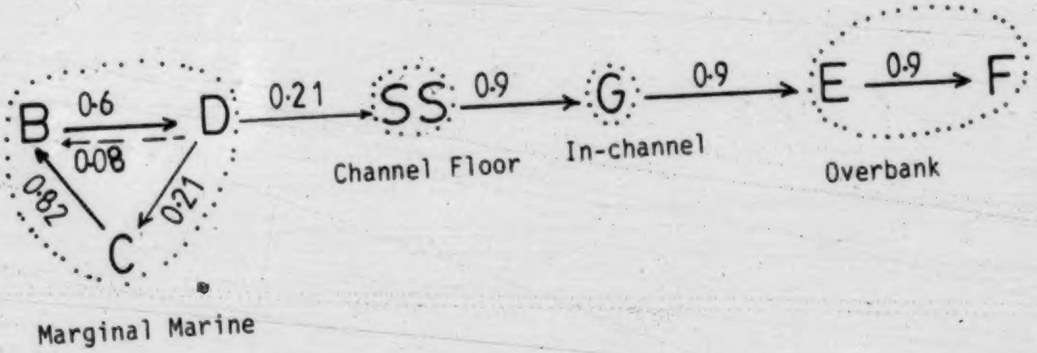
B
0·6
0·08
D
0·82
0·21
C
0·21
SS
0·9
G
0·9
E
0·9
F
Channel Floor
In-channel
Overbank
Marginal Marine

Oldman River Section

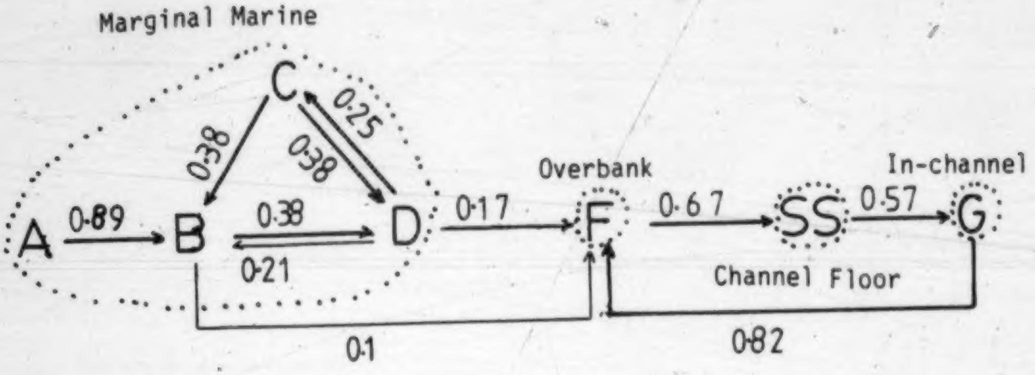
Marginal Marine
C
0·38
0·25
0·38
Overbank
In-channel
A
0·89
B
0·38
D
0·17
F
0·67
SS
0·57
G
0·21
Channel Floor
0·1
0·82

Trap Creek Section

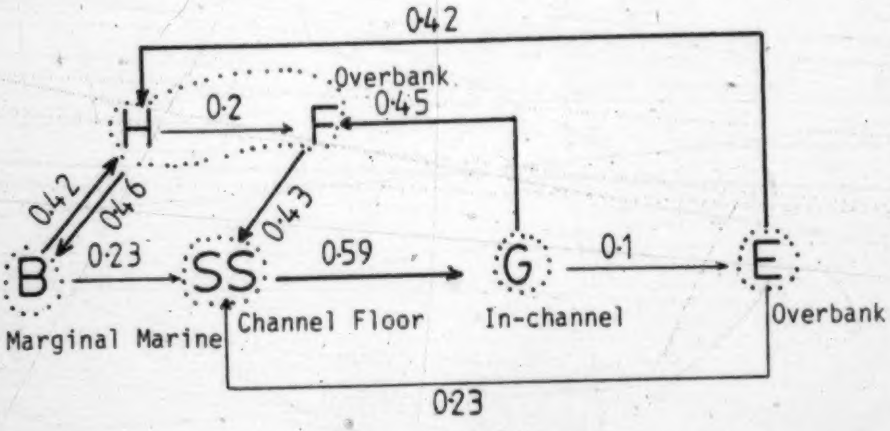
0·42
Overbank
H
0·2
F
0·45
0·42
0·46
0·43
B
0·23
SS
0·59
G
0·1
E
Marginal Marine
Channel Floor
In-channel
Overbank
0·23

Sheep River (Turner Valley) Section

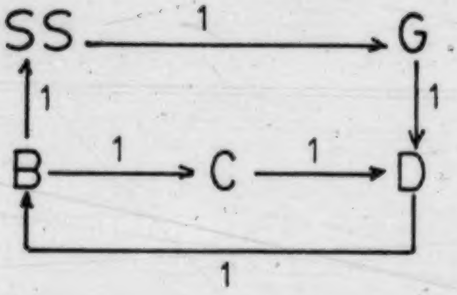

Highwood River Section. (Unsimplified 'spider' diagram; numbers above or beside the arrows indicate actual numbers of transitions observed).

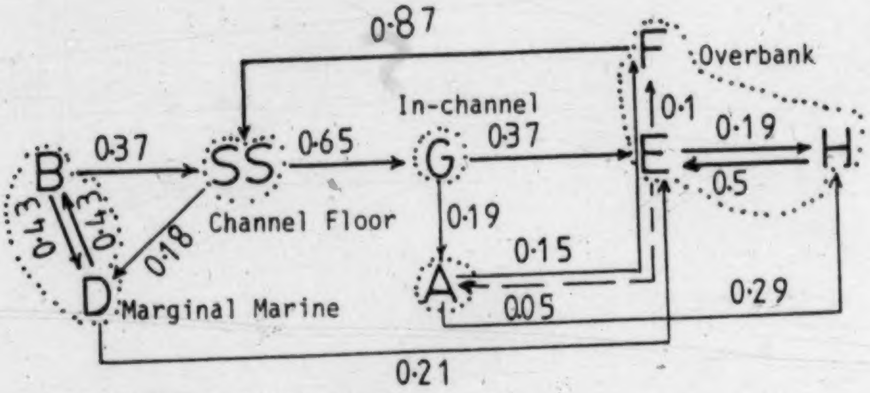
0·87
F
Overbank
In-channel
0·1
B
0·37
SS
0·65
G
0·37
E
0·19
H
0·5
0·43
0·43
Channel Floor
0·19
0·18
0·15
A
D
Marginal Marine
0·05
0·29
0·21

Jumpingpound (J1) Section

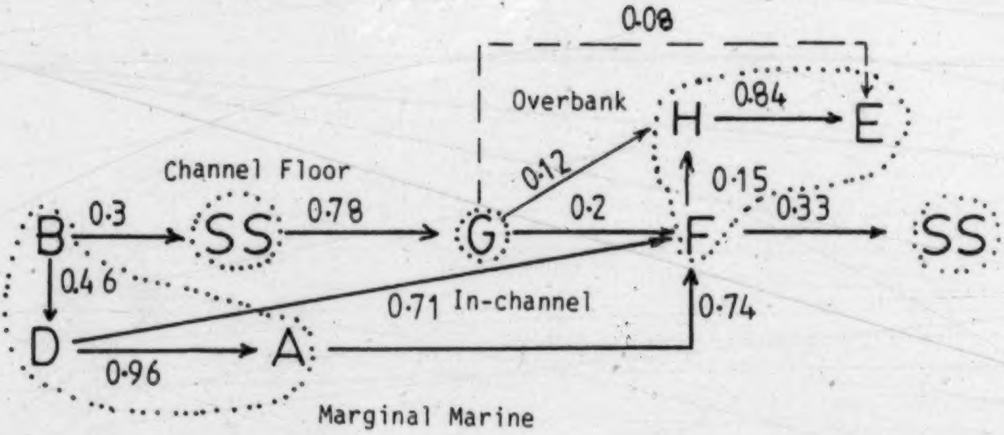
0·08
Overbank
H
0·84
E
Channel Floor
0·12
0·15
B
0·3
SS
0·78
G
0·2
F
0·33
SS
0·4 6
0·71
In-channel
0·74
D
0·96
A
Marginal Marine

Jumpingpound (J2) Section

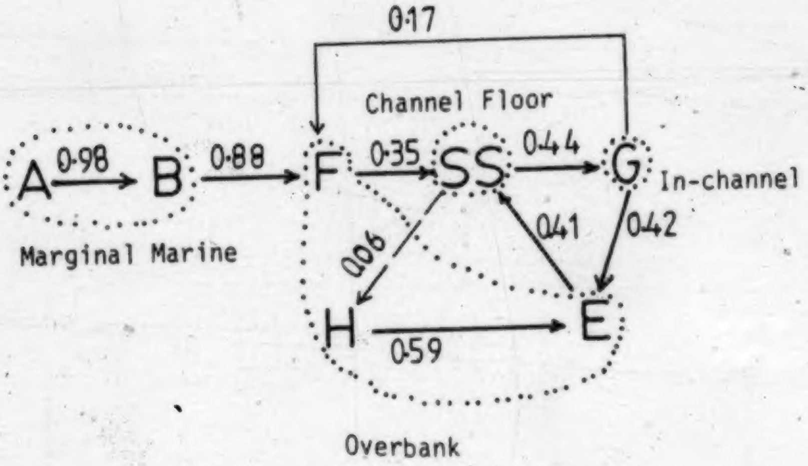
0·17
Channel Floor
A
0·98
B
0·88
F
0·35
SS
0·44
G
In-channel
0·41
0·42
0·06
Marginal Marine
H
E
0·59
Overbank

James River Section

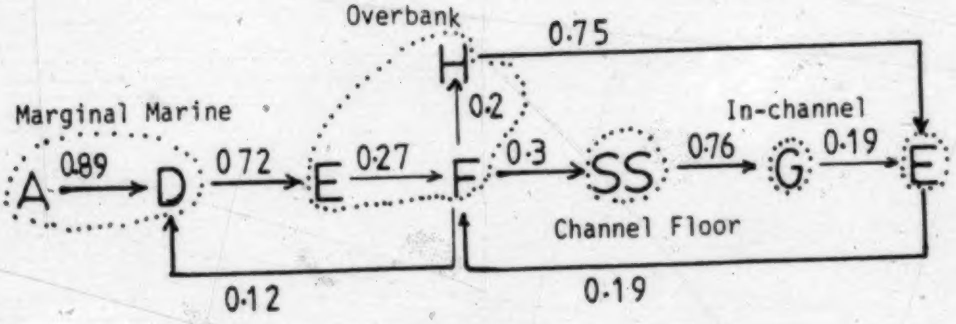
Overbank
H
0·75
0·2
Marginal Marine
In-channel
A
0·89
D
0·72
E
0·27
F
0·3
SS
0·76
G
0·19
E
Channel Floor
0·12
0·19

Little Red Deer River Section

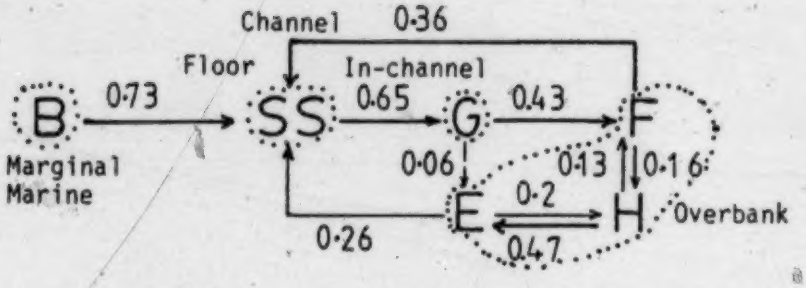
Channel
0·36
Floor
In-channel
B
0·73
SS
0·65
G
0·43
F
Marginal
Marine
0·06
0·13
0·1 6
E
0·2
H
Overbank
0·26
0·47

South Burnt Timber Creek Section

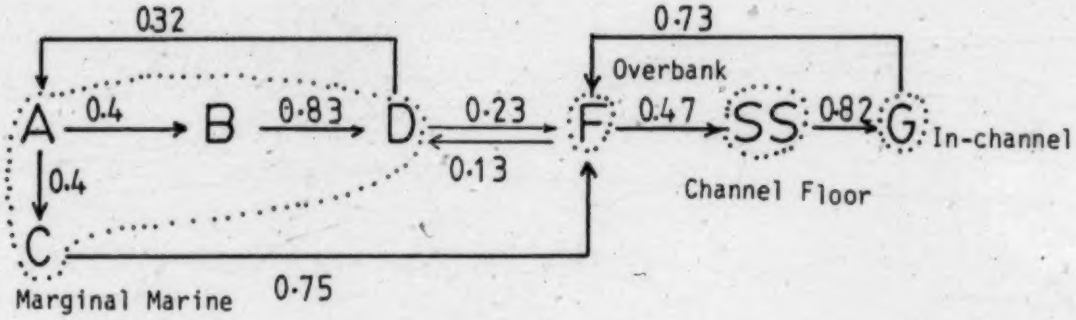
032
0·73
Overbank
A
0·4
B
0·83
D
0·23
F
0·47
SS
0·82
G
In-channel
0·4
0·13
Channel Floor
C
Marginal Marine
0·75

Ram River Section

APPENDIX C

Data sheet for the grain size analyses (using Humphries' Micrometer Eyepiece and the Counter Unit).

Sample D1

Grain size (Phi)	Number of grains	Percent of grains	Cumulative percent
1.875	1	0.167	0.167
2.375	5	0.833	1.000
2.625	5	0.833	1.833
2.875	24	4.000	5.833
3.125	77	12.833	18.667
3.375	115	19.167	37.833
3.625	133	22.167	60.000
3.875	107	17.833	77.833
4.125	77	12.833	90.667
4.375	56	9.333	100.000

Sample D2

Grain size (Phi)	Number of grains	Percent of grains	Cumulative percent
1.625	1	0.167	0.167
1.875	3	0.500	0.667
2.125	11	1.833	2.500
2.375	27	4.500	7.000
2.625	54	9.000	16.000
2.875	98	16.333	32.333
3.125	114	19.000	51.333
3.375	111	18.500	69.833
3.625	85	14.167	84.000
3.875	48	8.000	92.000
4.125	32	5.333	97.333
4.375	16	2.667	100.000

Sample D15B

Grain size (Phi)	Number of grains	Percent of grains	Cumulative percent
2.375	1	0.167	0.167
2.625	4	0.667	0.833
2.875	15	2.500	3.333
3.125	30	5.000	8.333
3.375	59	9.833	18.167
3.625	103	17.167	35.333
3.875	129	21.500	56.833
4.125	125	20.833	77.667
4.375	134	22.333	100.000

Sample D17B

Grain size (Phi)	Number of grains	Percent of grains	Cumulative percent
2.125	1	0.167	0.167
2.375	1	0.167	0.333
2.625	11	1.833	2.167
2.875	27	4.500	6.667
3.125	55	9.167	15.833
3.375	92	15.333	31.167
3.625	137	22.833	54.000
3.875	129	21.500	75.500
4.125	89	14.833	90.333
4.375	58	9.667	100.000

Sample D18

Grain size (Phi)	Number of grains	Percent of grains	Cumulative percent
2.375	1	0.167	0.167
2.625	8	1.333	1.500
2.875	18	3.000	4.500
3.125	49	8.167	12.667
3.375	88	14.667	27.333
3.625	152	25.333	52.667
3.875	112	18.667	71.333
4.125	103	17.167	88.500
4.375	69	11.500	100.000

Sample D23

Grain size (Phi)	Number of grains	Percent of grains	Cumulative percent
1.875	3	0.500	0.500
2.125	16	2.667	3.167
2.375	24	4.000	7.167
2.625	46	7.667	14.833
2.875	86	14.333	29.167
3.125	115	19.167	48.333
3.375	105	17.500	65.833
3.625	76	12.667	78.500
3.875	79	13.167	91.667
4.125	28	4.667	96.333
4.375	22	3.667	100.000

Sample D24B

Grain size (Phi)	Number of grains	Percent of grains	Cumulative percent
1.625	1	0.167	0.167
1.875	2	0.333	0.500
2.125	7	1.167	1.667
2.375	17	2.833	4.500
2.625	34	5.667	10.167
2.875	85	14.167	24.333
3.125	123	20.500	44.833
3.375	114	19.000	63.833
3.625	103	17.167	81.000
3.875	58	9.667	90.667
4.125	37	6.167	96.833
4.375	19	3.167	100.000

Sample D26B

Grain size (Phi)	Number of grains	Percent of grains	Cumulative percent
0.625	1	0.167	0.167
0.875	1	0.167	0.333
1.125	1	0.167	0.500
1.375	9	1.500	2.000
1.625	29	4.833	6.833
1.875	69	11.500	18.333
2.125	90	15.000	33.333
2.375	127	21.167	54.500
2.625	98	16.333	70.833
2.875	70	11.667	82.500
3.125	54	9.000	91.500
3.375	29	4.833	96.333
3.625	13	2.167	98.500
3.875	8	1.333	99.833
4.125	1	0.167	100.000

Sample D27(ii)

Grain size (Phi)	Number of grains	Percent of grains	Cumulative percent
1.125	2	0.333	0.333
1.375	6	1.000	1.333
1.625	21	3.500	4.833
1.875	58	9.667	14.500
2.125	85	14.167	28.667
2.375	96	16.000	44.667
2.625	110	18.333	63.000
2.875	85	14.167	77.167
3.125	58	9.667	86.833
3.375	32	5.333	92.167
3.625	28	4.667	96.833
3.875	14	2.333	99.167
4.125	3	0.500	99.667
4.375	2	0.333	100.000

Sample D30B

Grain size (Phi)	Number of grains	Percent of grains	Cumulative percent
1.375	3	0.500	0.500
1.625	16	2.667	3.167
1.875	48	8.000	11.167
2.125	66	11.000	22.167
2.375	106	17.667	39.833
2.625	112	18.667	58.500
2.875	89	14.833	73.333
3.125	85	14.167	87.500
3.375	41	6.833	94.333
3.625	18	3.000	97.333
3.875	14	2.333	99.667
4.125	2	0.333	100.000

Sample D34B

Grain size (Phi)	Number of grains	Percent of grains	Cumulative percent
1.125	1	0.167	0.167
1.375	2	0.333	0.500
1.625	13	2.167	2.667
1.875	48	8.000	10.667
2.125	105	17.500	28.167
2.375	124	20.667	48.833
2.625	112	18.667	67.500
2.875	82	13.667	81.167
3.125	49	8.167	89.333
3.375	37	6.167	95.500
3.625	13	2.167	97.667
3.875	10	1.667	99.333
4.125	4	0.667	100.000

Sample D37B

Grain size (Phi)	Number of grains	Percent of grains	Cumulative percent
0.625	15	2.500	2.500
0.875	20	3.333	5.833
1.125	30	5.000	10.833
1.375	58	9.667	20.500
1.625	82	13.667	34.167
1.875	103	17.167	51.333
2.125	92	15.333	66.667
2.375	73	12.167	78.833
2.625	46	7.667	86.500
2.875	42	7.000	93.500
3.125	22	3.667	97.167
3.375	11	1.833	99.000
3.625	5	0.833	99.833
4.125	1	0.167	100.000

Sample D47

Grain size (Phi)	Number of grains	Percent of grains	Cumulative percent
2.375	2	0.333	0.333
2.625	4	0.667	1.000
2.875	17	2.833	3.833
3.125	40	6.667	10.500
3.375	86	14.333	24.833
3.625	125	20.833	45.667
3.875	121	20.167	65.833
4.125	106	17.667	83.500
4.375	99	16.500	100.000

Sample D48B

Grain size (Phi)	Number of grains	Percent of grains	Cumulative percent
2.125	3	0.500	0.500
2.375	2	0.333	0.833
2.625	9	1.500	2.333
2.875	19	3.167	5.500
3.125	25	4.167	9.667
3.375	68	11.333	21.000
3.625	121	20.167	41.167
3.875	121	20.167	61.333
4.125	111	18.500	79.833
4.375	121	20.167	100.000

Sample OR3B

Grain size (Phi)	Number of grains	Percent of grains	Cumulative percent
2.625	1	0.167	0.167
2.875	7	1.167	1.333
3.125	13	2.167	3.500
3.375	40	6.667	10.167
3.625	56	9.333	19.500
3.875	96	16.000	35.500
4.125	134	22.333	57.833
4.375	253	42.167	100.000

Sample OR3

Grain size (Phi)	Number of grains	Percent of grains	Cumulative percent
1.875	1	0.167	0.167
2.625	3	0.500	0.667
2.875	11	1.833	2.500
3.125	28	4.667	7.167
3.375	56	9.333	16.500
3.625	84	14.000	30.500
3.875	126	21.000	51.500
4.125	143	23.833	75.333
4.375	149	24.833	100.167

Sample OR4T

Grain size (Phi)	Number of grains	Percent of grains	Cumulative percent
2.875	1	0.167	0.167
3.125	8	1.333	1.500
3.375	23	3.833	5.333
3.625	36	6.000	11.333
3.875	86	14.333	25.667
4.125	139	23.167	48.833
4.375	307	51.167	100.000

Sample OR5B

Grain size (Phi)	Number of grains	Percent of grains	Cumulative percent
2.375	1	0.167	0.167
2.625	5	0.833	1.000
2.875	8	1.333	2.333
3.125	18	3.000	5.333
3.375	40	6.667	12.000
3.625	91	15.167	27.167
3.875	131	21.833	49.000
4.125	136	22.667	71.667
4.375	170	28.333	100.000

Sample OR5T

Grain size (Phi)	Number of grains	Percent of grains	Cumulative percent
2.625	3	0.500	0.500
2.875	9	1.500	2.000
3.125	23	3.833	5.833
3.375	50	8.333	14.167
3.625	66	11.000	25.167
3.875	96	16.000	41.167
4.125	114	19.000	60.167
4.375	239	39.833	100.000

Sample OR6B

Grain size (Phi)	Number of grains	Percent of grains	Cumulative percent
2.375	1	0.167	0.167
2.875	5	0.833	1.000
3.125	11	1.833	2.833
3.375	31	5.167	8.000
3.625	67	11.167	19.167
3.875	105	17.500	36.667
4.125	127	21.167	57.833
4.375	253	42.167	100.000

Sample OR6T

Grain size (Phi)	Number of grains	Percent of grains	Cumulative percent
2.125	1	0.167	0.167
2.375	2	0.333	0.500
2.625	4	0.667	1.167
2.875	10	1.667	2.833
3.125	20	3.333	6.167
3.375	54	9.000	15.167
3.625	93	15.500	30.667
3.875	105	17.500	48.167
4.125	121	20.167	68.333
4.375	190	31.667	100.000

Sample OR8B

Grain size (Phi)	Number of grains	Percent of grains	Cumulative percent
2.125	1	0.167	0.167
2.375	2	0.333	0.500
2.625	6	1.000	1.500
2.875	7	1.167	2.667
3.125	17	2.833	5.500
3.375	37	6.167	11.667
3.625	65	10.833	22.500
3.875	108	18.000	40.500
4.125	134	22.333	62.833
4.375	223	37.167	100.000

Sample OR8T

Grain size (Phi)	Number of grains	Percent of grains	Cumulative percent
2.125	4	0.667	0.667
2.375	5	0.833	1.500
2.625	16	2.667	4.167
2.875	41	6.833	11.000
3.125	64	10.667	21.667
3.375	89	14.833	36.500
3.625	124	20.667	57.167
3.875	110	18.333	75.500
4.125	70	11.667	87.167
4.375	77	12.833	100.000

Sample OR10B

Grain size (Phi)	Number of grains	Percent of grains	Cumulative percent
2.125	1	0.167	0.167
2.375	1	0.167	0.333
2.625	6	1.000	1.333
2.875	14	2.333	3.667
3.125	38	6.333	10.000
3.375	65	10.833	20.833
3.625	107	17.833	38.667
3.875	121	20.167	58.833
4.125	117	19.500	78.333
4.375	130	21.667	100.000

Sample OR10T

Grain size (Phi)	Number of grains	Percent of grains	Cumulative percent
2.125	7	1.167	1.167
2.375	10	1.667	2.833
2.625	27	4.500	7.333
2.875	56	9.333	16.667
3.125	92	15.333	32.000
3.375	93	15.500	47.500
3.625	113	18.833	66.333
3.875	85	14.167	80.500
4.125	53	8.833	89.333
4.375	64	10.667	100.000

Sample OR11B

Grain size (Phi)	Number of grains	Percent of grains	Cumulative percent
1.625	1	0.167	0.167
2.125	2	0.333	0.500
2.375	11	1.833	2.333
2.625	21	3.500	5.833
2.875	72	12.000	17.833
3.125	97	16.167	34.000
3.375	130	21.667	55.667
3.625	120	20.000	75.667
3.875	92	15.333	91.000
4.125	28	4.667	95.667
4.375	26	4.333	100.000

Sample OR11T

Grain size (Phi)	Number of grains	Percent of grains	Cumulative percent
2.125	2	0.333	0.333
2.375	12	2.000	2.333
2.625	31	5.167	7.500
2.875	82	13.667	21.167
3.125	107	17.833	39.000
3.375	116	19.333	58.333
3.625	106	17.667	76.000
3.875	85	14.167	90.167
4.125	33	5.500	95.667
4.375	26	4.333	100.000

Sample OR12B

Grain size (Phi)	Number of grains	Percent of grains	Cumulative percent
1.875	2	0.333	0.333
2.125	6	1.000	1.333
2.375	14	2.333	3.667
2.625	34	5.667	9.333
2.875	69	11.500	20.833
3.125	97	16.167	37.000
3.375	136	22.667	59.667
3.625	92	15.333	75.000
3.875	79	13.167	88.167
4.125	44	7.333	95.500
4.375	27	4.500	100.000

Sample OR12T

Grain size (Phi)	Number of grains	Percent of grains	Cumulative percent
1.375	4	0.667	0.667
1.625	8	1.333	2.000
1.875	32	5.333	7.333
2.125	79	13.167	20.500
2.375	101	16.833	37.333
2.625	112	18.667	56.000
2.875	79	13.167	69.167
3.125	64	10.667	79.833
3.375	50	8.333	88.167
3.625	33	5.500	93.667
3.875	22	3.667	97.333
4.125	9	1.500	98.833
4.375	7	1.167	100.000

Sample OR14B1

Grain size (Phi)	Number of grains	Percent of grains	Cumulative percent
1.875	14	2.333	2.333
2.125	34	5.667	8.000
2.375	45	7.500	15.500
2.625	111	18.500	34.000
2.875	124	20.667	54.667
3.125	88	14.667	69.333
3.375	76	12.667	82.000
3.625	44	7.333	89.333
3.875	35	5.833	95.167
4.125	12	2.000	97.167
4.375	17	2.833	100.000

Sample OR14T1

Grain size (Phi)	Number of grains	Percent of grains	Cumulative percent
2.625	2	0.333	0.333
2.875	6	1.000	1.333
3.125	10	1.667	3.000
3.375	21	3.500	6.500
3.625	47	7.833	14.333
3.875	100	16.667	31.000
4.125	134	22.333	53.333
4.375	280	46.667	100.000

Sample OR14B2

Grain size (Phi)	Number of grains	Percent of grains	Cumulative percent
1.125	3	0.500	0.500
1.375	5	0.833	1.333
1.625	11	1.833	3.167
1.875	35	5.833	9.000
2.125	48	8.000	17.000
2.375	89	14.833	31.833
2.625	91	15.167	47.000
2.875	100	16.667	63.667
3.125	76	12.667	76.333
3.375	63	10.500	86.833
3.625	37	6.167	93.000
3.875	25	4.167	97.167
4.125	8	1.333	98.500
4.375	9	1.500	100.000

Sample OR14B3

Grain size (Phi)	Number of grains	Percent of grains	Cumulative percent
1.125	3	0.500	0.500
1.375	3	0.500	1.000
1.625	27	4.500	5.500
1.875	40	6.667	12.167
2.125	90	15.000	27.167
2.375	98	16.333	43.500
2.625	121	20.167	63.667
2.875	86	14.333	78.000
3.125	65	10.833	88.833
3.375	29	4.833	93.667
3.625	22	3.667	97.333
3.875	10	1.667	99.000
4.125	5	0.833	99.833
4.375	1	0.167	100.000

Sample OR14T3

Grain size (Phi)	Number of grains	Percent of grains	Cumulative percent
1.125	1	0.167	0.167
1.375	2	0.333	0.500
1.625	17	2.833	3.333
1.875	40	6.667	10.000
2.125	77	12.833	22.833
2.375	92	15.333	38.167
2.625	106	17.667	55.833
2.875	95	15.833	71.667
3.125	61	10.167	81.833
3.375	53	8.833	90.667
3.625	30	5.000	95.667
3.875	16	2.667	98.333
4.125	5	0.833	99.167
4.375	5	0.833	100.000

Sample M3

Grain size (Phi)	Number of grains	Percent of grains	Cumulative percent
1.125	3	0.500	0.500
1.375	2	0.333	0.833
1.625	4	0.667	1.500
1.875	3	0.500	2.000
2.125	7	1.167	3.167
2.375	21	3.500	6.667
2.625	37	6.167	12.833
2.875	51	8.500	21.333
3.125	76	12.667	34.000
3.375	93	15.500	49.500
3.625	91	15.167	64.667
3.875	86	14.333	79.000
4.125	59	9.833	88.833
4.375	67	11.167	100.000

Sample M5

Grain size (Phi)	Number of grains	Percent of grains	Cumulative percent
2.125	4	0.667	0.667
2.375	12	2.000	2.667
2.625	33	5.500	8.167
2.875	71	11.833	20.000
3.125	70	11.667	31.667
3.375	117	19.500	51.167
3.625	114	19.000	70.167
3.875	86	14.333	84.500
4.125	49	8.167	92.667
4.375	44	7.333	100.000

Sample M6

Grain size (Phi)	Number of grains	Percent of grains	Cumulative percent
0.875	4	0.667	0.667
1.125	9	1.500	2.167
1.375	21	3.500	5.667
1.625	62	10.333	16.000
1.875	91	15.167	31.167
2.125	109	18.167	49.333
2.375	82	13.667	63.000
2.625	86	14.333	77.333
2.875	63	10.500	87.833
3.125	37	6.167	94.000
3.375	17	2.833	96.833
3.625	12	2.000	98.833
3.875	3	0.500	99.333
4.125	4	0.667	100.000

Sample M8

Grain size (Phi)	Number of grains	Percent of grains	Cumulative percent
1.875	2	0.333	0.333
2.125	5	0.833	1.167
2.375	34	5.667	6.833
2.625	59	9.833	16.667
2.875	118	19.667	36.333
3.125	109	18.167	54.500
3.375	105	17.500	72.000
3.625	79	13.167	85.167
3.875	54	9.000	94.167
4.125	22	3.667	97.833
4.375	13	2.167	100.000

Sample M10

Grain size (Phi)	Number of grains	Percent of grains	Cumulative percent
1.125	1	0.167	0.167
1.875	1	0.167	0.333
2.125	6	1.000	1.333
2.375	15	2.500	3.833
2.625	25	4.167	8.000
2.875	46	7.667	15.667
3.125	76	12.667	28.333
3.375	113	18.833	47.167
3.625	96	16.000	63.167
3.875	95	15.833	79.000
4.125	67	11.167	90.167
4.375	59	9.833	100.000

Sample M12

Grain size (Phi)	Number of grains	Percent of grains	Cumulative percent
1.625	2	0.333	0.333
1.875	10	1.667	2.000
2.125	22	3.667	5.667
2.375	66	11.000	16.667
2.625	87	14.500	31.167
2.875	113	18.833	50.000
3.125	90	15.000	65.000
3.375	86	14.333	79.333
3.625	67	11.167	90.500
3.875	28	4.667	95.167
4.125	19	3.167	98.333
4.375	10	1.667	100.000

Sample M14

Grain size (Phi)	Number of grains	Percent of grains	Cumulative percent
2.375	1	0.167	0.167
2.625	6	1.000	1.167
2.875	24	4.000	5.167
3.125	41	6.833	12.000
3.375	100	16.667	28.667
3.625	122	20.333	49.000
3.875	129	21.500	70.500
4.125	84	14.000	84.500
4.375	93	15.500	100.000

Sample M15

Grain size (Phi)	Number of grains	Percent of grains	Cumulative percent
2.375	1	0.167	0.167
2.625	7	1.167	1.333
2.875	27	4.500	5.833
3.125	48	8.000	13.833
3.375	71	11.833	25.667
3.625	120	20.000	45.667
3.875	120	20.000	65.667
4.125	109	18.167	83.833
4.375	97	16.167	100.000

Sample M18B

Grain size (Phi)	Number of grains	Percent of grains	Cumulative percent
1.125	1	0.167	0.167
1.375	1	0.167	0.333
1.625	10	1.667	2.000
1.875	28	4.667	6.667
2.125	67	11.167	17.833
2.375	90	15.000	32.833
2.625	99	16.500	49.333
2.875	106	17.667	67.000
3.125	88	14.667	81.667
3.375	57	9.500	91.167
3.625	31	5.167	96.333
3.875	16	2.667	99.000
4.125	4	0.667	99.667
4.375	2	0.333	100.000

Sample M21B

Grain size (Phi)	Number of grains	Percent of grains	Cumulative percent
1.125	2	0.333	0.333
1.375	9	1.500	1.833
1.625	24	4.000	5.833
1.875	61	10.167	16.000
2.125	113	18.833	34.833
2.375	134	22.333	57.167
2.625	94	15.667	72.833
2.875	80	13.333	86.167
3.125	41	6.833	93.000
3.375	20	3.333	96.333
3.625	13	2.167	98.500
3.875	7	1.167	99.667
4.125	2	0.333	100.000

Sample M21T

Grain size (Phi)	Number of grains	Percent of grains	Cumulative percent
1.125	1	0.167	0.167
1.375	3	0.500	0.667
1.625	13	2.167	2.833
1.875	39	6.500	9.333
2.125	71	11.833	21.167
2.375	126	21.000	42.167
2.625	139	23.167	65.333
2.875	99	16.500	81.833
3.125	56	9.333	91.167
3.375	29	4.833	96.000
3.625	12	2.000	98.000
3.875	8	1.333	99.333
4.125	2	0.333	99.667
4.375	2	0.333	100.000

Sample M22B

Grain size (Phi)	Number of grains	Percent of grains	Cumulative percent
0.625	5	0.833	0.833
0.875	2	0.333	1.167
1.125	11	1.833	3.000
1.375	53	8.833	11.833
1.625	85	14.167	26.000
1.875	118	19.667	45.667
2.125	114	19.000	64.667
2.375	78	13.000	77.667
2.625	63	10.500	88.167
2.875	38	6.333	94.500
3.125	18	3.000	97.500
3.375	8	1.333	98.833
3.625	4	0.667	99.500
3.875	2	0.333	99.833
4.125	1	0.167	100.000

Sample M22T

Grain size (Phi)	Number of grains	Percent of grains	Cumulative percent
1.875	3	0.500	0.500
2.125	14	2.333	2.833
2.375	30	5.000	7.833
2.625	65	10.833	18.667
2.875	96	16.000	34.667
3.125	122	20.333	55.000
3.375	121	20.167	75.167
3.625	66	11.000	86.167
3.875	40	6.667	92.833
4.125	24	4.000	96.833
4.375	19	3.167	100.000

Sample M24B

Grain size (Phi)	Number of grains	Percent of grains	Cumulative percent
1.875	1	0.167	0.167
2.125	4	0.667	0.833
2.375	5	0.833	1.667
2.625	38	6.333	8.000
2.875	84	14.000	22.000
3.125	103	17.167	39.167
3.375	152	25.333	64.500
3.625	98	16.333	80.833
3.875	69	11.500	92.333
4.125	28	4.667	97.000
4.375	18	3.000	100.000

Sample M26B

Grain size (Phi)	Number of grains	Percent of grains	Cumulative percent
1.375	7	1.167	1.167
1.625	26	4.333	5.500
1.875	67	11.167	16.667
2.125	106	17.667	34.333
2.375	127	21.167	55.500
2.625	101	16.833	72.333
2.875	84	14.000	86.333
3.125	42	7.000	93.333
3.375	23	3.833	97.167
3.625	13	2.167	99.333
3.875	3	0.500	99.833
4.125	1	0.167	100.000

Sample M26T

Grain size (Phi)	Number of grains	Percent of grains	Cumulative percent
0.625	1	0.167	0.167
1.125	5	0.833	1.000
1.375	8	1.333	2.333
1.625	60	10.000	12.333
1.875	109	18.167	30.500
2.125	131	21.833	52.333
2.375	110	18.333	70.667
2.625	84	14.000	84.667
2.875	51	8.500	93.167
3.125	19	3.167	96.333
3.375	12	2.000	98.333
3.625	5	0.833	99.167
3.875	2	0.333	99.500
4.125	3	0.500	100.000

Sample M30B

Grain size (Phi)	Number of grains	Percent of grains	Cumulative percent
1.125	3	0.500	0.500
1.375	11	1.833	2.333
1.625	40	6.667	9.000
1.875	93	15.500	24.500
2.125	118	19.667	44.167
2.375	110	18.333	62.500
2.625	87	14.500	77.000
2.875	62	10.333	87.333
3.125	37	6.167	93.500
3.375	21	3.500	97.000
3.625	11	1.833	98.833
3.875	5	0.833	99.667
4.125	1	0.167	99.833
4.375	1	0.167	100.000

Sample M30T

Grain size (Phi)	Number of grains	Percent of grains	Cumulative percent
1.625	5	0.833	0.833
1.875	15	2.500	3.333
2.125	81	13.500	16.833
2.375	120	20.000	36.833
2.625	130	21.667	58.500
2.875	117	19.500	78.000
3.125	58	9.667	87.667
3.375	38	6.333	94.000
3.625	19	3.167	97.167
3.875	15	2.500	99.667
4.125	1	0.167	99.833
4.375	1	0.167	100.000

Sample S4/3-36

Grain size (Phi)	Number of grains	Percent of grains	Cumulative percent
1.875	3	0.500	0.500
2.125	7	1.167	1.667
2.375	21	3.500	5.167
2.625	35	5.833	11.000
2.875	66	11.000	22.000
3.125	82	13.667	35.667
3.375	94	15.667	51.333
3.625	107	17.833	69.167
3.875	89	14.833	84.000
4.125	39	6.500	90.500
4.375	56	9.333	99.833

Sample S6/3-36

Grain size (Phi)	Number of grains	Percent of grains	Cumulative percent
2.125	6	1.000	1.000
2.375	20	3.333	4.333
2.625	41	6.833	11.167
2.875	83	13.833	25.000
3.125	113	18.833	43.833
3.375	107	17.833	61.667
3.625	105	17.500	79.167
3.875	67	11.167	90.333
4.125	33	5.500	95.833
4.375	25	4.167	100.000

Sample S10/3-36

Grain size (Phi)	Number of grains	Percent of grains	Cumulative percent
0.625	9	1.500	1.500
0.875	7	1.167	2.667
1.125	12	2.000	4.667
1.375	9	1.500	6.167
1.625	20	3.333	9.500
1.875	22	3.667	13.167
2.125	41	6.833	20.000
2.375	54	9.000	29.000
2.625	77	12.833	41.833
2.875	76	12.667	54.500
3.125	69	11.500	66.000
3.375	59	9.833	75.833
3.625	65	10.833	86.667
3.875	39	6.500	93.167
4.125	22	3.667	96.833
4.375	19	3.167	100.000

Sample S11/3-36

Grain size (Phi)	Number of grains	Percent of grains	Cumulative percent
1.375	1	0.167	0.167
1.625	2	0.333	0.500
1.875	1	0.167	0.667
2.125	1	0.167	0.833
2.375	13	2.167	3.000
2.625	36	6.000	9.000
2.875	48	8.000	17.000
3.125	104	17.333	34.333
3.375	108	18.000	52.333
3.625	124	20.667	73.000
3.875	74	12.333	85.333
4.125	53	8.833	94.167
4.375	35	5.833	100.000

Sample S18/3-36

Grain size (Phi)	Number of grains	Percent of grains	Cumulative percent
2.375	2	0.333	0.333
2.625	6	1.000	1.333
2.875	33	5.500	6.833
3.125	58	9.667	16.500
3.375	71	11.833	28.333
3.625	95	15.833	44.167
3.875	114	19.000	63.167
4.125	95	15.833	79.000
4.375	126	21.000	100.000

Sample S21/3-36

Grain size (Phi)	Number of grains	Percent of grains	Cumulative percent
0.625	2	0.333	0.333
0.875	2	0.333	0.667
1.125	6	1.000	1.667
1.375	12	2.000	3.667
1.625	24	4.000	7.667
1.875	56	9.333	17.000
2.125	81	13.500	30.500
2.375	102	17.000	47.500
2.625	84	14.000	61.500
2.875	86	14.333	75.833
3.125	60	10.000	85.833
3.375	49	8.167	94.000
3.625	22	3.667	97.667
3.875	12	2.000	99.667
4.125	1	0.167	99.833
4.375	1	0.167	100.000

APPENDIX D: CUMULATIVE CURVES OF THE ANALYSED SAMPLES.

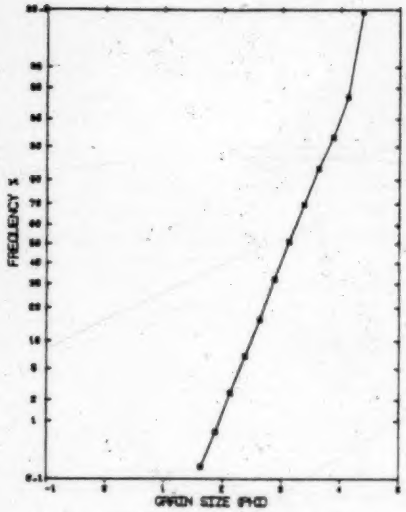

CUMULATIVE FREQUENCY CURVE -D2

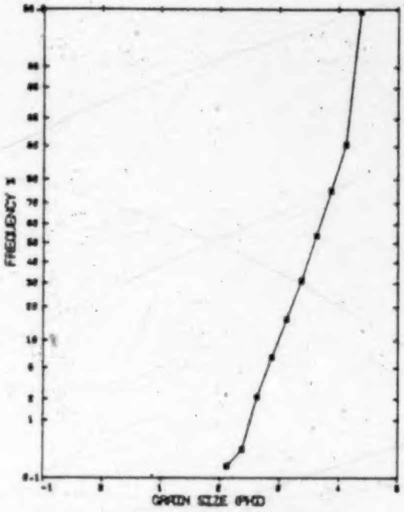

CUMULATIVE FREQUENCY CURVE -D17B

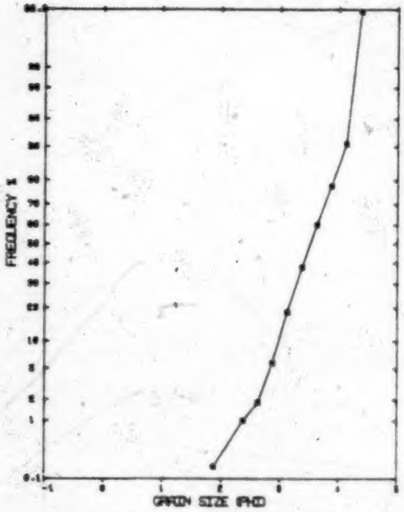

CUMULATIVE FREQUENCY CURVE -D1

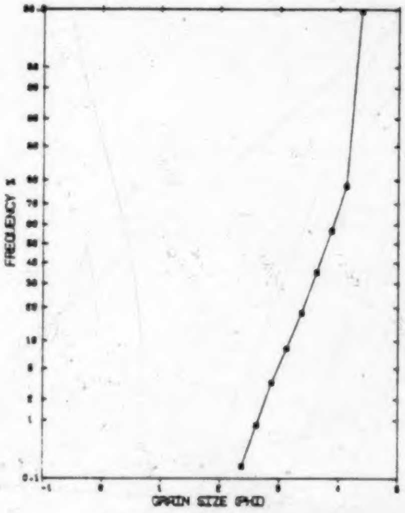

CUMULSTIVE FREQUENCY CURVE -D15B

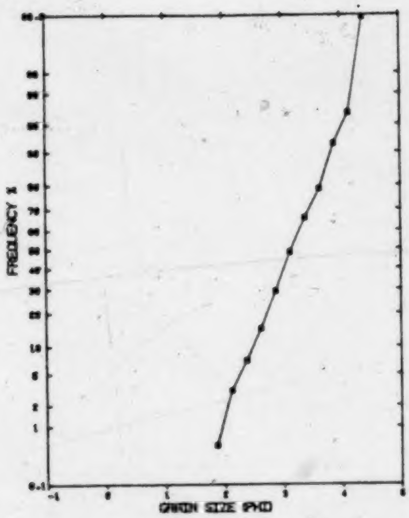

CUMULATIVE FREQUENCY CURVE -D23

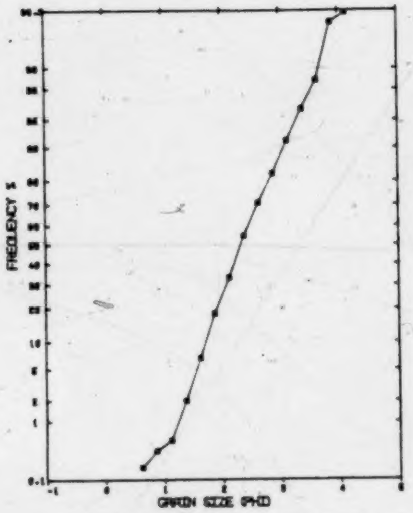

CUMULATIVE FREQUENCY CURVE -D26B

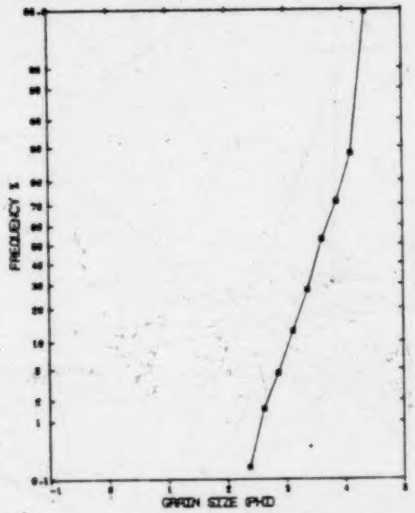

CUMULATIVE FREQUENCY CURVE -D18

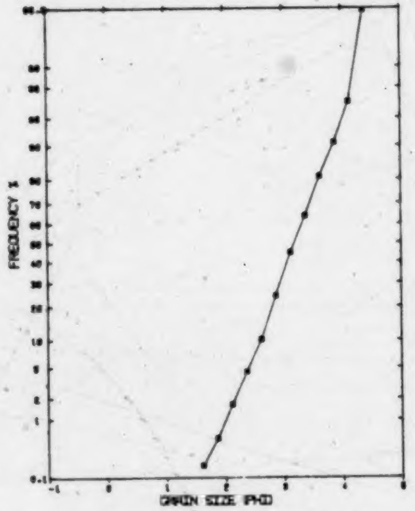

CUMULATIVE FREQUENCY CURVE -D24B

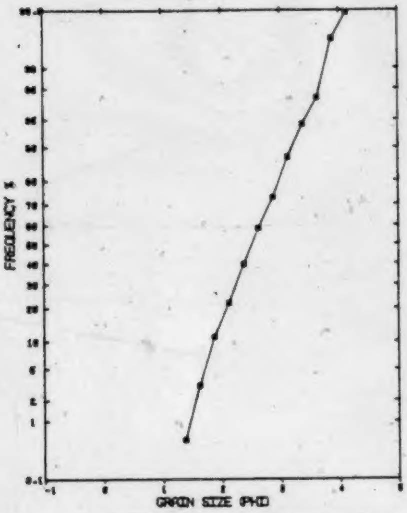

CUMULATIVE FREQUENCY CURVE -D30B

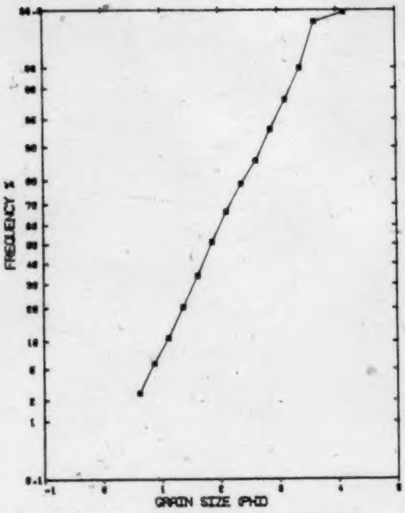

CUMULATIVE FREQUENCY CURVE -D37B

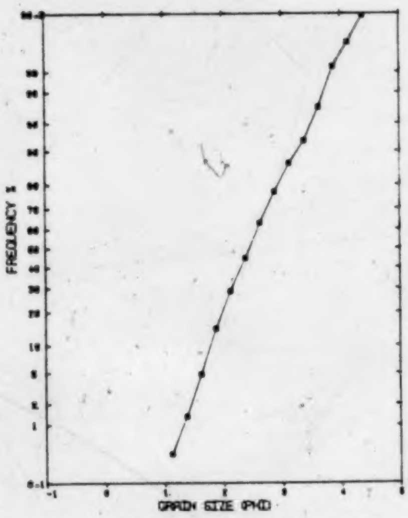

CUMULATIVE FREQUENCY CURVE -D27LL

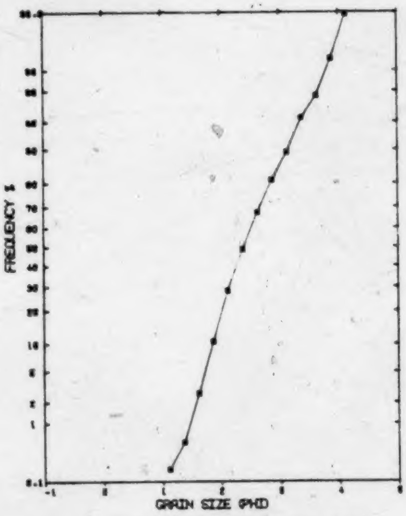

CUMULATIVE FREQUENCY CURVE -D34B

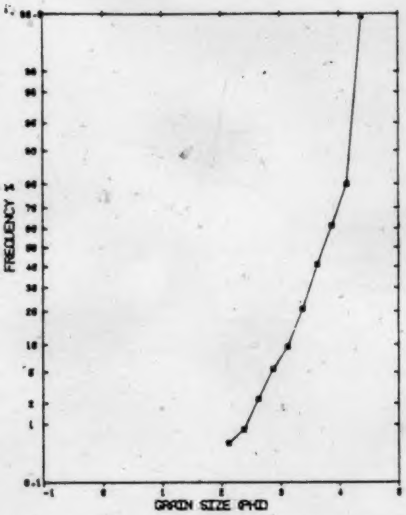

CUMULATIVE FREQUENCY CURVE -D48B

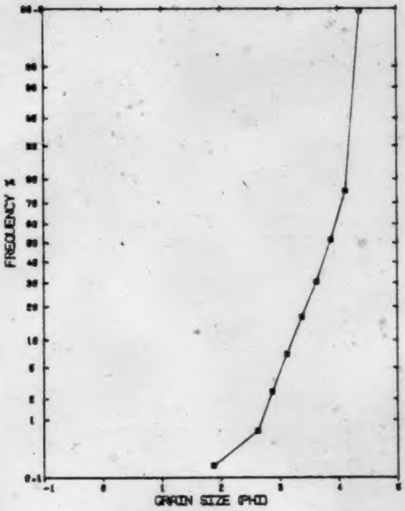

CUMULATIVE FREQUENCY CURVE -OR3T

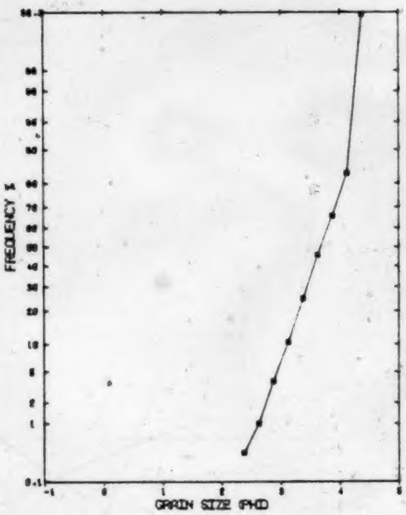

CUMULATIVE FREQUENCY CURVE -D47

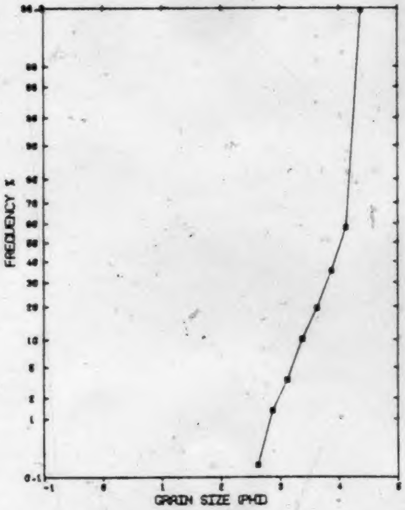

CUMULATIVE FREQUENCY CURVE -OR3B

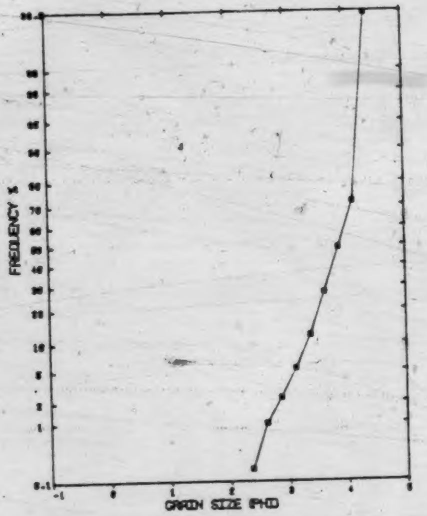

CUMULATIVE FREQUENCY CURVE -OR5B

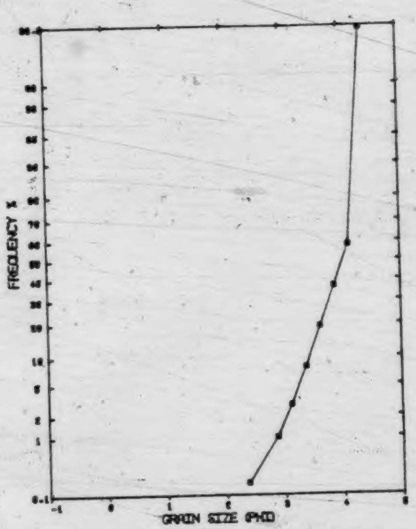

CUMULATIVE FREQUENCY CURVE -OR6B

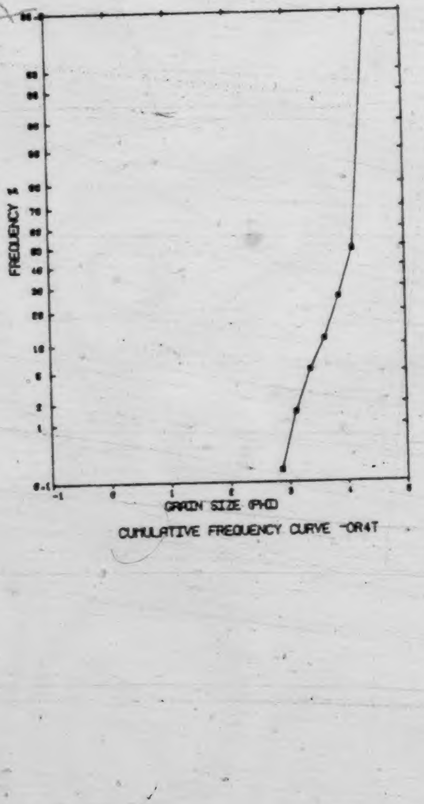

CUMULATIVE FREQUENCY CURVE -OR4T

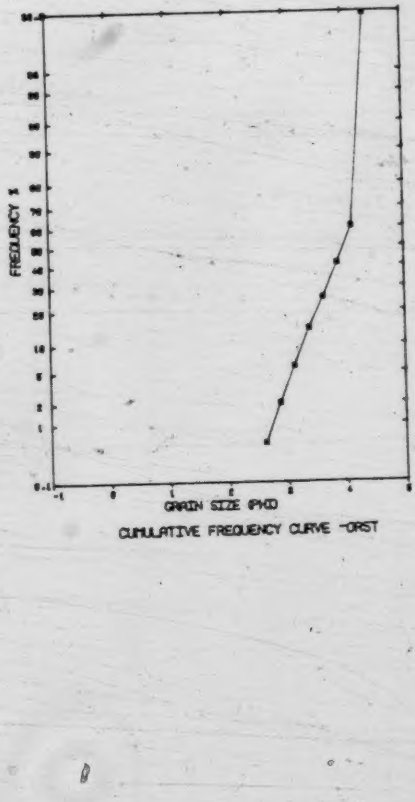

CUMULATIVE FREQUENCY CURVE -OR5T

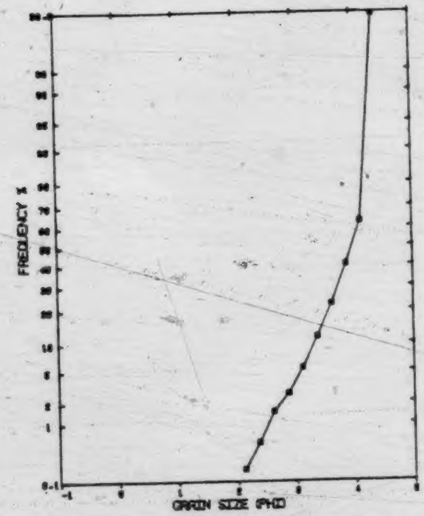

CUMULATIVE FREQUENCY CURVE -OR8B

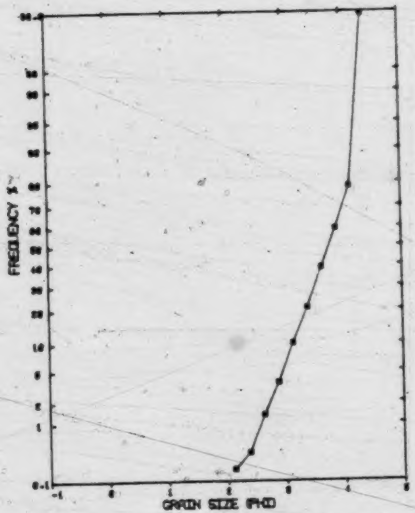

CUMULATIVE FREQUENCY CURVE -OR10B

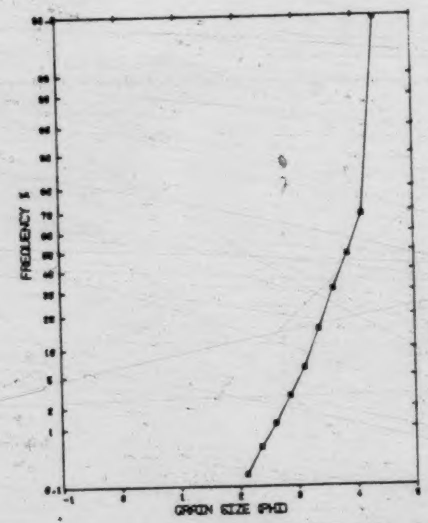

CUMULATIVE FREQUENCY CURVE -OR8T

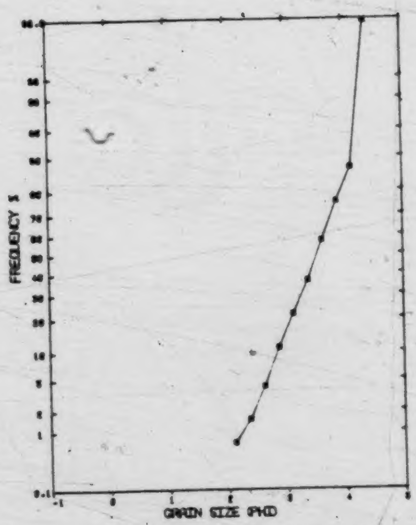

CUMULATIVE FREQUENCY CURVE -OR9T

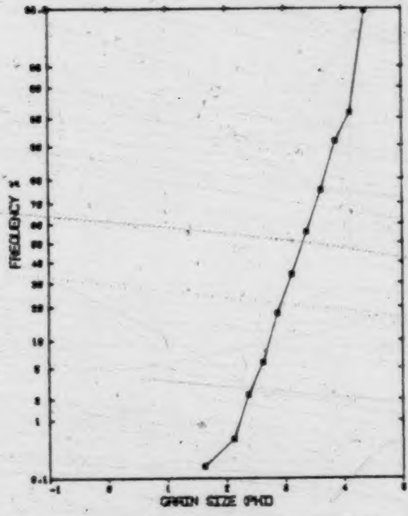

CUMULATIVE FREQUENCY CURVE -OR11B

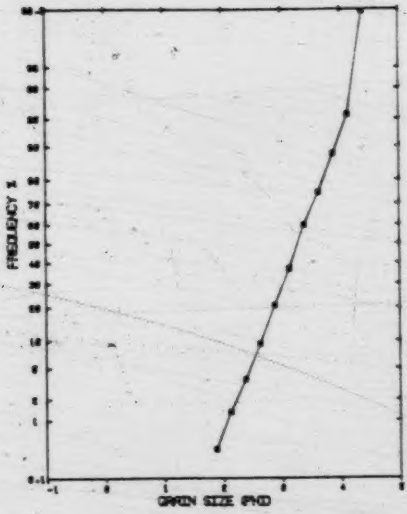

CUMULATIVE FREQUENCY CURVE -OR12B

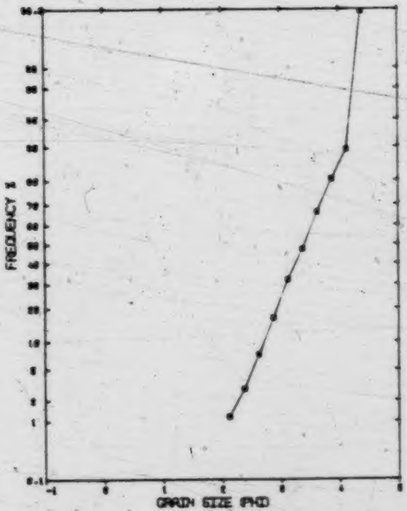

CUMULATIVE FREQUENCY CURVE -OR10T

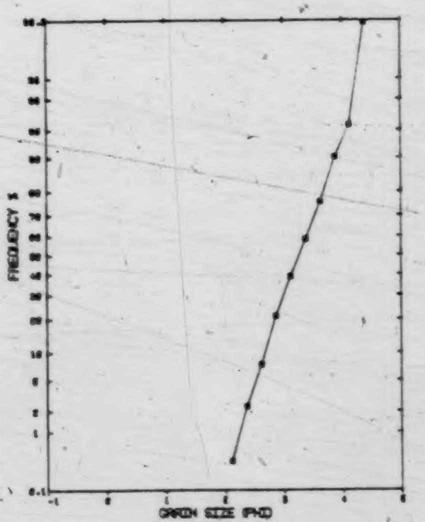

CUMULATIVE FREQUENCY CURVE -OR11T

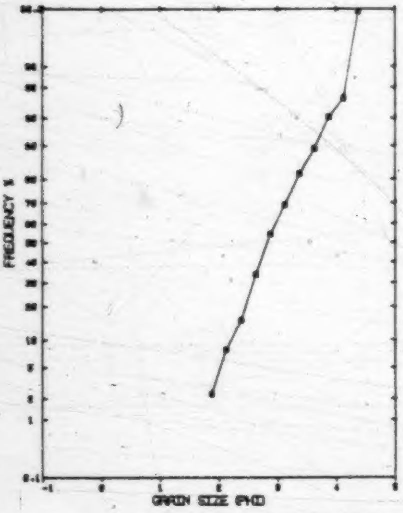

CUMULATIVE FREQUENCY CURVE -OR14B1

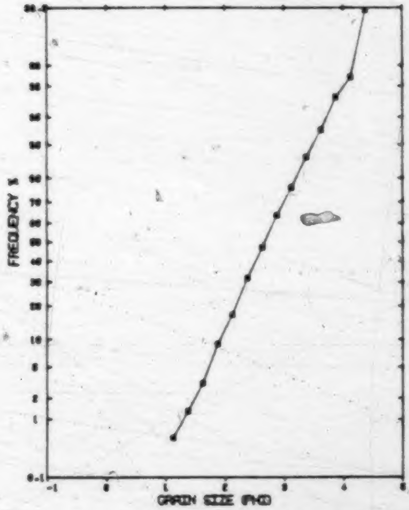

CUMULATIVE FREQUENCY CURVE -OR14B2

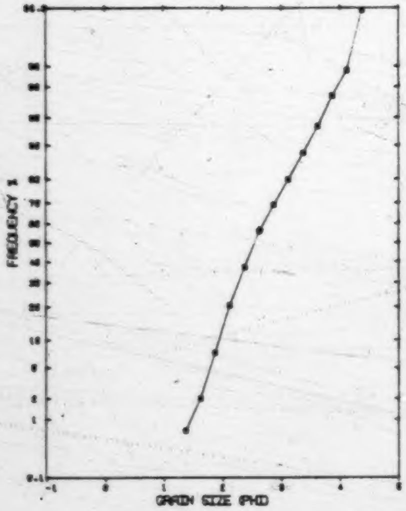

CUMULATIVE FREQUENCY CURVE -OR12T

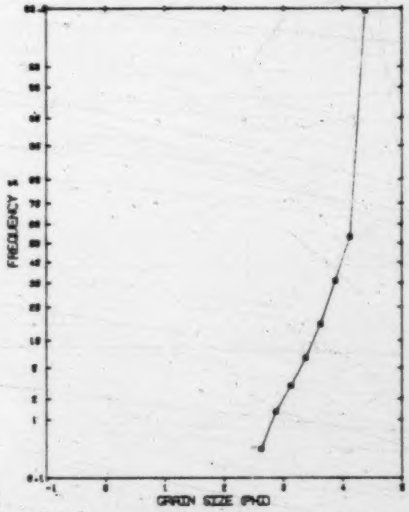

CUMULATIVE FREQUENCY CURVE -OR14T1

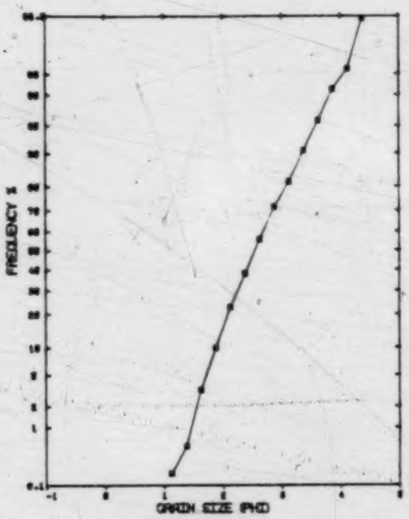

CUMULATIVE FREQUENCY CURVE -OR14T3

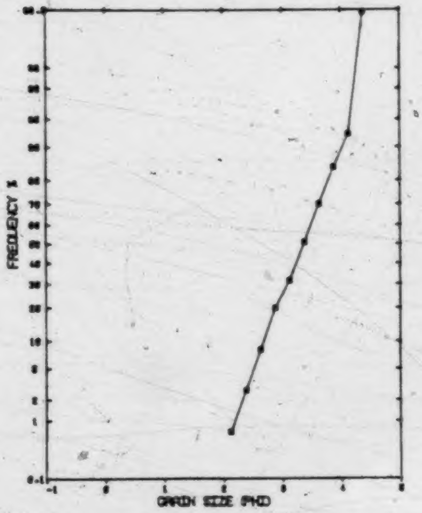

CUMULATIVE FREQUENCY CURVE -T5

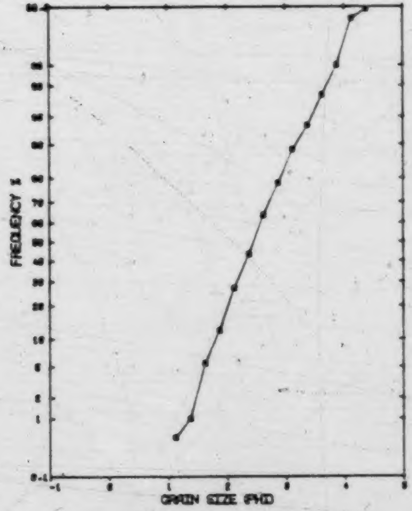

CUMULATIVE FREQUENCY CURVE -OR14B3

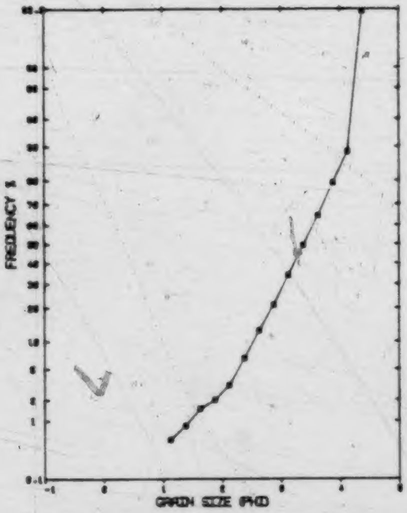

CUMULATIVE FREQUENCY CURVE -T3

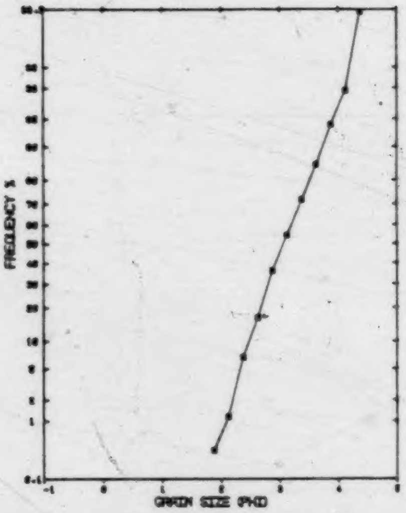

CUMULATIVE FREQUENCY CURVE -T18

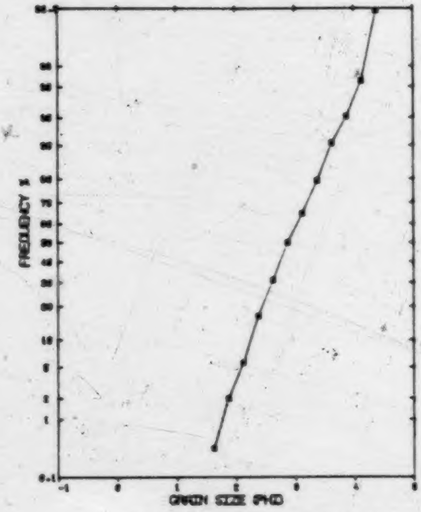

CUMULATIVE FREQUENCY CURVE -T112

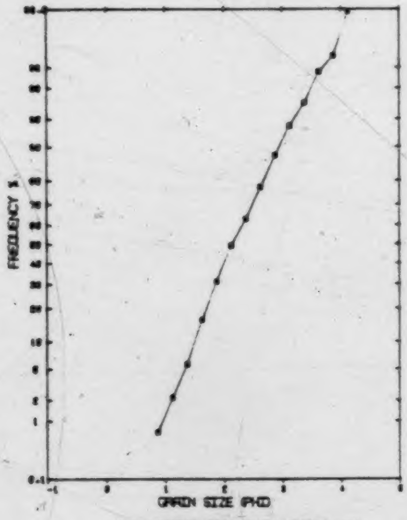

CUMULATIVE FREQUENCY CURVE -T16

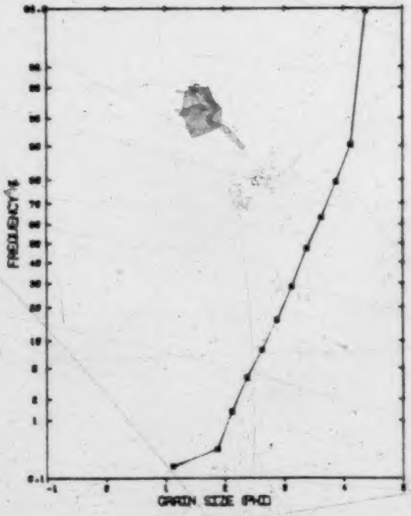

CUMULATIVE FREQUENCY CURVE -T110

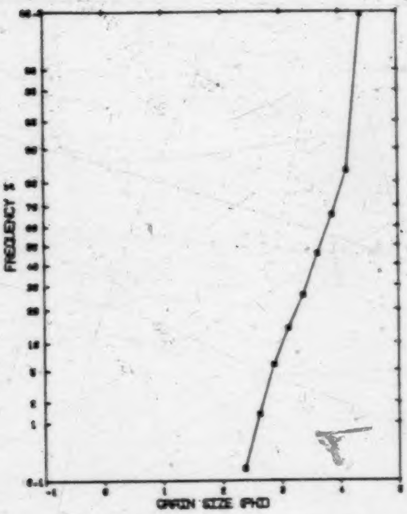

CUMULATIVE FREQUENCY CURVE -115

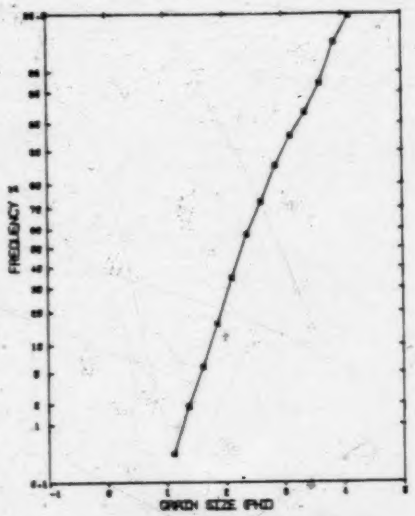

CUMULATIVE FREQUENCY CURVE -128

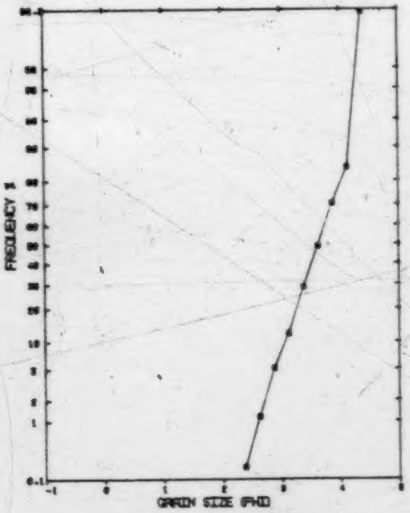

CUMULATIVE FREQUENCY CURVE -114

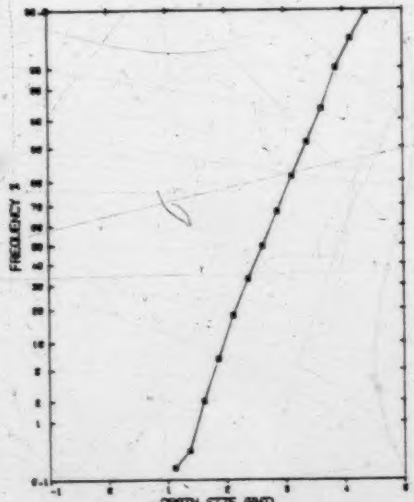

CUMULATIVE FREQUENCY CURVE -1188

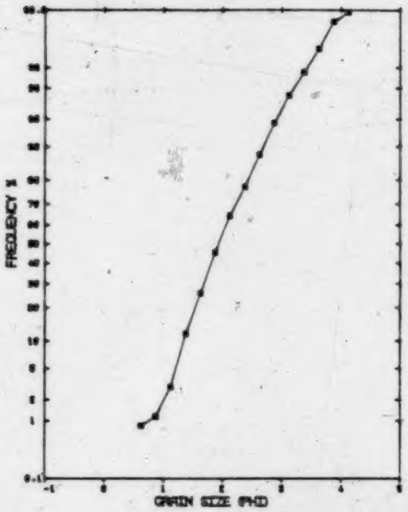

CUMULATIVE FREQUENCY CURVE H22B

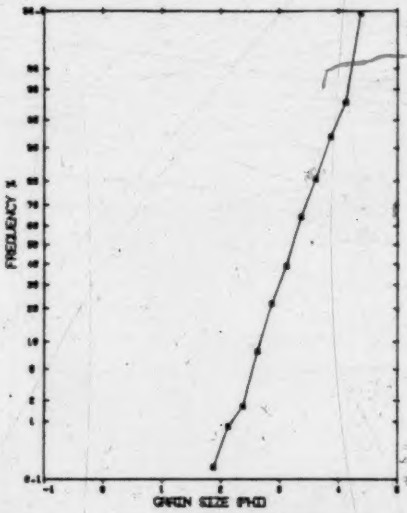

CUMULATIVE FREQUENCY CURVE H24B

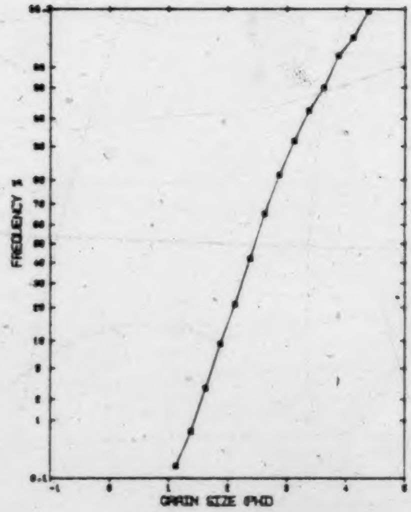

CUMULATIVE FREQUENCY CURVE H21T

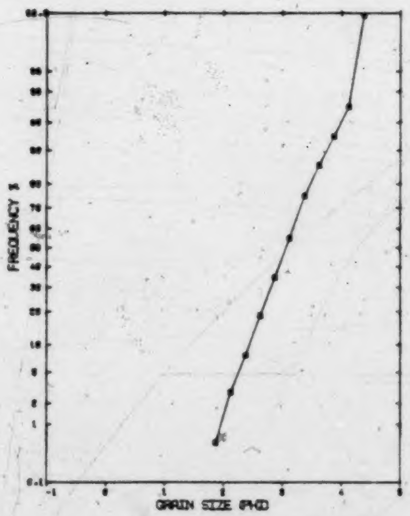

CUMULATIVE FREQUENCY CURVE H22T

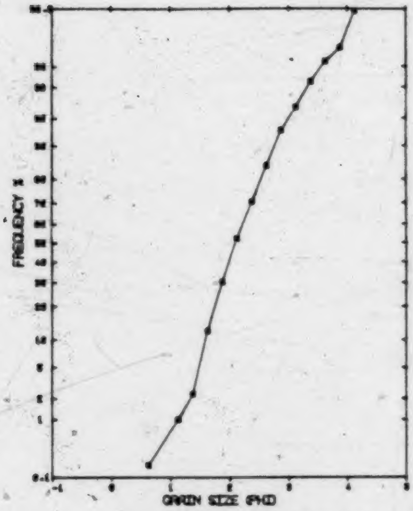

CUMULATIVE FREQUENCY CURVE -1128T

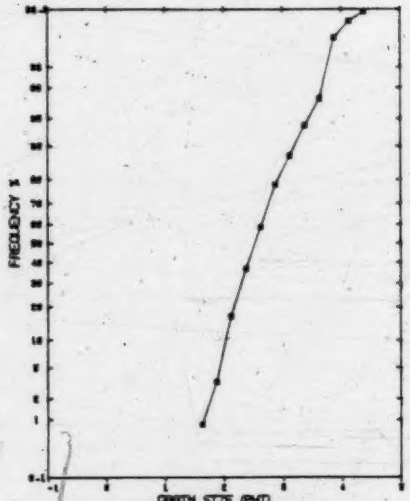

CUMULATIVE FREQUENCY CURVE -1130T

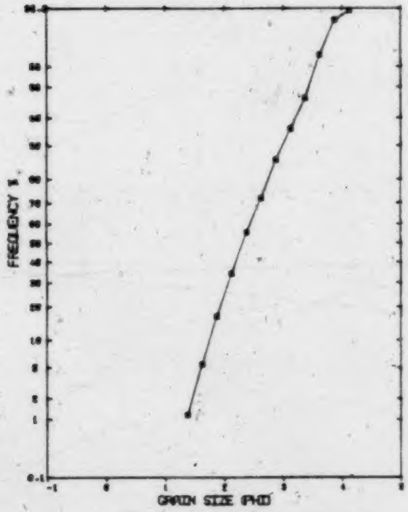

CUMULATIVE FREQUENCY CURVE -1128B

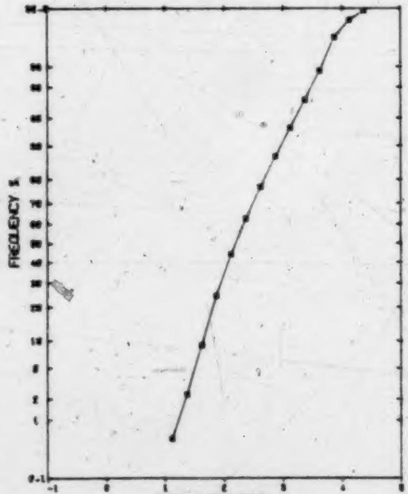

CUMULATIVE FREQUENCY CURVE -1130B

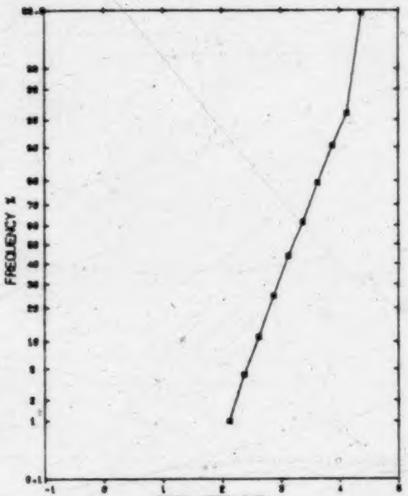

CUMULATIVE FREQUENCY CURVE-S8/3-36

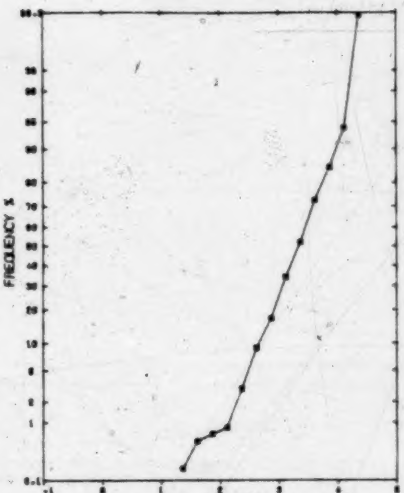

CUMULATIVE FREQUENCY CURVE-S11/3-36

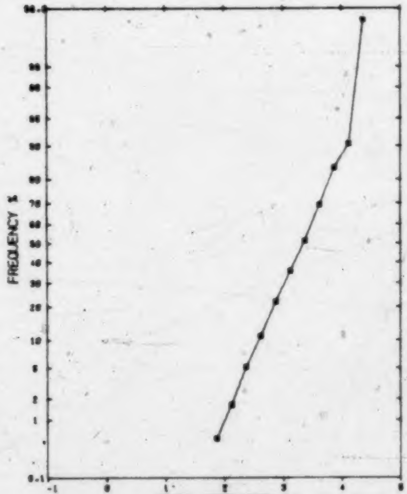

CUMULATIVE FREQUENCY CURVE-S4/3-36

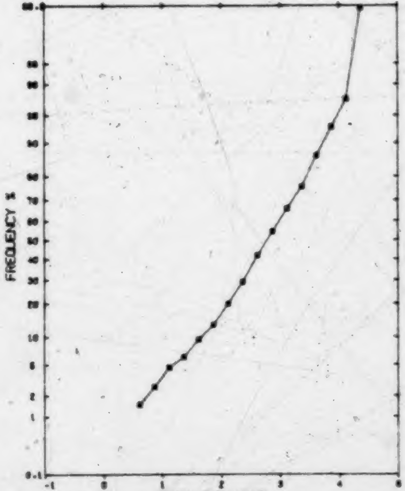

CUMULATIVE FREQUENCY CURVE-S10/3-36

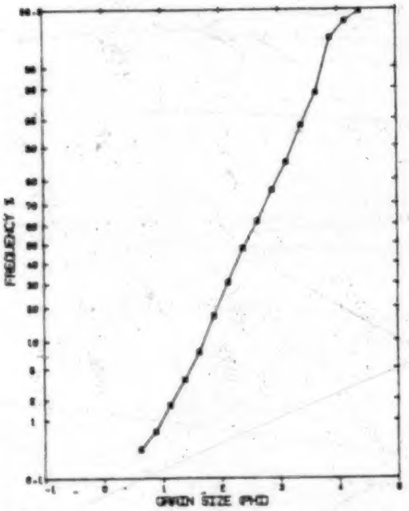

CUMULATIVE FREQUENCY CURVE-S21/3-36

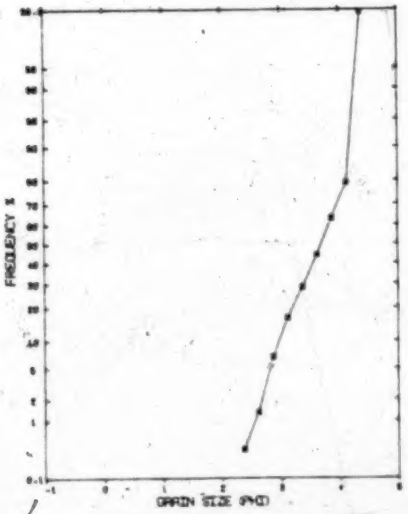

CUMULATIVE FREQUENCY CURVE-S18/3-36

APPENDIX E: HISTOGRAMS OF THE ANALYSED SAMPLES.

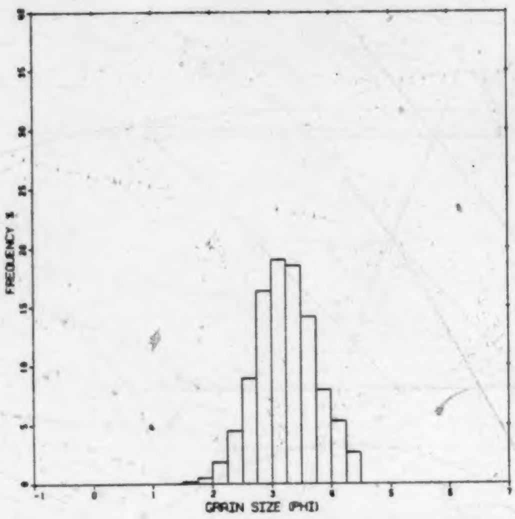

HISTOGRAM (SAMPLE D2)

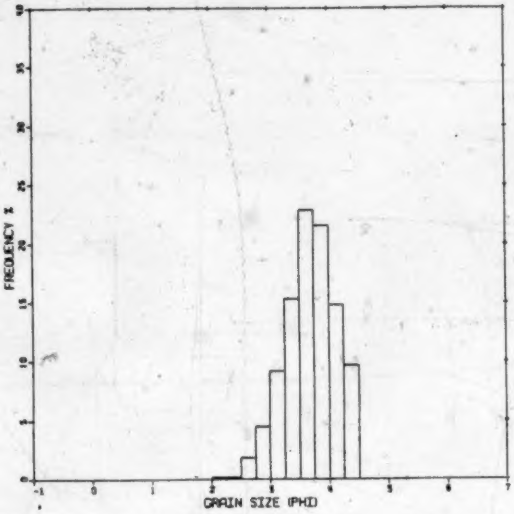

HISTOGRAM (SAMPLE D17B)

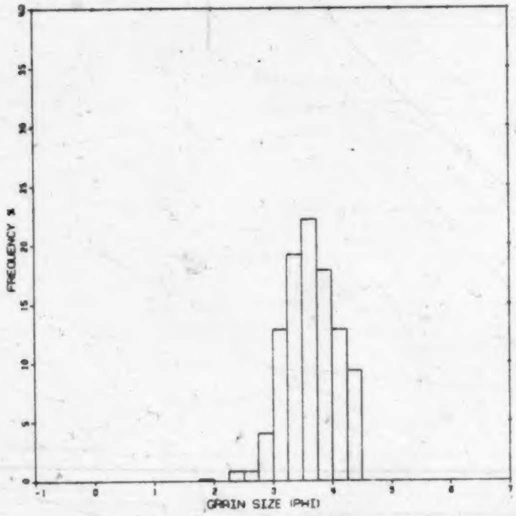

HISTOGRAM (SAMPLE D1)

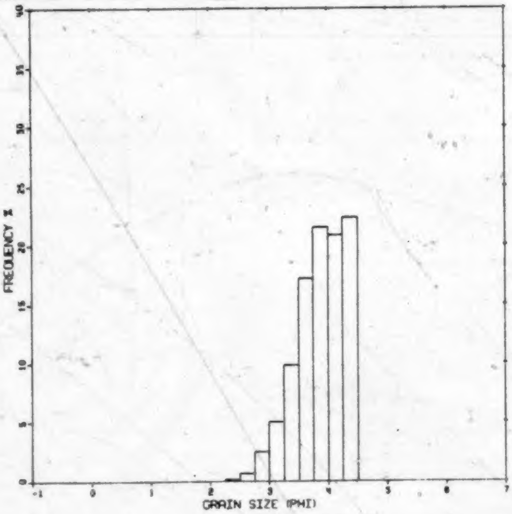

HISTOGRAM (SAMPLE D15B)

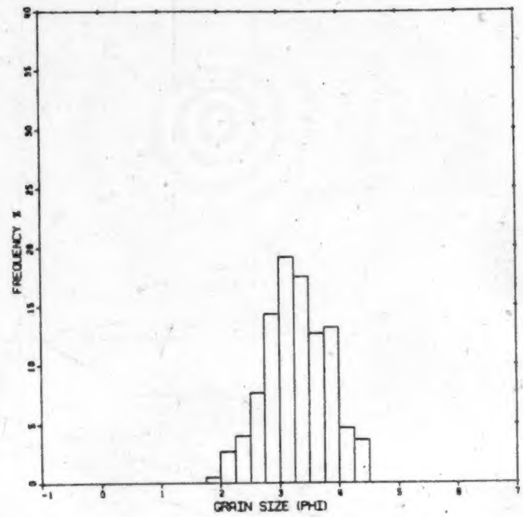

HISTOGRAM (SAMPLE D23)

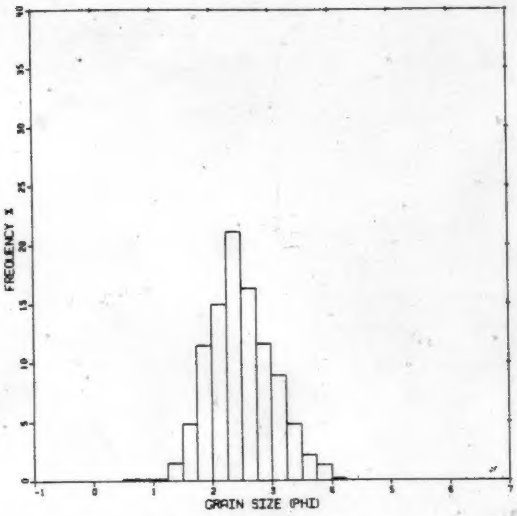

HISTOGRAM (SAMPLE D26B)

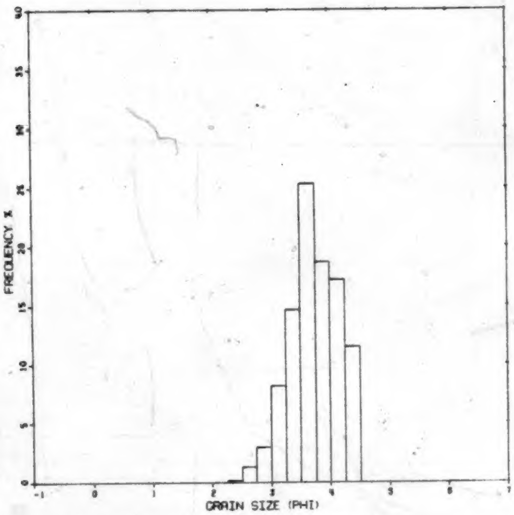

HISTOGRAM (SAMPLE D18)

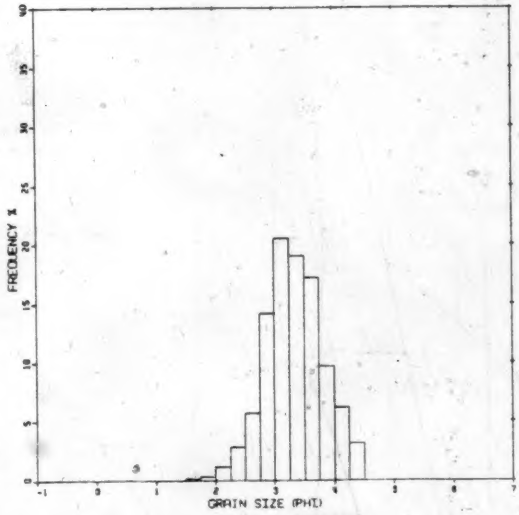

HISTOGRAM (SAMPLE D24B)

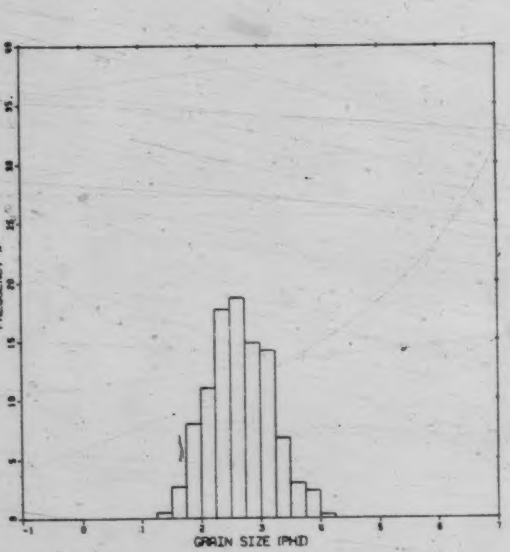

HISTOGRAM (SAMPLE D30B)

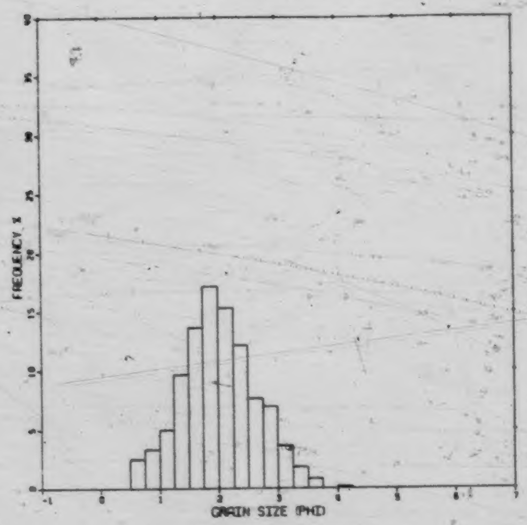

HISTOGRAM (SAMPLE D37B)

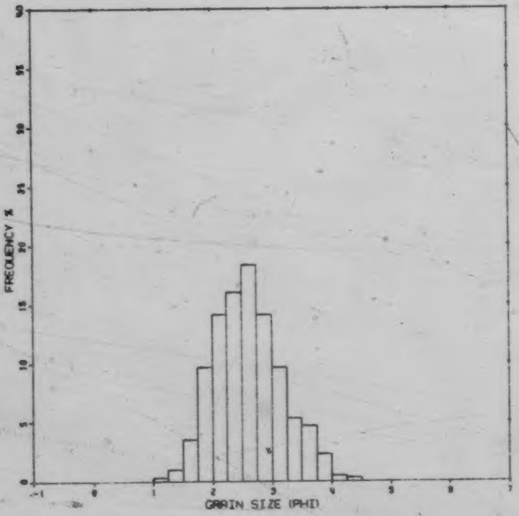

HISTOGRAM (SAMPLE D27XII)

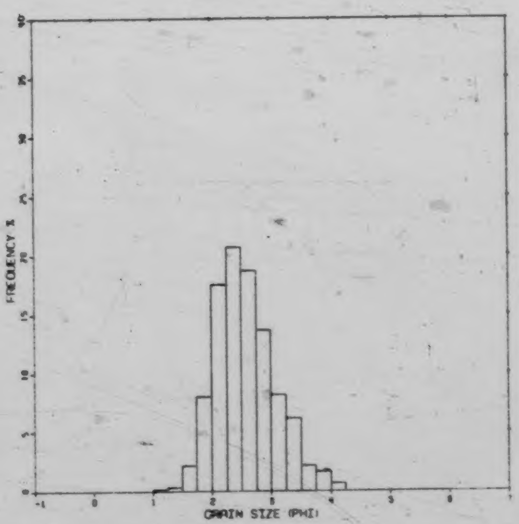

HISTOGRAM (SAMPLE D34B)

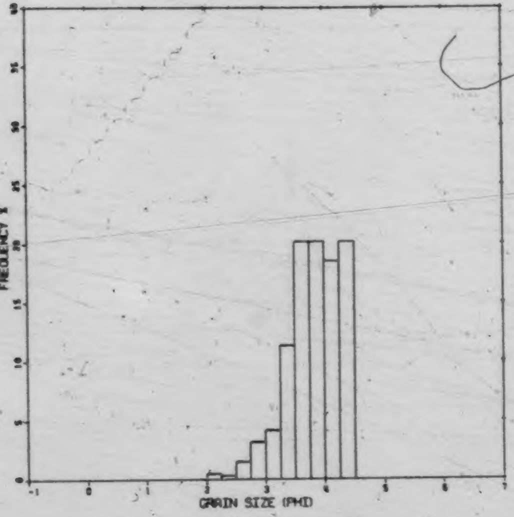

HISTOGRAM (SAMPLE D48B)

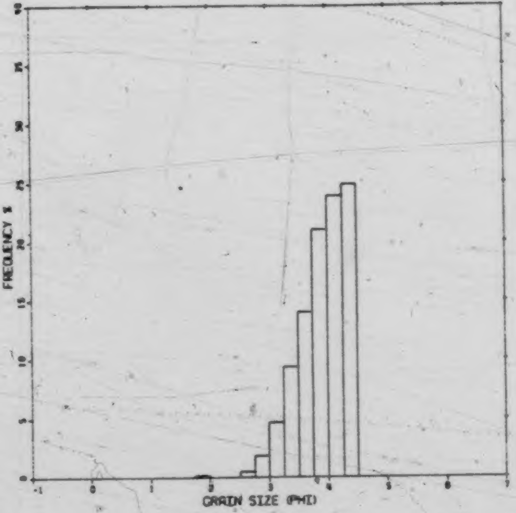

HISTOGRAM (SAMPLE OR3T)

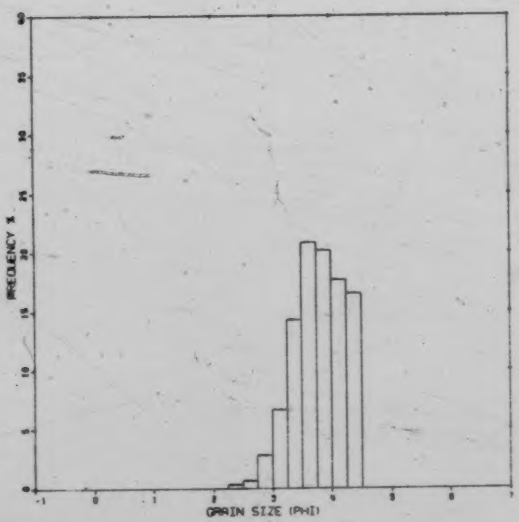

HISTOGRAM (SAMPLE D47)

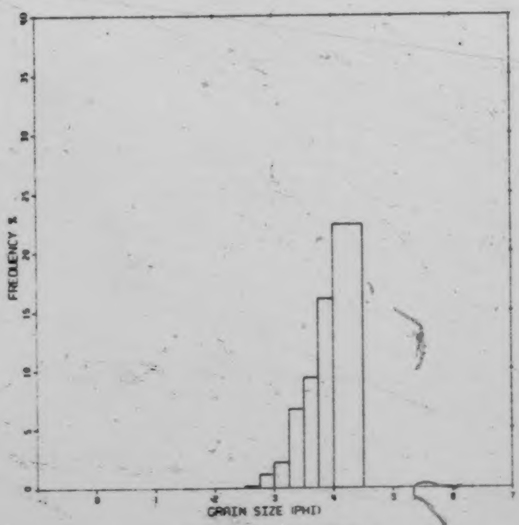

HISTOGRAM (SAMPLE OR3B)

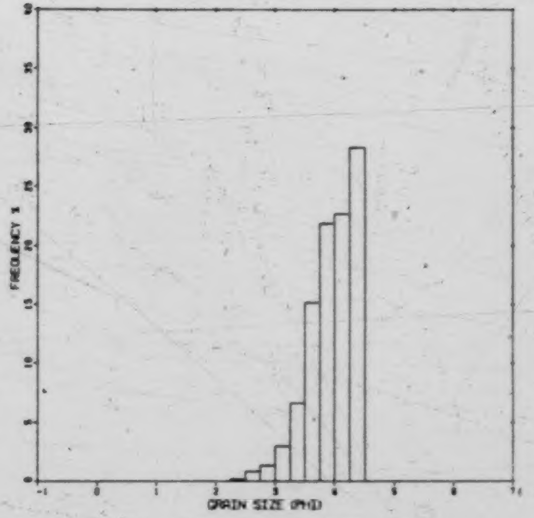

HISTOGRAM (SAMPLE OR5B)

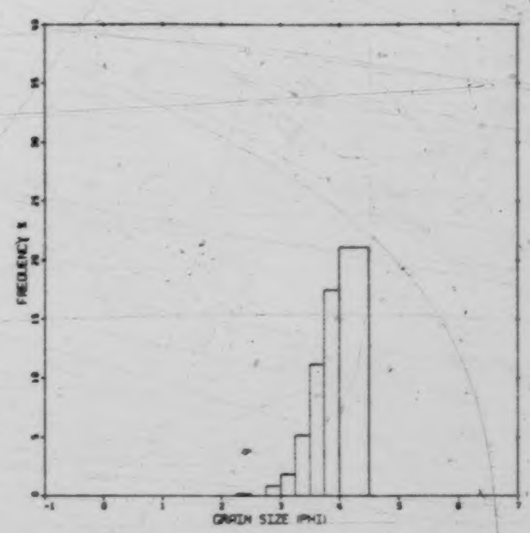

HISTOGRAM (SAMPLE OR6B)

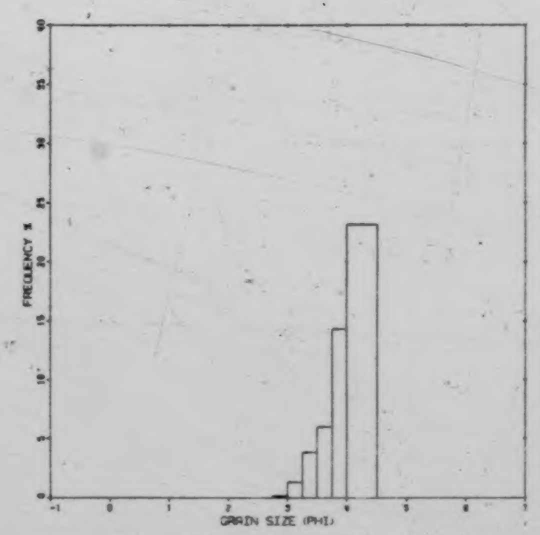

HISTOGRAM (SAMPLE OR4T)

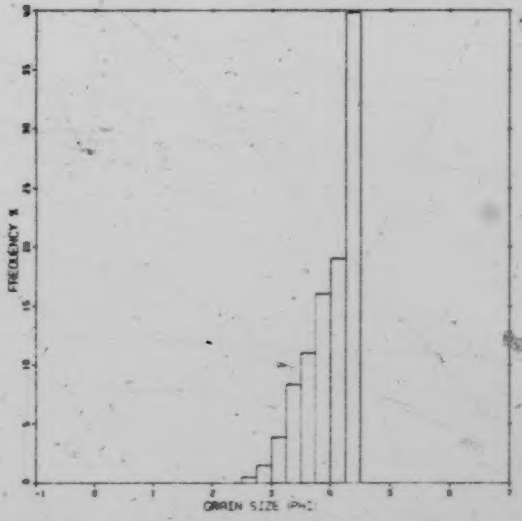

HISTOGRAM (SAMPLE OR5T)

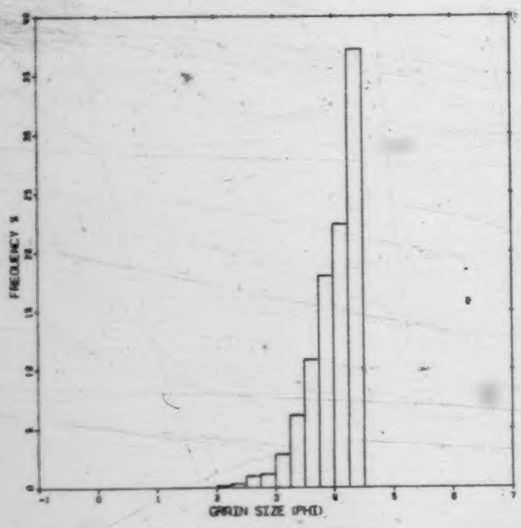

HISTOGRAM (SAMPLE OR8B)

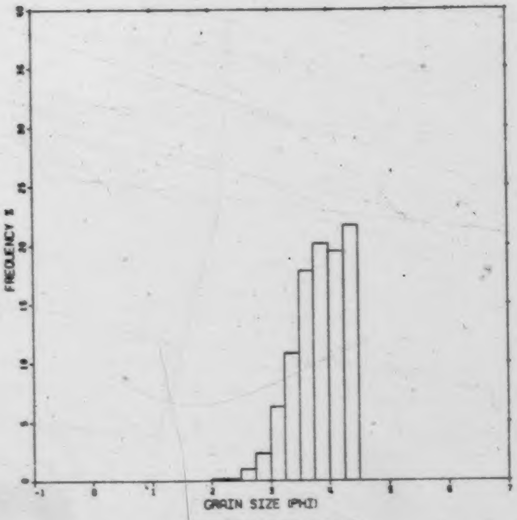

HISTOGRAM (SAMPLE OR10B)

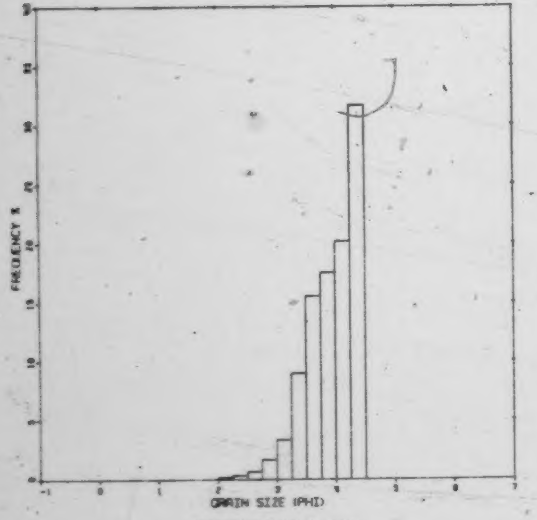

HISTOGRAM (SAMPLE OR6T)

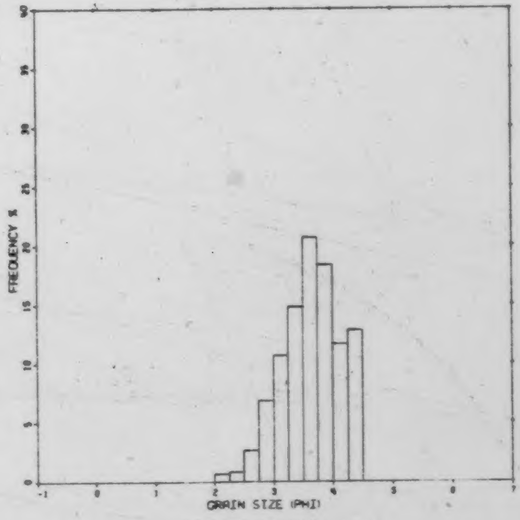

HISTOGRAM (SAMPLE OR8T)

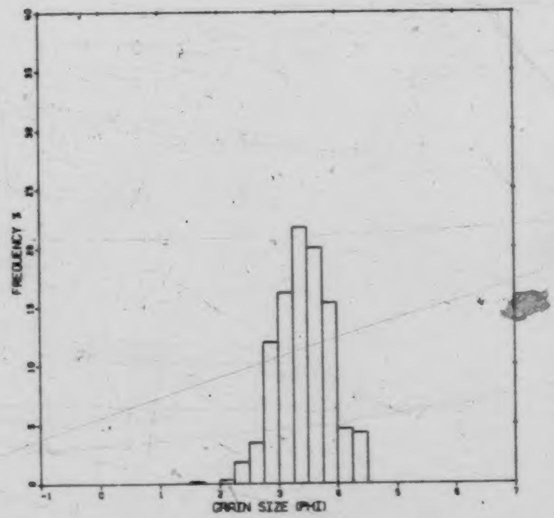

HISTOGRAM (SAMPLE OR11B)

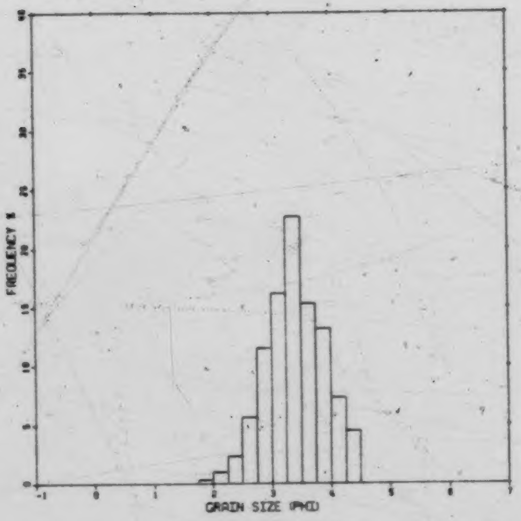

HISTOGRAM (SAMPLE OR12B)

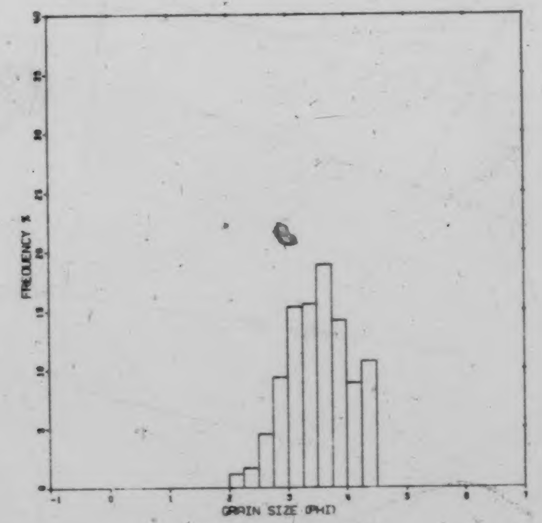

HISTOGRAM (SAMPLE OR10T)

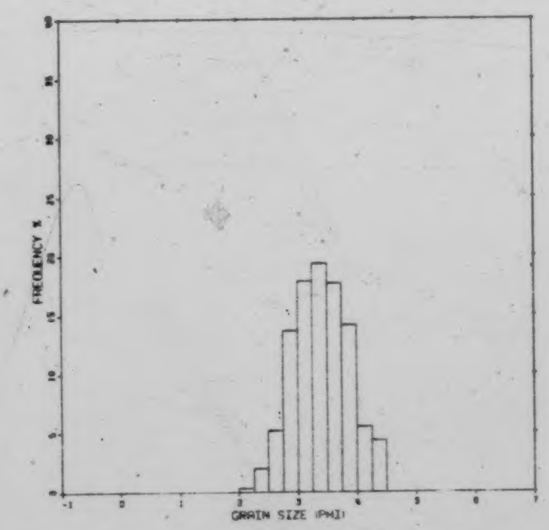

HISTOGRAM (SAMPLE OR11T)

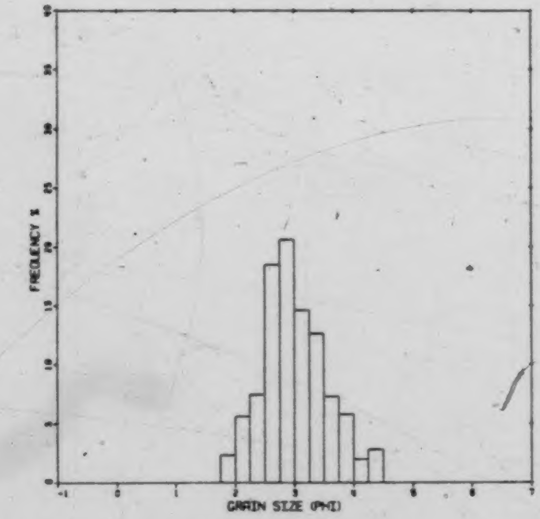

HISTOGRAM (SAMPLE OR14B3)

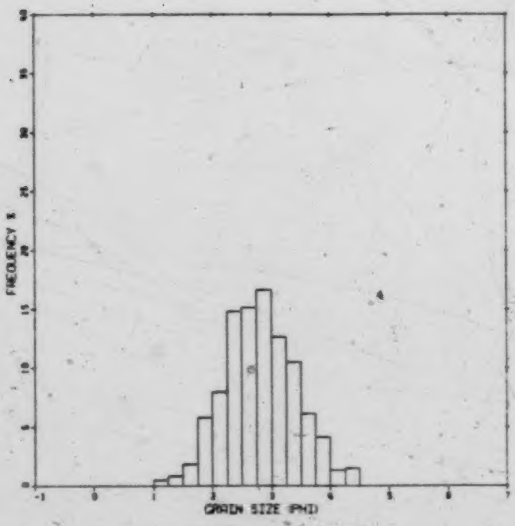

HISTOGRAM (SAMPLE OR14B2)

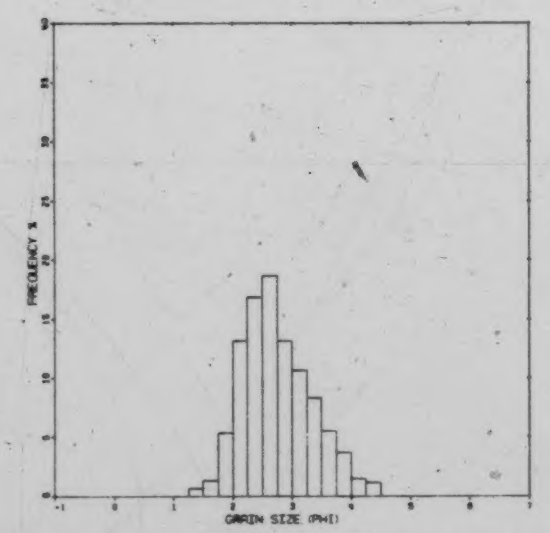

HISTOGRAM (SAMPLE OR12T)

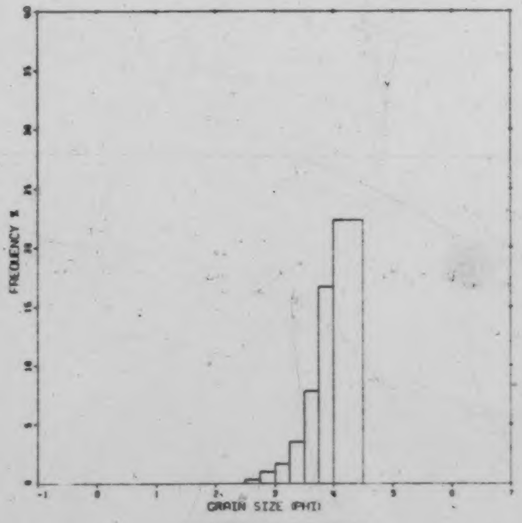

HISTOGRAM (SAMPLE OR14T)

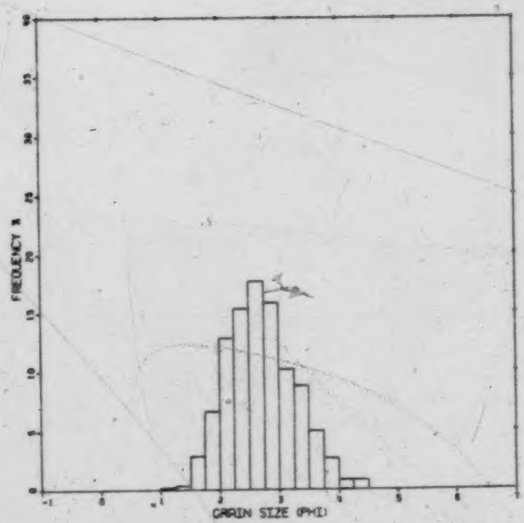

HISTOGRAM (SAMPLE OR14T3)

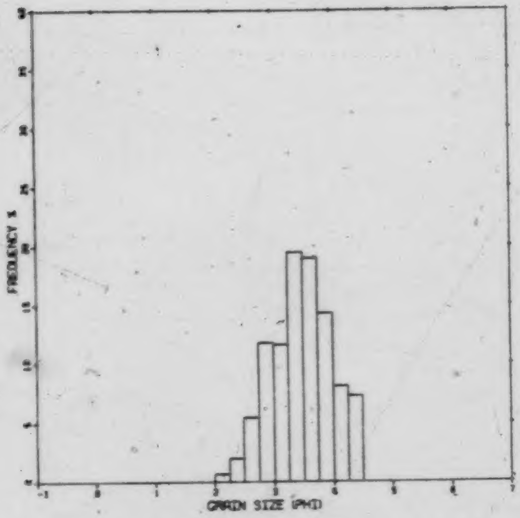

HISTOGRAM (SAMPLE M5)

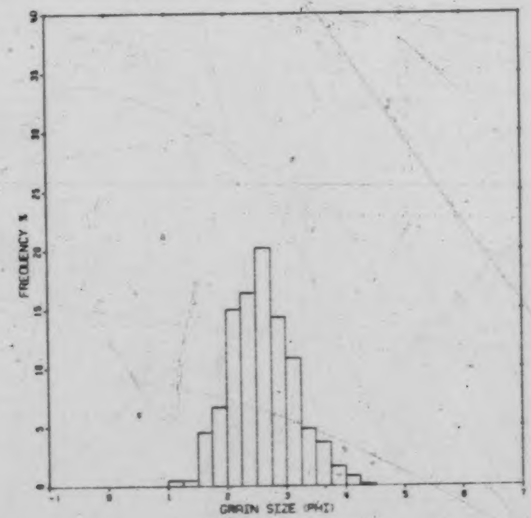

HISTOGRAM (SAMPLE OR14B3)

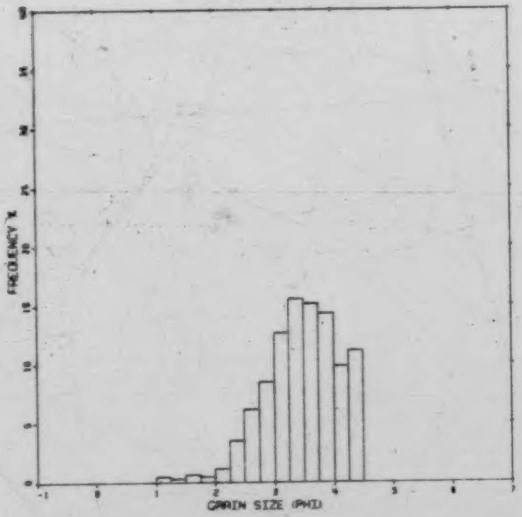

HISTOGRAM (SAMPLE M3)

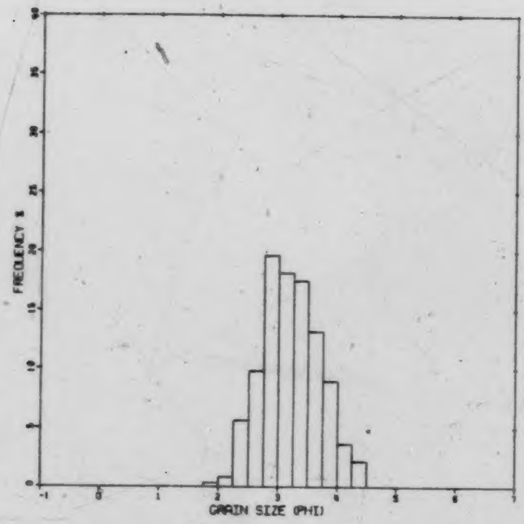

HISTOGRAM (SAMPLE M8)

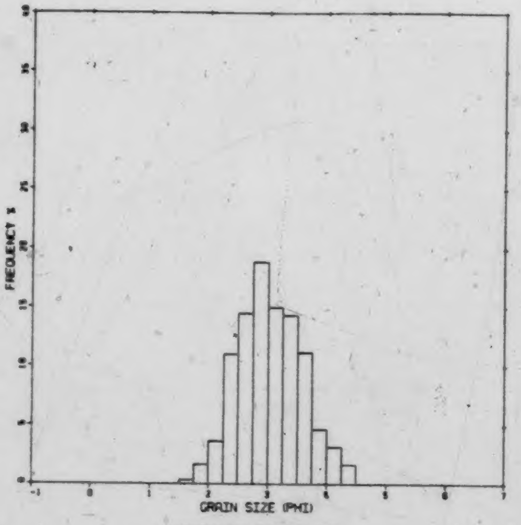

HISTOGRAM (SAMPLE M12)

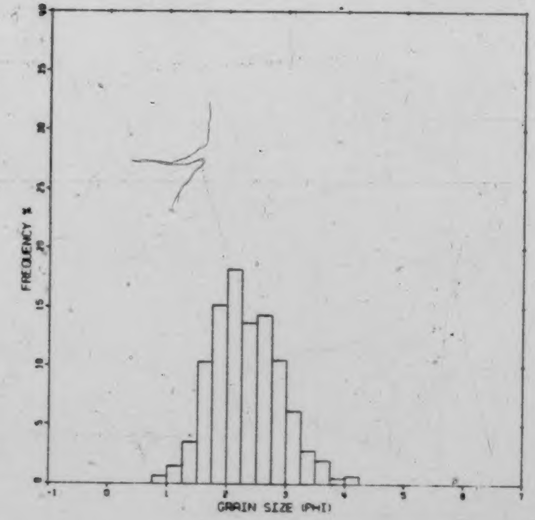

HISTOGRAM (SAMPLE M6)

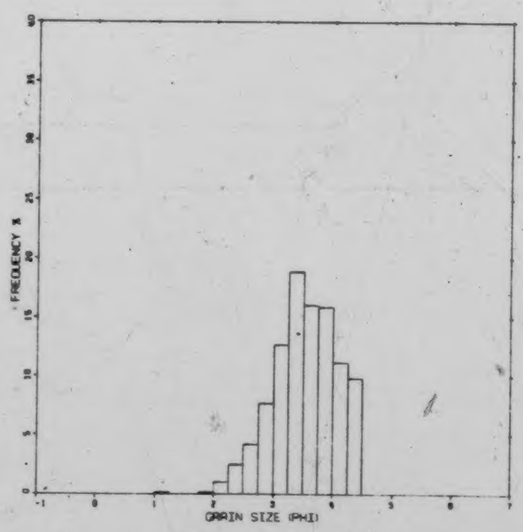

HISTOGRAM (SAMPLE M10)

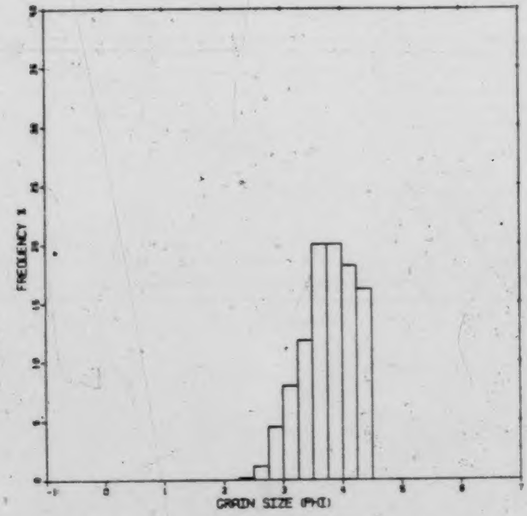

HISTOGRAM (SAMPLE M15)

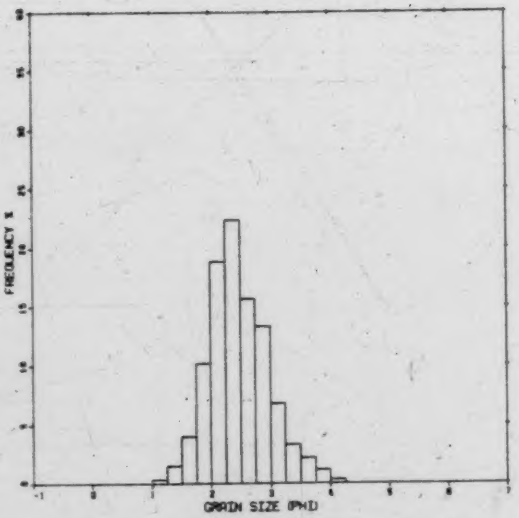

HISTOGRAM (SAMPLE M21B)

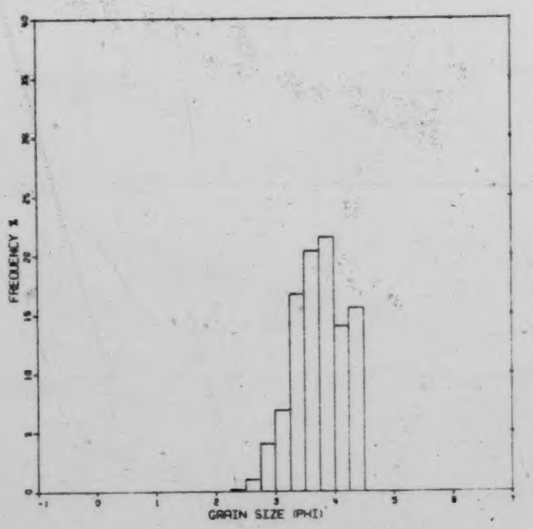

HISTOGRAM (SAMPLE M14)

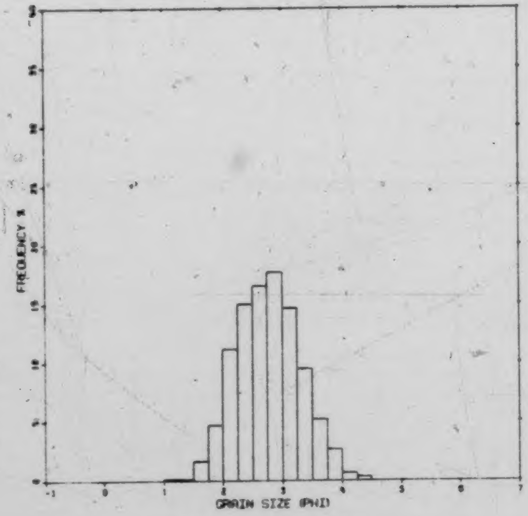

HISTOGRAM (SAMPLE M18B)

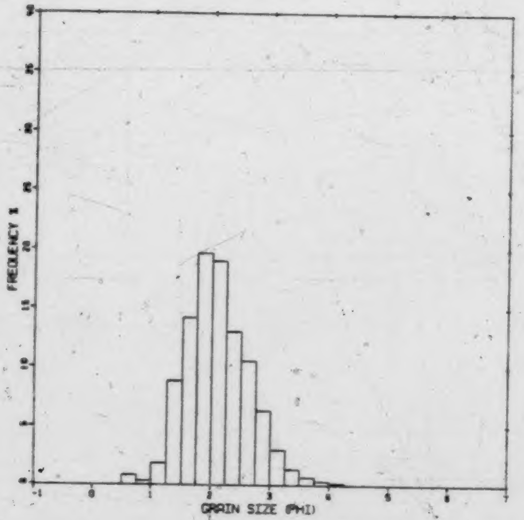

HISTOGRAM (SAMPLE M22B)

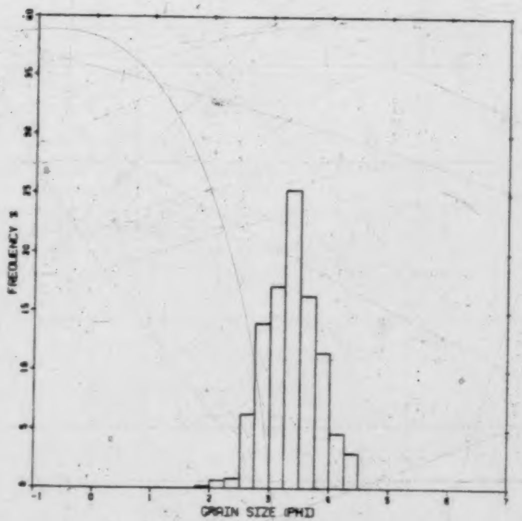

HISTOGRAM (SAMPLE M24B)

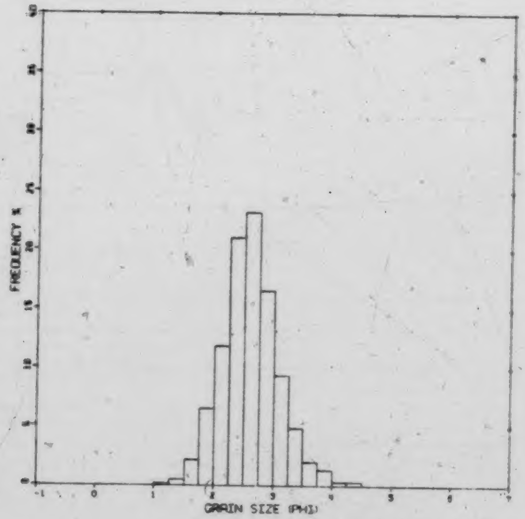

HISTOGRAM (SAMPLE M21T)

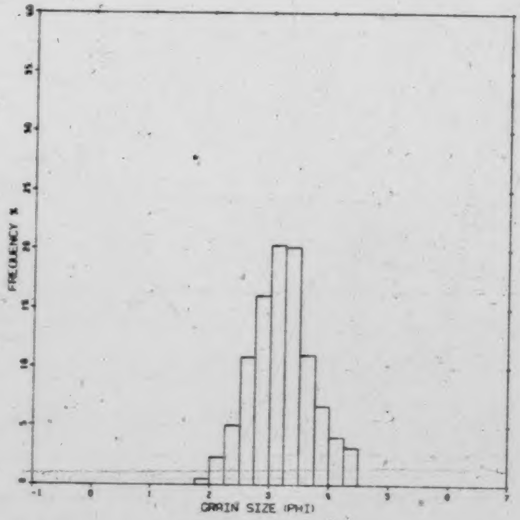

HISTOGRAM (SAMPLE M22T)

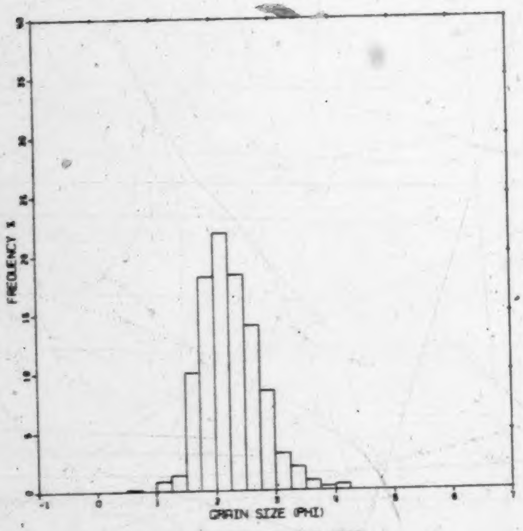

HISTOGRAM (SAMPLE M26T)

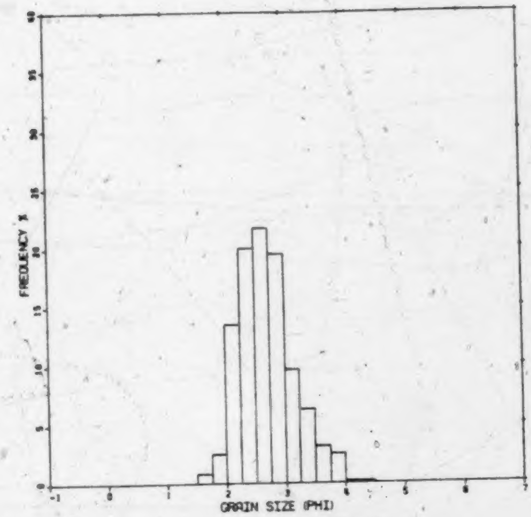

HISTOGRAM (SAMPLE M30T)

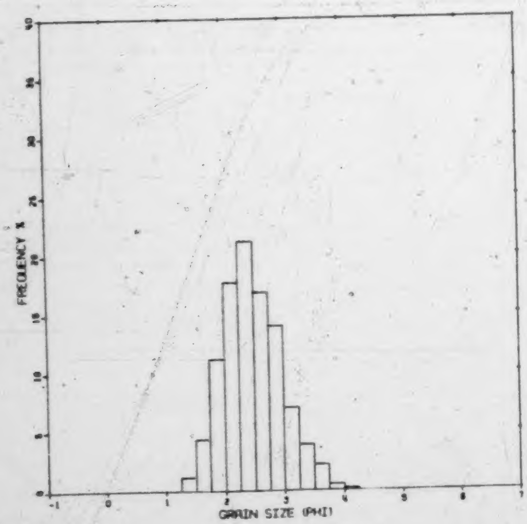

HISTOGRAM (SAMPLE M26B)

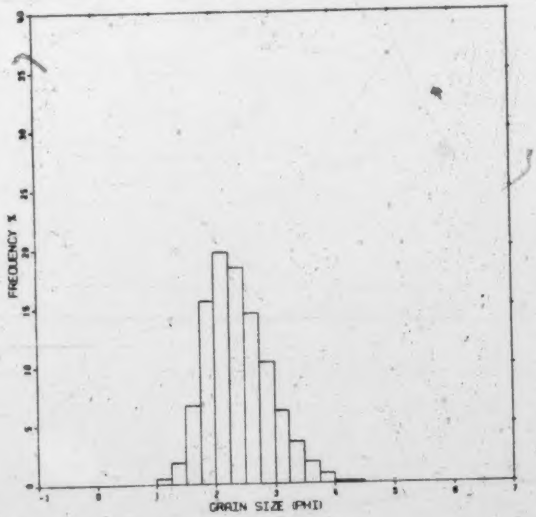

HISTOGRAM (SAMPLE M30B)

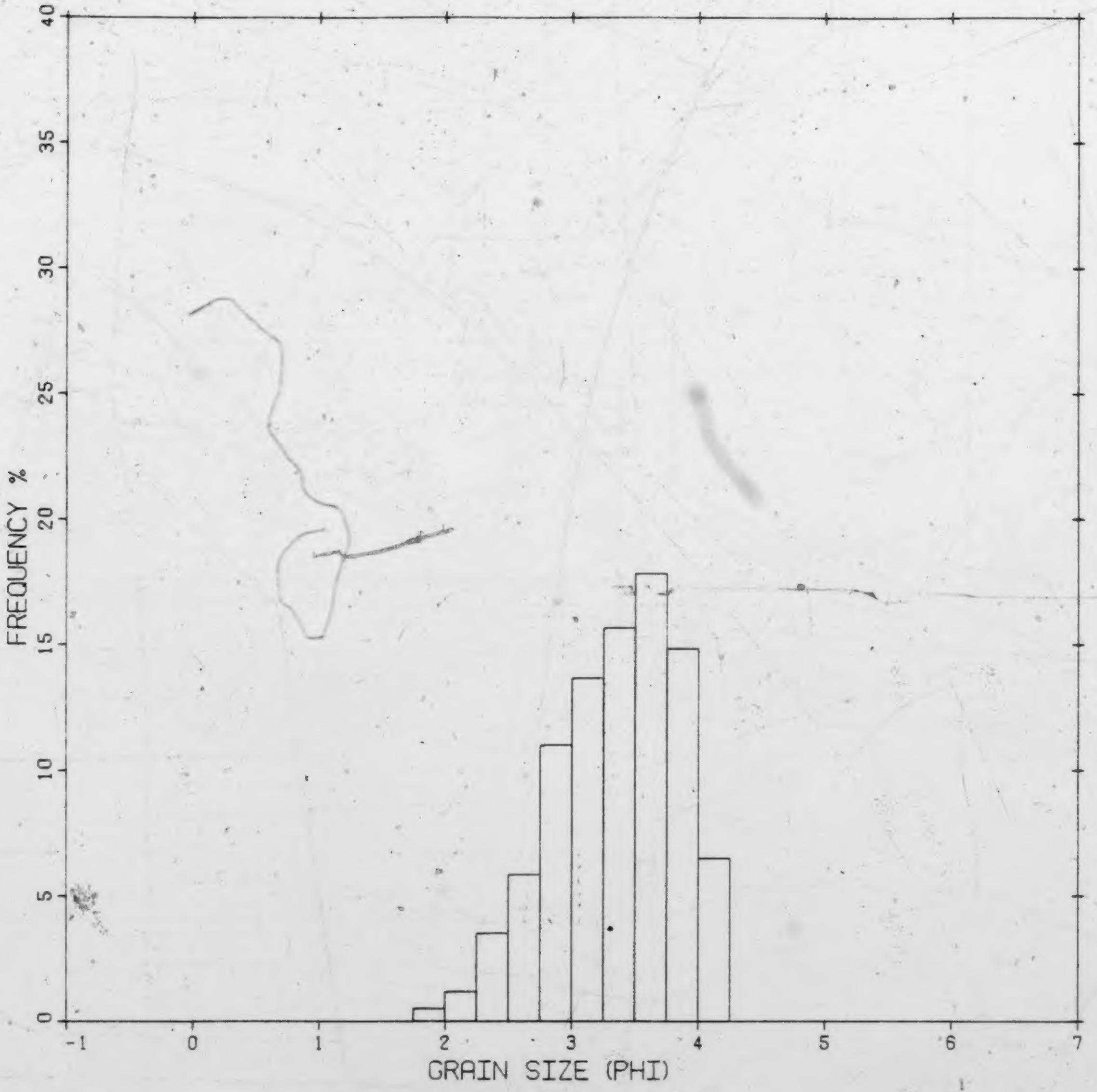

HISTOGRAM (SAMPLE S4/3-36)

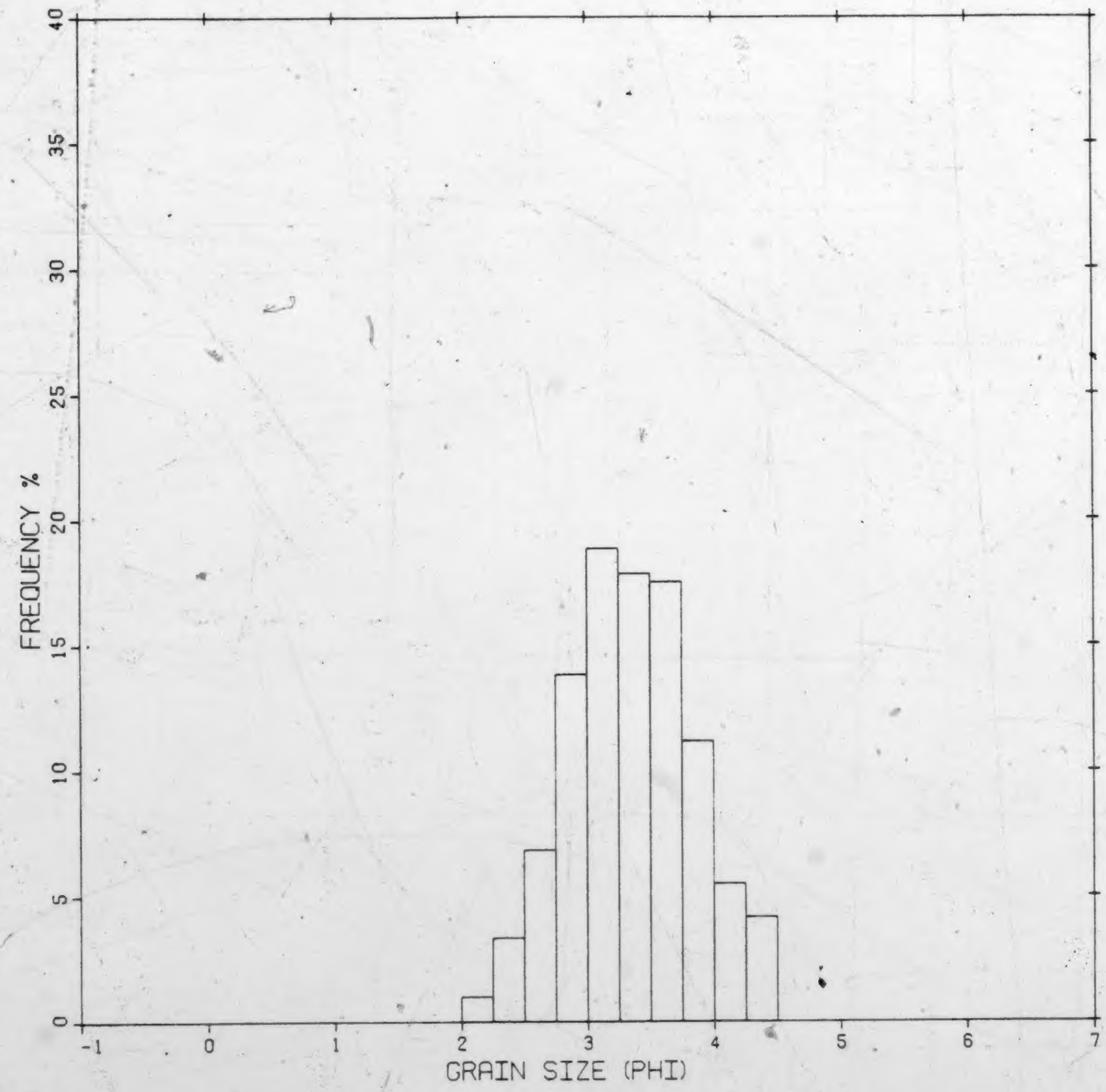

HISTOGRAM (SAMPLE S6/3-36)

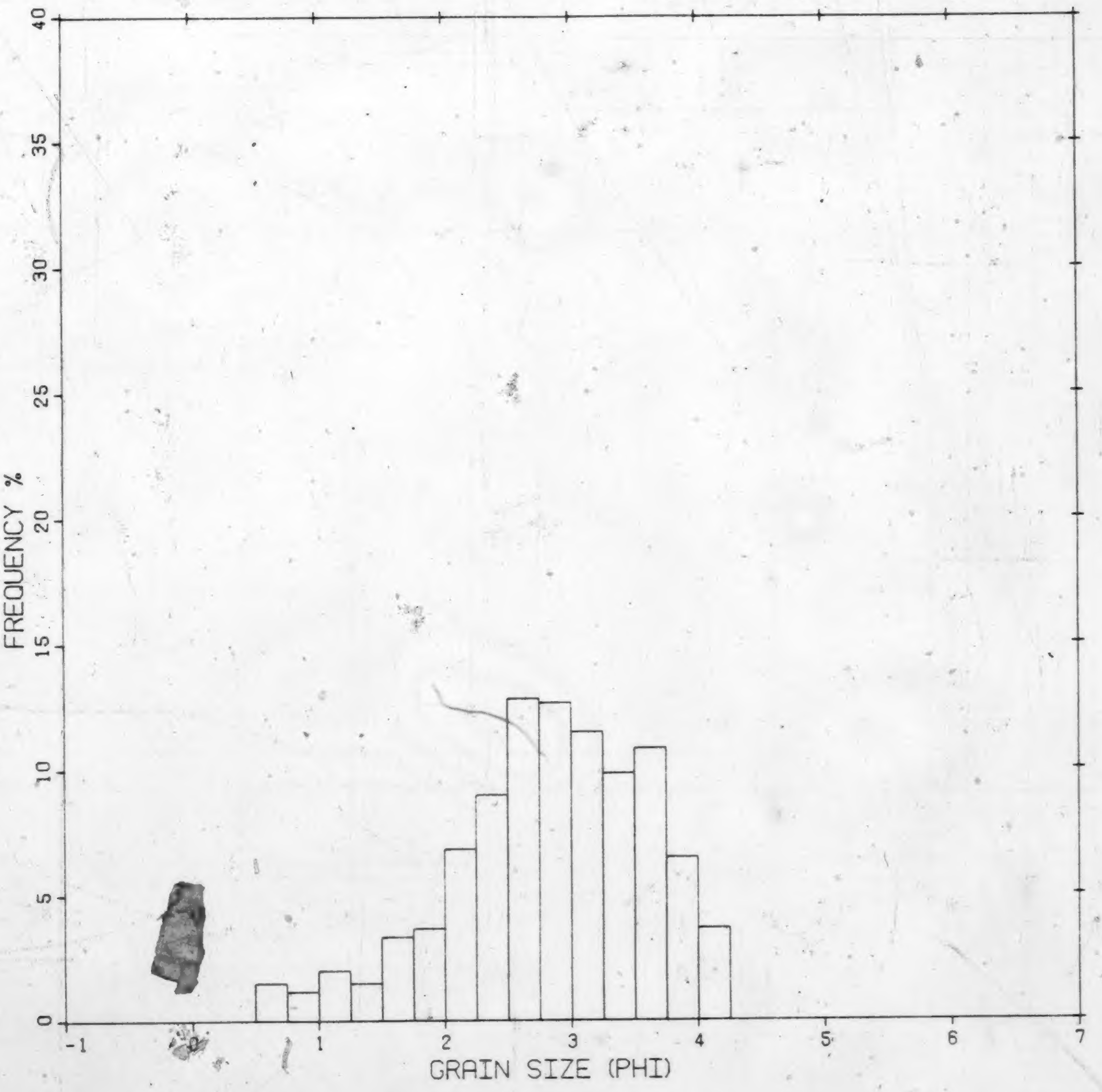

HISTOGRAM (SAMPLE S10/3-36)

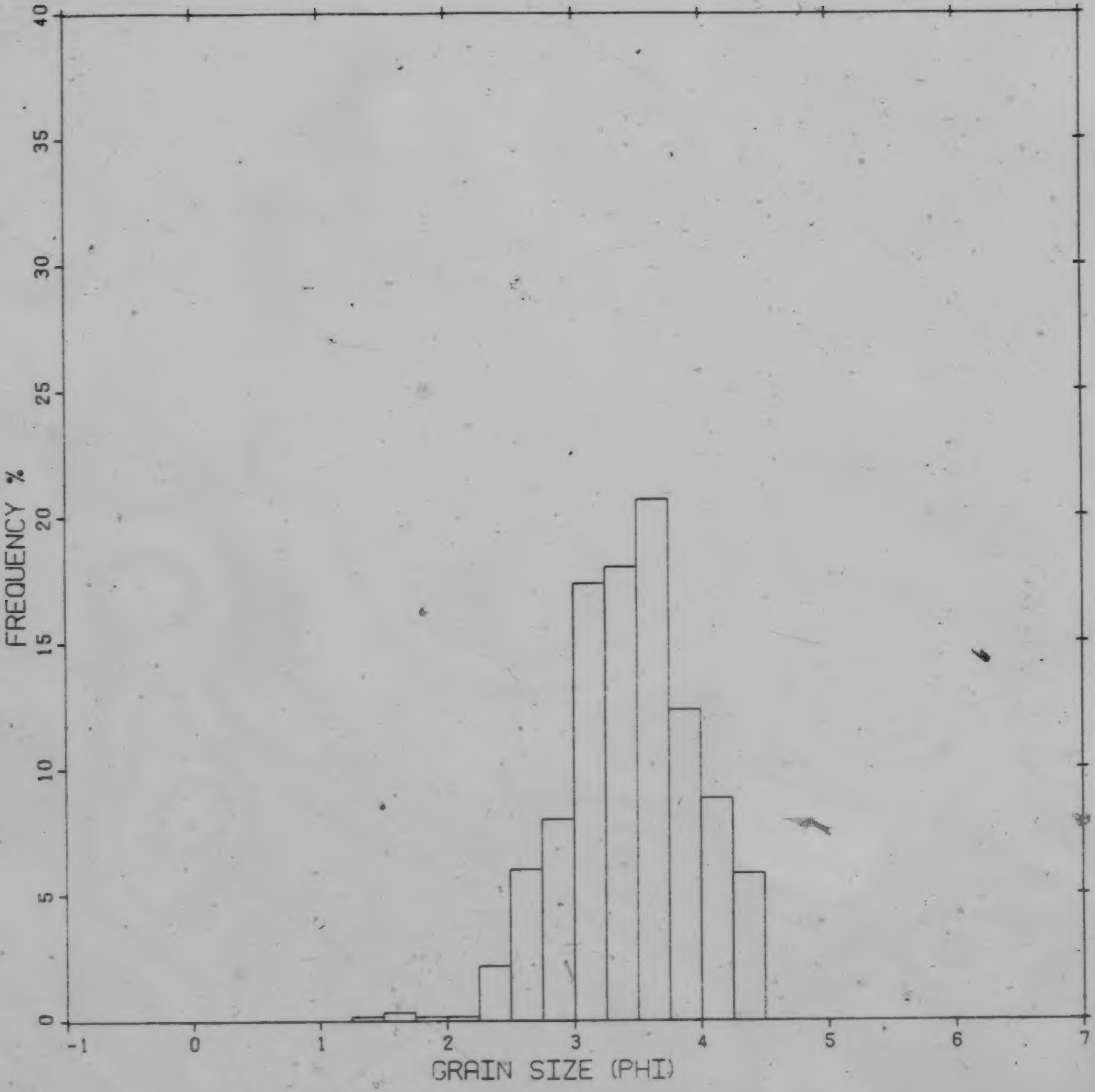

HISTOGRAM (SAMPLE S11/3-36)

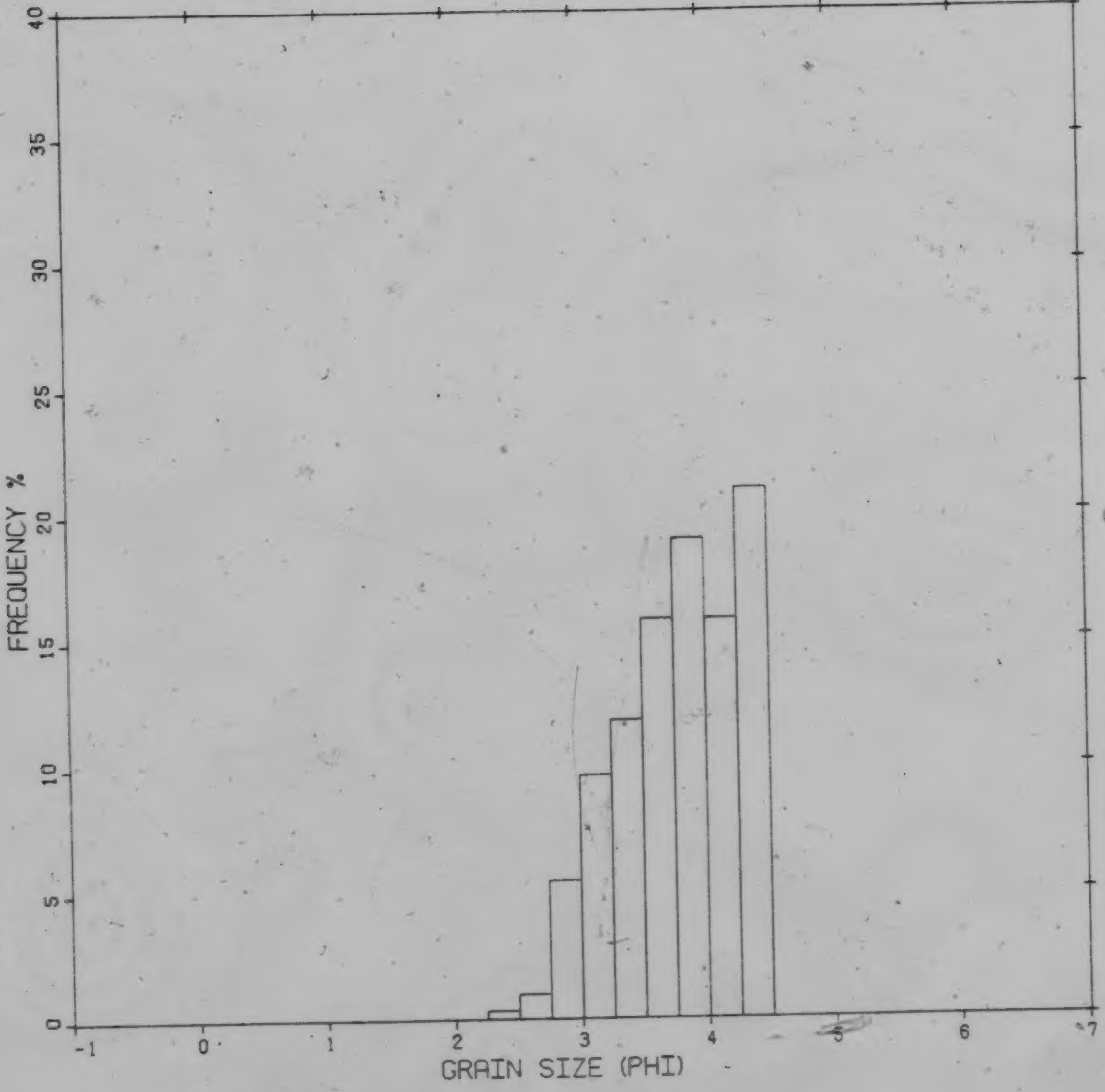

HISTOGRAM (SAMPLE S18/3-36)

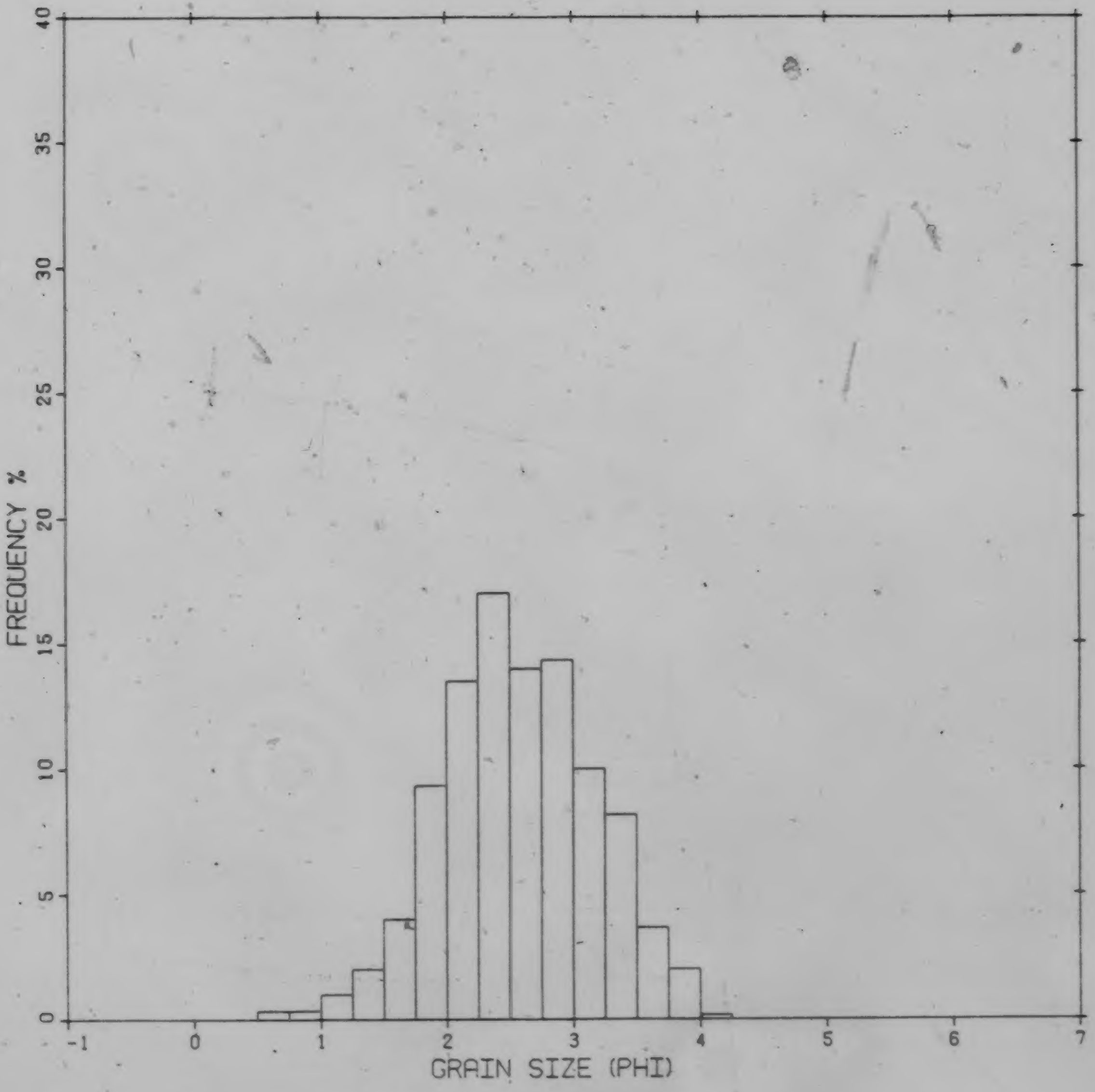

HISTOGRAM (SAMPLE S21/3-36)